WASHINGTON UNIVERSITY IN ST. LOUIS

Division of Biology and Biomedical Sciences
Computational and Systems Biology

Dissertation Examination Committee:
Jeffrey I. Gordon, Chair
Todd E. Druley
Daniel E. Goldberg
Lora. L. Iannotti
Michael A. Province

Impaired Gut Microbial Community Development in Undernourished Children

by

Sathish Subramanian

A dissertation presented to the
Graduate School of Arts and Sciences
of Washington University in
partial fulfillment of the
requirements for the degree
of Doctor of Philosophy

August 2015

St. Louis, Missouri

Table of Contents

Chapter 2

Persistent gut microbiota immaturity in malnourished Bangladeshi children

Chapter 3

An approach for identifying complementary foods that promote healthy gut microbiota development in children with undernutrition

Chapter 4

Future Directions

Acknowledgements

I would like to thank various family, mentors, colleagues and friends who have been a major source of support, comfort and motivation during my Ph.D. Firstly, I am deeply grateful to Jeffrey Gordon for the incredible opportunity to work in his laboratory under his inspirational mentorship. There are many fond experiences I have with Jeff who combines the best qualities one would seek for in a mentor, scientist and human being: kindness, creativity, passion, endurance, and someone who truly cares for all his students and colleagues. Jeff has always had an open-door policy, been interested in the views of others as well as possessing an intimate understanding of the on-goings in the laboratory. On rare occasions, a couple of weeks may go by without a conversation, but Jeff would resume our interaction as though he had been engaged, all the while, in a extrasensory 'mind-meld' with me. It is my honor to be a trainee of Dr. Gordon and his example and teachings form much of my philosophy as I aspire towards a future career in science. I wish him continued success in unlocking the mysteries of the gut microbiota and ultimately bringing much-needed benefit to children afflicted with undernutrition.

It is my belief that I was able to get the opportunity to join Jeff's lab, in large part due to the incredible support I have received from my previous mentors. My interest in biomedical research, medicine and undernutrition stems from my experience working with the late Ganapati Bhat at the University Teaching Hospital in Lusaka, Zambia. His generosity and desire to teach was so apparent that I could not resist the temptation to continue to study undernutrition several years later. It was Dr. Bhat who asked me to conduct my first research project to monitor the anthropometry of children in the pediatrics ward. I know that he would be very proud of my thesis and many times when I have doubted the overall significance of a scientific problem or experienced challenging situations, it is the memory of my time working with him and the children he treated that has motivated me to continue.

I am thankful to David Roos at the University of Pennsylvania who showed me, by example, how much fun science can be, and spurred me to follow a training route that combines

bench-work with computational analyses. I also want to thank Ponzy Lu who showed me through the Roy & Diana Vagelos Scholars in the Molecular Life Sciences program at the University of Pennsylvania that hard work and a fundamental training in mathematics, physics and biochemistry form the basis for research in the life sciences. I am also very thankful to Julian Rayner at the Wellcome Trust Sanger Institute for the interest he took in me to enable studying in his laboratory and the opportunity to spend a year doing research in England.

During my time in the Gordon Lab, I enjoyed several special interactions and formed meaningful friendships with colleagues. Brian Muegge and Tanya Yatsunenko were incredible graduate student mentors to me and represent a very happy, responsibility-free period of mine during the laboratory. Jeremiah Faith was also a big influence, as he piqued my interest in sequencing platforms and the innovative approaches he applied in this area. I would like to thank Ansel Hsiao for his thoughtful discussions and the opportunity to work with him in his interesting cholera study. I am especially grateful to Nicholas Griffin for his tutelage in statistical methods and for making my work-space an enjoyable environment. The latter half of my Ph.D. represents a second act consisting of a different set of main characters, one that also represents the ongoing succession in Jeff's lab. The arrival of Siddarth Venkatesh into the laboratory has had a huge impact on my thinking as a scientist, in particular his willingness to seek out opinions, frame problems logically and his genuine love of science. Through his collaboration, I have been inspired to consider post-doctoral training in exciting areas of biomedical research in future. I also want to thank and wish all the best to a consortium of youthful and exuberant students, Jeanette Gehrig, Tarek Salih, Hao-wei Chang and Derek Barisas as they continue with their respective theses. This thesis would not be possible without overwhelming levels of encouragement, technical assistance and supervision from Jessica Hoisington Lopez, Marty Meier, David O'Donell, Maria Karlsson, Laura Kyro, Su Deng, Jiye Cheng, Janaki Guruge, Justin Serugo, Sabrina Wagoner, Stephanie Amen, Eric Martin and Brian Koebbe.

I would also like to thank my fellow MSTP students Joseph Planer and Nicholas Semenkovich with whom I will fondly remember our time together in the lab. I am extremely thankful

to the Medical Scientist Training Program Director Wayne Yokoyama and Brian Sullivan for giving me the opportunity to attend the MSTP program. I am also thankful for funding from the Olin Foundation for my studies and the Bill & Melinda Gates Foundation for supporting our research.

Outside of Jeff's laboratory, I have had the great privilege of working with mentors in Bangladesh, Tahmeed Ahmed and Rashidul Haque, as well as William Petri from the University of Virginia, who have all been extremely generous, supportive and important figures in my thesis work. I hope to continue to interact with them in Bangladesh and to learn more about their research efforts and clinical study-sites. I have also really enjoyed my interactions with Sayeeda Huq, Mustafa Mahfuz and Munirul Islam, each of whom has provided great help to me during my thesis. Importantly, I wish to thank the parents and children from Dhaka, Bangladesh for their participation in the studies incorporated into my thesis.

I want to express thanks to members of my committee. I am grateful to Daniel Goldberg for his chairing of my committee and with whom I have felt a connection to because of my previous research experiences in Apicomplexan parasites. I would like to thank Michael Province for his counsel on statistical approaches in my analyses and his referral to Qunyuan Zhang, who spent much time helping me. I thank Todd Druley for his encouragement and mentorship towards future life as a M.D. Ph.D. I am also very grateful for Lora Iannotti's input on topics relating to undernutrition and the applicability of my research to important global health issues.

I reserve special thanks to my parents for their concern for my well-being, support of my choices and for their hard work and sacrifices that made it possible for me to study in the USA. I would like to thank my sister, Savitha Subramanian, for her older-sibling instincts over the years and the inspiration she provides to me by her public health work in several countries including Sierra Leone and Nepal. I am also grateful to my girlfriend, Swapnil Verma, for her carefree distractions away from science and her understanding during the journey of my Ph.D. as well as the generous support from her parents.

Dedication

In memory of Dr. Ganapati J. Bhat

Former Head of the Department of Paediatrics and Child Health

University Teaching Hospital, Lusaka, Zambia

ABSTRACT OF THE DISSERTATION

Impaired gut microbial community development in undernourished children

by

Sathish Subramanian

Doctor of Philosophy in Biology and Biomedical Sciences

Computational and Systems Biology Program

Washington University in St. Louis, 2015

Professor Jeffrey I. Gordon, Chair

The healthy growth of children is typically considered from an anthropometric perspective: i.e., changes in height and weight over time. Another feature of postnatal development involves the acquisition of our microbial communities, the largest of which resides in our gut. Malnutrition (undernutrition) in children, and its severity, is defined by the degree to which their anthropometric scores deviate from median values established by a World Health Organization reference cohort of 8440 individuals living in six countries. Epidemiologic studies have shown that moderate to severe forms of acute undernutrition are not due to food insecurity alone. The human gut microbiota can be thought of as a microbial 'organ' that plays important roles in extracting and metabolizing food ingredients, providing metabolites to the host and shaping development of the immune system. The central hypotheses of my thesis are that this microbial organ undergoes definable stages in its development following birth, that features of its developmental program are shared across biologically unrelated individuals living in distinct geographic locales and representing distinctive cultural traditions, that this developmental program is disrupted in undernourished children, and that such disruption is not merely an effect of undernutrition but is causally related to it. My thesis consists of three parts.

The first part is a 'Perspective' describing the hypotheses described above, and describing approaches that might be useful for linking the identification of bacterial taxa that define normal development of the gut microbiota during the first several years of postnatal life to (i) an analysis of how this developmental program may be linked to the risk for, or the expression of the manifestations of undernutrition, and (ii) how knowledge of complementary feeding practices could be applied to developing new ways to sponsor robust development of the microbiota in individuals where this program has already been perturbed.

In the second part, I define normal gut microbiota development in unrelated children with healthy growth phenotypes who live in an urban slum of Dhaka, Bangladesh. I did so by applying a machine-learning method (Random Forests) to bacterial 16S rRNA datasets generated from fecal samples collected monthly from birth through 24 months of life. I identified a group of 'age-discriminatory' bacterial strains whose changing representation in gut microbiota over time provide a signature of the developmental biology of the gut microbial community. I used this Random Forests-derived model to create two metrics that define the state of maturation of a given child's microbiota relative his/her chronologic age; 'relative microbiota maturity index' and 'microbiota-for-age Z score'. Using these metrics, I found that children with severe acute malnutrition (SAM) have immature gut microbiota (i.e. the configuration of their gut communities is younger than expected based on their chronologic age) and that this immaturity is incompletely and only transiently improved by two commonly used therapeutic food interventions.

In the third part, I expand my Random Forests-based modeling of gut microbiota development by studying members of birth cohorts living in India, South Africa, Peru, and Brazil; finding that features of microbiota development (age-discriminatory strains) are shared across populations representing diverse geographic locations and cultural traditions. I also present a preclinical model for identifying complementary foods that could be used to repair the persistent microbiota immaturity present in children with SAM. This model was created by (i) culturing nine age-discriminatory bacterial strains as well as seven SAM-associated strains from the fecal microbiota of Bangladeshi children, (ii) introducing these strains into germ-free mice, (iii) feeding the animals

different sequences of a prototypic Bangladeshi diet supplemented with different combinations of commonly consumed complementary foods, and (iv) analyzing 16S rRNA datasets generated from the recipient animal's fecal microbiota in order to identify foods that promote the representation of age-indicative but not SAM-associated strains. A follow-up study in gnotobiotic mice of one of the lead complementary foods discovered from these analyses confirmed that it promotes microbiota maturation, as well as sponsoring an increase in butyrate levels and the representation of colonic regulatory T cells.

Chapter 1

Introduction

Chapter 1 Introduction

Cultivating Healthy Growth and Nutrition through the Gut Microbiota

Sathish Subramanian[1,2], Laura V. Blanton[1,2], Steven A. Frese[3], Mark Charbonneau[1,2], David A. Mills[3], Jeffrey I. Gordon[1,2]

[1]Center for Genome Sciences and Systems Biology, Washington University School of Medicine, St. Louis, MO 63108, USA

[2]Center for Gut Microbiome and Nutrition Research, Washington University School of Medicine, St. Louis, MO 63108, USA

[3]Departments of Food Science & Technology and Viticulture & Enology, University of California, Davis, Davis, CA 95616, USA

This chapter corresponds to the complete and accepted version of a manuscript published as:

Subramanian, S. *et al.* Cultivating Healthy Growth and Nutrition through the Gut Microbiota. *Cell* **161,** 36–48 (2015).

Abstract

Microbiota assembly is perturbed in children with undernutrition, resulting in persistent microbiota immaturity that is not rescued by current nutritional interventions. Evidence is accumulating that this immaturity is causally related to the pathogenesis of undernutrition and its lingering sequelae. Preclinical models in which human gut communities are replicated in gnotobiotic mice have provided an opportunity to identify and predict the effects of different dietary ingredients on microbiota structure, expressed functions, and host biology. This capacity sets the stage for proof-of-concept tests designed to deliberately shape the developmental trajectory and configurations of microbiota in children representing different geographies, cultural traditions, and states of health. Developing these capabilities for microbial stewardship is timely given the global health burden of childhood undernutrition, the effects of changing eating practices brought about by globalization, and the realization that affordable nutritious foods need to be developed to enhance our capacity to cultivate healthier microbiota in populations at risk for poor nutrition.

Introduction

Understanding the determinants of the nutritional value of different foods has never been more important, with population stabilization being unlikely this century (Gerland et al., 2014) and growing challenges related to sustainable agriculture. An integral part of understanding how best to deliver nutritious food to a burgeoning population is understanding how the microbial community in our gut (the microbiota) is shaped by what we eat and how that community in turn shapes our development and health. Nowhere will this kind of insight be more crucial than in raising the world's children.

Current obstacles to achieving healthy and productive lives and societies are reflected in the United Nations' millennium development goals that include reductions in child mortality and hunger and improvements in maternal health (http://www.un.org/millenniumgoals/). The scope of the problem of childhood undernutrition is described by parameters such as the International Food Policy Research Institute's Global Hunger Index (http://www.ifpri.org/publication/2014-global-

hunger-index), which is an aggregate measure of calorie intake plus the rates of children being underweight and childhood mortality within a given region or country.

Much has been said about how changing patterns of food preferences brought about by economic development, globalization, and changes in food technology and food distribution systems are producing dramatic changes in how, what, and when we eat. These changes, combined with rapid population expansion and issues related to sustainable agriculture, create the need and the opportunity to drive innovation in the area of identifying new, affordable, and nutritious foods. Here, we focus on the importance of understanding the postnatal developmental biology of our gut microbial community—a highly adaptable microbial "organ" that is critically involved in the biotransformation of foods to products that can shape many aspects of human biology. In our view, studies of human gut microbial communities will markedly revise current thinking about many aspects of human nutrition. The knowledge gained could and should catalyze efforts to integrate agricultural policies, food production, and nutritional recommendations for consumers representing different ages, cultural traditions, and geographies. Preclinical research platforms are now available to evaluate the effects of foods that we currently consume and those that we envision creating in the future on the gut microbial community and host biology in ways that can inform clinical studies. Furthermore, studies of children with undernutrition are highlighting the importance of postnatal development of the gut microbiota for achieving healthy growth and providing us with a new set of metrics to define the efficacy of nutritional recommendations and interventions directed at infants, the maternal-infant dyad, and children. Finally, we emphasize the importance of addressing ethical, social, and regulatory issues related to research in this area now rather than later.

Defining Human Postnatal Development from a Microbial Perspective

The human gut microbiota is composed of all three domains of life; Bacteria, which predominate, Archaea, and Eukarya, plus viruses. The gut microbiota is composed of relatively few bacterial phyla compared to communities in other body habitats and is notable for its strain-level diversity. Application of low-error sequencing methods to PCR amplicons generated from the bacterial phy-

logenetic marker gene encoding the principal RNA in the small subunit of ribosomes (16S rRNA) has indicated that, once acquired, the majority of bacterial strains in a healthy adult are retained for long periods of time (Faith et al., 2013). Thus, early colonizers, once established in the gut ecosystem, have the potential to exert their effects on our biological features and health status for most and perhaps all of our adult lives. This latter finding emphasizes the importance of understanding whether there is a definable program of community assembly in healthy infants/children and whether such a program is shared or varies considerably across populations with distinct dietary habits and culinary traditions residing in different geographic locations. If such a developmental program were definable and a significant contributor to healthy growth, fostering its proper and full execution could represent the basis of an arm of preventive medicine designed to ensure long-term health through informed microbial stewardship.

Food is a major factor that shapes the proportional representation of microorganisms present in the gut microbiota and the relative abundance of its genes (the microbiome). Reciprocally, the configuration of the microbiota/microbiome influences the nutritional value of food. One illustration of this interrelationship comes from a culture-independent metagenomic analysis of the gut microbiomes of infants, children, and adults belonging to 150 families living in three countries located on three different continents (metropolitan areas of the USA plus rural villages in southern Malawi and the Amazonas state of Venezuela). The results revealed that the relative abundances of genes in the microbiome that are related to vitamin biosynthesis (e.g., folate, cobalamin, thiamine, and biotin), amino acid metabolism, and processing of complex polysaccharides change in an identifiable sequence during the postnatal period (Yatsunenko et al., 2012). In addition, differences between Westernized (USA) and non-Westernized populations were evident, with breastfed Malawian and Amerindian babies having higher relative abundances of microbial genes encoding enzymes involved in carbohydrate metabolism, vitamin biosynthesis (e.g., components of the biosynthetic pathway for riboflavin, a component of breast milk, dairy products, and meat), and urease (Yatsunenko et al., 2012). Urea represents up to 15% of breast milk nitrogen; its degradation to ammonia can be used for microbial biosynthesis of essential amino acids, potentially benefiting

both the microbiota and host when diets are deficient in protein. Significant differences in microbiome configuration were also observed between breast-fed and formula-fed infants, with the latter showing increased representation of genes involved in various aspects of carbohydrate and amino acid metabolism and cobalamin (vitamin B12) biosynthesis (Yatsunenko et al., 2012). Cobalamin is not only important for the host; the ability to transport cobalamin and other substituted corrins is an important determinant of survival for members of the microbiota (Degnan et al., 2014).

Together, these findings suggested that the gut community should be considered when assessing the nutritional requirements at different stages of the human life cycle and in different geographic/cultural settings. They also raised the question of whether perturbations in the functional development of the microbiota/microbiome were related to childhood undernutrition, the major cause of childhood deaths worldwide and a manifestation of a complex set of still poorly understood intra- and intergenerational factors, rather than food insecurity alone (Lazzerini et al., 2013, Caulfield et al., 2014 and Richard et al., 2014).

Undernutrition and Gut Microbiota Immaturity

The World Health Organization's (WHO) Multi-Center Growth Reference Study (http://www.who.int.beckerproxy.wustl.edu/childgrowth/mgrs/en/) defines three anthropometric (physical) parameters (weight-for-age, height-for-age, and weight-for-height Z scores) to describe normal early childhood growth and nutritional status from its evaluation of 8,440 infants and children living in six distinct sites around the world (USA, Oman, Norway, Brazil, Ghana, and India). A recent study provided another definition of healthy growth but from a microbial perspective (Chapter 2, Subramanian et al., 2014). It did so by examining gut microbiota assembly in 50 children residing in Dhaka, Bangladesh whose anthropometry during their first 2 years of life indicated healthy growth. Fecal samples were collected monthly from birth through the end of the second postnatal year, and the relative abundances of bacterial strains were analyzed by 16S rRNA amplicon sequencing. The results revealed that interpersonal variation in the bacterial component of their gut communities was significantly smaller than the variation associated with age. Applying Random

Forests, a machine-learning method, to regress relative abundances of bacterial taxa across these children revealed age-discriminatory bacterial strains. Separating these 50 children into training and validation cohorts, the regression was optimized to include the most informative taxa for accurate prediction of microbiota "age." The results were formally validated to prevent over-fitting and over-estimation of generalizability and produced a sparse model composed of 24 strains that could be used in aggregate as a microbial signature for describing a shared program of microbiota development in healthy individuals and two derived metrics for defining deviations from that normal program: "relative microbiota maturity" and "microbiota-for-age" Z (MAZ) score (Figure 1).

Severe acute malnutrition (SAM) is defined by weight-for-height Z (WHZ) scores more than 3 SDs below the median of children in the WHO reference cohort. Application of this sparse model to 64 Bangladeshi children with SAM (WHZ -4.2 ± 0.72 [SD]) revealed they had gut microbiota that appeared significantly "younger" than their chronological age (relative microbiota maturity of -6 ± 0.7 months and MAZ scores of -1.7 ± 0.2). Moreover, this immaturity was incompletely and only transiently rescued following a customary period of administration of either one of two types of ready-to-use therapeutic foods (RUTFs; typically given for 2 weeks until a 15% increase in weight gain is achieved; http://www.ClinicalTrials.gov, number NCT01331044). Bangladeshi children with moderate acute malnutrition (WHZ between -3 and -2) also exhibited significant microbiota immaturity, although less severe than children with SAM (Chapter 2, Subramanian et al., 2014). These results indicate that children with SAM have a persistent developmental abnormality affecting their gut microbial "organ" that is not durably repaired with existing therapy.

These observations raise a critical question: is microbiota immaturity a cause or an effect of childhood undernutrition? Many studies have shown that, although current protocols for treating children with (acute) undernutrition reduce mortality, they do not rescue its long-term morbidities, including stunting, immune dysfunction, and neurodevelopmental abnormalities (Victora et al., 2008, Gaayeb et al., 2014, Kosek et al., 2013 and Galler et al., 2012). For example, given the remarkable metabolic requirements of the neonatal brain, alterations in the normal postnatal de-

velopment of the gut microbiota may trigger marked impairments in brain development and lead to persistent disorders of cognition.

Support for a causal role for the gut microbiota in SAM comes from studies of gnotobiotic mice. In recent years, methods have been developed for transplanting previously frozen fecal samples from human donors into groups of germ-free mice at a selected stage of their lives (e.g., young, rapidly growing animals that have been recently weaned or older animals) and with a designated genetic background. If the human microbiota sample is frozen shortly after it is produced and maintained at −80°C, the bacterial strains represented in the donor's community can be transmitted efficiently and reproducibly to recipient mice (e.g., Turnbaugh et al., 2009a, Smith et al., 2013, Ridaura et al., 2013, Palm et al., 2014 and Kau et al., 2015). The recipient mice can be fed diets that contain ingredients used in foods consumed by the microbiota donor. Moreover, the ingredients and methods for preparing (cooking) such diets can be varied systematically. This approach allows myriad types of models to be constructed for studying the interaction of foods and the human gut microbiota in vivo. For example, diets can be given that are representative of those consumed by populations other than those of the donor to anticipate the effects of changes in food consumption patterns associated with Westernization or composed of ingredients that represent new potential sources of affordable, nutritious foods such as landraces and waste streams from current food manufacturing processes. Critically, these preclinical gnotobiotic animal models allow proof-of-concept tests of whether a donor phenotype is transmissible via his/her gut microbiota, the extent to which phenotypic transmission generalizes across different donor microbiota, and the sensitivity or robustness of phenotypic transmission to diet type. These preclinical models also permit simulations of existing or anticipated therapeutic interventions, including the opportunity to "randomize" a given individual's microbiota to not just one but multiple treatment arms in order to directly compare the effect (and effect size) of the treatments on both the microbiota and host, to characterize underlying mechanisms, and to identify surrogate- or mechanism-based biomarkers that could be translatable to the microbiota donor or donor population (Figure 2).

Transplanting fecal microbiota from same-gender Malawian twins discordant for kwashiorkor, a form of SAM, into separate groups of adult germ-free mice and feeding the recipient animals

a representative micro- and macronutrient-deficient Malawian diet disclosed that the healthy and kwashiorkor co-twins' microbiota transmitted discordant weight loss and metabolic phenotypes (as well as an enteropathy characterized by disruption of the small intestinal and colonic epithelial barrier in animals harboring kwashiorkor but not healthy microbiota) (Smith et al., 2013 and Kau et al., 2015). Unlike the transplanted healthy co-twins' microbiota, the kwashiorkor microbiota was structurally and metabolically labile, reconfiguring itself upon exposure to a peanut-based RUTF, but not in a sustained way when animals were returned to the Malawian diet. The combination of a nutrient-deficient Malawian diet and a kwashiorkor microbiota was required to produce pathology in the recipient "humanized" mice, including inhibition of steps within the tricarboxylic acid cycle in host cells (Smith et al., 2013). These findings not only provided evidence for a causal relationship between the gut microbiota and SAM but also highlighted the importance of diet-by-microbiota interactions in disease pathogenesis.

If we consider children with persistent microbiota immaturity from the perspective of developmental biology, we can pose a number of basic and applied scientific questions. One question is whether the developmental program defined in Bangladeshi infants and children is generalizable to other populations representing different geographic and cultural settings. If so, it would reveal a fundamental shared aspect of postnatal human development and raise mechanistic questions about the factors that specify a healthy microbial community "fate." Initial support for generalizability comes from an analysis of concordant healthy Malawian twin pairs, which showed that a number of the age-discriminatory bacterial strains with the highest feature importance scores in the Bangladeshi Random Forests model are also represented in the Malawian population (Chapter 2, Subramanian et al., 2014 and Yatsunenko et al., 2012). The designation "same strain" was based on the same 16S rRNA sequence; whole-genome sequencing of a given age-discriminatory strain identified by its 16S rRNA sequence will be needed to determine its degree of gene conservation across different Bangladeshi and Malawian hosts. Bacterial 16S rRNA analyses of fecal samples obtained at monthly intervals from infants and children with healthy growth phenotypes enrolled in birth cohorts living at multiple low-income countries allow country/community site-specific,

Random-Forests-based models of microbiota maturation to be constructed, as well as an aggregate model representing data pooled from all sites. "Generalizability" can be established through reciprocal tests of the accuracy of the site-specific models (and aggregate model) for healthy individuals living at the different sites and whether these models reveal similar relationships between anthropometry and relative microbiota maturity/MAZ scores for undernourished children living at each of these sites.

A second question has to do with the relationship between microbiota development, enteropathogen load, and environmental enteric dysfunction (EED, also known as environmental enteropathy), an enigmatic and as-yet-incompletely defined disorder of gut barrier function (Keusch et al., 2014 and Kosek et al., 2014). Does a primary failure to execute normal maturation of the microbiota directly influence risk for enteropathogen invasion, perturbations in development of mucosal immune system, and abnormalities in nutrient processing and absorption that ultimately results in growth faltering? Alternatively, is a holistic view required that considers each of these features of enteric biology as intimately and integrally related to one another? Large birth cohort studies such as MAL-ED and GEMS have provided an opportunity to measure the contributions of enteropathogen load/carriage and diarrheal incidence to growth faltering (MAL-ED Network Investigators, 2014, Platts-Mills et al., 2014 and Kotloff et al., 2013). Evidence is emerging that some of the age-discriminatory taxa that define normal microbiota maturation also protect the host from enteropathogen infection. Intriguingly, studies of Bangladeshi adults with acute cholera have shown that recovery from the diarrheal phase involves recapitulation of the sequence of appearance of the same age-discriminatory bacterial strains that define the normal pattern of assembly of the microbiota in healthy Bangladeshi infants/children, suggesting that an essential set of rules governs this assembly (successional) process (Hsiao et al., 2014). For example, *Ruminococcus obeum*, a bacterium that directly correlates with recovery from *Vibrio cholerae* infection in adult Bangladeshi subjects and defines later stages of normal gut microbiota maturation in healthy Bangladeshi children, restricts *V. cholerae* colonization of gnotobiotic mice harboring a representative human gut microbiota. Its mechanism involves production of an autoinducer-2 (AI-2) that causes

quorum-sensing mediated repression of *V. cholerae* colonization and virulence factor expression (Hsiao et al., 2014).

A third related question is the manner in which the mucosal immune system and the microbiota co-develop. How do these complex organs talk to and educate each other? The answers could help identify factors that legislate a normal developmental trajectory for a gut community and how developmental arrest of the microbiota could be become fixed and difficult to overcome/advance. Immaturity of the microbiota may be associated with relative immaturity of mucosal immunity in ways that impede responsiveness to vaccines or enteropathogens. If so, can we use members of the microbiota as next-generation adjuvants to prime the immune system in the context of a defined antigen (Yilmaz et al., 2014)? One way to characterize maturation of the mucosal immune system is to use fluorescence-activated cell sorting (FACS) to identify microbial taxa targeted by its IgA responses as a function of chronologic age in hosts with healthy growth phenotypes and in those with undernutrition (critically, IgA targeting is not simply a reflection of the abundances of organisms in the gut community; Kau et al., 2015). This method, named BugFACS, has identified bacterial targets of gut mucosal IgA responses using fecal samples from children with healthy growth phenotypes or those with varying degrees of undernutrition, as well as fecal samples harvested from gnotobiotic mice harboring transplanted microbiota from healthy and undernourished donors fed diets representative of those that these children consume. BugFACS-purified viable IgA-targeted bacterial taxa were subsequently introduced into germ-free animals fed nutrient-deficient or -sufficient diets to characterize their functional properties. The results disclosed that IgA responses to members of the microbiota can be used as biomarkers of growth faltering, that they are influenced by enteropathogen load, and that they mediate a diet-dependent enteropathy characterized by small intestinal and colonic epithelial barrier disruption. Moreover, treatment with IgA-targeted bacterial strains purified from healthy donor microbiota can prevent development of the enteropathy (Kau et al., 2015), indicating that this approach may have utility that extends beyond diagnostics to therapeutic lead discovery and defining mechanisms underlying EED pathogenesis.

A fourth and critical question is whether age-discriminatory taxa are not only just bio-

markers but also effectors of growth. If so, they become potential therapeutic agents and targets for manipulation, including food-based manipulations that allow for their establishment in an individual or population at the time of presentation with manifest disease or prior to that time. One way we are currently determining whether age-indicative taxa are also growth indicative is by transplanting microbial communities from children exhibiting varying degrees of growth faltering (defined by anthropometry), representing a particular geographic region, into young, actively growing germ-free animals fed diets representative of the donor population and then defining the effects of the different transplanted communities on the growth, metabolic and immunologic phenotypes of recipient gnotobiotic mice (Figure 2). 16S rRNA data sets generated from the animals' fecal samples can be used to correlate strain abundances to these phenotypes. These strains can then be cultured from the microbiota of different donor populations. Determining the effects of subsequently introducing these strains—singly or as components of defined consortia—into young gnotobiotic mice harboring microbiota from different undernourished donors represents a way to address several challenges that would be faced when designing and interpreting a clinical study. For example, these preclinical studies could help to (1) define criteria used to select strains beyond their feature importance scores in the Random Forests models and cultivability (e.g., the extent of representation of virulence determinants in their genomes); (2) assess how to encapsulate these organisms, including anaerobes, in ways that permit their long-term storage and viability; (3) determine the extent to which consortia can invade and establish themselves in different microbiota representing individuals from a given population or different populations; (4) assess the nature of their effects on growth (e.g., gain of lean body mass), metabolism, and gut barrier function as a function of the degree of donor undernutrition and microbiota immaturity; and (5) ascertain the degree to which invasion and establishment of these strains in the targeted microbiota and their host effects are impacted by diet. Determining whether these strains are interchangeable between countries will influence the generalizability of microbial interventions or whether there would have to be local sourcing of these biological resources by or for the communities who are themselves afflicted by undernutrition.

Establishing Microbiota and the Maternal Influence

The origins of the microbes that colonize an infant's gastrointestinal tract are complex, given that infants are exposed to different environmental sources. A major source is the mother and includes microbes from her vagina, skin, gut, and as some have reported, breast milk and possibly the placenta (Dominguez-Bello et al., 2010, Hunt et al., 2011, Grönlund et al., 2011, Cabrera-Rubio et al., 2012 and Aagaard et al., 2014).

A key knowledge gap relates to the "anthropology of microbes": knowing how practices associated with pregnancy, including micronutrient supplementation, as well as traditional (and changing) societal "prescriptions" for dietary practices, impact a mother's microbial ecology prior to and following parturition and how this may impact transmission of her microbes to her infant. A study of 91 pregnant Finnish women showed that the maternal microbiota changes between the first and third trimester (Koren et al., 2012) (Figure 3). Another analysis of Bangladeshi mothers revealed marked changes in their gut microbiota in the first month post-partum, followed by less substantial changes in the ensuing nine months (Chapter 2, Subramanian et al., 2014). One testable hypothesis is that the maternal microbiota, much like the infant microbiota, undergoes stereotypical alterations during normal pregnancy designed to enhance maternal health and to promote transfer of strains to the infant. Testing this hypothesis will require detailed time series sampling of maternal microbiota throughout pregnancy and of the maternal-infant dyad, plus other environmental sources, including other family members and caregivers. If a program of pregnancy-associated changes in the maternal gut microbiota can be identified using approaches analogous to those described above to characterize maturation of the infant microbiota, it could provide an opportunity to use the most indicative or transmissible taxa as biomarkers of nutritional status and as reporters of the effects of different dietary practices or the efficacy of prescribed prenatal nutritional interventions.

Pregnancy is also a time of increased susceptibility to infection. Rowe et al. (2011) demonstrated that pregnant mice show increased bacterial burden in models of *Listeria monocytogenes*

and *Salmonella typhimurium* infection, mediated via active immune suppression by a population of FoxP3+ regulatory T cells (Tregs). Moreover, ablation of the Treg compartment resulted in near-complete resorption of fetuses, indicating a delicate balance between immunological tolerance of the fetus and defense against enteropathogens (Rowe et al., 2011). It is not known how this period of deliberate immune suppression impacts the maternal microbiota and, in turn, transfer of pathogens (and other microbial community members) to the infant.

The Impact of First Foods

Breast Milk

The association between healthy postnatal growth and exclusive breastfeeding has led to the WHO's recommendation for a minimum of six months of exclusive breastfeeding (Kramer and Kakuma, 2002). Human milk is composed of lipids (tri-, di-, and monoglycerides, phospholipids, glycolipids, and free fatty acids), protein components (including immunoglobulins, lactoferrin, lysozyme, and cytokines), and a large repertoire of human milk oligosaccharides (HMOs). Over time, this composition changes from colostrum, which is HMO rich, to mature milk, which contains fewer HMOs and protein while the fat content remains relatively stable (Coppa et al., 1993 and Lemons et al., 1982).

HMOs and other milk glycoconjugates pass undigested through the proximal gut (Engfer et al., 2000) and serve as nutrient substrates for saccharolytic microbiota in the colon. The microbiota of healthy exclusively breastfed infants is dominated by members of the genus *Bifidobacterium* (Figure 1; Yatsunenko et al., 2012 and Chapter 2, Subramanian et al., 2014). These infant-associated bifidobacteria, notably *Bifidobacterium longum subsp. infantis*, possess a suite of genes involved in importing complex fucosylated and sialylated milk glycans, their further degradation, and subsequent utilization (Sela et al., 2008). The functions encoded by this suite of genes allow them to outcompete other saccharolytic taxa (Marcobal et al., 2010). Bifidobacteria also actively reshape milk composition. For example, they release N-linked glycans conjugated to

milk glycoproteins for use as a growth substrate. However, the effect of deglycosylation on milk protein digestibility and function is as-yet unknown (Garrido et al., 2012 and Garrido et al., 2013).

Colonization by *Bifidobacterium* species during nursing is associated with a range of benefits, including improved vaccine responses (Huda et al., 2014) and enhanced gut barrier function (Ewaschuk et al., 2008 and Weng et al., 2014), including stabilized epithelial tight junctions noted in both animal models (Bergmann et al., 2013) and human cell lines (Chichlowski et al., 2012). Recent work has shown that infants with high *Bifidobacterium* population densities exhibit a corresponding decrease in fecal milk glycans (De Leoz et al., 2015 and Wang et al., 2015), a relationship that could serve as the basis for developing inexpensive diagnostics to monitor development of a healthy gut microbiota in nursing infants.

Development of a healthy infant gut microbiota can be threatened by maternal undernutrition and premature birth. Maternal undernutrition during pregnancy increases risk for underweight and preterm births (Kramer et al., 1992). Children of undernourished mothers receive substantially less than the recommended intake of priority micronutrients during lactation (Allen, 2005). Fortified milk obtained from donors who have had a full-term pregnancy likely does not provide sufficient protein to preterm infants (Arslanoglu et al., 2009). Even when mothers of preterm infants can produce sufficient milk, alterations in milk fat, protein, oligosaccharide content (Weber et al., 2001 and De Leoz et al., 2012), and the repertoire of immunoactive components (Castellote et al., 2011) are observed, leading to a call for identifying additional elements for nutritional support of these infants (Gabrielli et al., 2011 and De Leoz et al., 2012).

A vicious cycle of maternal undernutrition and poor infant nutritional status can reflect alterations in the immune, HMO, and/or other components of mother's milk. This has critical implications for infant health. Poor maternal health is associated with variations in breast milk immunoglobulins and glycoprotein structures during lactation (Smilowitz et al., 2013) and with decreased lactoferrin, a protein with antimicrobial activities (Hennart et al., 1991). Parasite-specific breast milk IgA titers to *Entamoeba histolytica* and *Cryptosporidium* spp. correlate with nutritional

status in a Bangladeshi infant population in which the burden of infection with these enteropathogens is very high (Korpe et al., 2013). Preterm delivery is associated with atypical variations in milk glycan structures (De Leoz et al., 2012), which poses additional risks. As HMOs have structural similarities to epithelial cell surface and mucus glycans, they can have anti-adhesive effects on enteropathogens. Sialic acid or fucose moieties are key determinants of this activity. Thus, variations in fucosylated HMOs associated with preterm birth may reduce the efficacy of milk oligosaccharides as anti-adhesive decoy molecules for pathogens (Ruiz-Palacios et al., 2003 and Jantscher-Krenn et al., 2012).

Understanding how breast milk glycan repertoires correlate with normal microbiota assembly and with impaired microbiota maturation and undernutrition provides an opportunity to identify new glycan streams that could be used to treat undernourished infants. Commercial prebiotics are commonly added to infant formula, where they increase bifidobacteria titers in infant feces (Haarman and Knol, 2005, Knol et al., 2005 and Boehm et al., 2002) and lower the incidence of pathogens (Knol et al., 2005). However, current prebiotics, namely fructooligosaccharides and galactooligosaccharides, do not represent the constellation of complex glycan structures delivered in human milk. Moreover, their consumption is not restricted to the population of microbes that define normal gut microbiota maturation (Everard et al., 2014 and Dewulf et al., 2013). Numerous efforts to recreate the glycan landscape present in human milk are underway. The technology for chemical and chemoenzymatic construction of complex "milk" oligosaccharides has advanced tremendously, enabling wholesale construction of a limited number of HMO-like structures present in milk (Muthana et al., 2009). Alternatively, purification from animal milks presents another opportunity for rapid and large-scale acquisition of milk oligosaccharides and glycoconjugates. At present, a number of enriched or purified bovine milk glycoproteins, including immunoglobins, lactoferrin, and glycomacropeptide, and glycolipids are commercially available or could be readily produced at scale for use in preclinical and clinical studies. Bovine milk contains a relatively low concentration of free oligosaccharides, but the distribution of structures observed roughly matches the most abundant species present in HMOs (Aldredge et al., 2013). Importantly, bovine milk

oligosaccharides (BMOs) can be sourced from numerous points in dairy processing, including cheese whey, suggesting an opportunity for large-scale production of fractions enriched for given (or similar) structures (Zivkovic and Barile, 2011).

Serial Introduction of Complementary Foods in Ways that Promote Maturation of the Gut Microbiota

A recent study compared the microbiota and immune system in bottle-fed versus breastfed macaques. The results showed that breastfed infant macaques develop more robust T_H17 cells in the memory pool, suggesting that the timing and trajectory of dietary exposures during early life may have lasting functional consequences beyond that period (Ardeshir et al., 2014). In breastfed humans, the transition to formula feeding and family foods (complementary feeding practices) varies considerably in terms of which food types are consumed, the order of their presentation, and the duration of their consumption. Documenting which foods growing infants consume and in what quantities has required innovative approaches, particularly in low-income countries where undernutrition is prevalent (Caulfield et al., 2014) (Figure 3). For example, data collection protocols across eight different countries have been harmonized to enable quantification of variations in child feeding practices in the MAL-ED consortium (Caulfield et al., 2014).

The co-linearity between the introduction of various types of solid foods, reduction in breast milk consumption, and maturation of the gut microbiota makes it challenging to identify causal relationships between specific ingredients and the representation of specific microbes through human studies. However, studies in gnotobiotic mice colonized with defined collections of cultured (and sequenced) human gut-derived bacteria have been successful in interrogating specific food-microbe associations (Faith et. al., 2011). These relationships were identified using an experimental design in which a given gnotobiotic animal harboring a defined microbial consortium received a sequence of diets, composed of several different combinations of foods, whose concentrations are intentionally varied between diets. The order of presentation of the different diets was also varied between different mice in order to limit confounding from hysteresis

effects. This approach has identified associations between various commercially available foods given in the USA during the complementary feeding period and specific microbes independent of their order of presentation, which would be virtually impossible to identify in clinical studies of developing human infants (Faith et al., 2011). This approach can be applied to young mice colonized with the age- and healthy growth-associated bacterial strains identified using the methods described above to determine which complementary foods promote their representation and expressed functional features. The results could lead to a recommended sequence of complementary feeding that reflects local food availability, affordability, and cultural practices and that sponsors healthy microbiota maturation. This information would advance current recommendations, which are not microbiota based and quite general (Kleinman, 2000).

Additional Considerations Regarding the Developmental Biology of the Gut Microbiota

Obesity

Although we have emphasized the global challenge of undernutrition in children, another vexing global health problem is the growing burden of obesity and associated metabolic dysfunction in children. Increasing attention is being paid to delineating differences in the gut microbiota of children who become obese in the hopes that early recognition of perturbed microbiota development may permit early interventions in at risk populations. For example, a recent culture-independent study of a Singaporean birth cohort disclosed that precocious maturation of the microbiota during the first 6 months of postnatal life was associated with significantly increased adiposity at 18 months (Dogra et al., 2015). Specifically, an unsupervised clustering approach based on bacterial 16S rRNA sequence data sets revealed three clusters of fecal microbiota configurations. The number of samples that binned into one of these clusters (cluster 3), which is characterized by high levels of *Bifidobacteria* and *Collinsella* and low levels of *Streptococcus* and *Enterobacteriaceae*, increased with age. A faster time to achieving a cluster 3 configuration was associated with significantly greater adiposity measured at age 18 months. Given the rapid rate of change in eating practices and incidence of childhood obesity, longitudinal studies of this type are timely. They should

be strategically applied to populations representing different manifestations of these economic, anthropologic, and epidemiologic transitions and accompanied by comprehensive, quantitative assessments of food consumption during the pre-weaning, weaning, and postweaning periods.

Obesity is associated with reduced organismal and genetic diversity in the gut microbiota/microbiome of adults (Turnbaugh et al., 2009b and Le Chatelier et al., 2013). Transplantation of intact fecal microbiota samples, or derived culture collections, from adult twins stably discordant for obesity into germ-free mice transmitted the donors' discordant adiposity phenotypes, as well as obesity-associated metabolic dysfunction (Ridaura et al., 2013). Co-housing mice just after they received the obese donor's (Ob) microbiota with mice just after they received the lean co-twin's (Ln) microbiota, before their discordant adiposity/metabolic phenotypes became evident, prevented development of obesity and metabolic abnormalities in the Ob cagemate. This prevention was associated with unidirectional invasion of bacteria from the Ln cagemate's gut community to the Ob cagemate's microbiota. Invasion was diet dependent, occurring in mice fed a human diet formulated to reflect the lower third of saturated fat and upper third of fruit and vegetable consumption in the USA, but not when animals received an unhealthy diet representing the upper third of saturated fat and lower third of fruit and vegetable consumption (Ridaura et al., 2013). These results illustrate how niches can be filled in the Ob microbiota by Ln-derived bacterial taxa to prevent disease and how important diet is to the installation of these health-promoting strains. The results raise important questions about the origins of the reduced bacterial diversity observed in Ob microbiota.

Impact of Antibiotics

One active area of investigation is the role of frequent consumption of broad-spectrum antibiotics in determining the diversity and functional features of the developing microbiota. Studies in conventionally raised mice treated with low-dose penicillin from birth to 4, 8, or 28 weeks of age revealed that early and brief exposure was sufficient to produce durable changes in body composition (Cox et al., 2014). Practical issues (in many parts of the world, antibiotic consumption

in children is pervasive and poorly documented), ethical considerations, and the identification of suitable controls all confound the design of human studies that would seek to determine the effects of antibiotic administration on the developmental biology of the human infant gut microbiota and growth. In principle, pre-clinical tests that administer various classes of antibiotics in varying doses—together with representative human diets to gnotobiotic mice harboring transplanted microbiota from infants and children living in various parts of the world—followed by transplantation of their antibiotic-treated microbiota to a next generation of (antibiotic-free) gnotobiotic recipients, would provide one way to explore these questions.

Affordable Nutritious Foods: Societal Implications and Challenges

An imbalance of carbohydrate, fat, and protein consumption, food insecurity, and changing diets in low-income countries brought about by globalization, increases in food prices at the point of retail, and a global protein supply that needs to double by 2050 are some of the drivers for developing new types of affordable nutritious foods that are culturally acceptable, suitable for storage, and distributable given current and envisioned future infrastructure. A sustainable economic model in which local economies benefit from producing and/or distributing foods is also required to ensure long-term supplies. Moreover, there is a paucity of generally accepted metrics for defining foods that provide optimal nutrition at affordable cost (e.g., see the "nutrient-rich foods index" developed based on FDA recommendations; Drewnowski, 2010).

We propose that the gut microbiota provides a parameter that needs to be considered when developing nutrition options and that the type of preclinical gnotobiotic models described above will be useful for testing and defining dietary parameters. Studies with mice and other species provide means for characterizing interactions between food ingredients (at different levels of ingredient resolution and including culturally relevant spices and sweeteners), their methods of preparation and preservation, the gut microbiota of various consumer populations, and human metabolic,

immunologic, and other physiologic features. These research platforms offer the promise of yielding next-generation foods designed to be satiating, delicious, nutritious, and able to manipulate microbiota and host properties in ways that promote healthy growth and wellness. However, fulfilling this promise demands a holistic view of the nexus of human gut microbial ecology research, agricultural practices, food production, evolving consumer tastes in an era of rapid globalization, envisioned commercialization strategies, current regulatory structures/practices, ethical issues, and public education. For example, there is a need to more thoroughly and rapidly characterize, through readily searchable, accessible, well-annotated databases, emerging food consumption patterns in countries representing different cultural traditions, stages of economic development, and land/water resources. At the commercial level, there is an opportunity to define and differentiate foods based on their effects on different consumer populations with distinct biological phenotypes and with different gut microbial community configurations. There is an accompanying need to frame intellectual property laws in ways that provide appropriate incentives for private investment while protecting the public good.

To effectively and responsibly apply this knowledge in ways that benefit society, there is a need to work with government agencies to provide efficient and sensible regulatory schemes. These regulatory frameworks vary between nations and are evolving. Currently, the US Food and Drug Administration (FDA) defines "medical foods" as foods that make medical claims. A "dietary supplement" is a product intended for ingestion that contains a dietary ingredient designed to add further nutritional value to a diet. Dietary supplements can only contain ingredients that are "generally regarded as safe" (GRAS) or approved as food additives by the FDA after filing a "new dietary ingredient" (NDI) notification with full description of the ingredient and product in which it will be marketed, the basis for the manufacturer's conclusion that it is an NDI, recommended use and proposed labeling, plus a history of its use and evidence of its safety to support the proposed use. Probiotics have been defined in various ways, including "live microorganisms that, when administered in adequate amounts, confer a health benefit on the host" (Joint FAO/WHO Expert Consultation on Evaluation of Health and Nutritional Properties of Probiotics, 2001), whereas pre-

biotics have been considered to be "a selectively fermented ingredient that allows specific changes both in the composition and/or activity of the gastrointestinal microbiota that confer benefits upon host well-being and health" (Roberfroid, 2007). Synbiotics are combinations of prebiotics and probiotics. Regulation of prebiotics, probiotics, and synbiotics remains a work in progress, although any health claims they make will likely require a clinical development pathway that is the same as that employed for biologics.

Opening the Public Discussion

For public acceptance and societal benefit, a thoughtful proactive, science-based, educational outreach is needed with an understandable vocabulary tailored to targeted consumer populations and respectful of their cultural traditions. The goal would be to objectively describe the extent to which the nutritional value of food is related to a consumer's microbiota and how food ingredients, food choices, and the microbiota are connected to health benefits.

We suggest that one way of framing a public discussion regarding the impact of human gut microbiome research on the nexus of food, agriculture, and nutrition is to divide it into three "sectors": science and technology, ethics, and policy and governance.

Science and Technology

Ongoing and new studies will help to define (1) methods for selection and production of new food sources, (2) design of new foods/diets, (3) definitions of nutritional value and benefit and metrics for differentiation of foods, and (4) the role of the gut microbiota in determining nutritional status in pregnant women, infants and children, and adults throughout the course of their lives.

Ethics

The impact of gut microbiota research extends beyond conceptions of health to human rights. Key issues include (1) concepts of self and ownership of microbes and the shaping of these views by cultural, religious, socio-economic, educational, and political factors; (2) use of a person's mi-

crobes to improve nutritional status within and beyond family, community, and country; (3) strategies for responsible stewardship of our (human) microbial resources; and (4) personal, familial, and societal impact (and shared benefit) of methods envisioned to promote intergenerational transmission of beneficial microbes and to effect durable repair of defective gut microbial community development early in life or functional restoration later in life.

Policy and Governance

Advances in gut microbiota research will have long-term impact on regulatory and other governmental policies and agencies as they relate to agriculture, food, and nutritional health. These effects include (1) definitions of food safety, including the products of microbial biotransformation of food ingredients; (2) definitions of nutritional benefit within and outside of the context of specific human health claims; (3) laws concerning ownership of microbial strains and their distribution within and across national borders (for example, in October 2014, the Convention on Biological Diversity/Nagoya Protocol on Access to Genetic Resources and the Fair and Equitable Sharing of Benefits from their Utilization entered into international force "stringent requirements for prior informed consent and benefit sharing for research and commercial activities involving genetic resources from plants, animals, and microorganisms" [http://www.cbd.int/abs/]); (4) laws concerning intellectual property related to microbes, microbial consortia, and the products of microbial interactions with food ingredients, including diagnostics and therapeutics; (5) policies related to standards of manufacture, purity, and composition of probiotics and synbiotics; and (6) incentives for linking plans for food production and distribution with gut microbiota health. A key challenge is how to construe (1)–(6) in the context of a reference set of "representative" countries.

Closing Thoughts

Given the intricate links between first foods and long-term human health, ensuring availability of appropriate food sources is of high priority. Because undernutrition is such a widespread affliction, it is critical to consider how to categorize the targeted populations, the cost and economic

sustainability, the efficacy (effect size and durability), and the cultural acceptability of various therapeutic or preventative approaches, as well as the generalizability of both food-based and microbial interventions to large populations within and across national/societal boundaries. One way of conceptualizing this complex set of challenges for treatment and prevention is to place, on one end of the spectrum of undernutrition, children with already manifest SAM and significant microbiota immaturity who could be treated with locally produced, readily and reproducibly manufactured, affordable and safe, culturally acceptable next-generation RUTFs, with or without microbial interventions of the type described above. Moving along this continuum, another group would consist of individuals who manifest growth faltering (stunting) in the first 1,000 days after conception, where the envisioned targets for interventions are pregnant and lactating women and their infants. At the other end of the continuum is a third group that are the targets of locally produced, consumer-focused, affordable nutrition products designed to improve dietary quality and increase the diversity of food choices.

Looking back over 800 million years of metazoan evolution, we appreciate more now than ever before the splendid innovation of having a gut that assembles microbial resources that enable efficient utilization of available nutrients (McFall-Ngai et al., 2013). We, humans, are now in a position to not only understand but to deliberately influence this process of microbial community acquisition in order to ensure its optimal execution. The challenges we face in designing and improving food systems and nutritional health are great and pressing. Hopefully, our gut instinct will be to honor and harness the intimate interrelationship between foods and “our” microbes in an attempt to address this challenge now and throughout the course of this defining century for our species and planet.

Acknowledgments

Work cited from the authors' labs was supported in part by grants from the Bill & Melinda Gates Foundation (BMGF) and the NIH (DK078669, DK30292, and DK70977). We thank our colleagues in the BMGF-sponsored Breast Milk, Gut Microbiome, and Immunity Project, Tahmeed Ahmed and other members of our collaboration with the International Center for Diarrheal Disease Research, Bangladesh (ICDDR,B), Michael Barratt, Jeanette Gehrig, Siddarth Venkatesh and other members of our laboratories, plus William Petri and Andrew Serazin for their insights and inspiration. J.I.G. is a co-founder of Matatu, Inc., a company characterizing the role of diet-by-microbiota interactions in animal health. D.A.M. is a co-founder and President of Evolve Biosystems, Inc., a company focused on diet-based manipulation of the gut microbiota.

References

Aagaard, K., Ma, J., Antony, K.M., Ganu, R., Petrosino, J., and Versalovic, J. (2014). The Placenta Harbors a Unique Microbiome. Sci Transl Med *6*, 237ra65–237ra65.

Aldredge D. L., M. R. Geronimo, S. Hua, C. C. Nwosu, C. B. Lebrilla, D. Barile. (2013). Annotation and structural elucidation of bovine milk oligosaccharides and determination of novel fucosylated structures. Glycobiology *23*, 664-676.

Allen LH: Multiple micronutrients in pregnancy and lactation: an overview. (2005). Am J Clin Nutr. *81*, 51206S-1212S.

Ardeshir, A., Narayan, N.R., Méndez-Lagares, G., Lu, D., Rauch, M., Huang, Y., Rompay, K.K.A.V., Lynch, S.V., and Hartigan-O'Connor, D.J. (2014). Breast-fed and bottle-fed infant rhesus macaques develop distinct gut microbiotas and immune systems. Sci Transl Med *6*, 252ra120–252ra120.

Arslanoglu S., Moro G.E., Ziegler E.E. (2009). Preterm infants fed fortified human milk receive less protein than they need. J Perinatol *29,* 489–492.

Bergmann K.R., Liu S.X.L., Tian R., Kushnir A., Turner J.R., Li H.L., Chou P.M., Weber C.R., De Plaen I.G. (2013). Bifidobacteria stabilize claudins at tight junctions and prevent intestinal barrier dysfunction in mouse necrotizing enterocolitis. Am J Pathology *182,* 1595–1606.

Bogin, B. (1999). Patterns of human growth (Cambridge University Press).

Boehm G., Lidestri M., Casetta P., Jelinek J., Negretti F., et al. (2002). Supplementation of a bovine milk formula with an oligosaccharide mixture increases counts of faecal bifidobacteria in preterm infants. Arch Dis Child Fetal Neonatal Ed. *86*, F178-81.

Cabrera-Rubio, R., Collado, M.C., Laitinen, K., Salminen, S., Isolauri, E., and Mira, A. (2012). The human milk microbiome changes over lactation and is shaped by maternal weight and mode of delivery. Am J Clin Nutr *96*, 544–551.

Castellote C., Casillas R., Ramirez-Santana C., Perez-Cano F.J., Castell M., Gloria Moretones M., Carmen Lopez-Sabater M., Franch A. (2011). Premature Delivery Influences the Immunological Composition of Colostrum and Transitional and Mature Human Milk. J Nutr *141,* 1181–1187.

Caulfield, L.E., Bose, A., Chandyo, R.K., Nesamvuni, C., Moraes, M.L. de, Turab, A., Patil, C., Mahfuz, M., Ambikapathi, R., and Ahmed, T. (2014). Infant Feeding Practices, Dietary Adequacy, and Micronutrient Status Measures in the MAL-ED Study. Clin Infect Dis *59*, S248–S254.

Chichlowski M., De Lartigue G., German J.B., Raybould H.E., Mills D.A. (2012). Bifidobacteria isolated from infants and cultured on human milk oligosaccharides affect intestinal epithelial function. J Pediatr Gastroenterol Nutr *55,* 321–327.

Coppa G.V., Gabrielli O., Pierani P., Catassi C., Carlucci A., Giorgi P.L. (1993). Changes in carbohydrate composition in human milk over 4 months of lactation. Pediatrics *91,* 637–641.

Cox, L.M., Yamanishi, S., Sohn, J., Alekseyenko, A.V., Leung, J.M., Cho, I., Kim, S.G., Li, H., Gao, Z., Mahana, D., et al. (2014). Altering the intestinal microbiota during a critical developmental window has lasting metabolic consequences. Cell *158*, 705–721.

Degnan, P.H., Barry, N.A., Mok, K.C., Taga, M.E., and Goodman, A.L. (2014). Human Gut Microbes Use Multiple Transporters to Distinguish Vitamin B12 Analogs and Compete in the Gut. Cell Host & Microbe *15*, 47–57.

De Leoz, M.L.A., Gaerlan, S.C., Strum, J.S., Dimapasoc, L.M., Mirmiran, M., Tancredi, D.J., Smilowitz, J.T., Kalanetra, K.M., Mills, D.A., German, J.B., et al. (2012). Lacto N Tetraose, Fucosylation, and Secretor Status are Highly Variable in Human Milk Oligosaccharides From Women Delivering Preterm. J Proteome Res *11*, 4662–4672.

De Leoz, M.L.A., Kalanetra, K.M., Bokulich, N.A., Strum, J.S., Underwood, M.A., German, J.B., Mills, D.A., and Lebrilla, C.B. (2015). Human Milk Glycomics and Gut Microbial

Genomics in Infant Feces Show a Correlation between Human Milk Oligosaccharides and Gut Microbiota: A Proof-of-Concept Study. J. Proteome Res. *14*, 491–502.

Dewulf, E. M., Cani, P. D., Claus, S. P., Fuentes, S., Puylaert, P. G., Neyrinck, A. M., Bindels, L.B., de Vos, W.M., Gibson, G.R., Thissen, J.P., and Delzenne, N. M. (2013). Insight into the prebiotic concept: lessons from an exploratory, double blind intervention study with inulin-type fructans in obese women. Gut *62*, 1112-21.

Dogra, S., Sakwinska, O., Soh, S.-E., Ngom-Bru, C., Brück, W.M., Berger, B., Brüssow, H., Lee, Y.S., Yap, F., Chong, Y.-S., et al. (2015). Dynamics of infant gut microbiota are influenced by delivery mode and gestational duration and are associated with subsequent adiposity. mBio *6*, e02419–14.

Dominguez-Bello, M.G., Costello, E.K., Contreras, M., Magris, M., Hidalgo, G., Fierer, N., and Knight, R. (2010). Delivery mode shapes the acquisition and structure of the initial microbiota across multiple body habitats in newborns. Proc Natl Acad Sci USA *107*, 11971–11975.

Drewnowski, A. (2010). The Nutrient Rich Foods Index helps to identify healthy, affordable foods. Am J Clin Nutr. *91*, 1095S–1101S.

Engfer M.B., Stahl B., Finke B., Sawatzki G., Daniel H. (2000). Human milk oligosaccharides are resistant to enzymatic hydrolysis in the upper gastrointestinal tract. Am J Clin Nutr *71,* 1589–1596.

Everard, A., Lazarevic, V., Gaïa, N., Johansson, M., Ståhlman, M., Backhed, F., Delzenne, N.M., Schrenzel, J., François, P., and Cani, P. D. (2014). Microbiome of prebiotic-treated mice reveals novel targets involved in host response during obesity. ISME J *8*, 2116-2130.

Ewaschuk J.B., Diaz H., Meddings L., Diederichs B., Dmytrash A., Backer J., Langen M.L-V., Madsen K.L. (2008). Secreted bioactive factors from Bifidobacterium infantis enhance epithelial cell barrier function. Am J Physiol Gastrointest Liver Physiol *295,* G1025–G1034.

Faith, J.J., McNulty, N.P., Rey, F.E., and Gordon, J.I. (2011). Predicting a human gut microbiota's response to diet in gnotobiotic mice. Science *333*, 101–104.

Faith, J.J., Guruge, J.L., Charbonneau, M., Subramanian, S., Seedorf, H., Goodman, A.L., Clemente, J.C., Knight, R., Heath, A.C., Leibel, R.L., Rosenbaum, M., and Gordon, J.I. The long-term stability of the human gut microbiota. Science *341*, 1237439 doi: 10.1126/science.1237439 (2013).

Gaayeb, L., Sarr, J.B., Cames, C., Pinçon, C., Hanon, J.-B., Ndiath, M.O., Seck, M., Herbert, F., Sagna, A.B., Schacht, A.-M., et al. (2014). Effects of malnutrition on children's immunity to bacterial antigens in Northern Senegal. Am J Trop Med Hyg *90*, 566–573.

Gabrielli O., Zampini L., Galeazzi T., Padella L., Santoro L., Peila C., Giuliani F., Bertino E., Fabris C., Coppa G.V. (2011). Preterm milk oligosaccharides during the first month of lactation. Pediatrics *128,* e1520–e1531.

Galler, J.R., Bryce, C., Waber, D.P., Zichlin, M.L., Fitzmaurice, G.M., and Eaglesfield, D. (2012). Socioeconomic outcomes in adults malnourished in the first year of life: a 40-year study. Pediatrics *130*, e1–e7.

Garrido D., Nwosu C., Ruiz-Moyano S., Aldredge D., German J.B., Lebrilla C.B., Mills D.A. (2012). Endo- -N-acetylglucosaminidases from Infant Gut-associated Bifidobacteria Release Complex N-glycans from Human Milk Glycoproteins. Mol & Cell Proteomics *11,* 775–785.

Garrido D., Dallas D.C., Mills D.A. (2013). Consumption of human milk glycoconjugates by infant-associated bifidobacteria: mechanisms and implications. Microbiology *159,* 649–664.

Gerland, P., Raftery, A.E., Ševčíková, H., Li, N., Gu, D., Spoorenberg, T., Alkema, L., Fosdick, B.K., Chunn, J., Lalic, N., et al. (2014). World population stabilization unlikely this century. Science *346*, 234–237.

Goyal, M.S., Hawrylycz, M., Miller, J.A., Snyder, A.Z., and Raichle, M.E. (2014). Aerobic glycolysis in the human brain is associated with development and neotenous gene expression. Cell Metab. *19*, 49–57.

Grönlund, M.-M., Grześkowiak, Ł., Isolauri, E., and Salminen, S. (2011). Influence of mother's intestinal microbiota on gut colonization in the infant. Gut Microbes *2*, 227–233.

Haarman M., Knol J. (2005). Quantitative real-time PCR assays to identify and quantify fecal Bifidobacterium species in infants receiving a prebiotic infant formula. Appl Environ Microbiol *71*, 2318-24.

Hennart P.F., Brasseur D.J., Delognedesnoeck J.B., Dramaix M.M., Robyn C.E. (1991). Lysozyme, Lactoferrin, and Secretory Immunoglobulin-a Content in Breast-Milk - Influence of Duration of Lactation, Nutrition Status, Prolactin Status, and Parity of Mother. Am J Clin Nutr *53,* 32–39.

Hsiao, A., Ahmed, A.M., Subramanian, S., Griffin, N., Ahmed, T., Haque, R., and Gordon, J.I. (2014) Members of the human gut microbiota involved in recovery from *Vibrio cholerae* infection. Nature**,** *515*, 423-426.

Huda M.N., Lewis Z., Kalanetra K.M., Rashid M., Ahmad S.M., Raqib R., Qadri F., Underwood M.A., Mills D.A., Stephensen C.B. (2014). Stool microbiota and vaccine responses of infants. Pediatrics *134,* e362–72.

Hunt, K.M., Foster, J.A., Forney, L.J., Schütte, U.M.E., Beck, D.L., Abdo, Z., Fox, L.K., Williams, J.E., McGuire, M.K., and McGuire, M.A. (2011). Characterization of the Diversity and Temporal Stability of Bacterial Communities in Human Milk. PLoS ONE *6*, e21313.

Jantscher-Krenn E., Lauwaet T., Bliss L.A., Reed S.L., Gillin F.D., Bode L. (2012). Human milk oligosaccharides reduce Entamoeba histolytica attachment and cytotoxicity in vitro. Br J Nutr *108,* 1839–1846.

Joint FAO/WHO Expert Consultation on Evaluation of Health and Nutritional Properties of Probiotics. (2001). Health and nutrition properties of probiotics in food including powder

milk with live lactic acid bacteria. In Probiotics in Food: Health and Nutritional Properties and Guidelines for Evaluation (FAO and WHO), pp. 1–30.

Kau, A.L., Planer, J.D., Liu, J., Rao, S., Yatsunenko, T., Trehan, I., Manary, M.J., Liu, T.-C., Stappenbeck, T.S., Maleta, K.M., et al. (2015). Functional characterization of IgA-targeted bacterial taxa from undernourished Malawian children that produce diet-dependent enteropathy. Sci Transl Med *7*, 276ra24–ra276ra24.

Keusch, G.T., Denno, D.M., Black, R.E., Duggan, C., Guerrant, R.L., Lavery, J.V., Nataro, J.P., Rosenberg, I.H., Ryan, E.T., Tarr, P.I., et al. (2014). Environmental enteric dysfunction: pathogenesis, diagnosis, and clinical consequences. Clin. Infect. Dis. *59 Suppl 4*, S207–S212.

Kleinman, R.E. (2000). American Academy of Pediatrics recommendations for complementary feeding. Pediatrics *106*, 1274.

Knights, D., Kuczynski, J., Charlson, E.S., Zaneveld, J., Mozer, M.C., Collman, R.G., Bushman, F.D., Knight, R., and Kelley, S.T. (2011). Bayesian community-wide culture-independent microbial source tracking. Nat Meth *8*, 761–763.

Knol J., Boehm G., Lidestri M., Negretti F., Jelinek J., et al. (2005). Increase of faecal bifidobacteria due to dietary oligosaccharides induces a reduction of clinically relevant pathogen germs in the faeces of formula-fed preterm infants. Acta Paediatr Suppl. *94*(449), 31-3.

Koren, O., Goodrich, J.K., Cullender, T.C., Spor, A., Laitinen, K., Bäckhed, H.K., Gonzalez, A., Werner, J.J., Angenent, L.T., Knight, R., et al. (2012). Host remodeling of the gut microbiome and metabolic changes during pregnancy. Cell *150*, 470–480.

Korpe, P.S., Liu, Y., Siddique, A., Kabir, M., Ralston, K., Ma, J.Z., Haque, R., and Petri, W.A. (2013). Breast milk parasite-specific antibodies and protection from amebiasis and cryptosporidiosis in Bangladeshi infants: a prospective cohort study. Clin. Infect. Dis. *56*, 988–992.

Kosek, M., Guerrant, R.L., Kang, G., Bhutta, Z., Yori, P.P., Gratz, J., Gottlieb, M., Lang, D., Lee, G., Haque, R., et al. (2014). Assessment of environmental enteropathy in the MAL-ED cohort study: theoretical and analytic framework. Clin. Infect. Dis. *59 Suppl 4*, S239–S247.

Kosek, M., Haque, R., Lima, A., Babji, S., Shrestha, S., Qureshi, S., Amidou, S., Mduma, E., Lee, G., Yori, P.P., et al. (2013). Fecal markers of intestinal inflammation and permeability associated with the subsequent acquisition of linear growth deficits in infants. Am J Trop Med Hyg *88*, 390–396.

Kotloff, K.L., Nataro, J.P., Blackwelder, W.C., Nasrin, D., Farag, T.H., Panchalingam, S., Wu, Y., Sow, S.O., Sur, D., Breiman, R.F., et al. (2013). Burden and aetiology of diarrhoeal disease in infants and young children in developing countries (the Global Enteric Multicenter Study, GEMS): a prospective, case-control study. Lancet *382*, 209–222.

Kramer M.S., McLean F.H., Eason E.L., Usher R.H. (1992). Maternal Nutrition and Spontaneous Preterm Birth. Am J Epidemiol *136,* 574–583.

Kramer, M.S., and Kakuma, R. (2002). Optimal duration of exclusive breastfeeding. Cochrane Database Syst Rev CD003517.

Lazzerini, M., Rubert, L., and Pani, P. (2013). Specially formulated foods for treating children with moderate acute malnutrition in low- and middle-income countries. Cochrane Database Syst Rev *6*, CD009584.

Le Chatelier, E., Nielsen, T., Qin, J., Prifti, E., Hildebrand, F., Falony, G., Almeida, M., Arumugam, M., Batto, J.-M., Kennedy, S., et al. (2013). Richness of human gut microbiome correlates with metabolic markers. Nature *500*, 541–546.

Lemons J.A., Moye L., Hall D., Simmons M. (1982). Differences in the composition of preterm and term human milk during early lactation. Pediatr Res *16,* 113–117.

MAL-ED Network Investigators (2014). The MAL-ED study: a multinational and multidisciplinary approach to understand the relationship between enteric pathogens, malnutrition, gut

physiology, physical growth, cognitive development, and immune responses in infants and children up to 2 years of age in resource-poor environments. Clin Infect Dis *59 Suppl 4*, S193–206.

Marcobal A., Barboza M., Froehlich J.W., Block D.E., German J.B., Lebrilla C.B., Mills D.A. (2010). Consumption of Human Milk Oligosaccharides by Gut-Related Microbes. J Agric Food Chem *58,* 5334–5340.

McFall-Ngai, M., Hadfield, M.G., Bosch, T.C.G., Carey, H.V., Domazet-Lošo, T., Douglas, A.E., Dubilier, N., Eberl, G., Fukami, T., Gilbert, S.F., et al. (2013). Animals in a bacterial world, a new imperative for the life sciences. PNAS *110*, 3229–3236.

Muthana S., Cao H., Chen X. (2009). Recent progress in chemical and chemoenzymatic synthesis of carbohydrates. Curr Opin Chem Biol *13*, 573-81.

Palm, N.W., de Zoete, M.R., Cullen, T.W., Barry, N.A., Stefanowski, J., Hao, L., Degnan, P.H., Hu, J., Peter, I., Zhang, W., et al. (2014). Immunoglobulin A coating identifies colitogenic bacteria in inflammatory bowel disease. Cell *158*, 1000–1010.

Platts-Mills, J.A., McCormick, B.J.J., Kosek, M., Pan, W.K., Checkley, W., Houpt, E.R., and MAL-ED Network Investigators (2014). Methods of analysis of enteropathogen infection in the MAL-ED Cohort Study. Clin Infect Dis *59 Suppl 4*, S233–238.

Richard, S.A., McCormick, B.J.J., Miller, M.A., Caulfield, L.E., Checkley, W., and MAL-ED Network Investigators (2014). Modeling environmental influences on child growth in the MAL-ED cohort study: opportunities and challenges. Clin Infect Dis *59 Suppl 4*, S255–260.

Ridaura, V.K., Faith, J.J., Rey, F.E., Cheng, J., Duncan, A.E., Kau, A.L., Griffin, N.W., Lombard, V., Henrissat, B., Bain, J.R., et al. (2013). Gut microbiota from twins discordant for obesity modulate metabolism in mice. Science *341*, 1241214.

Roberfroid, M. (2007). Prebiotics: the concept revisited. J Nutr *137*, 830S–7S.

Rowe, J.H., Ertelt, J.M., Aguilera, M.N., Farrar, M.A., and Way, S.S. (2011). Foxp3(+) regulatory T cell expansion required for sustaining pregnancy compromises host defense against prenatal bacterial pathogens. Cell Host & Microbe *10*, 54–64.

Ruiz-Palacios G.M., Cervantes L.E., Ramos P., Chavez-Munguia B., Newburg D.S. (2003) Campylobacter jejuni binds intestinal H(O) antigen (Fuc alpha 1, 2Gal beta 1, 4GlcNAc), and fucosyloligosaccharides of human milk inhibit its binding and infection. J Biol Chem *278,* 14112–14120.

Sela D.A., Chapman J., Adeuya A., Kim J.H., Chen F., Whitehead T.R., Lapidus A., Rokhsar D.S., Lebrilla C.B., German J.B. (2008). The genome sequence of Bifidobacterium longum subsp. infantis reveals adaptations for milk utilization within the infant microbiome. Proc Natl Acad Sci USA *105,* 18964–18969.

Smilowitz J.T., Totten S.M., Huang J., Grapov D., Durham H.A., Lammi-Keefe C.J., Lebrilla C., German J.B. (2013). Human Milk Secretory Immunoglobulin A and Lactoferrin N-Glycans Are Altered in Women with Gestational Diabetes Mellitus. J Nutr *143,* 1906–1912.

Smith, M.I., Yatsunenko, T., Manary, M.J., Trehan, I., Mkakosya, R., Cheng, J., Kau, A.L., Rich, S.S., Concannon, P., Mychaleckyj, J.C., et al. (2013). Gut Microbiomes of Malawian Twin Pairs Discordant for Kwashiorkor. Science *339*, 548–554.

Sonnenburg, J.L., Xu, J., Leip, D.D., Chen, C.-H., Westover, B.P., Weatherford, J., Buhler, J.D., and Gordon, J.I. (2005). Glycan Foraging in Vivo by an Intestine-Adapted Bacterial Symbiont. Science *307*, 1955–1959.

Subramanian, S., Huq, S., Yatsunenko, T., Haque, R., Mahfuz, M., Alam, M.A., Benezra, A., DeStefano, J., Meier, M.F., Muegge, B.D., et al. (2014). Persistent gut microbiota immaturity in malnourished Bangladeshi children. Nature *510*, 417–421.

Turnbaugh, P.J., Ridaura, V.K., Faith, J.J., Rey, F.E., Knight, R., and Gordon, J.I. (2009). The Effect of Diet on the Human Gut Microbiome: A Metagenomic Analysis in Humanized Gnotobiotic Mice. Sci Transl Med *1*, 6ra14–6ra14.

Turnbaugh, P.J., Hamady, M., Yatsunenko, T., Cantarel, B.L., Duncan, A., Ley, R.E., Sogin, M.L., Jones, W.J., Roe, B.A., Affourtit, J.P., et al. (2009). A core gut microbiome in obese and lean twins. Nature *457*, 480–484.

Victora, C.G., Adair, L., Fall, C., Hallal, P.C., Martorell, R., Richter, L., Sachdev, H.S., Maternal and Child Undernutrition Study Group (2008). Maternal and child undernutrition: consequences for adult health and human capital. Lancet *371*, 340–357.

Weber A., Loui A., Jochum F., Bührer C., Obladen M. (2001). Breast milk from mothers of very low birthweight infants: variability in fat and protein content. Acta Paediatr *90,* 772–775.

Weng, M., Ganguli, K., Zhu, W., Shi, H.N., and Walker, W.A. (2014). Conditioned medium from Bifidobacteria infantis protects against Cronobacter sakazakii-induced intestinal inflammation in newborn mice. American Journal of Physiology - Gastrointestinal and Liver Physiology *306*, G779–G787.

Yatsunenko, T., Rey, F.E., Manary, M.J., Trehan, I., Dominguez-Bello, M.G., Contreras, M., Magris, M., Hidalgo, G., Baldassano, R.N., Anokhin, A.P., et al. (2012). Human gut microbiome viewed across age and geography. Nature *486*, 222–227.

Yilmaz, B., Portugal, S., Tran, T.M., Gozzelino, R., Ramos, S., Gomes, J., Regalado, A., Cowan, P.J., d'Apice, A.J.F., Chong, A.S., et al. (2014). Gut Microbiota Elicits a Protective Immune Response against Malaria Transmission. Cell *159*, 1277–1289.

Zivkovic, A. M. and D. Barile. (2011). Bovine milk as a source of functional oligosaccharides for improving human health. Adv Nutr *2*, 284-9.

Figure Legends

Figure 1 – Developing metrics for describing gut microbial community development. (a) Bacterial taxa that discriminate different stages of development were identified by a machine learning-based (Random Forests) regression of 16S rRNA datasets produced from monthly fecal samples collected from anthropometrically healthy infants and children living in an urban slum in Dhaka, Bangladesh during their first two years of postnatal life to their respective chronologic ages at the time of sample collection (Subramanian et. al, 2014). Shown are depictions of the typical distributions of these age-discriminatory taxa across the population. Taxa were selected based on their relative importance to the accuracy of the Random Forests model using a permutation-based 'feature importance'. (b) The most discriminatory taxa, as defined by their feature importance, were used as inputs into a sparse 24-taxon model whose output ('microbiota age') is a microbiota-based prediction of the chronologic age of a healthy child. The plot on the left of the panel shows microbiota age against chronologic age of healthy children used as a training set to fit the regression (each dot is a fecal sample from an individual child). The plot on the right of the panel shows application of the sparse model to a validation set composed of a different group of children living in the same location that were not used to train the model. Applying the model to a separate validation set controls for over-fitting of the model to the training set, and ensures its wider usability. (c) Two metrics of microbiota maturation based on application of the model to two separate validation sets of singletons and a separate study of Bangladeshi twins/triplets. 'Relative microbiota maturity' is the deviation, in months, from a smooth-spline fit of microbiota age values with respect to chronologic age, fitted using the validation datasets (see black dashed curve). The red dot represents a fecal sample collected from a focus child that is 11 months below the spline fit, indicating negative relative microbiota maturity (i.e., an immature microbiota). A microbiota-for-age Z score (MAZ) is computed by dividing the difference between the focal child's microbiota age and the median microbiota age of healthy controls in the same monthly chronologic age bin over the standard deviation within the same age bin. The median and standard deviation of each bin are computed using the validation datasets. The distribution of microbiota maturity and MAZ scores in birth-co-

hort studies have been studied using linear mixed models that take into account random variation specific to each serially-sampled child and family while estimating the fixed variation attributable to a factor observed across different children (e.g., diarrheal episodes) (Chapter 2, Subramanian et al., 2014).

Note that using Random Forests to study microbiota maturation is advantageous because of its non-parametric assumptions and utility in the context of high dimensional datasets (large numbers of predictors). Nonetheless, it is one of several methods that can be useful. For example, the rank-order Spearman correlation metric has been applied to infant microbiome datasets to detect monotonic relationships between microbiome-encoded functions/bacterial taxa and postnatal age (Yatsunenko et. al, 2012).

Figure 2 – Integration of existing clinical observational and interventional studies into gnotobiotic mouse models to identify interactions between the gut microbiota, food, and host biology. The discovery process depicted by the left circle illustrates how gnotobiotic animal models colonized with human donor microbiota and fed human diets can lead to a greater understanding of how diet-by-microbiota interactions are causally related to healthy growth and to phenotypes associated with undernutrition: e.g., immune system development, brain development and host and microbial community metabolism. New surrogate- or mechanism-based biomarkers of nutritional state emanating from these gnotobiotic models can be validated using biospecimens collected from the donors used to construct these gnotobiotic models, as well as from other members of the study population. The discovery/development process depicted on the right illustrates how dietary and microbial 'leads' can be tested in the context of humanized gnotobiotic animals to assess how they modulate biological processes already known, discovered or postulated to be involved in healthy growth and/or the pathogenesis of undernutrition. The downward pointing arrow in the middle of the figure points to next steps in clinical translation. See the main text for a discussion of the regulatory, ethical, societal and commercial implications of these efforts. Abbreviation: IND, Investigational New Drug.

Figure 3 – Co-variation in gut microbiota assembly/maturation, dietary patterns and other facets of human postnatal development. (a) Illustration of the rate of change occurring in gut microbiota structure of both mother and child. Note that infant variation curves are known from both longitudinal and cross-sectional study designs (Yatsunenko et al., 2012, Chapter 2, Subramanian et al., 2014). In the case of mothers, the curve is interpolated based on studies of pregnant Finnish mothers prior to delivery (Koren et al., 2012) and Bangladeshi mothers following parturition (Chapter 2, Subramanian et al., 2014). (b) The food consumption pattern shown is at a population level and does not depict the great deal of temporal variation observed in food consumption patterns within a given child. Depicting the fractional contribution of each food to the consumption patterns of children in Bangladesh underscores how dietary changes occur simultaneously (lowering of breast-milk and increase in legumes and cow's milk) and not in an orderly fashion (small fluctuations from month-to-month; re-entry and dropout of certain foods). It also underscores the challenge encountered in ascertaining how food and the microbiota interact to effect maturation of the community. (c) Major processes related to growth and how they vary in rate and magnitude over time. Curves are adapted from Bogin (1999). Note that the newborn brain represents 12% of body weight (a value six times greater than in adults). By the end of the first decade, the brain represents 6% of body weight and consumes twice the amount of glucose and 1.5 times the amount of oxygen as the adult brain. Approximately 30% of the glucose consumed by the infant brain is accounted for by aerobic glycolysis (versus 12% in adults) (Goyal et al., 2014). The dramatic changes in brain metabolism that occur over the first two decades of life coincide with the initial proliferation and then pruning of synapses to adult levels. Central questions that need to be addressed in this area include the biological effects of the gut microbial community on neurogenesis, synaptic connectivity, gliogenesis and glial-neuron interactions, neural circuit function and higher cognitive processes in the context of healthy growth versus undernutrition, and whether/how the gut-brain axis operates to influence/regulate other aspects of host physiology, metabolism and immunity in the infant/child. Moreover, if persistent immaturity of the gut microbiota is causally related to undernutrition and its long-term sequelae, including neurodevelopmental abnormalities,

does durable repair of this immaturity require that nutritional interventions be administered earlier before disease becomes fully manifest (and the microbial ecosystem is so perturbed that restoration becomes very difficult)? Do nutritional interventions need to be applied for more sustained periods of time? Do new types of therapeutic foods need to be developed or is a microbial intervention also needed?

Figures

Figure 1.

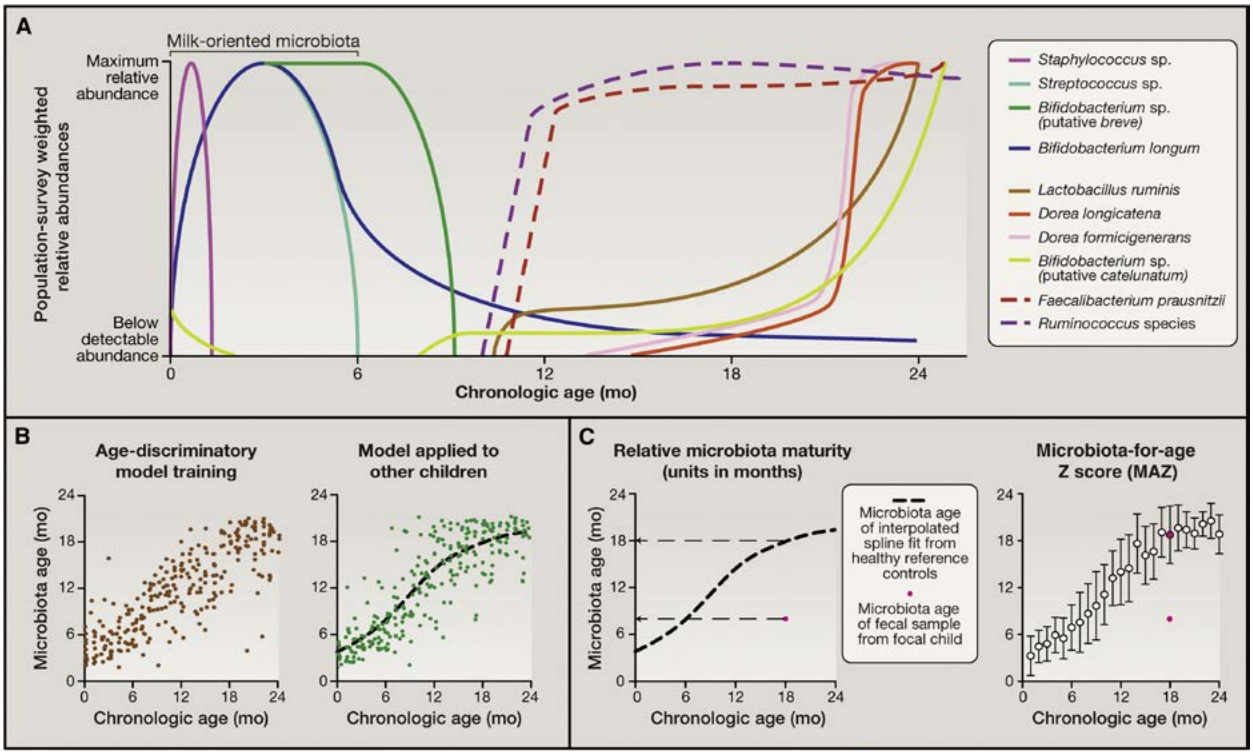

Figure 2.

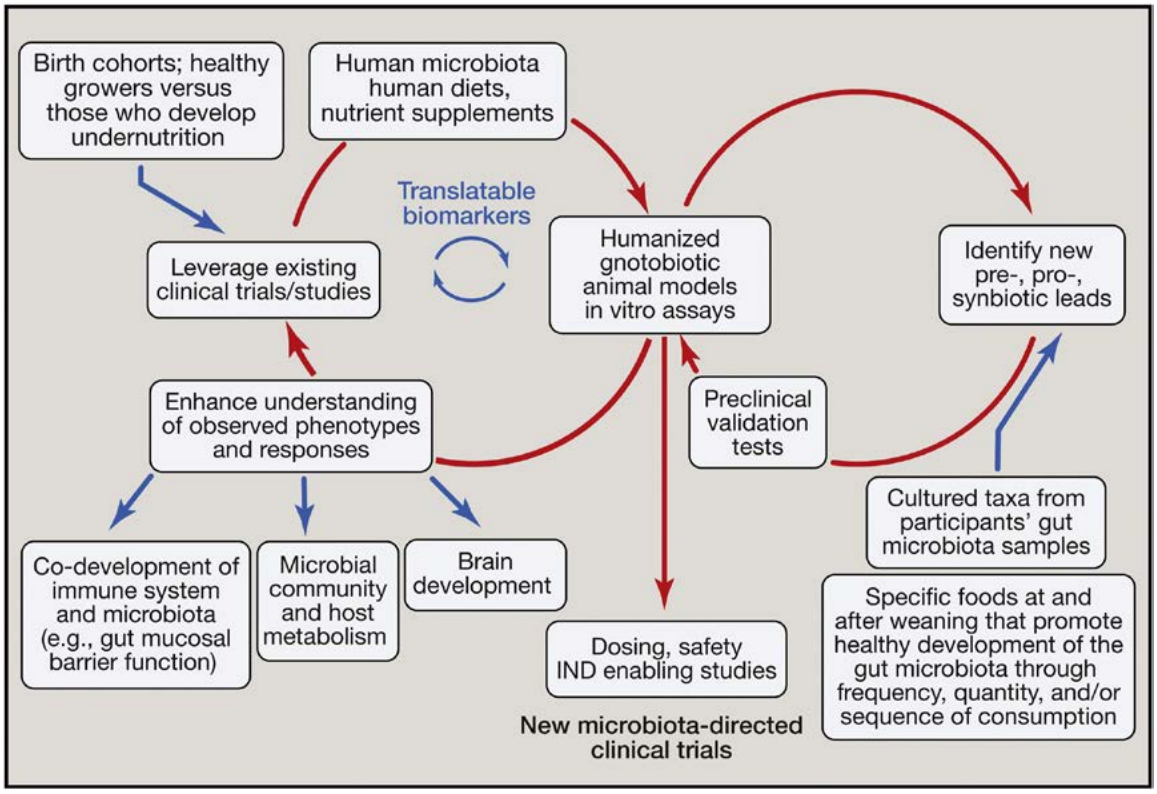
Birth cohorts; healthy growers versus those who develop undernutrition
Human microbiota human diets, nutrient supplements
Translatable biomarkers
Leverage existing clinical trials/studies
Humanized gnotobiotic animal models in vitro assays
Identify new pre-, pro-, synbiotic leads
Enhance understanding of observed phenotypes and responses
Preclinical validation tests
Cultured taxa from participants' gut microbiota samples
Co-development of immune system and microbiota (e.g., gut mucosal barrier function)
Microbial community and host metabolism
Brain development
Dosing, safety IND enabling studies
Specific foods at and after weaning that promote healthy development of the gut microbiota through frequency, quantity, and/or sequence of consumption
New microbiota-directed clinical trials

Figure 3.

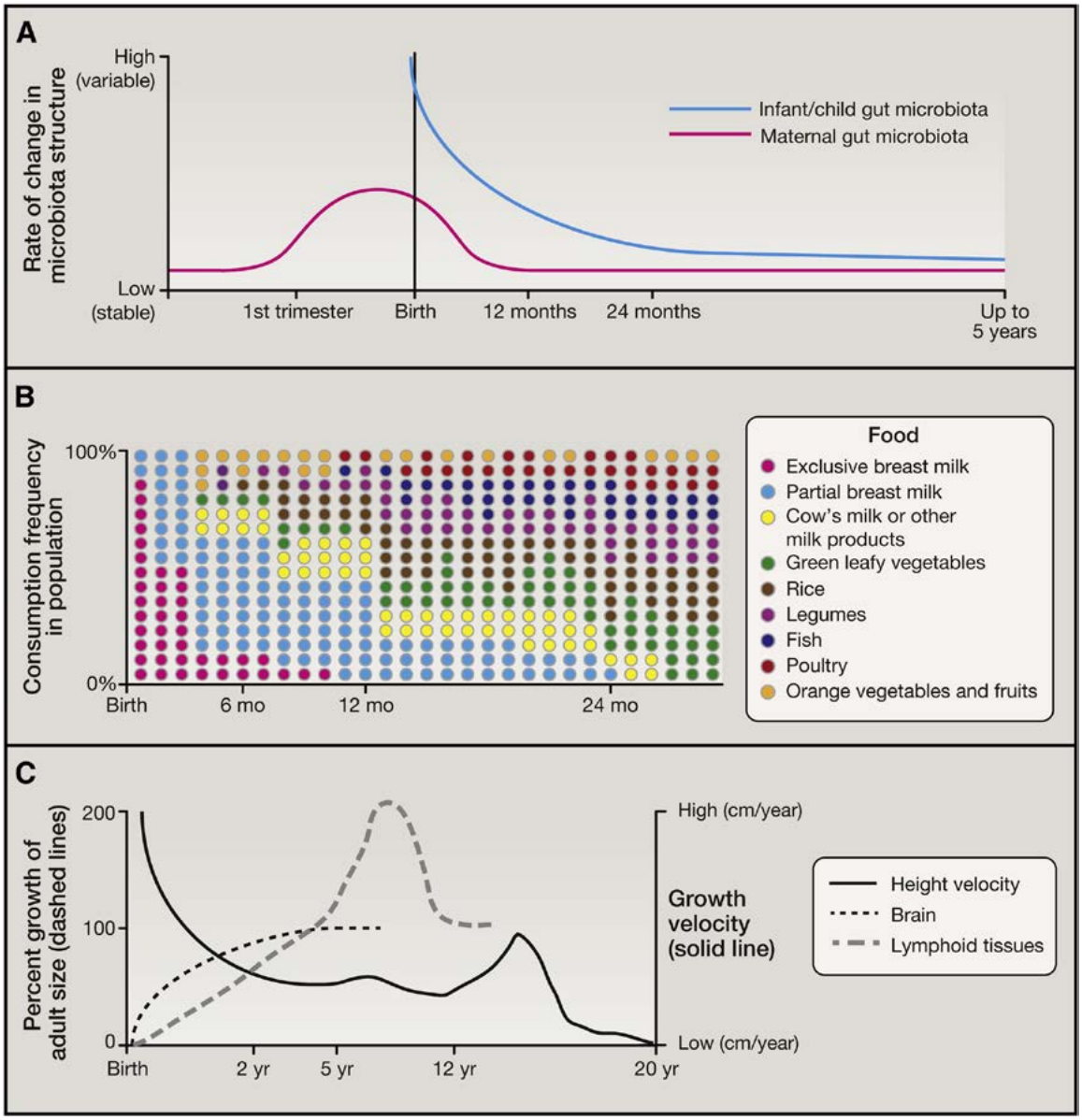
A
Rate of change in microbiota structure
High (variable)
Low (stable)
Infant/child gut microbiota
Maternal gut microbiota
1st trimester
Birth
12 months
24 months
Up to 5 years
B
Consumption frequency in population
100%
0%
Birth
6 mo
12 mo
24 mo
Food
Exclusive breast milk
Partial breast milk
Cow's milk or other milk products
Green leafy vegetables
Rice
Legumes
Fish
Poultry
Orange vegetables and fruits
C
Percent growth of adult size (dashed lines)
200
100
0
Birth
2 yr
5 yr
12 yr
20 yr
High (cm/year)
Growth velocity (solid line)
Low (cm/year)
Height velocity
Brain
Lymphoid tissues

Chapter 2

Persistent gut microbiota immaturity in malnourished Bangladeshi children

Chapter 2

Persistent gut microbiota immaturity in malnourished Bangladeshi children

Sathish Subramanian[1], Sayeeda Huq[2], Tanya Yatsunenko[1], Rashidul Haque[2], Mustafa Mahfuz[2], Mohammed A. Alam[2], Amber Benezra[3], Joseph DeStefano[1], Martin F. Meier[1], Brian D. Muegge[1], Michael J. Barratt[1], Laura G. VanArendonk[1], Qunyuan Zhang[4], Michael A. Province[4], William A. Petri Jr[5], Tahmeed Ahmed[2] & Jeffrey I. Gordon[1]

[1]Center for Genome Sciences and Systems Biology, Washington University in St. Louis, St. Louis, Missouri 63108, USA

[2]Centre for Nutrition and Food Security, International Centre for Diarrhoeal Disease Research, Dhaka 1212, Bangladesh

[3]Department of Anthropology, New School for Social Research, New York, New York 10003, USA

[4]Division of Statistical Genomics, Washington University in St. Louis, St. Louis, Missouri 63108, USA

[5]Departments of Medicine, Microbiology and Pathology, University of Virginia School of Medicine, Charlottesville, Virginia 22908, USA

This chapter corresponds to the complete and accepted version of a manuscript published as:

Subramanian, S. *et al.* Persistent gut microbiota immaturity in malnourished Bangladeshi children. *Nature* **510,** 417–421 (2014).

Abstract

Therapeutic food interventions have reduced mortality in children with severe acute malnutrition (SAM), but incomplete restoration of healthy growth remains a major problem[1,2]. The relationships between the type of nutritional intervention, the gut microbiota, and therapeutic responses are unclear. In the current study, bacterial species whose proportional representation define a healthy gut microbiota as it assembles during the first two postnatal years were identified by applying a machine-learning-based approach to 16S ribosomal RNA data sets generated from monthly faecal samples obtained from birth onwards in a cohort of children living in an urban slum of Dhaka, Bangladesh, who exhibited consistently healthy growth. These age-discriminatory bacterial species were incorporated into a model that computes a 'relative microbiota maturity index' and 'microbiota-for-age Z-score' that compare postnatal assembly (defined here as maturation) of a child's faecal microbiota relative to healthy children of similar chronologic age. The model was applied to twins and triplets (to test for associations of these indices with genetic and environmental factors, including diarrhoea), children with SAM enrolled in a randomized trial of two food interventions, and children with moderate acute malnutrition. Our results indicate that SAM is associated with significant relative microbiota immaturity that is only partially ameliorated following two widely used nutritional interventions. Immaturity is also evident in less severe forms of malnutrition and correlates with anthropometric measurements. Microbiota maturity indices provide a microbial measure of human postnatal development, a way of classifying malnourished states, and a parameter for judging therapeutic efficacy. More prolonged interventions with existing or new therapeutic foods and/or addition of gut microbes may be needed to achieve enduring repair of gut microbiota immaturity in childhood malnutrition and improve clinical outcomes.

Introduction

Severe acute malnutrition and moderate acute malnutrition (MAM) are typically defined by anthropometric measurements: children are classified as having SAM if their weight-for-height *Z*-scores (WHZ)[3] are below three standard deviations (−3 s.d.) from the median of the World Health Organization (WHO) reference growth standards, whereas those with WHZ between −2 and −3 s.d. are categorized as having MAM. SAM and MAM typically develop between 3 and 24 months after birth [4]. A standardized treatment protocol for SAM and its complications has been developed in Bangladesh[1]. The result has been a reduction in mortality rate, although the extent to which this protocol results in long-term restoration of normal growth and development needs to be ascertained through longitudinal studies[5, 6]. There is similar lack of clarity about the long-term efficacy of nutritional interventions for MAM[7, 8].

Food is a major factor that shapes the proportional representation of organisms present in the gut microbial community (microbiota), and its gene content (microbiome). The microbiota and microbiome in turn have an important role in extracting and metabolizing dietary ingredients[9, 10, 11, 12, 13, 14]. To investigate the hypothesis that healthy postnatal development (maturation) of the gut microbiota is perturbed in malnutrition[12], we monitored 50 healthy Bangladeshi children monthly during the first 2 years after birth (25 singletons, 11 twin pairs, 1 set of triplets; 996 faecal samples collected monthly; see Methods and Supplementary Tables 1–3). By identifying bacterial taxa that discriminate the microbiota of healthy children at different chronologic ages, we were able to test our hypothesis by studying 6- to 20-month-old children presenting with SAM, just before, during, and after treatment with two very different types of food intervention, as well as children with MAM. The results provide a different perspective about malnutrition; one involving disruption of a microbial facet of our normal human postnatal development.

Results

Bacterial taxonomic biomarkers for defining gut-microbiota maturation in healthy Bangladeshi children during the first two years of life

To characterize gut microbiota maturation across unrelated healthy Bangladeshi children living in separate households, faecal samples were collected at monthly intervals up to 23.4 ± 0.5 months of age in a training set of 12 children who exhibited consistently healthy anthropometric scores (WHZ, −0.32 ± 0.98 (mean ± s.d.) 22.7 ± 1.5 faecal samples per child; Supplementary Table 4a). The bacterial component of their faecal microbiota samples was characterized by V4-16S rRNA sequencing (Supplementary Table 5) and assigning the resulting reads to operational taxonomic units (OTUs) sharing ≥ 97% nucleotide sequence identity (see Methods; a 97%-identity OTU is commonly construed as representing a species-level taxon). The relative abundances of 1,222 97%-identity OTUs that passed our filtering criterion[15] were regressed against the chronologic age of each child at the time of faecal sample collection using the Random Forests machine learning algorithm[16]. The regression explained 73% of the variance related to chronologic age. The significance of the fit was established by comparing fitted to null models in which age labels of samples were randomly permuted with respect to their 16S rRNA microbiota profiles (P = 0.0001, 9,999 permutations). Ranked lists of all bacterial taxa, in order of 'age-discriminatory importance', were determined by considering those taxa, whose relative abundance values when permuted have a larger marginal increase in mean squared error, to be more important (see Methods). Tenfold cross-validation was used to estimate age-discriminatory performance as a function of the number of top-ranking taxa according to their feature importance scores. Minimal improvement in predictive performance was observed when including taxa beyond the top 24 (see Supplementary Table 6 for the top 60). The 24 most age-discriminatory taxa identified by Random Forests are shown in Fig. 1a in rank order of their contribution to the predictive accuracy of the model and were selected as inputs to a sparse 24-taxon model.

To test the extent to which this sparse model could be applied, we applied it, with no further parameter optimization, to additional monthly faecal samples collected from two other healthy groups of children: 13 singletons (WHZ, −0.4 ± 0.8 (mean ± s.d.)) and 25 children from a birth-cohort study of twins and triplets, (WHZ, −0.5 ± 0.7 (mean ± s.d.)), all born and raised in Mirpur, Bangladesh (Supplementary Table 4b, c). We found that the model could be applied to both groups (r^2 = 0.71 and 0.68, respectively), supporting the consistency of the observed taxonomic signature of microbiota maturation across different healthy children living in this geographic locale (Fig. 1b, c).

Two metrics of microbiota maturation were defined by applying the sparse model to the 13 healthy singletons and 25 members of twin pairs and triplets that had been used for model validation. The first metric, relative microbiota maturity, was calculated as follows:

$$\text{relative microbiota maturity} = \text{microbiota age of child} - \text{microbiota age of healthy children of similar chronologic age}$$

where microbiota age values for healthy children were interpolated across the first two years of life using a spline fit (Fig. 1b). The second metric, microbiota-for-age *Z* score, was calculated as follows:

$$\text{MAZ} = \frac{\text{(microbiota age} - \text{median microbiota age of healthy children of same chronologic age)}}{\text{(s.d. of microbiota age of healthy children of the same chronologic age)}}$$

where MAZ is the microbiota-for-age *Z*-score, and median and s.d. of microbiota age were computed for each month up to 24 months. The MAZ accounts for the variance of predictions of microbiota age as a function of different host age ranges (when considered in discrete monthly bins) (see Extended Data Figure 1 for the calculation of each metric, and Supplementary Notes for discussion of how this approach defines immaturity as a specific recognizable state rather than as a lack of maturity).

To study the influences of genetic and environmental factors on these microbiota maturation indices, we examined their distribution in healthy Bangladeshi twins and triplets. Monozy-

gotic twins were not significantly more correlated in their maturity profiles compared to dizygotic twins, and within the set of triplets, the two monozygotic siblings were not more correlated than their fraternal sibling (monozygotic pairs, 0.1 ± 0.5 (Spearman's Rho ± s.d.); dizygotic pairs, 0.33 ± 0.3; in the e of the triplets, values for the monozygotic pair and fraternal sibling were 0.1; and 0.24 ± 0.3, respectively). Maturity was significantly decreased in faecal samples obtained during and 1 month after diarrhoeal episodes ($P < 0.001$ and $P < 0.01$, respectively) but not beyond that period (Extended Data Figure 2). There was no discernable effect of recent antibiotic usage (1 week before sampling) on relative microbiota maturity, whereas intake of infant formula was associated with significantly higher maturity values (Supplementary Table 7). Family membership explained 29% of the total variance in relative microbiota maturity measurements (log-likelihood ratio = 102.1, $P < 0.0001$; linear mixed model) (see Supplementary Notes, Supplementary Tables 8 and 9, and Extended Data Figure 3 for analyses of faecal microbiota variation in mother–infant dyads and fathers).

Persistent immaturity of the gut microbiota in children with SAM

To investigate the effects of SAM on microbiota maturity, 64 children with SAM who had been admitted to the Nutritional Rehabilitation Unit of the International Centre for Diarrhoeal Disease Research, Bangladesh (ICDDR,B), Dhaka Hospital, were enrolled in a study to investigate the configuration of their faecal microbiota before, during and after treatment with either an imported, internationally used ready-to-use therapeutic food (RUTF; Plumpy'Nut) or a locally produced, lower-cost nutritional food combination (Khichuri–Halwa). Children ranged in age from 6 to 20 months of age at the time of enrollment and were randomly assigned to either of the treatment arms. At enrollment, WHZ averaged −4.2 ± 0.7 (mean ± s.d.) (see Supplementary Tables 10–12 for patient metadata and Fig. 2a for study design). In the initial 'acute phase' of treatment, infection control was achieved with parenteral administration of ampicillin and gentamicin for 2 and 7 days, respectively, and oral amoxicillin for 5 days (from days 3 to 7 of the antibiotic treatment protocol). Children with SAM were initially stabilized by being fed the milk-based gruel, 'suji', followed

by randomization to either an imported peanut-based RUTF intervention or an intervention with locally produced, rice-and-lentil-based therapeutic foods (Khichuri and Halwa; see Methods and Supplementary Table 13 for compositions of all foods used during nutritional rehabilitation). During this second 'nutritional rehabilitation phase' (1.3 ± 0.7 weeks long) children received 150–250 kcal kg^{-1} body weight per day of RUTF or Khichuri–Halwa (3–5 g protein kg^{-1} per day), plus micronutrients including iron. Children were discharged from the hospital after the completion of this second phase; during the 'post-intervention phase', periodic follow-up examinations were performed to monitor health status. Faecal samples were obtained during the acute phase before treatment with Khichuri–Halwa or RUTF, then every 3 days during the nutritional rehabilitation phase, and monthly thereafter during the post-intervention follow-up period.

There was no significant difference in the rate of weight gain between the RUTF and Khichuri–Halwa groups (10.9 ± 4.6 versus 10.4 ± 5.4 g kg^{-1} body weight per day (mean ± s.d.); Student's *t*-test, $P = 0.7$). The mean WHZ at the completion of nutritional rehabilitation was significantly improved in both treatment groups (−3.1 ± 0.7 (mean ± s.d.) RUTF, $P < 0.001$; and −2.7 ± 1.6 Khichuri–Halwa, $P < 0.0001$), but not significantly different between groups ($P = 0.15$). During follow-up, WHZ remained significantly lower compared to healthy children (−2.1 ± 1.2, Khichuri–Halwa; −2.4 ± 0.8 RUTF versus −0.5 ± 1.1 for healthy, $P < 0.0001$; Extended Data Figure 4a). Children in both treatment arms also remained markedly below normal height and severely underweight throughout the follow-up period (Extended Data Figure 4b, c).

The Random Forests model derived from healthy children was used to define relative microbiota maturity for children with SAM at the time of enrollment, during treatment, at the end of either nutritional intervention, and during the months of follow-up. The results revealed that compared to healthy children, children with SAM had significant microbiota immaturity at the time that nutritional rehabilitation was initiated and at cessation of treatment (Dunnett's post-hoc test, $P < 0.0001$ for both groups; Fig. 2b). Within 1 month of follow-up, both groups had improved significantly. However, improvement in this metric was short-lived for the RUTF and Khichuri–Halwa groups, with regression to significant immaturity relative to healthy children beyond 4 months

after treatment was stopped (Fig. 2b and Supplementary Table 14). MAZ, like relative microbiota maturity, indicated a transient improvement after RUTF intervention that was not durable beyond 4 months. In the Khichuri–Halwa group, relative microbiota maturity and MAZ improved following treatment, but subsequently regressed, exhibiting significant differences relative to healthy children at 2–3 months, and >4 months after cessation of treatment (Fig. 2b and Supplementary Table 14).

Both food interventions had non-durable effects on other microbiota parameters. The reduced bacterial diversity associated with SAM persisted after Khichuri–Halwa and only transiently improved with RUTF (Extended Data Figure 5 and Supplementary Table 14). We identified a total of 220 bacterial taxa that were significantly different in their proportional representation in the faecal microbiota of children with SAM compared to healthy children; 165 of these 220 97%-identity OTUs were significantly diminished in the microbiota of children with SAM during the longer term follow-up period in both treatment groups (Extended Data Figs 6 and 7, and Supplementary Table 15).

Although the majority of children in both treatment arms of the SAM study were unable to provide faecal samples before the initiation of antibiotic treatment due to the severity of their illness, a subset of nine children each provided one or two faecal samples (n = 12) before administration of parenteral ampicillin and gentamicin, and oral amoxicillin. Microbiota immaturity was manifest at this early time-point before antibiotics in these nine children (relative microbiota maturity: -5.15 ± 0.9 months versus -0.03 ± 0.1 for the 38 reference healthy controls; Mann–Whitney, $P < 0.0001$). Sampling these nine children after treatment with parenteral and oral antibiotics but before initiation of RUTF or Khichuri–Halwa (6 ± 3.6 days after hospital admission) showed that there was no significant effect on microbiota maturity (Wilcoxon matched-pairs rank test, $P = 1$). When pre-antibiotic faecal samples from these nine children were compared to samples collected at the end of all treatment interventions (dietary and antibiotic, 20 ± 9 days after admission), no significant differences in relative microbiota maturity (Wilcoxon, $P = 0.7$), MAZ, bacterial diversity (or WHZ) were found (Extended Data Figure 8a–d). This is not to say that these interventions were

without effects on overall community composition: opposing changes in the relative abundance of Streptococcaceae and Enterobacteriaceae were readily apparent (Extended Data Figure 8e, f; note that the Random Forests model classified both the microbiota of children with SAM sampled before and at the conclusion of all treatment interventions as immature, indicating lack of a generic immature state). Although these findings indicate that the relative microbiota immaturity associated with SAM was not solely attributable to the antibiotics used to treat these children, we could not, in cases where children were unable to provide pre-intervention faecal samples, measure the effects of other antibiotics, consumed singly or in various combinations during the acute infection control and nutritional rehabilitation phases, on their metrics of microbiota maturation (see Supplementary Notes and Supplementary Table 16 for further evidence indicating antibiotic use in the follow-up period did not correlate with the persistence of microbiota immaturity in children with SAM).

SAM affects approximately 4% of children in developing countries. MAM is more prevalent, particularly in South Central Asia, where it affects approximately 19% (30 million children)[7]. Epidemiological studies indicate that periods of MAM are associated with progression to SAM, and with stunting which affects >40% of children under the age of five in Bangladesh[17]. Therefore, we extended our study to children from the singleton cohort at 18 months of age, when all had transitioned to solid foods (n = 10 children with WHZ lower than −2 s.d., the threshold for MAM; 23 children with healthy WHZ; Supplementary Table 17). The relationship between relative microbiota maturity, MAZ and WHZ was significant (Spearman's Rho = 0.62 and 0.63, $P < 0.001$, respectively; Extended Data Figure 9a, b). Comparing children with MAM to those defined as healthy revealed significantly lower relative microbiota maturity, MAZ and differences in the relative abundances of age-discriminatory taxa in the malnourished group (Extended Data Figs 9d–l and 10a, b). These results suggest that microbiota immaturity may be an additional pathophysiological component of moderately malnourished states.

Discussion

In conclusion, definition of microbiota maturity using bacterial taxonomic biomarkers that are highly discriminatory for age in healthy children has provided a way to characterize malnourished states, including whether responses to food interventions endure for prolonged periods of time beyond the immediate period of treatment. RUTF and Khichuri–Halwa produced improvements in microbiota maturity indices that were not sustained. Addressing the question of how to achieve durable responses in children with varying degrees of malnutrition may involve extending the period of administration of existing or new types of food interventions[7]. One testable hypothesis is that a population's microbiota conditioned for generations on a diet will respond more favourably to nutrient supplementation based on food groups represented in that diet. Next-generation probiotics using gut-derived taxa may also be required in addition to food-based interventions. The functional roles (niches) of the age-discriminatory taxa identified by our Random Forests model need to be clarified since they themselves may be therapeutic candidates and/or form the basis for low cost field-based diagnostic assessments.

Systematic analyses of microbiota maturation in different healthy and malnourished populations living in different locales, representing different lifestyles and cultural traditions[11, 18], may yield a taxonomy-based model that is generally applicable to many countries and types of diagnostic and therapeutic assessments. Alternatively, these analyses may demonstrate a need for geographic specificity when constructing such models (and diagnostic tests or therapeutic regimens). Two observations are notable in this regard. First, expansion of our sparse model from 24 to 60 taxa yielded similar results regarding the effects of diarrhoea in healthy individuals, MAM and SAM (and its treatment with RUTF and Khichuri–Halwa) on microbiota maturity (see Supplementary Notes). Second, we applied the model that we used for Bangladeshi children to healthy children in another population at high risk for malnutrition. The results show that the model generalizes (r^2 = 0.6) to a cohort of 47 Malawian twins and triplets, aged 0.4–25.1 months, who were concordant for healthy status in a previous study[11] (WHZ, −0.23 ± 0.97 (mean ± s.d.); Supplementary Table 18). Age-discriminatory taxa identified in healthy Bangladeshi children show similar age-dependent

changes in their representation in the microbiota of healthy Malawian children, as assessed by the Spearman rank correlation metric (Extended Data Figure 10c, d).

The question of whether microbiota immaturity associated with SAM and MAM is maintained during and beyond childhood also underscores the need to determine the physiologic, metabolic and immunologic consequences of this immaturity, and how they might contribute to the associated morbidities and sequelae of malnutrition, including increased risk for diarrhoeal disease, stunting, impaired vaccine responses, and cognitive abnormalities[2, 19]. Our study raises a testable hypothesis: namely, that assessments of microbiota maturation, including in the context of the maternal–infant dyad, will provide a more comprehensive view of normal human development and of developmental disorders, and generate new directions for preventive medicine. Testing this hypothesis will require many additional clinical studies but answers may also arise from analyses of gut microbiota samples that have already been stored from previous studies.

Methods

Singleton birth cohort

Full details of the design of this now-complete birth cohort study have been described previously[21]. Faecal microbiota samples were profiled from 25 children who had consistently healthy anthropometric measures based on quarterly (every three months) measurements (Supplementary Table 1). The WHZ threshold used for 'healthy' (on average above −2 s.d.) was based on median weight and height measurements obtained from age- and gender-matched infants and children by the Multi-Centre Growth Reference study of the World Health Organization[3]. Clinical parameters, including diarrhoeal episodes and antibiotic consumption associated with each of their faecal samples are provided in Supplementary Table 2.

A second group studied from this singleton cohort consisted of 33 children sampled cross-sectionally at 18 months, including those who were incorporated as healthy reference controls, and those with a WHZ < −2 who were classified with MAM (Supplementary Table 17).

Twins and triplets birth cohort

Mothers with multiple pregnancy, identified by routine clinical and sonographic assessment at the Radda Maternal Child Health and Family Planning (MCH-FP) Clinic in Dhaka, were enrolled in a prospective longitudinal study (n = 11 mothers with twins, 1 mother with triplets). The zygosity of twin pairs and triplets was determined using plasma DNA and a panel of 96 polymorphic single-nucleotide polymorphisms (SNPs) (Center for Inherited Disease Research, Johns Hopkins University). Four twin pairs were monozygotic, six were dizygotic, and the set of triplets consisted of a monozygotic pair plus one fraternal sibling (Supplementary Table 1; note that one of the 11 twin pairs could not be tested for zygosity because plasma samples were not available). Information about samples from healthy twins, triplets and their parents, including clinical parameters associated with each faecal sample, is provided in Supplementary Tables 2 and 3.

The three healthy Bangladeshi groups used for model training and validation had the following WHZ scores: -0.32 ± 1 (mean ± s.d.; 12 singletons randomized to the training set), -0.44 ± 0.8 (13 singletons randomized to one of the two validation sets), and -0.46 ± 0.7 (twins and triplets in the other validation set) (Supplementary Table 4). The average number of diarrhoeal episodes in the singleton training set, the singleton validation set, and the twin and triplet validation set (4, 4.6 and 1.7, respectively) was comparable to values reported in previous surveys of another cohort of 0–2-year-old Bangladeshi children (4.25 per child per year)[22].

There were no significant differences in the number of diarrheal episodes per year per child and the number of diarrhoeal days per year per child between the singleton training and validation sets (Student's t-test, P = 0.5). Moreover, across all training and validation sets, neither of these diarrheal parameters correlated with mean age-adjusted Shannon diversity indices (Spearman's Rho, −0.18 and −0.12, P = 0.22 and 0.4, respectively). The fraction of faecal samples collected from each child where oral antibiotics had been consumed within the prior 7 days was not significantly different between the training and two validation sets (one-way ANOVA, P = 0.14; see Supplementary Table 4).

Severe acute malnutrition study

Sixty-four children in the Nutritional Rehabilitation Unit of ICDDR,B, Dhaka Hospital suffering from SAM (defined as having a WHZ less than −3 s.d. and/or bilateral pedal oedema) were enrolled in a randomized interventional trial to compare an imported peanut-based RUTF, Plumpy'Nut (Nutriset Plumpyfield, India) and locally produced Khichuri–Halwa (clinical trial NCT01331044). Initially, children were stabilized by rehydration and feeding 'suji', which contains whole bovine milk powder, rice powder, sugar and soybean oil (approximately 100 kcal kg^{-1} body weight per day, including 1.5 g protein kg^{-1} per day). Children were then randomized to the Khichuri–Halwa or RUTF groups. Khichuri consists of rice, lentils, green leafy vegetables and soybean oil; Halwa consists of wheat flour (atta), lentils, molasses and soybean oil. Children randomized to the Khichuri–Halwa treatment arm also received milk suji '100' during their nutritional rehabilitation phase (a form of suji with a higher contribution of calories from milk powder compared to suji provided during the acute phase). RUTF is a ready-to-use paste that does not need to be mixed with water; it consists of peanut paste mixed with dried skimmed milk, vitamins and minerals (energy density, 5.4 kcal g^{-1}). Khichuri and Halwa are less energy-dense than RUTF (1.45 kcal g^{-1} and 2.4 kcal g^{-1}, respectively, see Supplementary Table 13 for a list of ingredients for all foods used during nutritional rehabilitation).

The primary outcome measurement, rate of weight gain (g kg^{-1} per day), along with improvement in WHZ after nutritional rehabilitation are reported by child in Supplementary Table 10. Faecal samples were collected before randomization to the RUTF and Khichuri–Halwa treatment arms, every 3 days during nutritional rehabilitation and once a month during the follow-up period (information associated with each faecal sample is provided in Supplementary Table 11).

Anthropologic study

To obtain additional information about household practices in the Mirpur slum of Dhaka, in-depth semi-structured interviews and observations were conducted over the course of 1 month in nine households (n = 30 individuals). This survey, approved by the Washington University and

ICDDR,B IRBs, involved three ICDDR,B field research assistants, and three senior scientific staff in the ICDDR,B Centre for Nutrition and Food Security, plus two anthropologists affiliated with Washington University in St. Louis. Parameters that might affect interpretation of metagenomic analyses of gut microbial-community structure were noted, including information about daily food preparation, food storage, personal hygiene and childcare practices.

Characterization of the bacterial component of the gut microbiota by V4-16S rRNA sequencing

Faecal samples were frozen at −20 °C within 30 min of their collection and subsequently stored at −80 °C before extraction of DNA. DNA was isolated by bead-beating in phenol and chloroform, purified further (QIAquick column), quantified (Qubit) and subjected to polymerase chain reaction (PCR) using primers directed at variable region 4 (V4) of bacterial 16S rRNA genes. Bacterial V4-16S rRNA data sets were generated by multiplex sequencing of amplicons prepared from 1,897 faecal DNA samples (26,580±26,312 (mean±s.d.) reads per sample, paired-end 162- or 250-nucleotide reads; Illumina MiSeq platform; Supplementary Table 5). Reads of 250 nucleotides in length were trimmed to 162 nucleotides, then all reads were processed using previously described custom scripts, and overlapped to 253-nucleotide fragments spanning the entire V4 amplicon[15]. 'Mock' communities, consisting of mixtures of DNAs isolated from 48 sequenced bacterial members of the human gut microbiota combined in one equivalent and two intentionally varied combinations, were included as internal controls in the Illumina MiSeq runs. Data from the mock communities were used for diversity and precision-sensitivity analyses employing methods described previously[15, 23].

Reads with≥97% nucleotide sequence identity (97%-identity) across all studies were binned into operational taxonomic units (OTUs) using QIIME (v 1.5.0), and matched to entries in the Greengenes reference database (version 4feb2011)[24, 25]. Reads that did not map to the Greengenes database were clustered *de novo* with UCLUST at 97%-identity and retained in further analysis. A total of 1,222 97%-identity OTUs were found to be present at or above a level of confident

detection (0.1% relative abundance) in at least two faecal samples from all studies. Taxonomy was assigned based on the naive Bayesian RDP classifier version 2.4 using 0.8 as the minimum confidence threshold for assigning a level of taxonomic classification to each 97%-identity OTU. Raw V4-16S rRNA data sets before trimming, processing and abundance-filtering steps are available at http://www.ebi.ac.uk/ena/data/view/PRJEB5482.

Definition of gut-microbiota maturation in healthy children using Random Forests

Random Forests regression was used to regress relative abundances of OTUs in the time-series profiling of the microbiota of healthy singletons against their chronologic age using default parameters of the R implementation of the algorithm (R package 'randomForest', ntree = 10,000, using default mtry of p/3 where p is the number of input 97%-identity OTUs (features))[26]. The Random Forests algorithm, due to its non-parametric assumptions, was applied and used to detect both linear and nonlinear relationships between OTUs and chronologic age, thereby identifying taxa that discriminate different periods of postnatal life in healthy children. A rarefied OTU table at 2,000 sequences per sample served as input data. Ranked lists of taxa in order of Random Forests reported 'feature importance' were determined over 100 iterations of the algorithm. To estimate the minimal number of top ranking age-discriminatory taxa required for prediction, the rfcv function implemented in the 'randomForest' package was applied over 100 iterations. A sparse model consisting of the top 24 taxa was then trained on the training set of 12 healthy singletons (272 faecal samples). Without any further parameter optimization, this model was validated in other healthy children (13 singletons, 25 twins and triplets) and then applied to samples from children with SAM and MAM. A smoothing spline function was fit between microbiota age and chronologic age of the host (at the time of faecal sample collection) for healthy children in the validation sets to which the sparse model was applied.

Alpha diversity comparisons

Estimates of within-sample diversity were made at a rarefaction depth of 2,000 reads per sample. A linear regression was fit between the Shannon diversity index (SDI) and postnatal age in the 50 healthy children using a mixed model (see the additional details regarding statistical methods, below). An estimate of the coefficient for the slope of SDI with age and intercept was extracted, residuals of this regression were defined as a ΔSDI metric, and associations of this metric with clinical parameters were tested in the cohort of healthy twins and triplets. To test for differences in SDI as a function of health status and chronologic age in malnourished children, we compared the distribution of age-adjusted ΔSDIs in children with SAM between treatment phases.

Detection of associations of bacterial taxa with nutritional status and other parameters

Relative abundances of 97%-identity OTUs were used in linear mixed models as response variables to test for associations with clinical metadata as predictors. For each comparison, we restricted our analysis to 97%-identity OTUs and bacterial families whose relative abundance values reached a level of confident detection (0.1%) in a minimum of 1% of samples in each comparison. Pseudocounts of 1 were added to 97%-identity OTUs to account for variable depth of sequencing between samples, and relative abundances were arcsin-square-root-transformed to approximate homoscedasticity when applying linear models. *P* values of associations of factors with the relative abundance of bacterial taxa were computed using ANOVA type III (tests of fixed effects), subjected to Benjamini–Hochberg false discovery rate (FDR) correction.

Enteropathogen testing

Clinical microscopy was performed for all faecal samples collected at monthly intervals from the singleton birth cohort and from healthy twins and triplets, and screened for *Entamoeba histolytica*, *Entamoeba dispar, Escherichia coli*, *Blastocystis hominis*, *Trichomonas hominis*, *Blastocystis hominis*, Coccidian-like bodies, *Giardia lamblia*, *Ascaris lumbricoides*, *Trichuris Tricuria*, *Ancylostoma duodenale/Necator americanus*, *Hymenolepsis nana*, *Endolimax nana*, *Iodamoeba*

butschlii and *Chilomastix mesnili.* The effects of enteropathogens, detected by microscopy on relative microbiota maturity, MAZ and SDI were included in our analysis of multiple environmental factors in Extended Data Figure 2 and Supplementary Table 7. In cases in which children presented with SAM plus diarrhoea, faecal samples collected before nutritional rehabilitation were cultured for *Vibrio cholerae*, *Shigella flexneri*, *Shigella boydi*, *Shigella sonnei*, *Salmonella enterica*, *Aeromonas hydrophila* and *Hafnia alvae*. See Supplementary Tables 10 and 19 for results of enteropathogen testing.

Additional details regarding statistical methods

Linear mixed models were applied to test for associations of microbiota metrics (relative microbiota maturity, MAZ and SDI) with genetic and environmental factors in twins and triplets. Log-likelihood ratio tests and *F* tests were used to perform backward elimination of non-significant random and fixed effects[27]. Relative microbiota maturity, MAZ and SDI were defined at different phases of treatment and at defined periods of follow-up (<1 month, 1–2, 3–4 and >4 months after completion of the RUTF or Khichuri–Halwa nutritional intervention) in children with SAM relative to healthy children. 'Treatment phase' was specified as a categorical multi-level factor in a univariate mixed model with random by-child intercepts. Dunnett's post-hoc comparison procedure was performed to compare each treatment phase relative to healthy controls and relative to samples collected at enrollment in each food intervention group.

References

1. Ahmed, T. *et al*. Mortality in severely malnourished children with diarrhoea and use of a standardised management protocol. *Lancet* **353**, 1919–1922 (1999)

2. Ashraf, H. *et al*. A follow-up experience of 6 months after treatment of children with severe acute malnutrition in Dhaka, Bangladesh. *J. Trop. Pediatr.* **58**, 253–257 (2012)

3. World Health Organization Department of Nutrition for Health and Development WHO child growth standards growth velocity based on weight, length and head circumference: methods and development. (World Health Organization, 2009)

4. Victora, C. G., de Onis, M., Hallal, P. C., Blössner, M. & Shrimpton, R. Worldwide timing of growth faltering: revisiting implications for interventions. *Pediatrics* **125**, e473–e480 (2010)

5. Ahmed, T. & Begum, B. Badiuzzaman, Ali, M. & Fuchs, G. Management of severe malnutrition and diarrhea. *Indian J. Pediatr.* **68**, 45–51 (2001)

6. Ahmed, T. *et al*. P0580 Use of a standardized protocol based on local diet results in satisfactory rates of weight gain of severely malnourished children undergoing nutritional rehabilitation. *J. Pediatr. Gastroenterol. Nutr.* **39**, S277 (2004)

7. Lazzerini, M., Rubert, L. & Pani, P. Specially formulated foods for treating children with moderate acute malnutrition in low- and middle-income countries. *Cochrane Database Syst. Rev.* CD009584 (2013)

8. Prentice, A. M. *et al*. Critical windows for nutritional interventions against stunting. *Am. J. Clin. Nutr.* **97**, 911–918 (2013)

9. Muegge, B. D. *et al*. Diet drives convergence in gut microbiome functions across mammalian phylogeny and within humans. *Science* **332**, 970–974 (2011)

10. Wu, G. D. *et al*. Linking long-term dietary patterns with gut microbial enterotypes. *Science* **334**, 105–108 (2011)

11. Yatsunenko, T. *et al*. Human gut microbiome viewed across age and geography. *Nature* **486**, 222–227 (2012)

12. Smith, M. I. *et al*. Gut microbiomes of Malawian twin pairs discordant for kwashiorkor. *Science* **339**, 548–554 (2013)

13. David, L. A. *et al*. Diet rapidly and reproducibly alters the human gut microbiome. *Nature* **505**, 559–563 (2014)

14. Tang, W. H. W. *et al*. Intestinal microbial metabolism of phosphatidylcholine and cardiovascular risk. *N. Engl. J. Med.* **368**, 1575–1584 (2013)

15. Faith, J. J. *et al*. The long-term stability of the human gut microbiota. *Science* **341**, (2013)

16. Breiman, L. Random Forests. *Mach. Learn.* **45**, 5–32 (2001)

17. Dewey, K. G. *et al*. Infant weight-for-length is positively associated with subsequent linear growth across four different populations. *Matern. Child Nutr.* **1**, 11–20 (2005)

18. Lin, A. *et al*. Distinct distal gut microbiome diversity and composition in healthy children from Bangladesh and the United States. *PLoS ONE* **8**, e53838 (2013)

19. Nahar, B. *et al*. Effects of a community-based approach of food and psychosocial stimulation on growth and development of severely malnourished children in Bangladesh: a randomised trial. *Eur. J. Clin. Nutr.* **66**, 701–709 (2012)

20. Bates, D., Maechler, M. & Bolker, B. lme4: Linear mixed-effects models using S4 classes. http://CRAN.R-project.org/package=lme4 (2011)

21. Mondal, D. *et al*. Contribution of enteric infection, altered intestinal barrier function, and maternal malnutrition to infant malnutrition in Bangladesh. *Clin. Infect. Dis.* **54**, 185–192 (2012)

22. Pathela, P. *et al*. Diarrheal illness in a cohort of children 0-2 years of age in rural Bangladesh: I. Incidence and risk factors. *Acta Paediatr.* **95**, 430–437 (2006)

23. Bokulich, N. A. *et al*. Quality-filtering vastly improves diversity estimates from Illumina amplicon sequencing. *Nature Meth*. **10**, 57–59 (2013)

24. Caparaso, J. G. *et al*. QIIME allows analysis of high-throughput community sequencing data. *Nature Meth*. **7**, 335–336 (2010)

25. McDonald, D. *et al*. An improved Greengenes taxonomy with explicit ranks for ecological and evolutionary analyses of bacteria and archaea. *ISME J*. **6**, 610–618 (2012)

26. Liaw, A. & Weiner, M. Classification and regression by randomForest. R package version 4.6-7. *R News* **2**, 18–22 (2002)

27. Kuznetsova, A., Brockhoff, P. B. & Christensen, R. H. B. lmerTest: tests for random and fixed effects for linear mixed effect models (lmer objects of lme4 package). http://CRAN.R-project.org/package=lmerTest (2013)

28. National Institute of Population Research and Training (NIPORT), Mitra and Associates, and ICF International. Bangladesh Demographic and Health Survey 2011. Dhaka, Bangladesh and Calverton, Maryland, USA: NIPORT, Mitra and Associates, and ICF International (2013)

Acknowledgements

We thank the parents and children from Dhaka, Bangladesh for their participation in this study, J. Hoisington-López and S. Deng for technical assistance, and N. Griffin, A. Kau, N. Dey and J. Faith for suggestions during the course of this work. This work was supported by the Bill & Melinda Gates Foundation. The clinical component of the SAM study was funded by the International Atomic Energy Agency. The birth cohort study of singletons was supported in part by the NIH (AI043596). S.S. is a member of the Washington University Medical Scientist Training Program. A.B. is the recipient of an SBE Doctoral Dissertation Research Improvement Grant (NSF Award no. SES-1027035).

Author Contributions S.S. and J.I.G. designed the metagenomic study, S.H, T.A, R.H, M.A.A, M.M, W.A.P. designed and implemented the clinical monitoring and sampling for the SAM trial, participated in patient recruitment, sample collection, sample preservation and/or clinical evaluations; S.S. generated the 16S rRNA data with assistance from M.F.M. and B.D.M.; A.B and J.D performed the anthropology study; S.S., T.Y., Q.Z, L.G.V-A., M.J.B, M.A.P, and J.I.G. analyzed the data; S.S. and J.I.G. wrote the paper.

Author Information 16S rRNA sequences, generated from fecal samples in raw format prior to post-processing and data analysis, have been deposited at the European Nucleotide Archive (Study accession number PRJEB5482). Reprints and permissions information are available at www.nature.com/reprints. Correspondence and requests for materials should be addressed to J.I.G (jgordon@wustl.edu).

Figure Legends

Figure 1: Bacterial taxonomic biomarkers for defining gut microbiota maturation in healthy Bangladeshi children during the first two years of life. a, Twenty-four age-discriminatory bacterial taxa were identified by applying Random Forests regression of their relative abundances in faecal samples against chronologic age in 12 healthy children (n = 272 faecal samples). Shown are 97%-identity OTUs with their deepest level of confident taxonomic annotation (also see Supplementary Table 6), ranked in descending order of their importance to the accuracy of the model. Importance was determined based on the percentage increase in mean-squared error of microbiota age prediction when the relative abundance values of each taxon were randomly permuted (mean importance ± s.d., n = 100 replicates). The insert shows tenfold cross-validation error as a function of the number of input 97%-identity OTUs used to regress against the chronologic age of children in the training set, in order of variable importance (blue line). **b**, Microbiota age predictions in a birth cohort of healthy singletons used to train the 24 bacterial taxa model (brown, each circle represents an individual faecal sample). The trained model was subsequently applied to two sets of healthy children: 13 singletons set aside for model testing (green circles, n = 276 faecal samples) and another birth cohort of 25 twins and triplets (blue circles, n = 448 faecal samples). The curve is a smoothed spline fit between microbiota age and chronologic age in the validation sets (right two panels of **b**), accounting for the observed sigmoidal relationship (see Methods). **c**, Heatmap of mean relative abundances of the 24 age-predictive bacterial taxa plotted against the chronologic age of healthy singletons used to train the Random Forests model, and correspondingly in the healthy singletons, and twins and triplets used to validate the model (hierarchical clustering performed using the Spearman rank correlation distance metric).

Figure 2: Persistent immaturity of the gut microbiota in children with SAM.

a, Design of the randomized interventional trial. **b**, Microbiota maturity defined during various phases of treatment and follow-up in children with SAM. Relative microbiota maturity in the upper portion of the panel is based on the difference between calculated microbiota age (Random-

Forests-based sparse 24-taxon model) and values calculated in healthy children of similar chronologic age, as interpolated over the first 2 years of life using a spline curve. In the lower portion of the panel, maturity is expressed as a microbiota-for-age *Z*-score (MAZ). Mean values ± s.e.m. are plotted. The significance of differences between microbiota indices at various stages of the clinical trial is indicated relative to healthy controls (arrows above the bars) and versus samples collected at enrollment for each intervention group (arrows below the bars) (post-hoc Dunnett's multiple comparison procedure of linear mixed models; $*P<0.05$, $**P<0.01$, $***P<0.001$). Healthy children not used to train the Random Forests model served as healthy controls ($n = 38$). **c–f**, Plot of microbiota age for each child with SAM at enrollment (**c**), at the conclusion of the food intervention phase (**d**), and within (**e**) and beyond (**f**) 3 months of follow-up. The curve shown in each panel was fit using predictions in healthy children: this curve is the same as that replicated across each plot in Fig. 1b.

Figures

Figure 1.

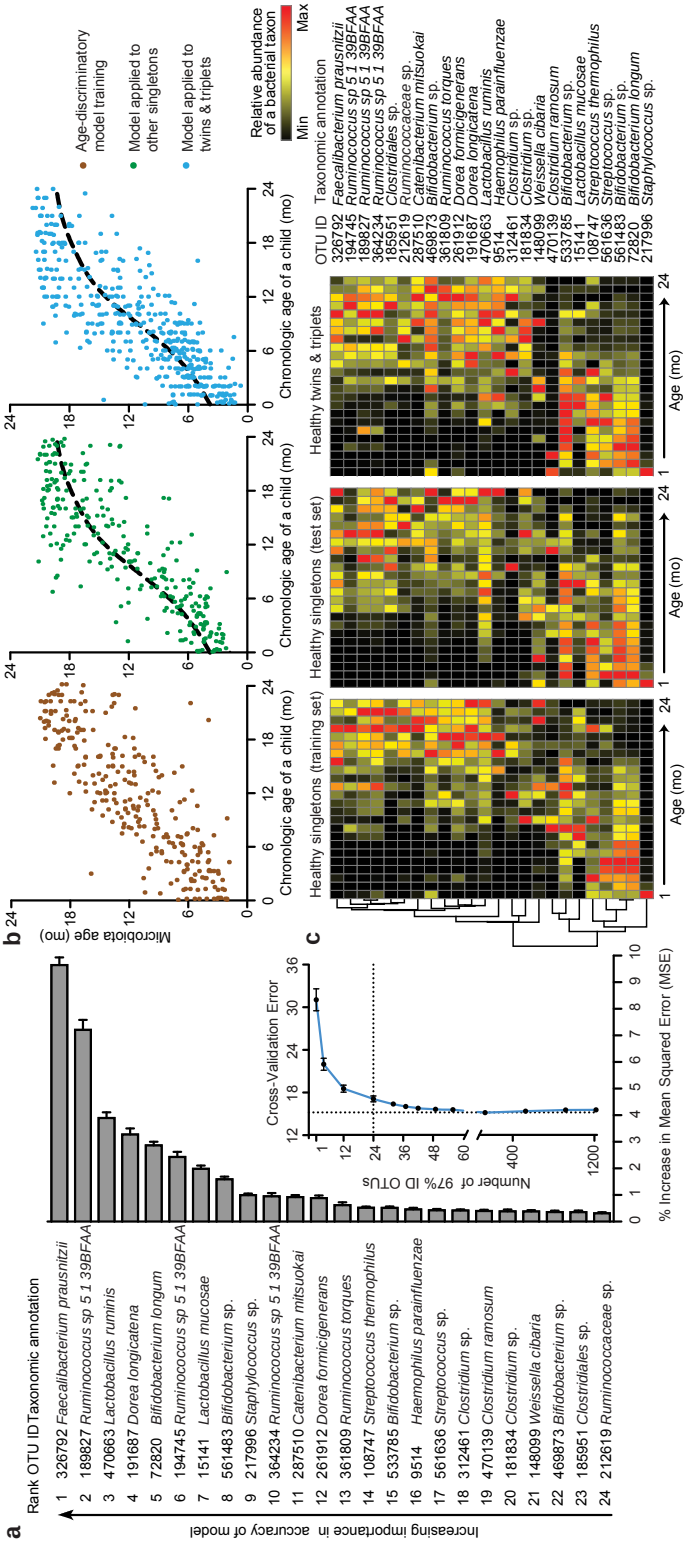

Figure 2.

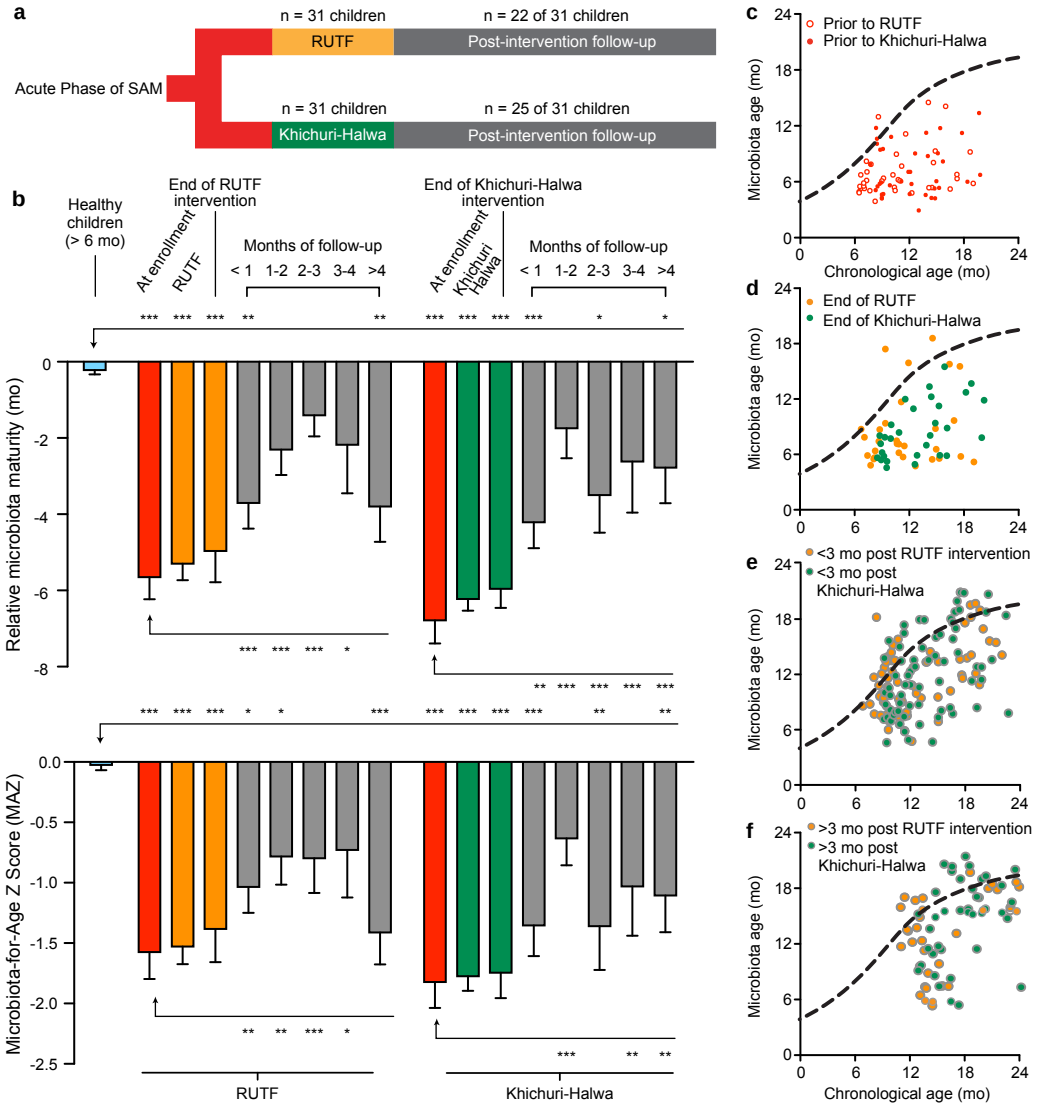
a
n = 31 children
RUTF
n = 22 of 31 children
Post-intervention follow-up
Acute Phase of SAM
n = 31 children
Khichuri-Halwa
n = 25 of 31 children
Post-intervention follow-up
b
Healthy children (> 6 mo)
At enrollment
End of RUTF intervention
RUTF
Months of follow-up
< 1 1-2 2-3 3-4 >4
At enrollment
End of Khichuri-Halwa intervention
Khichuri Halwa
Months of follow-up
< 1 1-2 2-3 3-4 >4
Relative microbiota maturity (mo)
Microbiota-for-Age Z Score (MAZ)
RUTF
Khichuri-Halwa
c
Prior to RUTF
Prior to Khichuri-Halwa
Microbiota age (mo)
Chronological age (mo)
d
End of RUTF
End of Khichuri-Halwa
e
<3 mo post RUTF intervention
<3 mo post Khichuri-Halwa
f
>3 mo post RUTF intervention
>3 mo post Khichuri-Halwa

Supplementary Materials

Supplementary Notes

Anthropologic assessment — The study population resided in the Mirpur slum of Dhaka, Bangladesh (23.8042°N 90.3667°E) in a catchment area consisting of 9,250 households. Most of the homes in this community consist of one main room (~220 square feet), composed of concrete floors and tin roofs with bamboo, metal, and in a few cases cement walls. The average number of household members ranges from 4-10 people, and average monthly family income is 4,000-10,000 Bangladeshi Taka (50 to 130 USD). Infants do not wear diapers, nor do they typically wear any clothing on the bottom halves of their bodies. The importance of hand washing before eating or child feeding is widely understood but rarely practiced due to lack of access to clean water. Families prepare food either on the floor or on a ground-level cement slab located at the entrance of the home; this slab typically straddles an open drain containing wastewater running along the street. Since few families have refrigerators, most food is stored on shelves or under the bed. Households may consist of more than one biological family: in these cases all individuals in the household share a gas stove and cooking area immediately outside the main room, although food, cooking pots and utensils are used separately by each biological family. All individuals share a common 'bathroom,' a small space containing a latrine, and sometimes the water pump, located next to the main room. The common practice is to wash the perianal area by hand with water contained in a small, special container called *bodna* in Bangla.

Fecal microbiota variation within and between family members during the first year of postnatal life - There are few reports of time-series studies charting assembly of the gut microbiota in healthy USA infants and even fewer studies in infants from non- Western populations. The results published to date have revealed pronounced intra- as well as interpersonal variation during the first year of life[11,29-31]. In contrast, the gut microbiota of healthy USA *adults* is quite stable over time, with signatures of within- individual and within-family similarity evident throughout sampling periods[15]. To obtain a view of gut microbiota development

in Bangladeshi infants and children as a function of time after birth and family structure, we collected monthly fecal samples from 11 twin pairs and 1 set of triplets and their parents. The first fecal sample was obtained from infants at the time of their enrollment (4±3 days of age). Monthly samples were subsequently obtained from each of these 25 infants and from their mothers while samples were collected from their fathers every three months. Families were followed for a total of 520±159 days (mean±SD). The duration of exclusive breastfeeding was 28±23 days (mean±SD). Diarrhoea occurred for 11±12 days (2±3 %of the total number of days followed during the study). Distances (degree of similarity) between all pairs of fecal microbiota samples in this birth cohort were computed using the Hellinger metric, an abundance-based ecological metric, as well as the phylogeny-based unweighted UniFrac metric where distance is calculated based on the degree to which any two communities share branch length on a bacterial tree of life[32]. In the case of triplets, we performed all possible pairwise comparisons (self-self; all three possible pairwise comparisons among siblings; each sibling against unrelated age-matched individuals; each sibling against their mother or father). We had previously noted that genetically unrelated co-habiting adults in the USA have more similar overall bacterial phylogenetic configurations in their fecal microbiota than unrelated adults living separately[11]. Comparing the difference (distance) of a Bangladeshi mother's microbiota during her first month post-partum to her microbiota three months later revealed a larger shift in overall structure compared to fathers sampled during the same three-month interval [P=0.01 (Hellinger); P=0.04 (unweighted UniFrac); **Extended Data Fig. 3b**], thus obscuring a microbial manifestation of their co-habitation. This signature of co-habitation emerged 10 months postpartum, at a time when the preceding marked temporal variation of the mother's microbiota had diminished (P=0.006 for difference between co-habiting spouses at 10 months postpartum versus non-co-habiting adults in the cohort as measured by the abundance based Hellinger metric; P=0.08 using the presence/absence unweighted UniFrac phylogenetic metric; see **Extended Data Fig. 3c**). During the first postnatal month, the bacterial configuration of the fecal microbiota of infants was more similar to mothers compared to fathers (P<0.001

Hellinger metric; P=0.07 with unweighted UniFrac; **Extended Data Fig. 3d**). Co-twins were more similar to one another than unrelated age-matched twins during the first postpartum year (P<0.001 Kruskall-Wallis; **Extended Data Fig. 3e**). An analysis of sources of variation in the microbiota of the twins and triplets over the course of the entire study revealed that age alone captured 19% and 37.7% of variance (Hellinger and unweighted UniFrac metrics, respectively) in contrast to dietary factors (presence/absence of 'breast milk', 'formula', 'solid foods') which explained only 2.5% and 3.8%, respectively (see **Supplementary Table 8** for partitioning of variance by metric and metadata; PERMANOVA as implemented with adonis function in R package vegan)[33]. We identified increases in the proportional representation of 97%-identity OTUs in the microbiota of mothers during the perinatal period, including a number of the age- discriminatory taxonomic biomarkers, notably Bifidobacteria in **Extended Data Fig. 3a** and **Supplementary Table 9.** This latter feature is not unique to Bangladesh: a recent study of 80 Finnish mother-infant pairs sampled at 1 and 6 months post-partum demonstrated that if a mother was positive for *B. bifidum* 1 month following delivery, the likelihood of her child being colonized was significantly higher[34]).

Transient reduction of gut microbiota diversity in healthy twins and triplets associated with diarrhoea - In addition to changes in the relative proportions of specific bacterial taxa incorporated into our Random Forests model-derived MAZ and relative microbiota maturity metrics, the developing gut microbiota of infants/children is also characterized by an increase in total community bacterial diversity as judged by the Shannon Diversity Index (SDI). SDI is an ecological measure of within-sample (alpha) diversity that incorporates both the concept of total community size as well as the evenness of the abundance of its members. Across the 50 healthy Bangladeshi children sampled, SDI increased linearly with age (0.11 units per month of life with an intercept of 1.6±0.1 units at birth; mixed model; P<0.0001). In twins and triplets, diarrhoea (n=36 episodes) was the only significant clinical parameter associated with a reduction in SDI (-0.44±0.1; P<0.01). This reduction showed a similar time course of recovery as

relative microbiota maturity, persisting for one month (-0.35±0.2 SDI; $P<0.05$) followed by subsequent recovery (**Extended Data Fig. 2**; **Supplementary Table 7c**).

Persistent reductions in diversity associated with SAM - As with measurements of microbiota maturity, the RUTF group showed significant improvement in SDI values between 1-3 months following cessation of treatment, followed by regression to a persistent lower than healthy SDI beyond 3 months. In the case of Khichuri-Halwa, improvement in SDI was only significant at 3-4 months of follow-up. SAM children in both treatment groups exhibited significant reductions in diversity compared to healthy Bangladeshi children at all phases of treatment and recovery, except for 1-3 months post- RUTF and 3-4 months post-Khichuri-Halwa (**Extended Data Fig. 5; Supplementary Table 14**).

Two hundred and twenty bacterial taxa that are significantly different in their proportional representation in microbiota of children with SAM compared to healthy at multiple treatment phases across both groups **-** During the acute phase, prior to nutritional rehabilitation, 116 97%-identity OTUs were significantly altered in SAM. The majority were lower in relative abundance compared to healthy children. The four 97%-identity OTUs with the largest reductions in abundance during the acute phase included three classified as belonging to the genus *Bifidobacterium* (*B. longum*, two unassigned to a species) and *Faecalibacterium prausnitzii,* of which two are age-discriminatory taxa (FDR- corrected P<0.05). Taxa that were enriched in children diagnosed with SAM compared to healthy children included those belonging to the family *Enterobacteriaceae* (genera *Escherichia* and *Klebsiella*) as well as *Enterococcus faecalis* (FDR-corrected $P<0.05$). In children with SAM, taxa that remain depleted throughout the follow-up period included members of the bacterial families *Ruminococcaceae*, *Veillonellaceae* and *Prevotellaceae*. Taxa enriched in the microbiota of children with SAM after the therapeutic food interventions belonged predominantly to the genus *Streptococcus*, including 97% ID OTUs identified as *Streptococcus lutentiensis, Streptococcus thermophilus* (also age-discriminatory) and other as yet unknown *Streptococcus* species (FDR-corrected $P<0.01$; see **Extended Data Fig. 6** and **Extended Data Fig. 7** for a heatmap depiction of all 97% ID OTUs

whose representation in the fecal microbiota is significantly altered in SAM relative to healthy before, during and after the nutritional rehabilitation period; also see **Supplementary Table 15**).

Assessing the effects of antibiotics on microbiota maturity during the follow-up period in children with SAM – As noted in the main text, we compared antibiotic use during the post-intervention periods for the two treatment arms. The results indicate that (i) the frequency of antibiotic consumption during this period was comparable to that of healthy children in our training and validation sets (P=0.5, one-way ANOVA); (ii) there was no significant difference in antibiotic use between treatment arms (P=1; Fisher's exact test; **Supplementary Table 12**); (iii) there was no significant association between recent antibiotic intake (defined as occurring seven or fewer days before collection of a fecal sample) and relative microbiota maturity values [difference in maturity values for samples with versus those without recent antibiotic intake: -0.37±0.8 (mean ± SEM) P=0.6 (ANOVA of linear mixed model; n=100 samples for the 22 children in the post RUTF arm); +0.17±0.9; P=0.9 (n=103 samples, 25 children in the Khichuri- Halwa arm)]. Similarly, we found that diarrhoea was not significantly associated with differences in maturity values in either arm during the post-intervention period (**Supplementary Table 16**).

Expanding the sparse Random Forests-based model from 24 to 60 taxa - It is logical to ask the following questions about our approach for defining microbiota maturity. *First,* are we defining "immaturity" entirely as a lack of maturity, rather than a specific, recognizable state in and of itself. Ours is a 'positive' composition-based classification. For example, the *Bifidobacterium longum* OTU in **Fig. 1a** ranks 5th in terms of its feature importance score in the 24-taxon Random Forests model. In samples from healthy infants less than 6 months old, this OTU is highly represented [relative abundance = 52.7±30% (mean±SD); >1% in 94% of samples from the training and validation sets). The remaining seven 97%-identity OTUs that comprise the cluster of early age- discriminatory taxa shown in **Fig. 1c** together represent 6.35±8% of the microbiota and are present at >1% abundance in 84% of samples. *Second,* was there an outlet

for samples containing very few or none the 24 taxa selected by the model? For example, were they deemed unclassifiable, or classified as "other", or were all samples "forced" onto the maturity scale? How were samples with low feature signal having few to no age-discriminant taxa classified? Only one of the 589 fecal samples in the SAM study had undetectable levels of the 24 age-discriminatory taxa. In the SAM cohort, only 10% of fecal samples (60/589) had an aggregate relative abundance of the 24 age-discriminatory taxa that was less than 10%. In healthy children, this was true for 36/960 samples. When we expanded our model to include the top 60 age-discriminatory taxa, we found that < 1% of SAM samples and none of the healthy samples had an aggregate relative abundance of the 60 age-discriminatory taxa that was less than 10%. Note that in expanding the model, we excluded OTUs that were deemed chimeric when using default BLAST thresholds to the Greengenes reference as implemented in QIIME. The performance of the 24 and 60 taxa models were similar. Predictions made by the two models when they were applied to the healthy validation datasets (all 724 samples considered), and when they were applied to the SAM datasets (all 589 samples considered), showed a strong correlation (r^2=0.98 and 0.93, respectively). Both yielded similar results for our analysis of (i) the effects of diarrhoea in healthy twins/triplets (microbiota immaturity was transient), (ii) the SAM trial (the effects of RUTF and Khichuri-Halwa produced transient non-durable improvements compared to healthy controls; antibiotics did not have a significant effect on microbiota maturity measurements either during the acute phase or during the post-intervention; note that the top 60 model includes *Enterobacteriaceae* and *Streptococcaceae* OTUs that are highly enriched in children with SAM relative to healthy); and (iii) the MAM study (a significant difference was observed between 18 month old healthy controls versus children with MAM) (data not shown).

Extended Data Figure Legends

Extended Data Figure 1: Illustration of the equations used to calculate 'relative microbiota maturity' and 'microbiota-for-age *Z*-score'. a, **b**, The procedure to calculate both microbiota maturation metrics are shown for a single faecal sample from a focal child (pink circle) relative to microbiota age values calculated in healthy reference controls. These reference values are computed in samples collected from children used to validate the Random-Forests-based sparse 24-taxon model and are shown in **a**, as a broken line of the interpolated spline fit and in **b**, as median ± s.d. values for each monthly chronologic age bin from months 1 to 24.

Extended Data Figure 2: Transient microbiota immaturity and reduction in diversity associated with diarrhoea in healthy twins and triplets. a, The transient effect of diarrhoea in healthy children. Seventeen children from 10 families with healthy twins or triplets had a total of 36 diarrhoeal illnesses where faecal samples were collected. Faecal samples collected in the months immediately before and following diarrhoea in these children were examined in an analysis that included multiple environmental factors in the 'healthy twins and triplets' birth cohort. Linear mixed models of these specified environmental factors indicated that 'diarrhoea', 'month following diarrhoea' and 'presence of formula in diet' have significant effects on relative microbiota maturity, while accounting for random effects arising from within-family and within-child dependence in measurements of this maturity metric. The factors 'postnatal age', 'presence or absence of solid foods', 'exclusive breastfeeding', 'enteropathogen detected by microscopy', 'antibiotics' as well as 'other periods relative to diarrhoea' had no significant effect. The numbers of faecal samples (n) are shown in parenthesis. Mean values ± s.e.m. are plotted. *$P < 0.05$, ***$P < 0.001$. See Supplementary Table 7 for the effects of dietary and environmental covariates. **b**, Effect of diarrhoea and recovery on age-adjusted Shannon diversity index (SDI). Mean values of effect on SDI ± s.e.m. are plotted. *$P < 0.05$, **$P < 0.01$.

Extended Data Figure 3: Gut microbiota variation in families with twins and triplets during the first year of life. a, Maternal influence. Heatmap of the mean relative abundances of 13 bac-

terial taxa (97%-identity OTUs) found to be statistically significantly enriched in the first month post-partum in the faecal microbiota of mothers (see column labelled 1) compared to microbiota sampled between the second and twelfth months post-partum (FDR-corrected $P < 0.05$; ANOVA of linear mixed-effects model with random by-mother intercepts). An analogous heatmap of the relative abundance of these taxa in their twin or triplet offspring is shown. Three of these 97%-identity OTUs are members of the top 24 age-discriminatory taxa (blue) and belong to the genus *Bifidobacterium*. **b–e**, comparisons of maternal, paternal and infant microbiota. Mean values ± s.e.m. of Hellinger and unweighted UniFrac distances between the faecal microbiota of family members sampled over time were computed. Samples obtained at postnatal months 1, 4, 10 and 12 from twins and triplets, mothers and fathers were analysed (n = 12 fathers; 12 mothers; 25 children). **b**, Intrapersonal variation in the bacterial component of the maternal microbiota is greater between the first and fourth months after childbirth than variation in fathers. **c**, Distances between the faecal microbiota of spouses (each mother–father pair) compared to distances between all unrelated adults (male–female pairs). The microbial signature of co-habitation is only evident 10 months following childbirth. **d**, **e**, The degree of similarity between mother and infant during the first post-partum month is significantly greater than the similarity between microbiota of fathers and infants (**d**) while the faecal microbiota of co-twins are significantly more similar to one another than to age-matched unrelated children during the first year of life (**e**). For all distance analyses, Hellinger and unweighted UniFrac distance matrices were permuted 1,000 times between the groups tested. P values represent the fraction of times permuted differences between tested groups were greater than real differences between groups. *$P < 0.05$, **$P < 0.01$, ***$P < 0.001$.

Extended Data Figure 4: Anthropometric measures of nutritional status in children with SAM before, during and after both food interventions. a–c, Weight-for-height Z-scores (WHZ) (**a**) height-for-age Z-scores (HAZ) (**b**) and weight-for-age Z-scores (WAZ) (**c**). Mean values ± s.e.m. are plotted and referenced to national average anthropometric values for children surveyed between the ages of 6 and 24 months during the 2011 Bangladeshi Demographic Health Survey (BDHS)[28].

Extended Data Figure 5: Persistent reduction of diversity in the gut microbiota of children with SAM. Age-adjusted Shannon diversity index for faecal microbiota samples collected from healthy children ($n = 50$), and from children with SAM at various phases of the clinical trial (mean values ± s.e.m. are plotted). The significance of differences between SDI at various stages of the clinical trial is indicated relative to healthy controls (above the bars) and versus the time of enrollment before treatment (below the bars). *$P < 0.05$, **$P < 0.01$, ***$P < 0.001$ (post-hoc Dunnett's multiple comparison procedure of linear mixed models). See Supplementary Table 14.

Extended Data Figure 6: Heatmap of bacterial taxa significantly altered during the acute phase of treatment and nutritional rehabilitation in the microbiota of children with SAM compared to similar-age healthy children. Bacterial taxa (97%-identity OTUs) significantly altered (FDR-corrected $P < 0.05$) in children with SAM are shown (see Supplementary Table 15 for P values and effect size for individual taxa). Three groups of bacterial taxa are shown: those enriched before the food intervention (**a**); those enriched during the follow-up phase compared to healthy controls (**b**); and those that are initially depleted but return to healthy levels (**c**). Members of the top 24 age-discriminatory taxa are highlighted in blue. Note that there were no children represented in the Khichuri–Halwa arm under the age of 12 months during the 'follow-up after 3 months' period.

Extended Data Figure 7: Heatmap of bacterial taxa altered during long-term follow-up in the faecal microbiota of children with SAM compared to similar-age healthy children. a, **b**, Bacterial taxa (97%-identity OTUs) significantly altered (FDR-corrected $P < 0.05$) in children with SAM are shown (see Supplementary Table 15 for P values and effect sizes for individual taxa). **a**, Taxa depleted across all phases of SAM relative to healthy. **b**, Those depleted during the follow-up phase. Members of the top 24 age-discriminatory taxa are highlighted in blue. Note that there were no children under the age of 12 months represented in the Khichuri–Halwa treatment arm during the 'follow-up after 3 months' period.

Extended Data Figure 8: Effects of antibiotics on the microbiota of children with SAM. Plots of microbiota and anthropometric parameters in nine children sampled before antibiotics (abx), after oral amoxicillin plus parenteral gentamicin and ampicillin, and at the end of the antibiotic and dietary interventions administered over the course of nutritional rehabilitation in the hospital. All comparisons were made relative to the pre-antibiotic sample using the non-parametric Wilcoxon matched-pairs rank test, in which each child served as his or her own control. **a–c**, Microbiota parameters, plotted as mean values±s.e.m., include relative microbiota maturity, microbiota-for-age *Z*-score (MAZ), and SDI. WHZ scores are provided in **d**. **e**, **f**, The two predominant bacterial family-level taxa showing significant changes following antibiotic treatment. ns, not significant; $^{**}P<0.01$.

Extended Data Figure 9: Relative microbiota maturity and MAZ correlate with WHZ in children with MAM. a–c, WHZ are significantly inversely correlated with relative microbiota maturity (**a**) and MAZ (**b**) in a cross-sectional analysis of 33 children at 18 months of age who were above and below the anthropometric threshold for MAM (Spearman's Rho = 0.62 and 0.63, respectively; $^{***}P<0.001$). In contrast, there is no significant correlation between WHZ and microbiota diversity (**c**). **d–l**, Relative abundances of age-discriminatory 97%-identity OTUs that are inputs to the Random Forests model that are significantly different in the faecal microbiota of children with MAM compared to age-matched 18-month-old healthy controls (Mann–Whitney *U*-test, $P<0.05$). Box plots represent the upper and lower quartiles (boxes), the median (middle horizontal line), and measurements that are beyond 1.5 times the interquartile range (whiskers) and above or below the 75th and 25th percentiles, respectively (points) (Tukey's method, PRISM software v6.0d). Taxa are presented in descending order of their importance to the Random Forests model. See Extended Data Fig. 10a, b.

Extended Data Figure 10: Cross-sectional assessment of microbiota maturity at 18 months of age in Bangladeshi children with and without MAM, plus extension of the Bangladeshi-based model of microbiota maturity to Malawi. a, **b**, Children with MAM (WHZ lower than −2 s.d.; grey) have significantly lower relative microbiota maturity (**a**) and MAZ (**b**) compared to

healthy individuals (blue). Mean values ± s.e.m. are plotted $^{**}P < 0.01$ (Mann–Whitney *U*-test). See Extended Data Fig. 9 for correlations of metrics of microbiota maturation with WHZ and box-plots of age-discriminatory taxa whose relative abundances are significantly different in children with MAM relative to healthy reference controls. **c**, Microbiota age predictions resulting from application of the Bangladeshi 24-taxon model to 47 faecal samples (brown circles) obtained from concordant healthy Malawian twins and triplets are plotted versus the chronologic age of the Malawian donor (collection occurred in individuals ranging from 0.4 to 25.1 months old). The results show the Bangladeshi model generalizes to this population, which is also at high risk for malnutrition (each circle represents an individual faecal sample collected during the course of a previous study[11]). **d**, Spearman rho and significance of rank order correlations between the relative abundances of age-discriminatory taxa, and the chronologic age of all healthy Bangladeshi children described in the present study as well as concordant healthy Malawian twins and triplets. $^{*}P < 0.05$.

Extended Data Figures

Extended Data Figure 1

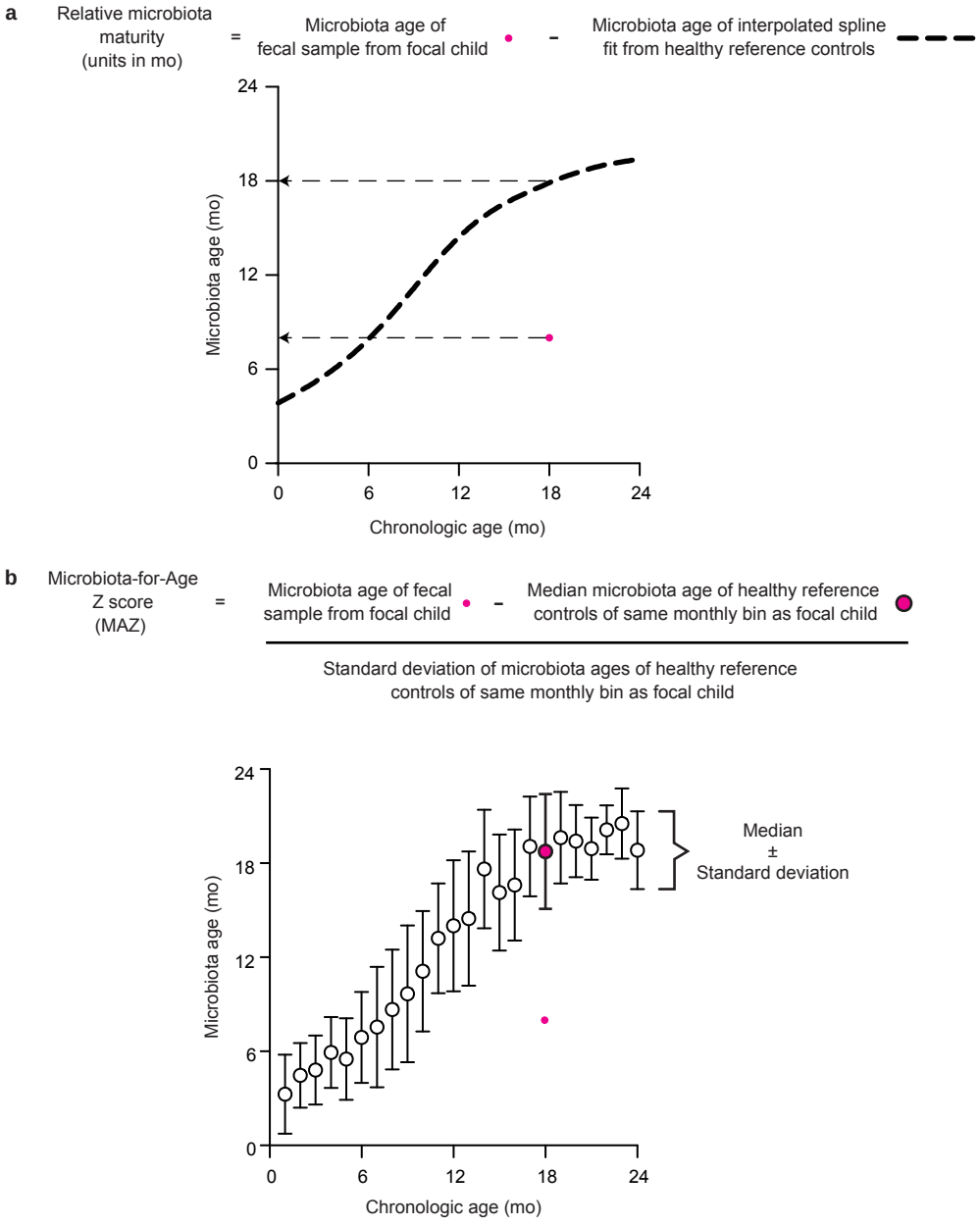

Extended Data Figure 2

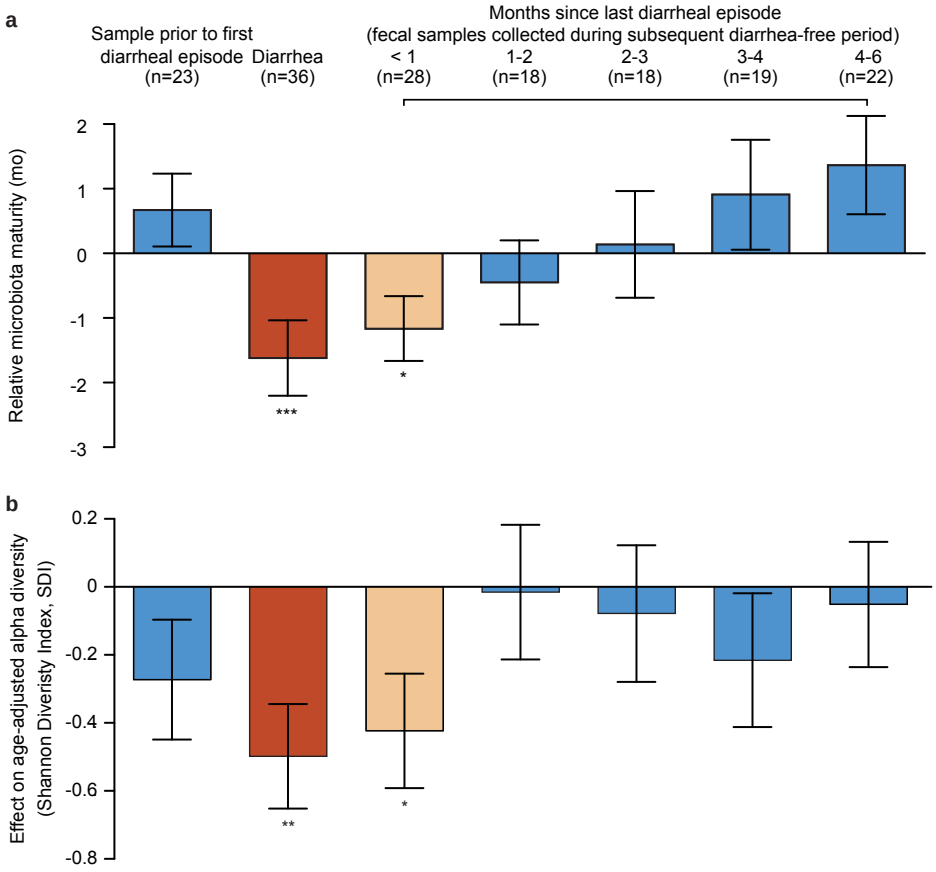

Extended Data Figure 3

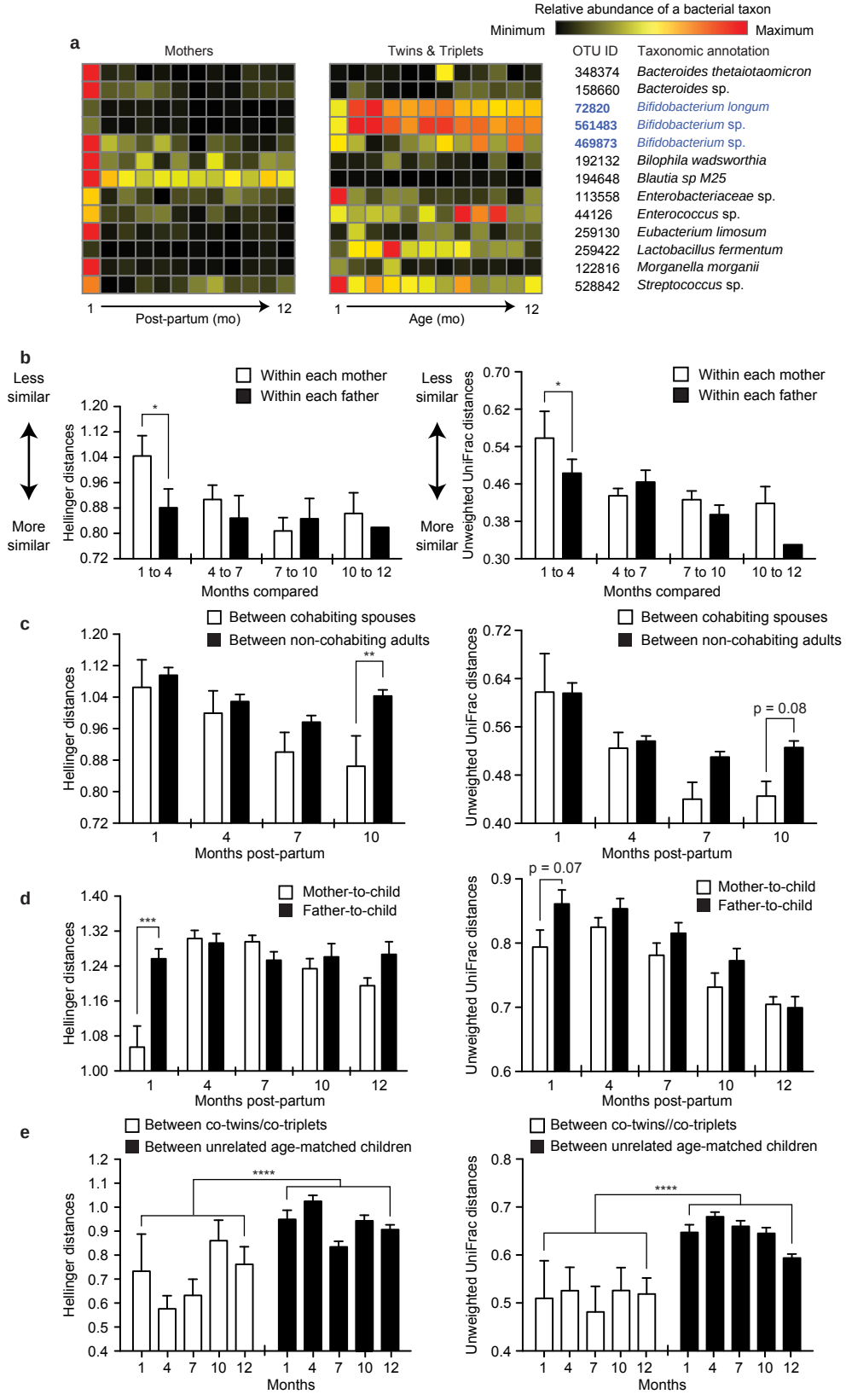

Extended Data Figure 4

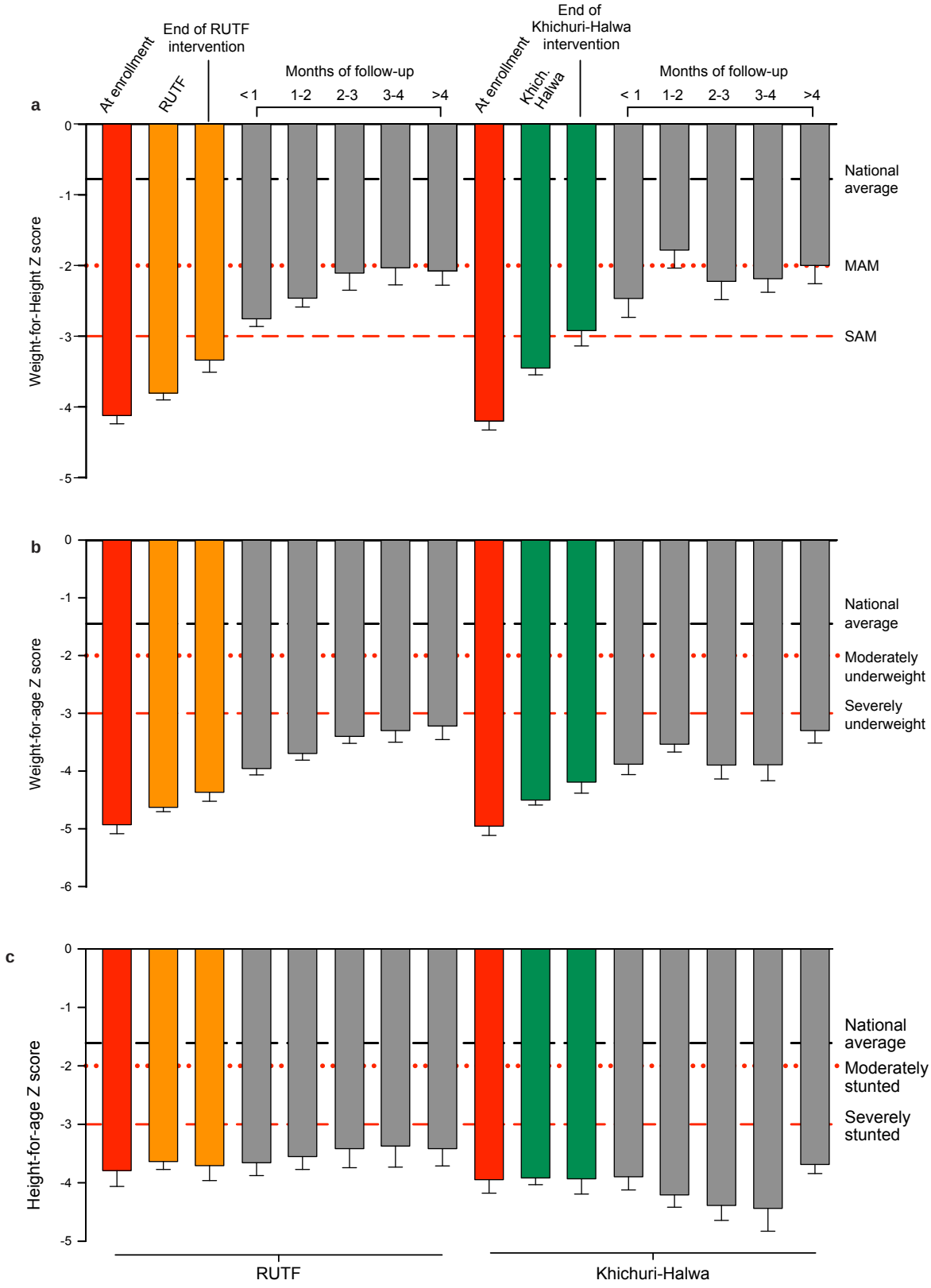

Extended Data Figure 5

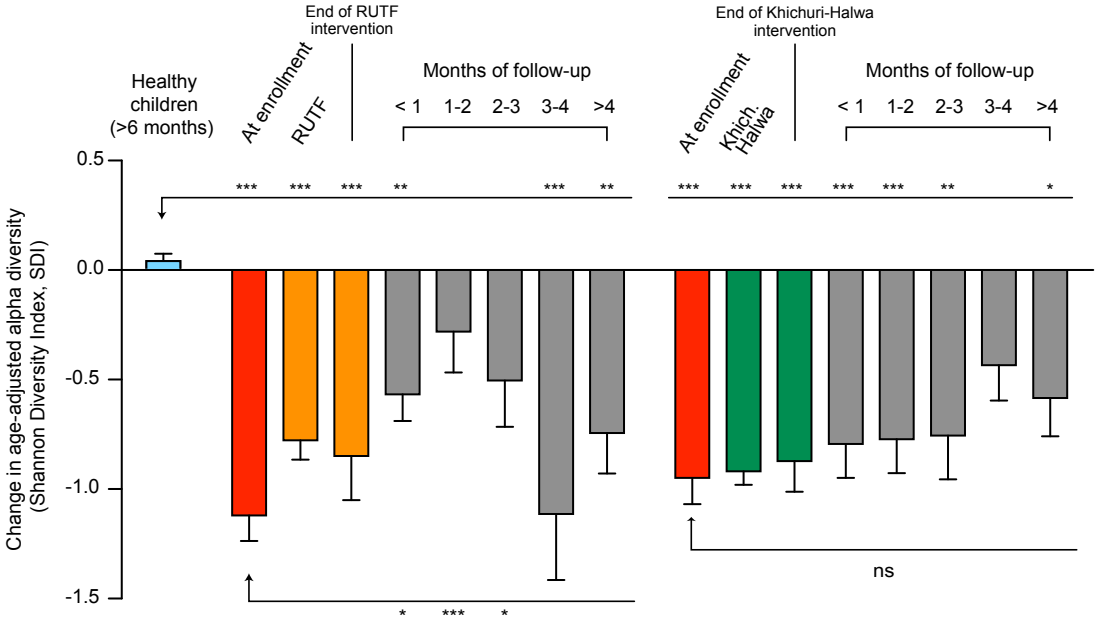

Extended Data Figure 6

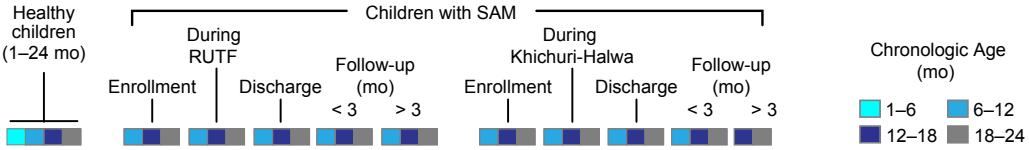

a Taxa enriched at enrollment in children with SAM relative to healthy

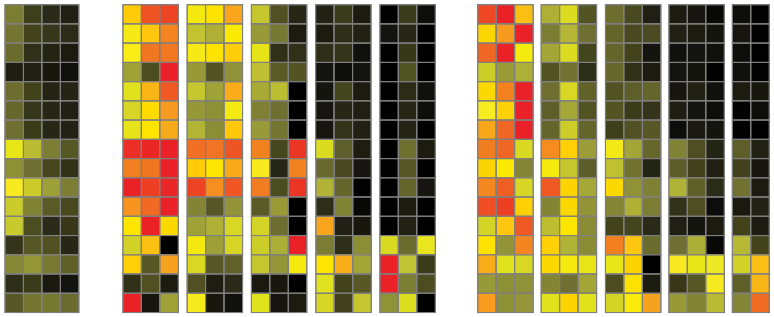

OTU ID	Taxonomic annotation
142054	*Enterobacteriaceae* sp.
210269	*Enterobacteriaceae* sp.
9715	*Enterobacteriaceae* sp.
563485	*Enterobacteriaceae* sp.
436723	*Enterobacteriaceae* sp.
512914	*Enterobacteriaceae* sp.
310265	*Enterobacteriaceae* sp.
307981	*Enterobacteriaceae* sp.
307080	*Escherichia* sp.
305760	*Escherichia coli*
113558	*Enterobacteriaceae* sp.
280706	*Enterobacteriaceae* sp.
540230	*Enterococcus faecalis*
15382	*Streptococcus* sp.
249155.c0	*Leuconostoc* sp.
316587	*Streptococcus gallolyticus*

b Taxa enriched during follow-up in children with SAM relative to healthy

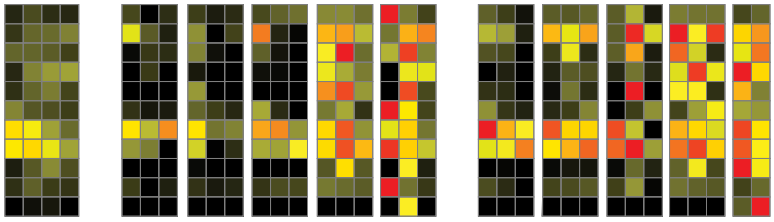

292424	*Streptococcus* sp.
148099	*Weissella cibaria*
628.d0	*Streptococcus* sp.
239.d0	*Lactobacillus* sp.
282068.c0	*Lactobacillus* sp.
528842	*Streptococcus parasanguinis*
108747	***Streptococcus thermophilus***
340.d0	*Bifidobacterium* sp.
73.d0	*Lactobacillaceae* sp.
294794	*Streptococcus* sp.
233573	*Erysipelotrichaceae* sp.

c Taxa depleted before but not after intervention in SAM relative to healthy

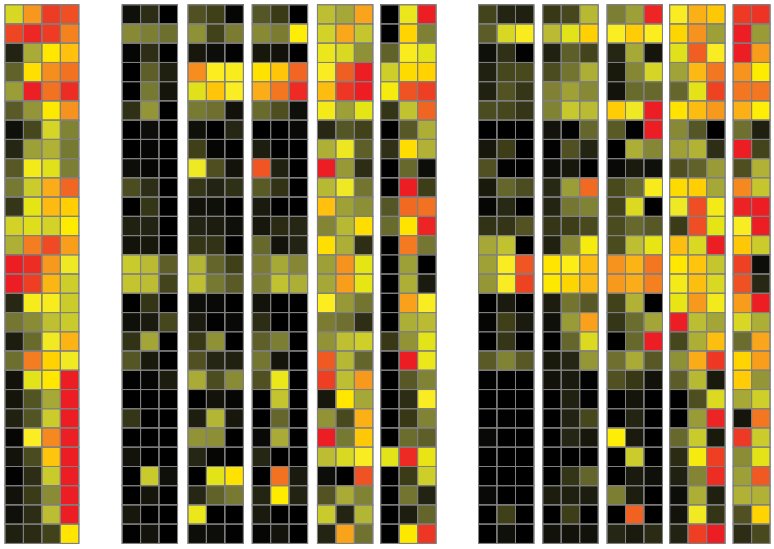

24773	*Bifidobacterium* sp.
131391	*Bifidobacterium* sp.
470663	***Lactobacillus ruminis***
186029	*Collinsella aerofaciens*
89679.c0	*Collinsella aerofaciens*
469873	***Bifidobacterium* sp.**
139221	*Coriobacteriaceae* sp.
15141	***Lactobacillus mucosae***
198251	*Ruminococcus gnavus*
292302	*Lactobacillus* sp.
250395	*Lactobacillus* sp.
326977	*Bifidobacterium* sp.
370431	*Actinomyces odontolyticus*
561483	***Bifidobacterium* sp.**
72820	***Bifidobacterium longum***
142448	*Lactobacillus* sp.
28727	*Lactobacillus* sp.
182804	*Coriobacteriaceae* sp.
470477	*Granulicatella adiacens*
302844	*Clostridium disporicum*
470369	*Eubacterium biforme*
295024	*Eubacterium biforme*
579564	*Clostridium disporicum*
594084	*Slackia isoflavoniconvertens*
178122	*Ruminococcus obeum*
182202	*Clostridium glycolicum*
100258	*Eubacterium sp cL 10 1 3*
471180	*Bifidobacterium* sp.

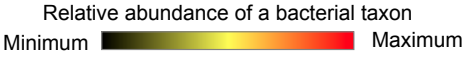

Extended Data Figure 7

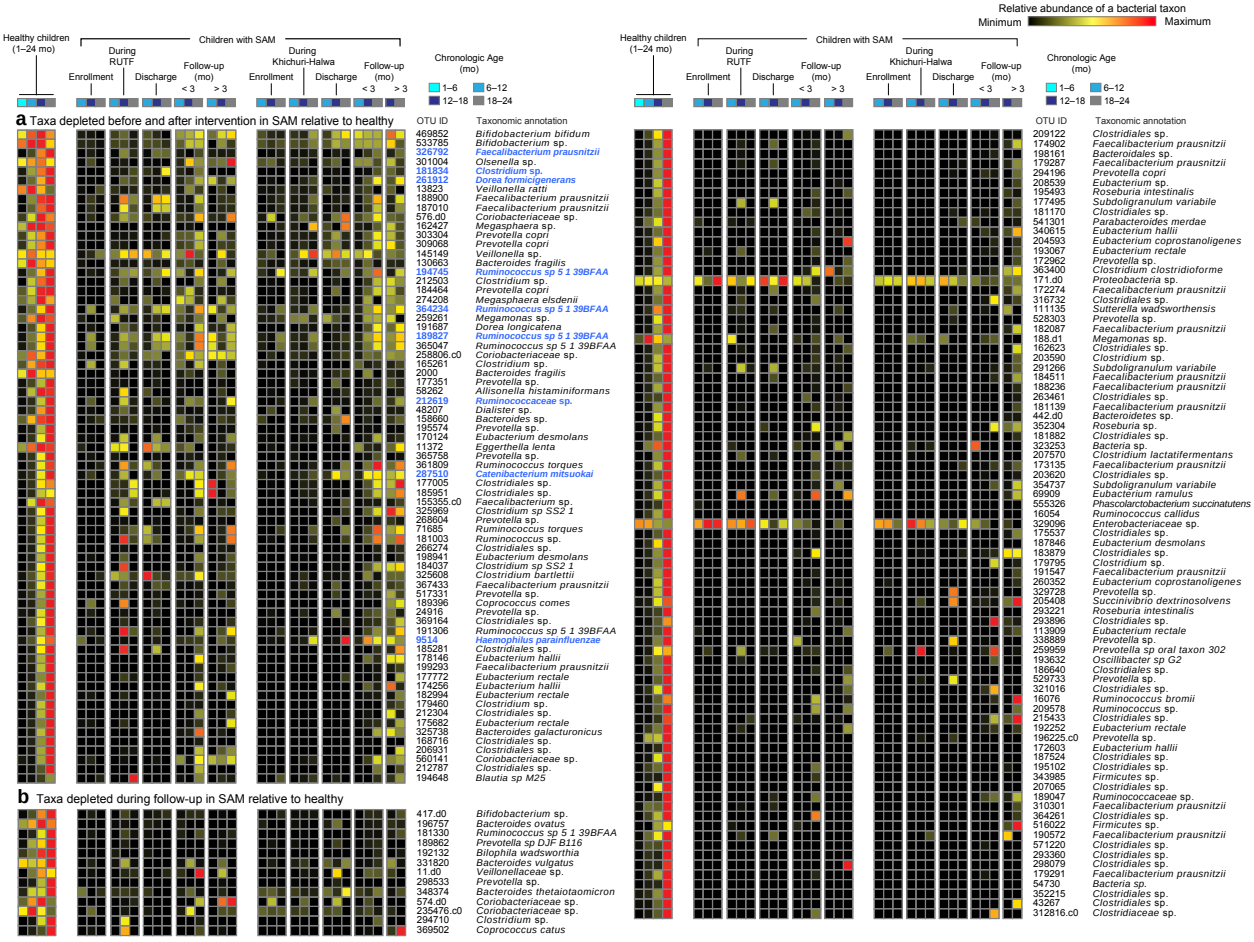

Extended Data Figure 8

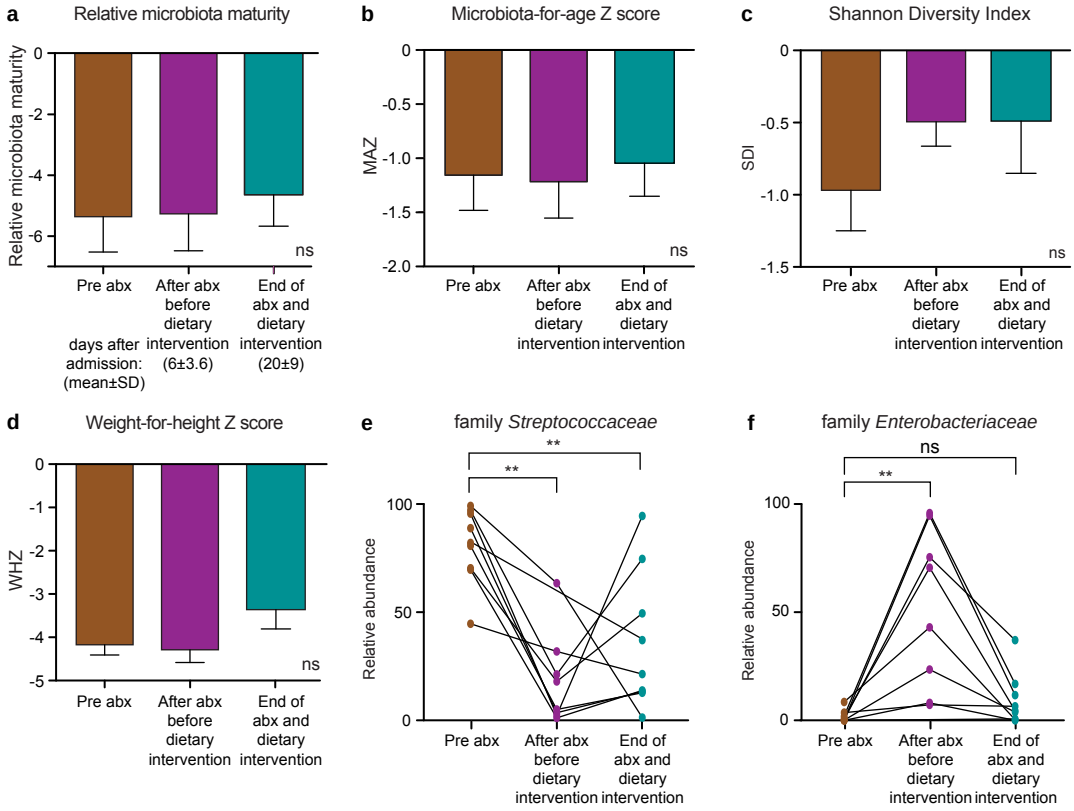

Extended Data Figure 9

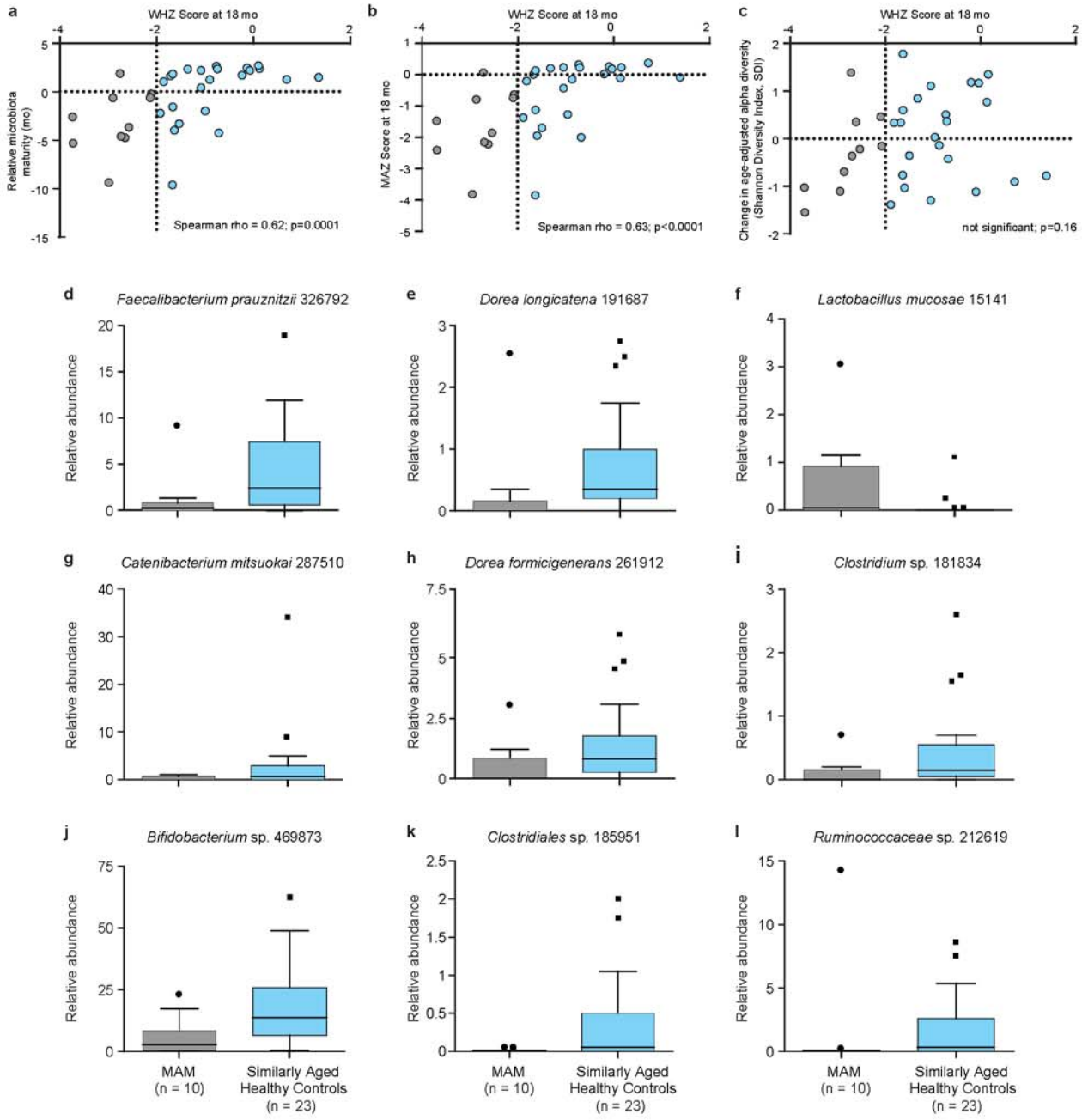

Extended Data Figure 10

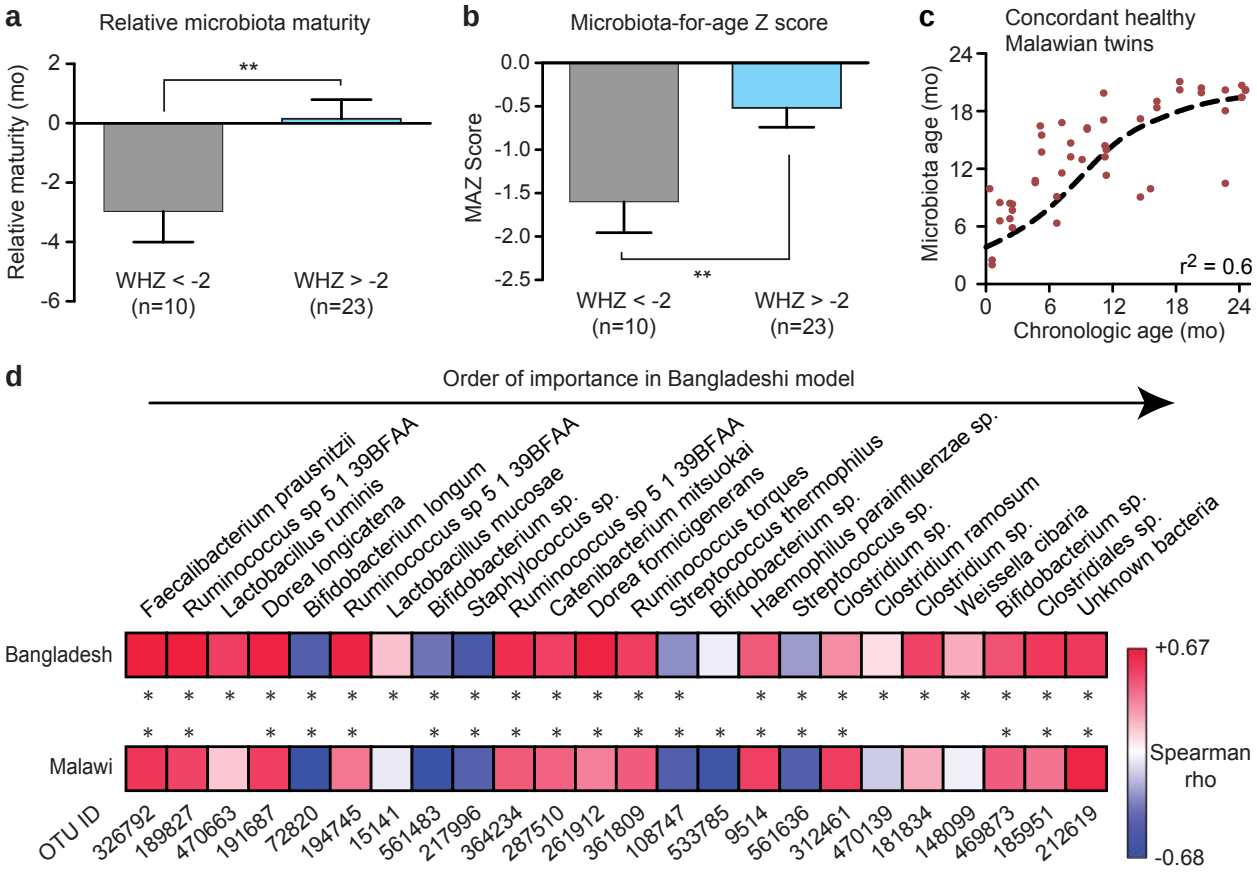

Supplementary Tables

Supplementary Table 1: Metadata for 50 healthy Bangladeshi children sampled monthly during the first two years of life

Supplementary Table 2: Information associated with individual fecal samples collected from healthy children in training and validation sets

Supplementary Table 3: Information associated with fecal samples collected from parents in twins and triplets birth cohort

Supplementary Table 4: Characteristics of children in training and validation sets used for Random Forests age-discriminatory model

Supplementary Table 5: Bacterial V4-16S rRNA sequencing statistics

Supplementary Table 6: 16S rRNA sequences and annotation of age-discriminatory bacterial taxa in order of feature importance

Supplementary Table 7: Associations between relative microbiota maturity, Microbiota-for-Age Z-score and age-adjusted Shannon Diversity Index (SDI) with clinical and dietary parameters in the healthy twins and triplets birth cohort

Supplementary Table 8: Identification of factors affecting variance in fecal microbiota configuration of healthy twins and triplets

Supplementary Table 9: Bacterial taxa enriched in the gut microbiota of Bangladeshi mothers during the first post-partum month compared to subsequent months 2 – 12

Supplementary Table 10: Metadata for Bangladeshi children with SAM in a randomized clinical trial of RUTF versus Khichuri-Halwa

Supplementary Table 11: Metadata associated with individual fecal samples collected over the course of the SAM trial

Supplementary Table 12: Contingency tables relating gender and antibiotics to food-intervention arms in the SAM trial

Supplementary Table 13: Ingredients of foods used during nutritional rehabilitation of children with SAM

Supplementary Table 14: Relative microbiota maturity, Microbiota-for-Age Z-score and age-adjusted Shannon Diversity Index comparisons in each treatment phase of each intervention arm in the SAM trial (compared to healthy controls and to values at enrollment)

Supplementary Table 15: 220 bacterial taxa whose abundances are significantly altered in the microbiota of children with SAM compared to similarly aged healthy children

Chapter 3

An approach for identifying complementary foods that promote healthy gut microbiota development in children with undernutrition

An approach for identifying complementary foods that promote healthy gut microbiota development in children with undernutrition

Sathish Subramanian[†1,2], Siddarth Venkatesh[†1,2], Jeanette L. Gehrig[1,2], Tarek Salih[1,2], Hao-wei Chang[1,2], Jiye Cheng[1,2], Philip P. Ahern[1,2], Ansel Hsiao[1,2], Janaki L. Guruge[1,2], Michael J. Barratt[1,2], Derek G. Barisas[1,2], Sayeeda Huq[3], Munirul Islam[3], Mustafa Mahfuz[3], Margaret Kosek[4], Gagandeep Kang[5], Pascal O. Bessong[6], Aldo A.M. Lima[5], William A. Petri Jr[3], Rashidul Haque[2], Tahmeed Ahmed[2] and Jeffrey I. Gordon[1*]

[†] contributed equally to this work

[1] Center for Genome Sciences and Systems Biology and [2]Center for Gut Microbiome and Nutrition Research, Washington University in St. Louis, St. Louis, MO 63108 USA.

[3] International Centre for Diarrhoeal Disease Research, Bangladesh, Dhaka, Bangladesh.

[4] Department of International Health, Johns Hopkins Bloomberg School of Public Health, Baltimore, Maryland; Biomedical Research Unit, Asociación Benéfica PRISMA, Iquitos, Peru.

[5] Division of Gastrointestinal Sciences, Christian Medical College, Vellore, TN, 632004, India.

[6] HIV/AIDS & Global Health Research Programme, Department of Microbiology, University of Venda, Thohoyandou 0950, South Africa.

[7] Center for Global Health, Department of Physiology and Pharmacology, Clinical Research Unit & Institute of Biomedicine, School of Medicine, Federal University of Ceará, Fortaleza, CE, Brazil.

[8] Departments of Medicine, Microbiology and Pathology, University of Virginia School of Medicine, Charlottesville, VA 22908.

*Correspondence to: jgordon@wustl.edu

Abstract

Culture-independent methods applied to fecal samples, collected monthly during the first two years of postnatal life from members of a Bangladeshi birth cohort living in an urban slum, combined with a machine learning method (Random Forests), have identified a set of bacterial strains whose relative abundances together define a normal program of assembly of the gut microbiota in healthy, biologically unrelated infants and children in this area. Applying this sparse Random Forests-derived model to Bangladeshi children with severe acute malnutrition (SAM), revealed that that they had perturbed microbiota development, with their gut communities appearing younger than those of chronologically age-matched children with healthy growth. Moreover, this immaturity was not repaired with existing therapeutic foods. These findings raise several questions. To what extent is this identified program of gut community assembly generalizable to other children raised in different geographic locations and representing different cultural traditions? To what extent does the gut microbiota continue to develop beyond the first two years of life and do the age-discriminatory strains present in the existing Random Forests-derived model of gut microbiota maturation persist beyond the first two years? What food or microbial interventions can be used to prevent or repair this immaturity and improve clinical outcomes? Therefore, we applied our modeling approaches to (i) bacterial 16S rRNA datasets generated from 50 healthy children, each sampled monthly from birth through the end of postnatal year 2, who live in urban, peri-urban or rural areas of four other countries (India, South Africa, Peru and Brazil) where the burden of childhood undernutrition is great, and (ii) datasets obtained from 36 healthy children living in an urban slum in Bangladesh who were each sampled monthly from 1-60 months. Single country Random Forests-derived models, as well as a model generated from 16S rRNA data aggregated from the four countries, were applied reciprocally to the different populations; the results revealed bacterial strains that define a program of gut microbiota development/maturation which is shared across children living very distinct geographic and cultural settings; the extended time series analysis conducted in Bangladesh established that this developmental program is largely but not fully completed by year three of postnatal life. We cultured and sequenced the genomes of nine age-discriminatory bacterial

strains as well as seven SAM-associated taxa from Bangladeshi donors, and then presented different sequences of different combinations of commonly consumed complementary foods, to gnotobiotic mice colonized with these cultured organisms. Analysis of 16S rRNA datasets generated from the recipient animal's fecal microbiota disclosed a number of complementary food ingredient–bacterial strain associations, with levels of chickpea positively correlating with the relative abundances of the greatest number of age-discriminatory strains (and without untoward effects on the representation of any of SAM-associated strains). Comparing gnotobiotic mice colonized with the consortium of SAM-associated strains and treated with (i) Khichuri-Halwa, a locally produced therapeutic food used for SAM or (ii) the chickpea-enriched microbiota-targeted complementary food (MDCF) formulation, with or without subsequent administration of a 'probiotic consortium' of these 9 age-discriminatory strains, disclosed that only the combination of the MCDF and 'probiotic' consortium produced a significant increase in microbial fermentation (notably levels of butyrate) and colonic $Foxp3^{+}$ $CD4^{+}$regulatory T cells. Together, these results illustrate a shared, microbial, feature of human development and a way for identifying and characterizing microbiota-directed interventions designed to support repair and/or prevent disruption of the normal program of community assembly.

Introduction

The transition in early postnatal life from breast-feeding to complementary foods coincides with a dramatic period of child development, including development of the gut microbiota. There has been a notable absence of detailed comparative time series studies of gut community assembly in members of birth cohorts who live in disparate geographic settings and represent distinct and diverse cultural and culinary traditions. As a consequence, we have insufficient knowledge of whether a common program of gut microbial community development exists. A related problem is that we lack understanding of how, and to what extent, complementary feeding practices during the suckling-weaning transition impact the developmental biology of the microbiota. From a meta-community perspective (i.e., local communities connected by dispersal), a better understanding of the spatial and temporal scales that affect variations in species co-existence, and patterns of local and regional microbial diversity within and between human guts is needed if we are to develop nutritional recommendations for infants and children that help sponsor normal development of their microbiota and healthy growth, as well as more effective food and/or microbial interventions that repair and ultimately prevent disruptions in this developmental program as occurs in children with SAM.

In the present report, we (i) identify shared features of gut microbiota development from a culture-independent (metagenomic) study of gut microbial community development in five birth cohorts living in five countries located on three continents, (ii) use the results as a guide to culture bacterial strains that are components of an ensemble of organisms that define this program; (iii) introduce these sequenced cultured strains into young gnotobiotic mice that were then subjected to a combinatorial screen of complementary foods to identify ingredients that promote the representation of these strains; and (iv) perform a preclinical proof of concept test of whether these ingredients, combined with these strains, when applied to an artificial model of a SAM microbiota, can impact features of microbial community function and host biology.

Results

Identifying shared features of gut microbiota development

We previously described an analysis of gut microbiota development in 50 Bangladeshi children who exhibited healthy growth, as defined by serial anthropometry, during their first two years of postnatal life (Subramanian et. al, 2014). Applying a non-parametric machine learning approach (Random Forests) to a dataset of bacterial 16S rRNA gene sequences generated from fecal samples collected each month from each individual yielded 'sparse' model composed of 24 of the most age-discriminatory strains whose relative abundances over this time period provided a 'microbial signature' that described normal development ('maturation') of the microbiota.

This Random Forests model was trained on a subset of 25 of the Bangladeshi children, and its performance subsequently evaluated on the remaining members of the healthy cohort. Using the 16S rRNA dataset generated from the Bangladeshi birth cohort, we performed a simulation to determine the minimum number of individuals (sample size) that would be required to construct a Random Forests model with comparable performance to larger sample sizes. The results showed that using ≥12 children who had been sampled monthly would produce a model with a comparable correlation coefficient and mean-squared error rate to a model generated from 25 children (**Extended Data Figure 1a,b**).

To test the extent to which gut microbial community assembly is comparable across children by sequencing the PCR products generated from variable region 4 of bacterial 16S rRNA genes present in the fecal microbiota of 50 anthropometrically healthy children who were members of birth cohorts from Loreto, Peru (peri-urban area; n=22 participants), Vellore, India (urban; n=14), Fortaleza, Brazil (urban; n=7), and Venda, South Africa (rural n=7) (see **Extended Data Tables 1** and **2** for information associated with each child and associated fecal samples). As in Bangladesh, fecal samples were collected monthly from each child from birth through 24 months of age (n=23±3 samples/child; 41,134±18,702 V4-16S rRNA reads/sample, mean±SD). 16S rRNA

reads were grouped based on a threshold nucleotide sequence identity of ≥97% into operational taxonomic units (97%ID OTUs).

We first used the sparse 24-taxon, Random Forests-derived model trained on the Bangladeshi dataset to predict the microbiota age of samples collected from all 50 children. The results indicated a significant correlation between the age of the child at the time of fecal sample collection and their predicted fecal microbiota age (r^2=0.65 across all four sites, r^2=0.75 for India and 0.72 for Peru; **Figure 1a,b**). Weaker correlations were found for datasets generated from smaller numbers of children (r^2=0.53 and 0.56 for Brazil and South Africa, respectively).

We next developed country-of-origin specific Random Forests models from the Peruvian and Indian datasets where the number of sampled children was ≥12. Model building for each country was initiated by regressing the relative abundance values of all identified OTUs in all fecal samples against the chronologic age of each donor at the time each sample was procured. For each country, OTUs were ranked based on their feature-importance scores (calculated from the observed increases in mean-squared error rate of the regression when values for that OTU were randomized). To determine, how many OTUs, ranked based on their feature importance scores, are required to create a Random Forests model that was comparable in accuracy to a model comprised of all OTUs, we performed an internal-cross-validation where models with sequentially fewer input OTUs were compared to one another (**Extended Data Figure 2**). Using the top 60 ranked OTUs for each country-specific model yielded error-rates that were indistinguishable from those obtained using all OTUs, while limiting the country specific model to the top 30 ranked OTUs had only minimal effects on accuracy (within 1% of mean-squared error obtained with all OTUs). Therefore, our subsequent analyses used sparse country-specific models, each comprised of their 30 top-ranked OTUs. The sparse Peruvian and sparse Indian models shared 16 OTUs with one another, and 14 with the sparse 24 OTU Bangladeshi model, noting that sharing here indicates alignment to the exact same 97%ID OTU cluster (**Extended Data Figure 2**).

Another test of degree to which features of normal microbiota development are shared across sites (countries) involved a series of reciprocal tests where each country-specific model (Bangladesh, India, Peru) was applied to datasets from the other two countries. In all six comparisons, the Pearson correlation values were remarkably similar (r^2 from 0.76 to 0.67; **Extended Data Figure 1c**).

Using a different approach, we created an "aggregate" model from the 16S rRNA datasets generated from all but the Bangladeshi birth cohort (n=50). To balance the representation of each country's contribution to the aggregate model, seven children from each of the four countries were randomly sampled. This random sampling was performed with 100 iterations, each iteration consisting of a different group of 28 children. Analogous to the procedure described above, for each iteration all OTUs were ranked based on their feature importance, and the minimum number of top ranked OTUs identified that yielded error-rates which were most similar to those obtained with all OTUs (in this case, the top 36 OTUs yielded error rates that were within 1% of the error rate obtained when all OTUs were used. 18 of the 36 OTUs in this sparse 'aggregate model' were present in the sparse Bangladeshi model, while 27 and 25 OTUs were present in the Indian and Peruvian models (**Figure 1c**). Applying the aggregate model to the Bangladeshi 16S rRNA datasets from 50 children yielded a Pearson correlation value (r^2) of 0.68. In addition, both the aggregate model and the "local" Bangladeshi model gave similar results when applied to microbiota samples from children with SAM ($r^2 = 0.78$; n=64 children).

Development of the gut microbiota during the first five postnatal years

These results provide a meta-community perspective about gut microbiota development; over the spatial and temporal scales represented by members of these five birth cohorts, the shared features of species co-existence in the gut provide evidence for habitat selection. Our findings, obtained from individuals sampled during the first two years of postnatal life, raise the question of how persistent these age-discriminatory strains are over a longer time scale. Therefore, we expanded our monthly sampling of the fecal microbiota to the 60th postnatal month for 36 Bangladeshi children

(n=1961 samples; 55±4 samples collected/child, 26,813±13,914 V4-16S rRNA reads/sample, see **Extended Data Table 3** for information associated with fecal samples). The cessation of breast milk, cow's milk or powdered milk consumption occurred at 34±10 months (mean±SD) in this cohort (see **Extended Data Figure 3** for a visual representation of the diet history for each child). Samples collected in a previous study from twelve unrelated Bangladeshi males living in the same urban slum and ranging in age from 23 to 41 years were used as representative adult microbiota.

To determine the degree to which a child's microbiota comes to resemble an adult microbiota during the first five years of postnatal life, we used the unweighted and weighted UniFrac metric to conduct an unsupervised analysis comparing the phylogenetic distances between each fecal sample collected from each child at each time point to the samples from each of the 12 unrelated adults. As a control, beta-diversity measurements were also computed using just adult samples. The mean 'child-to-adult' distance decreased to 'adult-to-adult' levels by 3 years of age (**Figure 2a,b**). This pattern of stabilization was also documented using the non-phylogenetic binary Jaccard and abundance-weighted Hellinger metrics (**Extended Data Figure 4a,b**). Shannon-Diversity and Phylogenetic Diversity indices of alpha diversity continued to increase up to five years (**Extended Data Figure 4c,d**).

We constructed a sparse Random Forests model using the 16S rRNA dataset generated from this longer time series study in order to describe gut microbiota development during the first five years of postnatal life. (Note that the dataset was first randomly split so that each child's time-series was allocated into either a training or validation set (see **Extended Data Table 3** for sample allocation and information). The 5-year model has a minimal error rate using the 36 OTUs with highest ranked feature importance scores, with no further improve in error if the top 60 were included) (**Figure 2c,d**). Like the 2-year model, it revealed significant microbiota immaturity when applied to the children with SAM (**Figure 2e**).

Sixteen of the OTUs incorporated into the sparse 5-year model were also present in the sparse two-year 24 OTU model. Of note, in both models the OTUs with the highest feature im-

portance scores were assigned to *F. prausnitzii*, although they correspond to three distinct 97%ID OTU clusters: all three are represented in the 5-year model; only one is in the 2-year model where it is the top ranked OTU (326792); this same OTU is ranked 23rd in the 5-year model. All three strains are present beyond 3 years of age, with the one that is top ranked in the 2-year model exhibiting a progressive reduction in its representation beyond two years as the other two emerge to prominence (**Extended Data Figure 5b**).

Generating a gnotobiotic mouse model to identify complementary foods that promote microbiota maturation

The identification of age-discriminatory OTUs that define a program of normal development of the microbiota, as well as its impairment in children with SAM, provides an opportunity to develop food-based interventions that promote the establishment/adequate representation of these taxa in the gut. Given that current ready-to-use therapeutic foods used to treat SAM, or ready-to-use supplementary foods (RUSFs) employed for the nutritional rehabilitation of children with moderate acute malnutrition, have not been formulated to target these age-discriminatory taxa in the developing gut microbial community, we reasoned that commonly consumed complementary foods represent a culturally acceptable source of dietary ingredients that could be tested for their ability to promote repair of microbiota immaturity in undernourished children or, ideally, prevent impaired microbiota development from occurring in the first place. To be therapeutically useful, a microbiota-directed complementary food (MDCF) should also not promote expansion of components of the microbiota, nor induce expression of their functions that have deleterious effects on healthy growth.

To identify microbiota-directed complementary foods (MDCFs), we constructed a gnotobiotic mouse model using a consortium of cultured, sequenced, age-discriminatory OTUs together with a set of cultured, sequenced bacterial taxa enriched in the microbiota of children with SAM. We were able to culture nine age-discriminatory bacterial, strains, under anaerobic culture conditions, from four fecal samples collected from three different Bangladeshi children aged 6-23

months who lived in Mirpur and had normal anthropometry (*Faecalibacterium prausnitzii*, *Dorea longicatena, Dorea formicigenerans, Ruminococcus obeum, Ruminococcus torques, Blautia luti, Bifidobacterium longum, Bifidobacterium breve,* and *Bifidobacterium catenulatum*). Sequencing V4-16S rRNA amplicons generated from these strains confirmed that they represented 97%ID OTU clusters in the sparse 2-year Bangladeshi, Indian, Peruvian and aggregate Random Forests models, as well as the 5-year sparse Bangladeshi model (**Table 1**). These nine OTUs vary in their pattern of change in relative abundance during the first two years of postnatal life: thus they embody different phases/features of gut community development.

We had previously compared the relative abundances of bacterial OTUs in the fecal microbiota of 64 Bangladeshi children with SAM relative to healthy controls, finding that OTUs belonging to the genera *Streptococcus*, *Enterococcus, Leuconostoc,* and *Bifidobacteria,* and to the families *Enterobacteriaceae* and *Lactobacillaceae*, were significantly enriched in those with SAM (Subramanian et al., 2014). Using the same medium and anaerobic culture conditions used to retrieve the age-discriminatory strains, we recovered seven bacterial strains from a fecal sample collected prior to a therapeutic food intervention from a 24-month old Bangladeshi child with SAM who lived in Mirpur: *Escherichia fergusonii, Streptococcus pasteurianus, Streptococcus constellatus, Streptococcus gordonii, Streptococcus salivarius, Enterococcus avium, Bifidobacteria pseudocatenulatum*. Three of these seven strains (*E. fergusonii, S. salivarius* and *S. pasteurianus*,) have V4-16S rRNA sequences that are exact matches to OTUs significantly enriched in SAM (**Extended Data Figure 6i-l**), while three of the remaining four strains belong to genera that are enriched. Six of the nine cultured age-discriminatory strains exhibit significant deficiency in their representation in the fecal microbiota of the 64 children with SAM compared to the 50 healthy Bangladeshi controls used to construct the 2-year Random Forests model: the exceptions are *R. obeum, B. longum, B. catenulatum* (**Extended Data Figure 6a-h**). Only two strains cultured from the SAM donor's microbiota share the same taxonomic annotation with a member of the set of nine age-discriminatory strains cultured from the healthy donors: *Bifidobacterium catenulatum* or *pseudocatenulatum*.

Importantly, this 16-member culture collection represents a defined artificial human gut microbiota community whose 97%ID OTUs directly match to 59.1±25% (mean±SD) of the V4-16S rRNA 97%ID sequences identified in 996 fecal samples collected from the 50 healthy Bangladeshi children living in Mirpur and 59.2±27% of the 97% ID OTUs identified in 589 fecal samples collected from the 64 children who had developed SAM. The genomes of each of the 16 Bangladeshi strains were sequenced (paired-end 150 nt reads with Illumina NextSeq; 32-138 fold coverage) and each genome was aligned to the nearest reference strain's genome using MIRA (see *Methods* for details of genome assembly and annotation, **Extended Data Table 4** for summaries of genome features, *Supplementary Results* for metabolic reconstructions, plus **Extended Data Table 5** and **Extended Data Figure 7** for genes with homology to entries in the Virulence Factors Database, including the notably high representation of these genes in the SAM-associated *Escherichia fergusonii* strain and three of the four SAM-associated *Streptoococcus* species).

Based on diet surveys conducted in the Mirpur population (see *Methods*), we chose twelve locally available, commonly consumed, complementary food ingredients to screen in various combinations at various dose levels in gnotobiotic mice (**Figure 3a**). To do so in an efficient and economical manner, we developed the diet-oscillation protocol shown in **Figure 3b**. The protocol was designed to minimize a number of potential confounding factors: (i) the order in which diets are presented to different treatment groups of animals would be sufficiently varied to find effects that are robust to order of presentation ('group' could be a single or multiple animals); (ii) there would be repetition built into the experiment with different ingredient-rich diets repeated over the course of an experiment encompassing different treatment groups to add confidence to the observed associations; (iii) there would be limited collinearity among ingredients so that observed effects can be clearly attributed to one ingredient over another; and (iv) there would be a broad range of concentrations for each ingredient, as well as several diets in which each ingredient was absent.

Twenty-four unique diets were designed by random sampling (see *Methods*). These diets and their sequence of administration satisfied the following four 'rules'. *First,* every diet contained six different ingredients at various dose levels. One of the ingredients was dominant in each

diet (47% or 37% by weight). Each diet consisted of a base of milk powder and soybean oil. The calculated energy, protein, fat, and micronutrient content for each diet was adequate for rodents (see **Table 2** plus **Extended Data Tables 6-9** for the composition of each diet). *Second,* each group of mice received a different sequence of diets. Diets were switched weekly and provided *ad libitum*. Mice were monitored daily for feeding behavior and weight changes. *Third,* no single mouse received a diet that was dominated by a particular food ingredient more than once during the course of the experiment. *Fourth,* within the same week, no two groups of mice were fed diets dominated by the same complementary food ingredient. If two explanatory variables (any two complementary food ingredients in this case) are highly correlated with each other, their effects cannot be disentangled from one another in a correlational analysis of resulting data. To verify that the individual complementary food ingredients are minimally correlated with each other, we selected a diet configuration where the Pearson correlation coefficient between any two ingredients was minimized (see **Table 3** for the results of a collinearity analysis). Each complementary food combination was cooked, and processed as a homogeneous blend, extruded into pellets, and the pellets sterilized by gamma irradiation. Culturing the pellets in rich medium revealed that 21 of the 24 diets were sterile; these 21 diets were advanced to oscillation screen.

Before the screen was initiated, a pilot experiment was performed to define conditions that were most conducive for successful colonization of the nine age-discriminatory strains. Complementary food combinations 1, 3, 9 and 11 that are rich in spinach, peanuts, chickpeas and whole wheat flour, respectively, were studied (47% by weight of each diet; see **Table 2**). In addition, three other diets were tested: an embodiment of the diet consumed by 18-month old children living in Mirpur (see *Methods* and **Extended Data Table 9** for details of how this 'Mirpur-18' diet was designed and its composition), plus two commercial low-fat, plant polysaccharide-rich mouse chows. Groups of five-week-old male germ-free C57Bl/6J mice were each started two days before gavage on one of these eight diets (2 mice, dually-caged/diet; total of 16 animals). The seven SAM-associated strains were gavaged first on 'day 0' of the experiment, as a mixture composed of equal numbers of each strain. Seven days later, the consortium of nine cultured age-discriminatory

strains was administered via single oral gavage of a mixture containing equal numbers of each component strain. Mice in each treatment group continued to receive their diet *ad libitum* for an additional 10 days. Fecal samples were collected daily from each mouse throughout the experiment. Based on the results of V4-16S rRNA sequencing of fecal DNA, successful colonization was defined as a strain achieving a relative abundance of >0.1% in the day 15 samples. Whole wheat flour rich and chickpea-rich complementary food combinations supported establishment and maintenance of the greatest number of age-discriminatory taxa (8); colonization with *F. prausnitzii* was not achieved with any of the eight diets. However, increasing the dose of this organism by 100-fold resulted in successful colonization when animals were given either the whole wheat flour- or chickpea-rich diets.

Based on these results, we adopted the colonization protocol shown in **Figure 3b** for the diet oscillation screen. The seven-member SAM-associated consortium was given first, by gavage, to five-week-old germ-free male C57Bl/6J mice: all animals (n=12) had been switched to the Mirpur-18 diet two days earlier. After four days had elapsed, all mice were switched to the chickpea-rich diet for three days. Three days later, the nine-member set of age-discriminatory strains was introduced by gavage, followed two days later by the concentrated dose of *F. prausnitzii*. An eight-week period of diet-oscillations followed (4 mice/diet oscillation sequence; two mice/cage) where diets were switched weekly and fecal samples were taken on days 1, 3, 5, 6 and 7 of each one-week diet 'block'. Bedding was changed on day 1 of each diet block to minimize contamination with the previous diet. Each fecal sample collected was profiled by V4-16S rRNA sequencing. Pearson's correlations were then computed between the relative abundances of the strains and the levels of complementary food ingredients in a given MCDF candidate (see **Figure 3c** for results obtained from this analysis of 21 different diets).

The chickpea ingredient provided the greatest number of positive correlations with age-discriminatory taxa. Intriguingly, the level of chickpea in the diets was significantly inversely correlated with the relative abundances of *Bifidobacterium longum* and *Bifidobacterium breve*, which dominate during the early phases of normal microbiota development, and positively associated

with the age-discriminatory OTUs that bloom later during the first two years of community maturation (**Figure 3c**). Moreover, the chickpea ingredient did not significantly increase the abundance of any of the SAM-associated strains while other ingredients, notably raw banana and peanuts, were positively associated with the relative abundances of *E. fergusonii* and *S. pasteurianus*, respectively (**Figure 3c**).

Comparing a microbiota-directed complementary food to an existing local therapeutic food

Given these results, we selected chickpea-rich complementary food combination 9 (**Table 2**) as the lead candidate MDCF and compared it to Khichuri-Halwa, a rice- and lentil-based, locally produced therapeutic food used to treat SAM. An experiment was designed to measure the effects of each diet, the effects of the age-discriminatory strains, and the effects of interactions between diet and the age-discriminatory strains, on features of the microbiota, gut immune function and host immune function. The study design is shown in **Figure 4a**. Each experimental group of five-week-old germ-free C57Bl/6J mice (4 groups, n=6 animals/group; three cages of dually-housed mice/group) was started on the Mirpur-18 diet two days before gavage of the 7-member SAM-associated cultured consortium (defined as experimental day 0). After 4 days had elapsed, all mice received Khichuri-Halwa or the chickpea MDCF candidate. Three days later, experimental day 7, half of the mice in each of the two diet arms were gavaged with the 9-member consortium of age-discriminatory strains, followed two days later by the concentrated dose of *F. prausnitzii* (groups I and III in **Figure 4a**). Groups II and IV did not receive this consortium of age-discriminatory strains. All mice were maintained on their designated diets for an additional 40 days. Fecal samples were collected from each animal on days 2, 7, 9, 15, 19, 21, 27, 33, 39, 45 and 49 for 16S rRNA analyses, and at selected time points multiple samples were obtained so that targeted gas-chromatography mass spectrometry (GC/MS) of short chain fatty acids and microbial RNA-Seq could be performed.

The results revealed that compared to Khichuri Halwa, the chickpea-rich MDCF candidate produced a significantly greater enrichment of *F. prausnitzii*, *Ruminococcus torques*, and *Dorea*

longicatena (**Figure 4c**, $p<0.0001$, repeated measures 2-way ANOVA; interaction between type of dietary intervention and time). The enrichment of *F. prausnitzi* peaked on experimental day 15, six days after it was last gavaged, at which time it represented 37±7% (mean±SD) of the community compared to 10±2% for Khichuri-Halwa treated fed animals (**Figure 4c**). A similar time course of enrichment was observed with *Blautia luti*, whose relative abundance also peaked 6 days after its introduction into mice harboring the 7-member SAM-associated consortium (24±3% in the chickpea-rich MDCF fed animals compared to 11±6% for Khichuri-Halwa treated fed animals; $p=0.0001$, repeated measures 2-way ANOVA; interaction between type of dietary intervention and time). All four age-discriminatory strains whose representation was significantly enhanced by the chickpea-rich MDCF relative to Khichuri-Halwa in this experiment had exhibited significant positive correlations with chickpea levels in the previous diet-oscillation screen (**Figure 3c**), providing confirmation of the findings in the screen (see **Extended Data Table 11** for the results of statistical tests of the significance of observed differences between experimental groups). Intriguingly, the combination of the chickpea-rich MDCF and age-discriminatory bacterial strain ('probiotic') intervention resulted in significant depletion of the SAM-associated taxa *Streptococcus pasteurianus* and *Enterococcus avium*. In the case of *E. fergusonii*, both dietary interventions, when combined with the age-discriminatory intervention produced comparable results, with significant depletion occurring relative to the diet intervention-only groups (**Figure 4d**).

The most abundant strain in the fecal microbiota of mice receiving the chickpea-rich MDCF intervention was *F prausnitzii*, a known butyrate producer. The genome assemblies of the age-discriminatory and SAM-associated strains had on average 97.7±1.3% identity alignments to the genomes of the taxonomically closest sequenced reference type strain genome. The *F. prausnitzii* genome cultured from the Bangladeshi donor shares 96.3% identity with the genome of the *F.prausnitzii* A2-165 type strain. (Note that this type strain was re-sequenced as a control for differences related to the sequencing platform or alignment procedures used; the resequenced genome had 99.9% identity with the publicly available genome sequence). The Bangladeshi strain we isolated, like the type strain contained a gene encoding butyryl-CoA:acetate CoA transferase

(EC:2.8.3.8) the enzymes which catalyzes the final step in butyrate synthesis. The other age-discriminatory strains whose abundances were significantly increased by the chickpea-rich MDCF, *Ruminococcus torques, Blautia luti* and *Dorea longicatena*, are related to strains that are known producers of short chain fatty acids, including butyrate.

GC/MS of fecal samples collected on experimental day 40 revealed that butyrate levels were significantly greater in the group of animals receiving the chickpea-rich diet plus age-discriminatory taxa compared to all other experimental groups (**Figure 5a**, $p<0.0001$; ANOVA followed by post-hoc Tukey's test). At the time of sacrifice on day 49, cecal levels of butyrate were significantly higher in both groups of mice that had been treated with the age-discriminatory strains (**Extended Data Figure 8a**), with a trend for higher levels in those that received the chickpea-rich MDCF ($p=0.1$). There was a highly significant correlation across both treatment groups between the relative abundance of *F.prausnitzii* and levels of cecal butyrate ($r^2=0.73$, $p<0.001$, Pearson's correlation, **Extended Data Figure 8b**). This association was not observed with any of the other age-discriminatory strains enriched in the fecal microbiota of mice fed the chickpea-rich MDCF compared to Khichuri-Halwa, including *D. longicatena*, *R. torques and B. luti* (insignificant Pearson's correlations, $r^2=-0.07$,$p=0.4$; $r^2=-0.03$, $p=0.6$; $r^2=0.1$, $p=0.3$). This finding was also consistent with the distribution of genes encoding butyryl-CoA:acetate CoA transferase, among these age-discriminatory strains.

Butyrate is a known mediator of regulatory T cell homeostasis, hence we used FACS to define compare the representation of $Foxp3^+$ $CD4^+$ T cells in the colons, mesenteric lymph nodes and spleens of all animals belonging to each of the four treatment groups. The percentage of colonic $Foxp3^+$ $CD4^+$ T cells was significantly greater in the group receiving the chickpea-rich MDCF diet plus age-discriminatory taxa, compared to all other groups (**Figure 5b**, all comparisons $p<0.01$, ANOVA followed by post-hoc Tukey's test). This induction of Tregs was specific for the colon and this treatment group; no significant differences in Tregs were observed in mesenteric lymph nodes or spleens harvested from any mice in any of the four experimental groups (data not shown).

A significant correlation was observed between fecal levels of *F.prausnitzii* and the percentage of colonic regulatory T cells (r^2=0.43, $p<0.05$; Pearson's correlation). In parallel with the observed patterns of colonic regulatory T cells representation, animals subjected to the chickpea-rich MDCF plus age-discriminatory strain intervention exhibited significant elevation in cecal levels of acetate and succinate compared to all other groups ($p<0.0001$, ANOVA followed by post-hoc Tukey's test). The extent to which this complementary food-by-microbiota interaction impacts other features of host metabolism is being assayed in serum, liver, gastrocnemius muscle, and brain.

Prospectus

The current study illustrates a way of applying machine learning methods to bacterial 16S rRNA datasets generated from fecal samples, collected monthly through the first several years of life from a modest number of children with healthy growth phenotypes enrolled in birth cohort studies, in order to identify age-discriminatory bacterial strains that define a program of gut microbial development which is shared across children representing geographically dispersed populations and embodying distinctive cultural traditions and culinary traditions. Knowledge of these strains and their temporal patterns of representation in a healthy gut community are useful for a number of reasons. First, they can serve as a guide for quantifying the effects of various factors, including dietary history, antibiotic usage, enteropathogen load, frequency and duration of diarrheal diseases, and biomarkers of environmental enteric dysfunction, on the development/maturation of the gut microbiota in healthy versus undernourished children, and by extension whether various combinations of these factors and the representation of these age-discriminatory taxa significantly correlate with, and are predictive of, anthropometric measures of growth phenotypes within and across different populations of children. *Second*, these age-discriminatory strains provide the starting point for identifying microbiota-directed complementary foods (MDCF) designed to produce durable repair of defects in community assembly or to prevent such defects from developing. This approach differs from current efforts to design more effective food-based interventions for children

with impaired linear and ponderal growth. Developing MDCFs that produce sustained repair of microbiota immaturity in undernourished children would enable follow-on proof-of-concept studies that test whether such repair produces better clinical outcomes compared to current therapy. If successful, the ability to use locally produced complementary foods for such interventions could yield products that are culturally acceptable, have desirable organoleptic properties, and whose manufacture and distribution promotes local economic development.

Gnotobiotic mouse models of the type described in this report are made possible by culturing strains that have been identified as high feature-importance age-discriminatory taxa in Random Forests models, by constructing diets combining various complementary foods represented at different levels, and by screening these candidate MDCFs using oscillation protocols that (i) minimize the numbers of animals that need to be used without precluding adequate replication across animals, (ii) account for potentially problematic hysteresis effects, and (iii) overcome the confounding problem of collinearity when trying to identify specific ingredient-microbe relationships by avoiding creation of multiple diet formulations where particular sets of ingredients inevitably co-occur. By including disease-associated taxa in the defined culture consortia introduced into these animals, the specificity of targeting of age-discriminatory taxa by candidate MDCFs can be ascertained. These models also allow the effects of a given MDCF on taxa that represent different stages of microbiota development to be determined; this capability provides an opportunity to design developmental stage/state-specific MDCFs and/or for identifying different MDCFs that might have to be sequentially applied in order sponsor full and sustained repair of a microbiota that takes several years to normally develop. Because a number of age-discriminatory OTUs appear to be shared across different populations of children the robustness of a given MDCF can be modeled in gnotobiotic animals harboring cultured consortia composed of sequenced age-discriminatory OTUs representing different donor origins or mixtures of OTUs from different donor countries. Additionally, the effectiveness of an MDCF in repairing microbiota function and associated host pathology can be tested in these models as a function of a given enteropathogen load, antibiotic treatment and/or synbiotic intervention involving a MDCF together with various combinations of age-discriminatory strains.

The current study also illustrates how these gnotobiotic models can be used to define the effects of MDCFs on features of host biology that are perturbed in undernourished children. Regulatory T cells affect gut barrier function and responses to vaccination, both of which are impaired in these children. For example, Tregs are the major helper cells for IgA responses to bacterial specific antigens derived from the microbiota (Cong et al., 2010). The effect size produced by the chickpea-rich MDCF on the proportion of colonic Tregs has been previously associated with improved rescue from ovalbumin-induced allergic diarrhea (Atarashi et al., 2013). The extent to which gut barrier function and vaccine responses are affected by interactions between a given MDCF and given member or members of the gut community can be modeled by including and excluding the taxon or taxa from a defined community that is introduced into gnotobiotic animals. An example of one attractive target that emerged from this report is *F. prausnitzii*, the butyrate-producing, age-discriminatory species with high feature importance score strain representatives across different country-specific Random Forests models, whose relative abundance positively correlates with the chickpea-rich MDCF-mediated increase in butyrate levels and colonic Treg representation.

Methods

Human studies

Human fecal samples were obtained from biospecimen collections assembled during the course of previous studies; these studies enrolled subjects and collected samples in accordance with procedures approved by local IRBs and the Washington University Human Studies Committee.

Animal Studies

All experiments involving mice were performed using protocols approved by the Washington University Animal Studies Committee. Mice belonging to the C57BL/6J inbred strain were maintained in plastic flexible film gnotobiotic isolators under a strict 12h light cycle (lights on at 0600).

Methods used for (i) collection of fecal samples and isolation of human fecal DNA, (ii) generation and sequencing of V4-16S rRNA amplicons and analysis of the resulting datasets (including generation of sparse Random Forests models), (iii) culturing age-discriminatory and SAM-associated bacterial strains from fecal samples obtained from Bangladeshi donors, (iv) sequencing, assembling and annotating the genomes of these cultured strains and performing metabolic reconstructions, (v) formulation of diets for gnotobiotic mouse experiments, (vi) colonization of mice with these strains and implementation of the diet oscillation experimental design, (vii) characterization of fecal and cecal samples obtained from these animals by V4-16S rRNA sequencing and by COmmunity PROfiling by short read shotgun DNA sequencing (COPRO-Seq), GC/MS and microbial RNA-Seq, and (viii) fluorescence activated cell sorting-based analysis of the representation of $Foxp3^+$ $CD4^+$ T cells in the colon, mesenteric lymph nodes and spleens of gnotobiotic mice, are described in Supplementary Information.

Accession Numbers

16S rRNA datasets, COPRO-Seq datasets, microbial RNA-Seq and draft genome sequences have been deposited in European Nucleotide Archive.

References

T. Ahmed *et al*., Development and acceptability testing of ready-to-use supplementary food made from locally available food ingredients in Bangladesh. *BMC Pediatr*. **14**, 164 (2014).

Atarashi, K. *et al*. Treg induction by a rationally selected mixture of Clostridia strains from the human microbiota. *Nature* **500,** 232–236 (2013).

S. Bartz *et al*., Severe acute malnutrition in childhood: hormonal and metabolic status at presentation, response to treatment, and predictors of mortality. *J. Clin. Endocrinol. Metab*. **99**, 2128–2137 (2014).

J. J. Faith, P. P. Ahern, V. K. Ridaura, J. Cheng, J. I. Gordon, Identifying Gut Microbe–Host Phenotype Relationships Using Combinatorial Communities in Gnotobiotic Mice. *Sci Transl Med*. **6**, 220ra11–220ra11 (2014).

Furusawa, Y. *et al*. Commensal microbe-derived butyrate induces the differentiation of colonic regulatory T cells. *Nature* **504,** 446–450 (2013

A. L. Goodman *et al*., Extensive personal human gut microbiota culture collections characterized and manipulated in gnotobiotic mice. *Proc. Natl. Acad. Sci. U.S.A*. **108**, 6252–6257 (2011).

E. K. Gough *et al*., The impact of antibiotics on growth in children in low and middle income countries: systematic review and meta-analysis of randomised controlled trials. *BMJ*. **348**, g2267 (2014).

A. Lin *et al*., Distinct distal gut microbiome diversity and composition in healthy children from Bangladesh and the United States. *PLoS ONE*. **8**, e53838 (2013).

C. Lozupone *et al*., Identifying genomic and metabolic features that can underlie early successional and opportunistic lifestyles of human gut symbionts. *Genome Res*. **22**, 1974–1984 (2012).

M. Kerac *et al*., Probiotics and prebiotics for severe acute malnutrition (PRONUT study): a double-blind efficacy randomised controlled trial in Malawi. *Lancet*. **374**, 136–144 (2009).

N. P. McNulty *et al*., The impact of a consortium of fermented milk strains on the gut microbiome of gnotobiotic mice and monozygotic twins. *Sci Transl Med*. **3**, 106ra106 (2011).

M. Pop *et al*., Diarrhea in young children from low-income countries leads to large-scale alterations in intestinal microbiota composition. *Genome Biology*. **15**, R76 (2014).

V. K. Ridaura *et al*., Gut microbiota from twins discordant for obesity modulate metabolism in mice. *Science*. **341**, 1241214 (2013).

M. I. Smith, T. Yatsunenko *et al*., Gut microbiomes of Malawian twin pairs discordant for kwashiorkor. *Science*. **339**, 548–554 (2013).

S. Subramanian *et al*., Persistent gut microbiota immaturity in malnourished Bangladeshi children. *Nature*. **510**, 417–421 (2014)

I. Trehan *et al*., Antibiotics as Part of the Management of Severe Acute Malnutrition. *New England J Med* **368**, 425–435 (2013).

T. Yatsunenko *et al*., Human gut microbiome viewed across age and geography. *Nature*. **486**, 222–227 (2012).

Acknowledgements

We thank David O'Donnell, Maria Karlsson, Marty Meier, Sabrina Wagoner, Su Deng, Justin Serugo and J. Hoisington-López, for superb technical assistance. This work was supported by the Bill & Melinda Gates Foundation. The five-year birth cohort study of Bangladeshi children was supported in part by the NIH (AI043596). S.S. is a member of the Washington University Medical Scientist Training Program. We thank the parents and children from each study site for their participation in this study.

Figure Legends

Figure 1. Generalizability of Bangladeshi Random Forests model of gut microbiota maturation model to children raised in other geographies. (a,b) The sparse 24-taxon Bangladeshi Random Forests model was applied to bacterial V4-16S rRNA datasets generated from monthly fecal samples collected from children with healthy growth phenotypes (as defined by anthropometry) who were enrolled in two birth cohorts, one from an urban area of India (Vellore; n=14 children, 349 fecal samples) and the other from a peri-urban area of Peru (Loreto, n=22 children, 505 fecal samples). Each point represents a fecal sample. The x-axis indicates the chronologic age of each child at the time of fecal sample collection; the y-axis is the prediction of microbiota age at the time of collection as defined using the sparse 24-taxon Forests model generated from Bangladeshi children living in the Mirpur urban slum in Dhaka Bangladesh. The correlation coefficients are shown in the bottom right of each panel. (**c**) An aggregate Random Forests-based model of gut microbiota maturation was developed by combining V4-16S rRNA datasets generated from monthly fecal sampled from children in birth cohorts from India, Peru, plus Fortaleza, Brazil (urban; n=7), and Venda, South Africa (rural n=7). To balance the representation of each country's contribution to the aggregate model, seven children from each of the four countries were randomly sampled (100 iterations, each iteration consisting of a different group of 28 children).

The increase in mean-squared error of the aggregate Random Forests model in plotted in ascending order of age-discriminatory importance for the top 30 OTUs. The OTUs are colored based on their overlap with OTUs in the Bangladeshi model (gold= one of the top 24 OTUs ranked in terms of their feature importance scores, green= one of the top 24 to 60 OTUs, black=absent from the top 60 OTUs). The inset shows the results of cross-validation, which indicates that beyond the top 60 taxa there is no improvement compared to all 1128 OTUs detected in all of the V4-16S rRNA datasets. The taxa cultured from the fecal microbiota of Bangladeshi children and incorporated into the artificial, defined, community used for studies in gnotobiotic mice are indicated by a blue asterisk. Two asterisks indicate that multiple isolates were obtained that correspond to the same V4-16S rRNA OTU.

Figure 2. Maturation of the gut microbiota in members of Bangladeshi birth cohort is largely executed by, but nonetheless continues beyond, the first three postnatal years. (a,b) UniFrac a beta-diversity metric that measures the degree to which any two communities share branch length on a bacterial phylogenetic tree, was used to calculate the distances (degree of dissimilarity) between each sampled child's microbiota at each time point of fecal collection (n=36 children, 1961 samples) relative to samples profiled from unrelated adults who also lived in the Mirpur slum (n=12 males, 49 samples). Panels a and b show unweighted and weighted UniFrac distances, respectively, plotted as mean and standard deviation values for each month up to 60 months. The lower the mean distance in a given monthly bin, the more similar the overall bacterial phylogenetic configuration is between samples collected from children at that time point and adults. As a control comparison, the distance between adult samples relative to one another are plotted on the far right of each panel. See **Extended Data Figure 4** for analyses of other metrics of alpha and beta diversity. (**c,d**) In addition to the unsupervised techniques applied in panels a and b, the training and validation of the supervised approach of Random Forests is shown for the 5-year Bangladeshi model. Each point represents a fecal sample collected from a child randomized to the training set (brown points in panel c) and validation set (blue points in panel d). In the validation set, a LOWESS curve has been fit to the dataset to account for the non-linearity observed at older ages. (e) The 5-year model was applied to samples obtained from the 64 children from Mirpur that were diagnosed with SAM. Correlation coefficients are shown in each panel of the validation set and the SAM dataset.

Figure 3. A diet oscillation screen to identify complementary food ingredients that boost the relative abundance of age-discriminatory strains in an artificial defined human gut microbiota assembled in gnotobiotic mice. (**a,b**) Experimental design for delineating the interrelationships between diet components and members of the 16-member defined community. Twenty-four unique diets, each composed of 6 ingredients in various combinations, each with one dominant ingredient, were designed by random sampling of 12 commonly consumed, locally available Bangladeshi foods and the application of the rules outlined at the bottom of panel b. An optimal diet

configuration is one in which the individual ingredients are minimally correlated with each other. Panel b shows the time course for colonization with the 7-member consortium of cultured bacterial taxa enriched in SAM followed by colonization with the 9-member cultured consortium of age-indicative strains. (c) Pearson's coefficient of correlation between the relative abundance of each bacterial strain in the fecal microbiota of recipient mice, and the levels of the food ingredient. The variation in the coefficients is indicated using a three-color scheme. The orange colored boxes indicate coefficients that are statistically significant, $p<0.05$, after applying a false-discovery rate correction. The green colored boxes indicate a positive correlation, white indicates no correlation and yellow indicates a negative correlation between the levels of ingredients and the relative abundances of the indicated strains.

Figure 4. The effects of the chickpea enriched microbiota-directed food formulation versus a locally produced therapeutic food on members of the defined artificial human gut microbiota. (a) The experimental design comparing the effects of chickpea-rich microbiota-directed complementary food combination 9, enriched in chickpea and secondarily in raw banana compared to the standard locally available ready-to-use therapeutic food, Khichuri-Halwa. Four groups of six 5-week-old mice were colonized by oral gavage with the SAM-associated strains while being fed Mirpur-18, the prototypic Bangladeshi diet. Four days later mice were switched to either the chickpea-rich MDCF or Khichuri-Halwa. For each diet treatment group, half of the mice were gavaged with a consortium of nine cultured, age-discriminatory strains on day 7 and to ensure colonization with *Faecalibacterium prausnitzii*, the taxon with the highest feature importance score in the 2-year Bangladeshi and Peruvian Random Forests models and among the top three in the aggregate and Indian models, a high-dose gavage 1.5×10^8 CFUs was delivered two days later (day 9). The other half of each dietary group did not receive the age-discriminatory strains. Mice from all groups were maintained on diets without oscillation for six more weeks. (**b**) The composition of both diets (see **Extended Data Table 9** for further details about nutritional analysis of these diets**).** (**c**) Comparing the abundance of age-discriminatory strains in the groups of mice that were gavaged with the age-discriminatory strains fed either chickpea-rich diet or a Khichuri-Halwa

therapeutic food reveals the OTUs that are significantly enriched over time in the chickpea-rich MDCF group. *Blautia luti* also showed a similar pattern but has lower relative abundance than the taxa displayed (for further details of responses of all strains to both diets see **Extended Data Table 11**). ****, p< 0.0001 (repeated measures 2-way ANOVA, interaction between type of dietary intervention and time). (d) SAM-associated strains whose abundances are significantly different in the fecal microbiota of mice treated with the chickpea-rich MDCF. ***, p< 0.001; ****, p< 0.0001 (repeated measures ANOVA with post-hoc Tukey's comparisons to group A shown in panel a)

Figure 5. An interaction between the chickpea-enriched MDCF diet and members of the consortium of age-discriminatory strains increases butyrate production by the model human gut microbiota and increases regulatory T-cells in the colons of gnotobiotic mice. The design of this experiment is shown in **Figure 4a**. (**a**) Fecal butyrate levels were elevated significantly in mice receiving the combination of the chickpea-enriched MDCF and the consortium of age-discriminatory taxa group compared to all other experimental groups (analysis of samples obtained on experimental day 40; ****, p<0.0001; ANOVA followed by post-hoc Tukey's comparisons). (**b**) At the time of sacrifice on experimental day 49, after 46 days of consumption of the chickpea MDCF and 40 days after administration of the consortium of nine age-discriminatory strains, the percentage of $Foxp3^+$ among colonic $CD4^+$ T cells was significantly elevated in compared to all other treatment groups (**, p<0.01; ***, p<0.001; ****, p<0.0001; ANOVA followed by post-hoc Tukey's comparisons).

Figures

Figure 1.

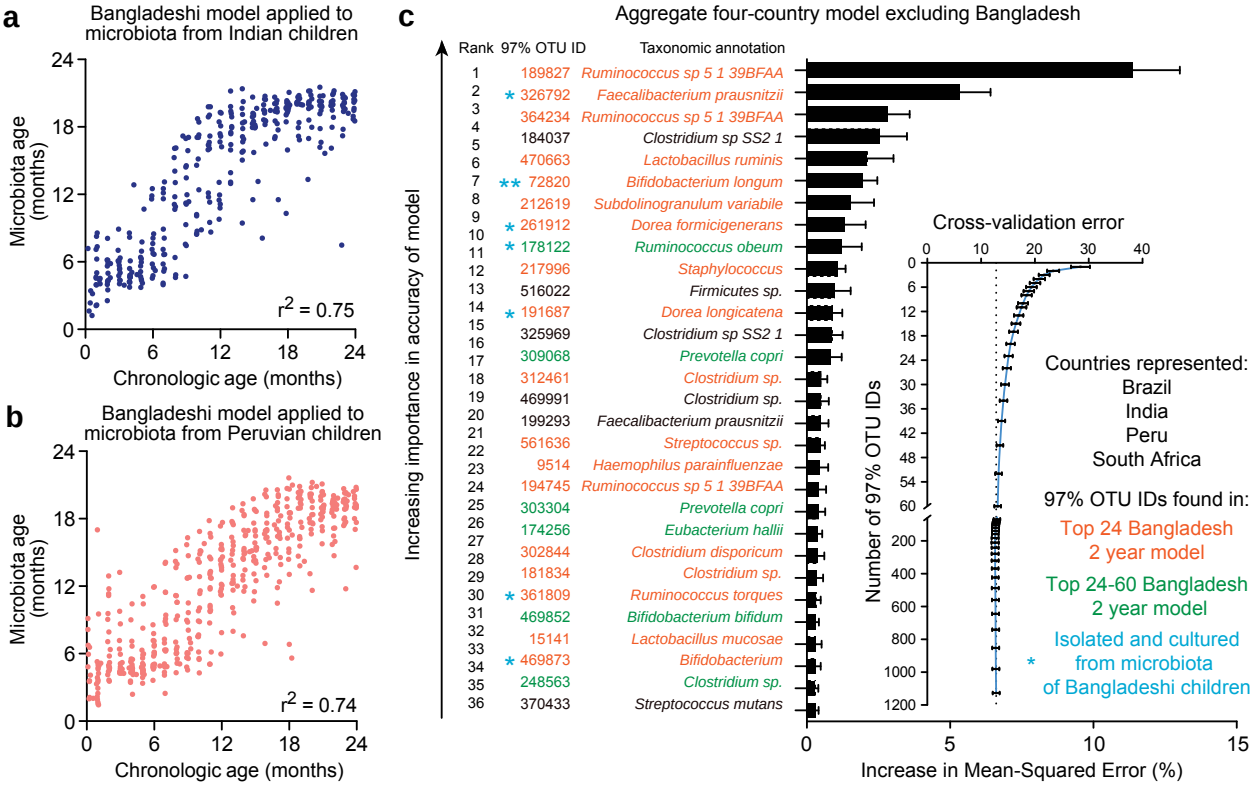

Figure 2.

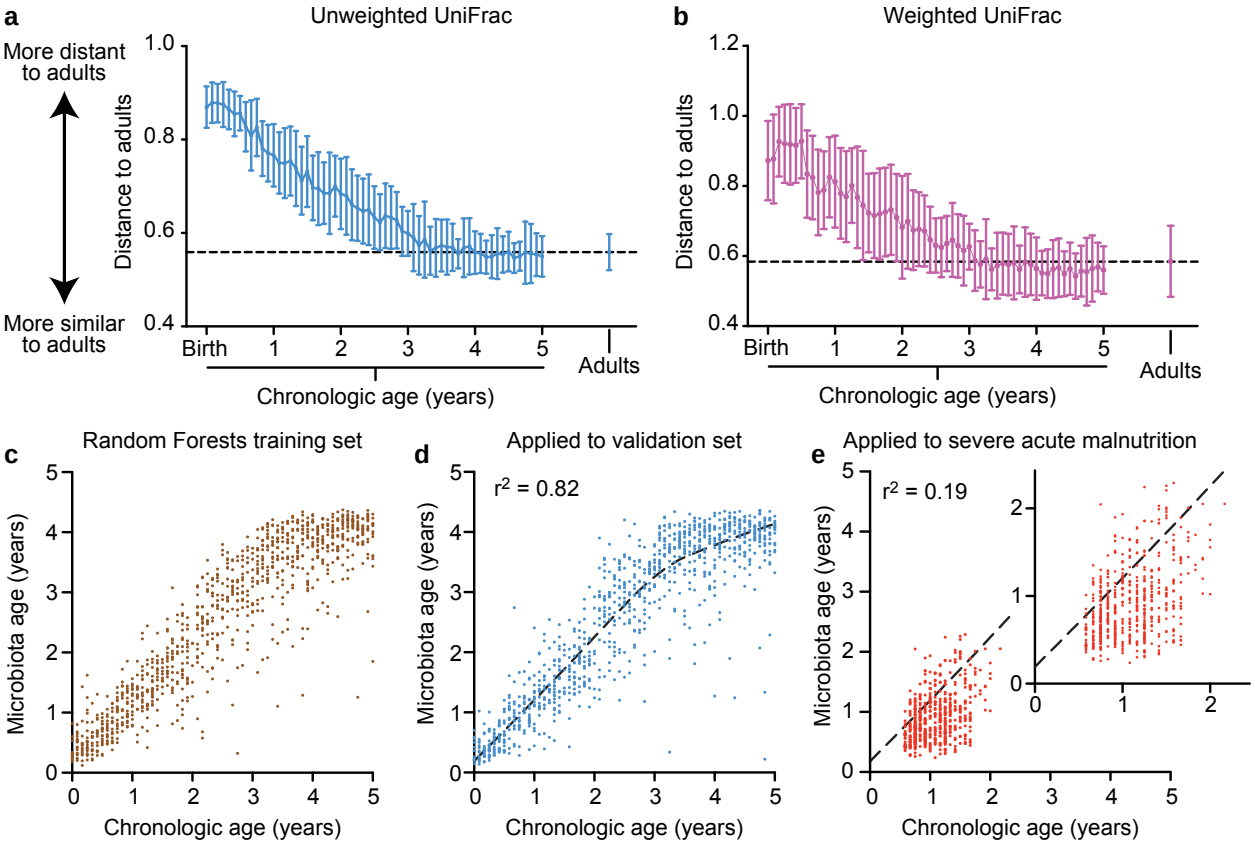
a
Unweighted UniFrac
More distant to adults
More similar to adults
Distance to adults
1.0
0.8
0.6
0.4
Birth
1
2
3
4
5
Adults
Chronologic age (years)
b
Weighted UniFrac
1.2
1.0
0.8
0.6
0.4
c
Random Forests training set
Microbiota age (years)
d
Applied to validation set
r2 = 0.82
e
Applied to severe acute malnutrition
r2 = 0.19

Figure 3.

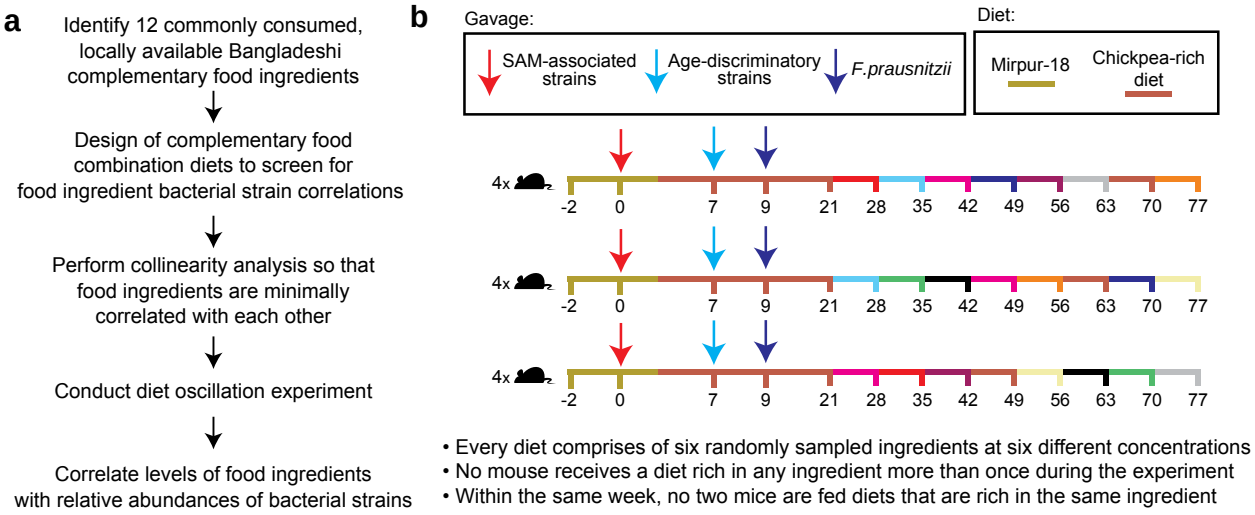

c

Age-discriminatory strains	Chickpeas	Raw banana	Peanuts	Tilapia	Whole wheat flour	Red lentils	Rice	Sweet pumpkin	Spinach	Egg	Potato
Faecalibacterium prausnitzii	0.64	0.42	0.16	0.20	0.00	-0.25	-0.06	-0.40	-0.08	-0.34	-0.39
Dorea longicatena	0.50	0.26	0.41	0.40	0.24	-0.24	-0.19	-0.33	-0.14	-0.50	-0.54
Dorea formicigenerans	-0.08	0.06	0.71	-0.06	-0.01	0.07	-0.18	0.05	-0.08	-0.43	-0.42
Blautia luti	0.52	0.20	0.18	0.36	0.41	0.20	-0.26	-0.14	-0.21	-0.53	-0.58
Ruminococcus torques	0.54	0.08	-0.09	0.10	-0.11	-0.08	0.04	-0.22	-0.26	-0.01	0.03
Ruminococcus obeum	0.16	0.64	0.17	-0.05	-0.15	-0.13	-0.10	-0.16	-0.04	-0.29	-0.26
Bifidobacterium longum / breve	-0.35	-0.25	-0.13	-0.30	0.01	0.54	0.30	0.31	-0.19	0.25	0.12
SAM-associated strains											
Streptococcus pasteurianus	0.14	-0.06	0.56	0.01	-0.05	-0.20	-0.11	-0.18	0.17	-0.33	-0.32
Enterococcus avium	-0.18	-0.19	-0.32	0.08	0.23	0.30	0.30	0.00	-0.16	0.37	-0.08
Escherichia fergusonii	0.14	0.71	0.08	0.02	-0.08	-0.24	-0.06	-0.31	0.17	-0.27	-0.35

p = <.05 (false discovery corrected)

Pearson's r: 0.71 — 0 — -0.58

Figure 4.

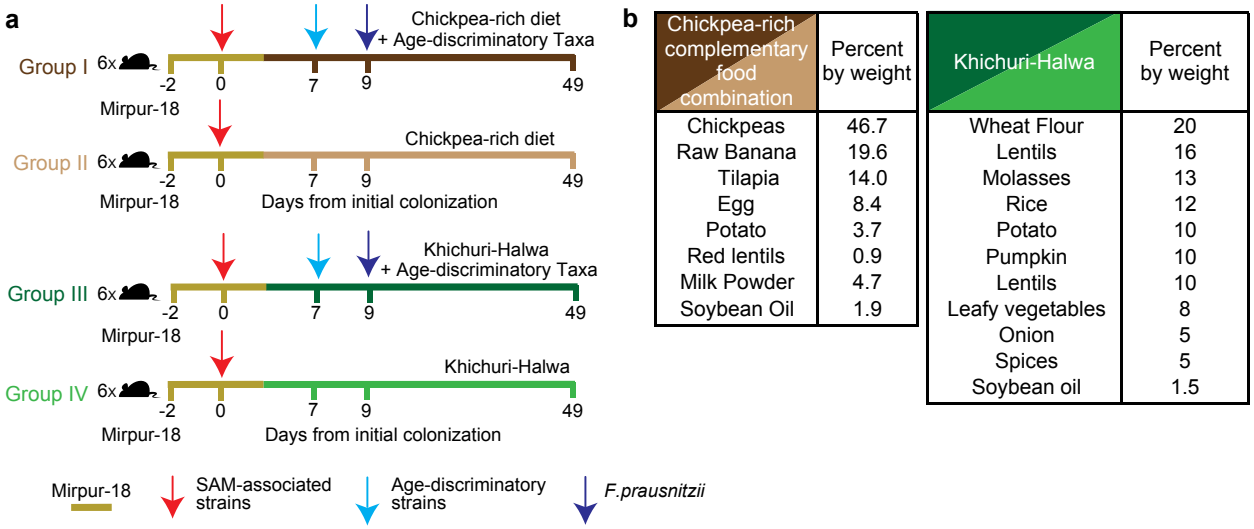

b

Chickpea-rich complementary food combination	Percent by weight
Chickpeas	46.7
Raw Banana	19.6
Tilapia	14.0
Egg	8.4
Potato	3.7
Red lentils	0.9
Milk Powder	4.7
Soybean Oil	1.9

Khichuri-Halwa	Percent by weight
Wheat Flour	20
Lentils	16
Molasses	13
Rice	12
Potato	10
Pumpkin	10
Lentils	10
Leafy vegetables	8
Onion	5
Spices	5
Soybean oil	1.5

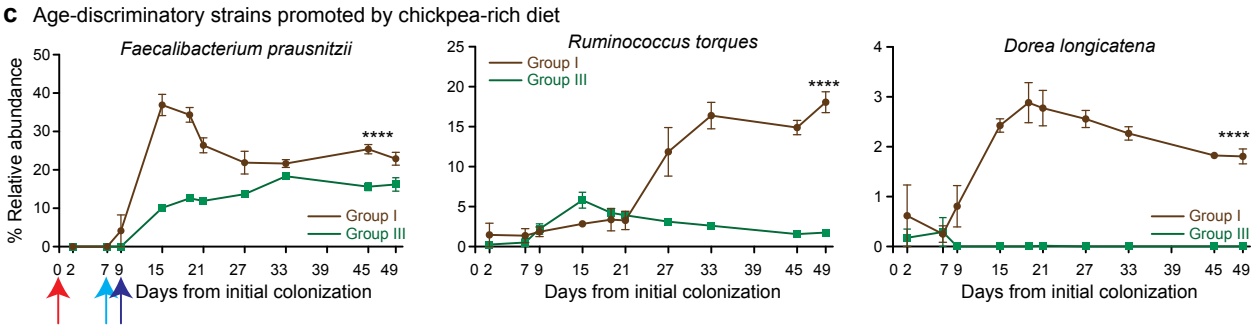

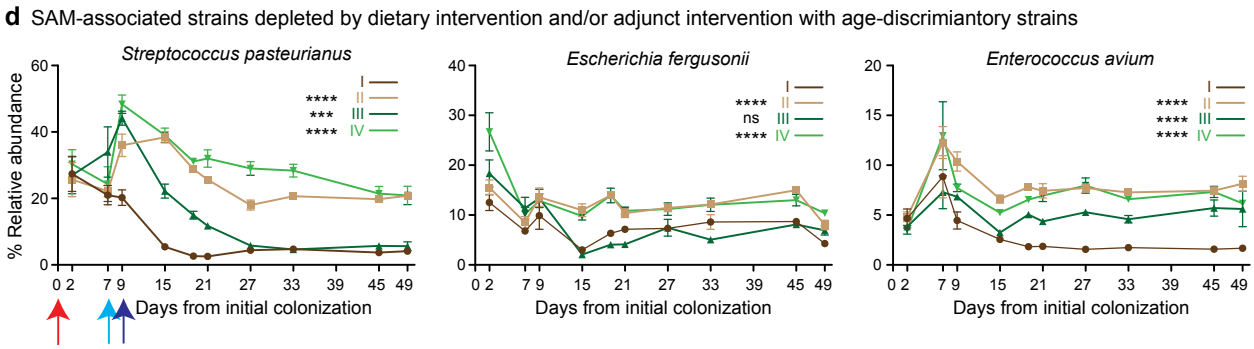

Figure 5.

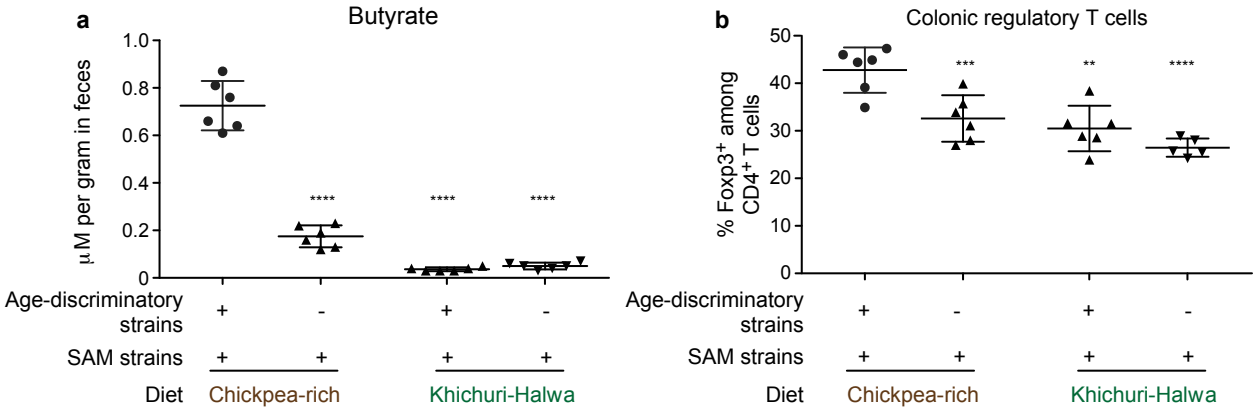
a
Butyrate
μM per gram in feces
1.0
0.8
0.6
0.4
0.2
0
****
****
****
Age-discriminatory strains
+
-
+
-
SAM strains
+
+
+
+
Diet
Chickpea-rich
Khichuri-Halwa
b
Colonic regulatory T cells
% Foxp3+ among CD4+ T cells
50
40
30
20
10
0
***
**
****
Age-discriminatory strains
+
-
+
-
SAM strains
+
+
+
+
Diet
Chickpea-rich
Khichuri-Halwa

Table Legends

Table 1 – Age-discriminatory and SAM-associated strains cultured from Bangladeshi donors.

Table 2 – Composition of complementary food diets. The red asterisk denotes irradiated diets that did not pass sterility testing and were excluded from further analysis in gnotobiotic mice.

Table 3 – Testing for collinearity among ingredients in the diet oscillation experiment in gnotobiotic mice colonized with age-discriminatory and SAM-associated strains. The Pearson's correlation matrix between each ingredient's levels with the levels of all other ingredients during each diet oscillation week is shown. The maximum collinearity observed was 0.63 between levels of milk-powder and red lentils.

Tables

Table 1.

97% OTU ID	Age discriminatory feature importance ranking					Full-length 16S-based taxonomy	Donor Sample	Cohort
	Bangladesh 2 year	Aggregate 2 year	India 2 year	Peru 2 year	Bangladesh 5 year			
72820	5	6	2	5	14	*Bifidobacterium breve*	Bgsng463m5.93	Bangladesh Healthy
72820	5	6	2	5	14	*Bifidobacterium longum*	Bgsng463m5.93	Bangladesh Healthy
361809	13	25	15	75	42	*Ruminococcus torques*	Bgsng7063.m22	Bangladesh Healthy
185951	23	36	4	38	51	*Blautia luti*	Bgsng7063.m22	Bangladesh Healthy
326792	1	2	3	1	23	*Faecalibacterium prausnitzii*	Bgsng7063.m22	Bangladesh Healthy
469873	22	28	20	4	12	*Bifidobacterium catenulatum*	Bgsng468m22.84	Bangladesh Healthy
191687	4	12	8	2	35	*Dorea longicatena*	Bgsng7063.m19	Bangladesh Healthy
178122	32	9	7	43	6	*Ruminococcus obeum*	Bgsng7063.m19	Bangladesh Healthy
261912	12	8	13	3		*Dorea formicigenerans*	Bgsng7063.m19	Bangladesh Healthy
554755	36	41	37	16		*Enterococcus avium*	BgSAM2.39.S1	Bangladesh SAM
den5505						*Bifidobacterium pseudocatelunatum*	BgSAM2.39.S1	Bangladesh SAM
50448						*Streptococcus gordonii*	BgSAM2.39.S1	Bangladesh SAM
50448						*Streptococcus constellatus*	BgSAM2.39.S1	Bangladesh SAM
316587						*Streptococcus pasteriuanus*	BgSAM2.39.S1	Bangladesh SAM
305760	37	49	52	52		*Escherichia fergusonni*	BgSAM2.39.S1	Bangladesh SAM
108747	14	60		27	44	*Streptococcus salivarius*	BgSAM2.39.S1	Bangladesh SAM

Isolated age-discriminatory strains and SAM-associated strains

Table 2.

Complementary food combination 1	Complementary food combination 2	Complementary food combination 3	Complementary food combination 4	Complementary food combination 5	Complementary food * combination 6	Complementary food combination 7	Complementary food * combination 8	Complementary food combination 9	Complementary food combination 10	Complementary food combination 11	Complementary food combination 12	%	G/kg
Spinach	Potato	Peanuts	Raw banana	Tllapia	Rice	Milk powder	Red lentils	Chickpeas	Sweet pumpkin	Whole wheat flour	Egg	46.7	467.3
Egg	Rice	Milk powder	Spinach	Chickpeas	Red lentils	Whole wheat flour	Tllapia	Raw banana	Potato	Peanuts	Sweet pumpkin	19.6	196.3
Potato	Egg	Red lentils	Peanuts	Milk powder	Chickpeas	Sweet pumpkin	Whole wheat flour	Tllapia	Rice	Spinach	Raw banana	14.0	140.2
Milk powder	Red lentils	Sweet pumpkin	Rice	Whole wheat flour	Peanuts	Spinach	Raw banana	Egg	Chickpeas	Potato	Tllapia	8.4	84.1
Sweet pumpkin	Milk powder	Spinach	Chickpeas	Raw banana	Whole wheat flour	Egg	Peanuts	Potato	Red lentils	Tllapia	Rice	3.7	37.4
Rice	Chickpeas	Whole wheat flour	Egg	Sweet pumpkin	Tllapia	Raw banana	Potato	Red lentils	Spinach	Milk powder	Peanuts	0.9	9.3
Milk powder	Milk powder	Milk powder	Milk powder	Milk powder	Milk powder	Milk powder	Milk powder	Milk powder	Milk powder	Milk powder	Milk powder	4.7	46.7
Soybean oil	Soybean oil	Soybean oil	Soybean oil	Soybean oil	Soybean oil	Soybean oil	Soybean oil	Soybean oil	Soybean oil	Soybean oil	Soybean oil	1.9	18.7

Complementary food combination 13	Complementary food combination 14	Complementary food combination 15	Complementary food combination 16	Complementary food combination 17	Complementary food * combination 18	Complementary food combination 19	Complementary food combination 20	Complementary food combination 21	Complementary food combination 22	Complementary food combination 23	Complementary food combination 24	%	G/kg
Potato	Egg	Red lentils	Peanuts	Milk powder	Chickpeas	Sweet pumpkin	Whole wheat flour	Tllapia	Rice	Spinach	Raw banana	37.38	373.83
Egg	Rice	Milk powder	Spinach	Chickpeas	Red lentils	Whole wheat flour	Tllapia	Raw banana	Potato	Peanuts	Sweet pumpkin	22.43	224.30
Sweet pumpkin	Milk powder	Spinach	Chickpeas	Raw banana	Whole wheat flour	Egg	Peanuts	Potato	Red lentils	Tllapia	Rice	15.89	158.88
Milk powder	Red lentils	Sweet pumpkin	Rice	Whole wheat flour	Peanuts	Spinach	Raw banana	Egg	Chickpeas	Potato	Tllapia	11.21	112.15
Rice	Chickpeas	Whole wheat flour	Egg	Sweet pumpkin	Tllapia	Raw banana	Potato	Red lentils	Spinach	Milk powder	Peanuts	4.67	46.73
Spinach	Potato	Peanuts	Raw banana	Tllapia	Rice	Milk powder	Red lentils	Chickpeas	Sweet pumpkin	Whole wheat flour	Egg	1.87	18.69
Milk powder	Milk powder	Milk powder	Milk powder	Milk powder	Milk powder	Milk powder	Milk powder	Milk powder	Milk powder	Milk powder	Milk powder	4.67	46.73
Soybean oil	Soybean oil	Soybean oil	Soybean oil	Soybean oil	Soybean oil	Soybean oil	Soybean oil	Soybean oil	Soybean oil	Soybean oil	Soybean oil	1.87	18.69

Composition of complementary food combinations

* - did not pass sterility testing

Table 3.

	Chickpeas	Egg	Milk powder	Peanuts	Potato	Raw banana	Red lentils	Rice	Spinach	Sweet pumpkin	Tilapia	Whole wheat flour
Chickpeas	1.00	-0.09	-0.37	-0.24	-0.17	0.28	-0.30	-0.12	-0.33	-0.25	0.39	-0.24
Egg	-0.09	1.00	0.17	-0.35	0.18	-0.24	-0.16	0.19	0.11	-0.05	-0.30	-0.23
Milk powder	-0.37	0.17	1.00	0.17	-0.24	-0.48	0.62	-0.23	0.03	0.02	-0.01	-0.19
Peanuts	-0.24	-0.35	0.17	1.00	-0.34	0.04	0.02	-0.21	0.01	-0.10	-0.15	0.07
Potato	-0.17	0.18	-0.24	-0.34	1.00	-0.31	-0.07	0.45	-0.05	0.12	-0.27	-0.21
Raw banana	0.28	-0.24	-0.48	0.04	-0.31	1.00	-0.37	-0.18	0.05	-0.27	0.06	0.01
Red lentils	-0.30	-0.16	0.62	0.02	-0.07	-0.37	1.00	0.18	-0.04	0.06	-0.34	-0.14
Rice	-0.12	0.19	-0.23	-0.21	0.45	-0.18	0.18	1.00	-0.18	-0.10	-0.37	-0.33
Spinach	-0.33	0.11	0.03	0.01	-0.05	0.05	-0.04	-0.18	1.00	-0.03	-0.36	-0.21
Sweet pumpkin	-0.25	-0.05	0.02	-0.10	0.12	-0.27	0.06	-0.10	-0.03	1.00	-0.27	0.06
Tilapia	0.39	-0.30	-0.01	-0.15	-0.27	0.06	-0.34	-0.37	-0.36	-0.27	1.00	0.42
Whole wheat flour	-0.24	-0.23	-0.19	0.07	-0.21	0.01	-0.14	-0.33	-0.21	0.06	0.42	1.00

Numbers indicate Pearson's coefficient of correlation to determine collinearity between any two ingredients across all diets

Extended Data Figure Legends

Extended Data Figure 1 – Sample size estimation for Random Forests model training and the reciprocal application of sufficiently powered sparse country-specific models from Bangladesh, India and Peru. To determine the adequate sample size needed for our studies of gut microbiota assembly in children raised in different countries, a subsampling of the training set of healthy Bangladeshi children (n=25) was performed and validated on a separate set of 25 children in this two year birth cohort study. (a,b) As the number of children incorporated into a model reduces there is a reduction in the correlation coefficients (panel a) and an increase in the mean-squared error rate (panel b). These effects plateau after above 12 children are included in the model training. (c) Based on the sample-size estimation, two country-specific datasets in India (n=14 participants) and Peru (n=22) have sufficient replication to warrant construction of country-specific Random Forests models of gut microbiota development. A given country-specific model was reciprocally applied to datasets generated from members of the birth cohorts studied in the other two countries. Each plot details the country in which the model was generated, the country the 16S rRNA dataset originates from and the correlation coefficient observed between the chronologic age of the child when a sample was obtained and the predicted age of his/her fecal microbiota.

Extended Data Figure 2 – Age-discriminatory taxa in India and Peru ranked by their feature importance scores. (a,b) The most discriminatory taxa in the Random Forests models constructed in India and Peru respectively are shown. The x-axis plots the increase in mean-squared error when values from each OUT are randomly permuted. The inset shows the cross-validation curves that result from reducing the number of 97% ID OTUs used for model training.

Extended Data Figure 3 – Daily dietary data collected from 36 Bangladeshi children sampled monthly during the first 60 months of postnatal life. Diet profiles are sorted in ascending order of the fraction of time each child was fed exclusively with family foods. The legend indicates the types of food and the associated abbreviations. Abbreviations: BM, breast milk; CM, liquid cows milk, PM, powdered milk; Ata*, Bangla* term synonymous with whole wheat.

Extended Data Figure 4 – Beta and alpha diversity measurement of fecal microbiota sampled monthly during the first 5 postnatal years in a Bangladeshi birth cohort living in Mirpur. (a,b) Non-phylogenetic metrics of beta-diversity were calculated for each sampled child (n=36 children, 1961 samples) relative to samples profiled from unrelated adults (n=12 adult Bangladeshi males, 49 samples) using Binary-Jaccard and Hellinger distances. Mean values ± SD are plotted for each monthly bin up to 60 months. As a reference control, the distances between adult samples relative to one another are plotted on the far right of each plot. (**c,d**) The metrics of alpha-diversity (Shannon Diversity Index and Phylogenetic Distance) are also plotted for each monthly bin and for adult samples. Mean values ± SD are plotted.

Extended Data Figure 5 – Ranking of feature importance scores in the 5-year Bangladeshi Random Forests model, and their relative abundances in the fecal microbiota of the study population. (**a**) The top ranked 36 most age-discriminatory taxa in the 5-year model are shown here in order of decreasing feature importance. The x-axis shows mean-squared error for each of OTU and the inset of a shows the results of cross-validation, i.e., the error-rate as a function of the number of 97% OTU ID predictors used. (**b)** Heatmap showing the monthly distribution of relative abundances of the top 60 most age-discriminatory taxa in the 5-year model. Note that a subset of the age-discriminatory discriminatory strains in the sparse 2-year Random Forests model remain at 5 years, included the same strains of *Faecalibacterium prausnitzii*, *Ruminococcus obeum* and *Bifidobacterium longum*. Of note, taxa with the same taxonomic annotation but different temporal patterns of relative abundances are observed with *Faecalibacterium prausnitzii* and *Ruminococcus obeum*. The significance of this strain-level and temporal variation is unknown.

Extended Data Figure 6 – Relative abundances of cultured age-discriminatory and SAM-associated strains in the fecal microbiota of Bangladeshi children with SAM compared to the cohort of healthy subjects. (**a-h**) Relative abundances of nine of the age-discriminatory strains in fecal samples collected monthly from healthy subjects (n=50) samples from SAM subjects prior to nutritional rehabilitation (n=75). Note that *Bifidobacterium breve* and *longum* cannot be distinguished based on their V4-16S rRNA sequences. (i-l) Relative abundances of four of the

SAM-associated strains in these two groups. Data for the healthy reference cohort is plotted as the mean±SD for each monthly bin. Each red dot represents a fecal sample collected from a child with SAM prior to nutritional rehabilitation.

Extended Data Figure 7 –Genes in the Virulence Factor Database with homologs in the genomes of age-discriminatory and SAM-associated strains. Virulence factors were screened using BLAST (e-value cutoff, 10^{-3}) against the virulence factor database (VFDB). The number of unique virulence factors found in each genome is plotted. The age-discriminatory strains and SAM-associated strains are sorted in ascending order of number of genes detected.

Extended Data Figure 8 – Cecal short-chain fatty acid levels in gnotobiotic mice treated with the chickpea-enriched MDCF with or without the 9-member consortium of cultured age-discirminatory strains, and correlations between levels of different short chain fatty acids and relative abundance of *F. prausnitzii* in the fecal microbiota of these mice. The experimental design is shown in **Figure 4a**. (**a**) Butyrate, measured in cecal contents, is plotted for each experimental group. Cecal butyrate levels are significantly greater when the age-discriminatory taxa are introduced in both dietary contexts (****, $p<0.0001$; ANOVA followed by post-hoc Bonferonni adjustment). (**b**) Correlation between the relative abundance of *F. prausnitzii* in cecal contents and levels of butyrate (Pearson's $r^2=0.73$, $p<0.001$). (**c**) Correlation between fecal levels of *F.prausnitzii* and colonic levels of $Foxp3^+$ $CD4^+$ T cells (Pearson's r, $p<0.01$). (**d**,**e**) Levels of acetate and succinate in cecal contents show a similar pattern to the colonic regulatory T cell patterns observed in panel b. Cecal acetate and succinate levels are significantly elevated in the group of animals treated with the chickpea-rich MDCF plus age-discriminatory strain consortium compared to all other experimental groups (**, $p<0.01$; ***, $p<0.001$;****, $p<0.0001$; ANOVA followed by post-hoc Tukey's comparisons).

Extended Data Figures

Extended Data Figure 1

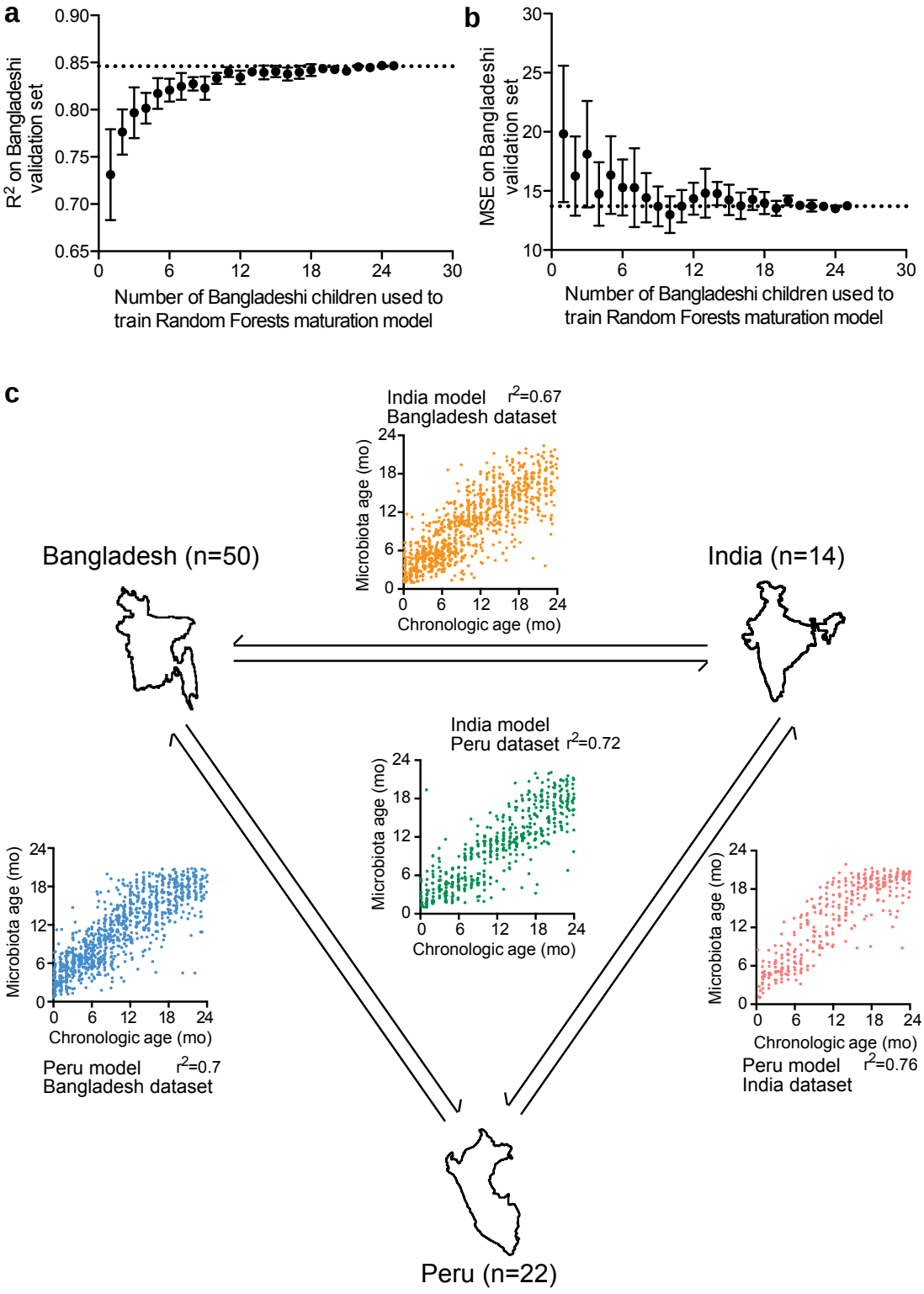

Extended Data Figure 2.

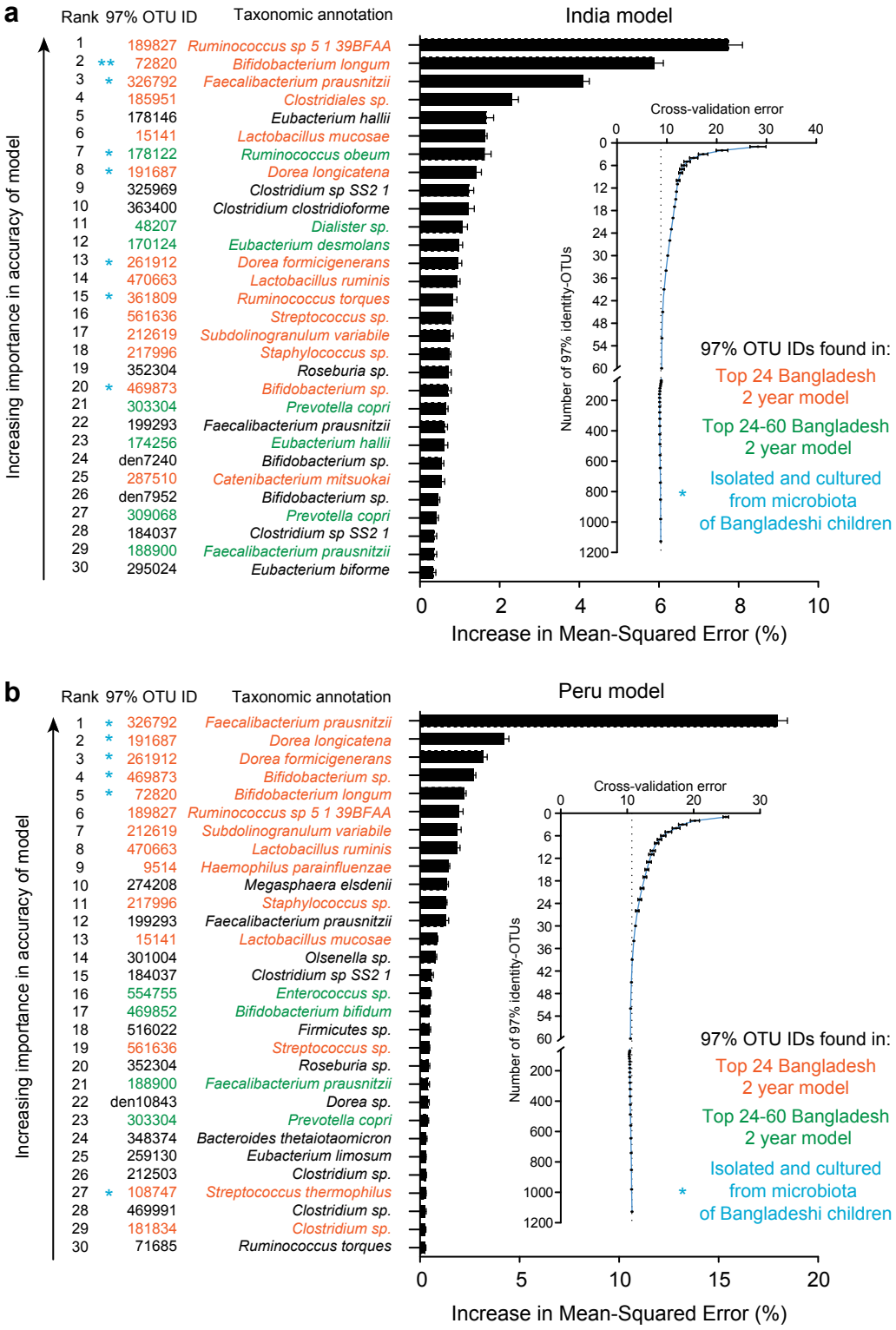

Extended Data Figure 3

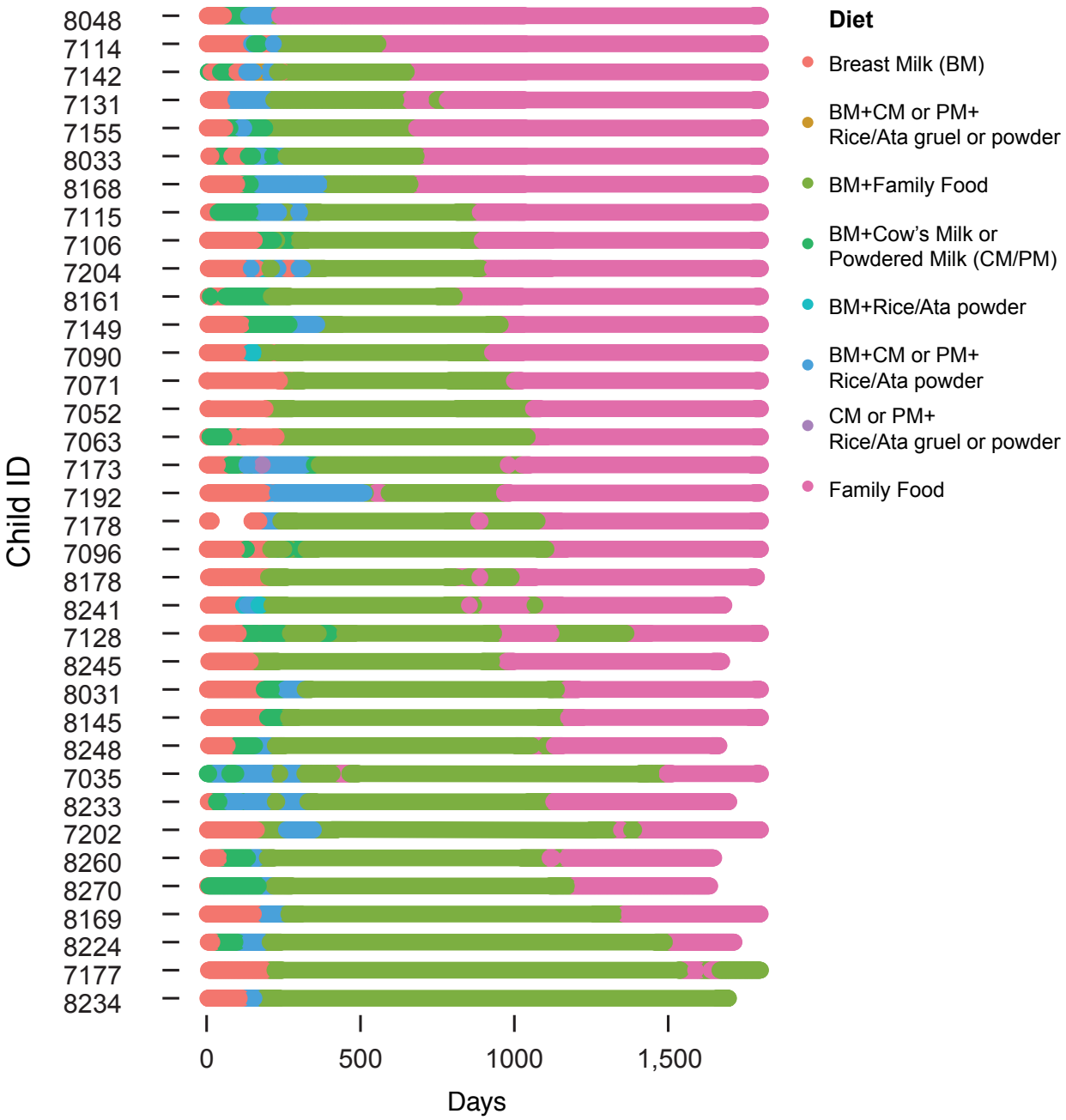

Extended Data Figure 4

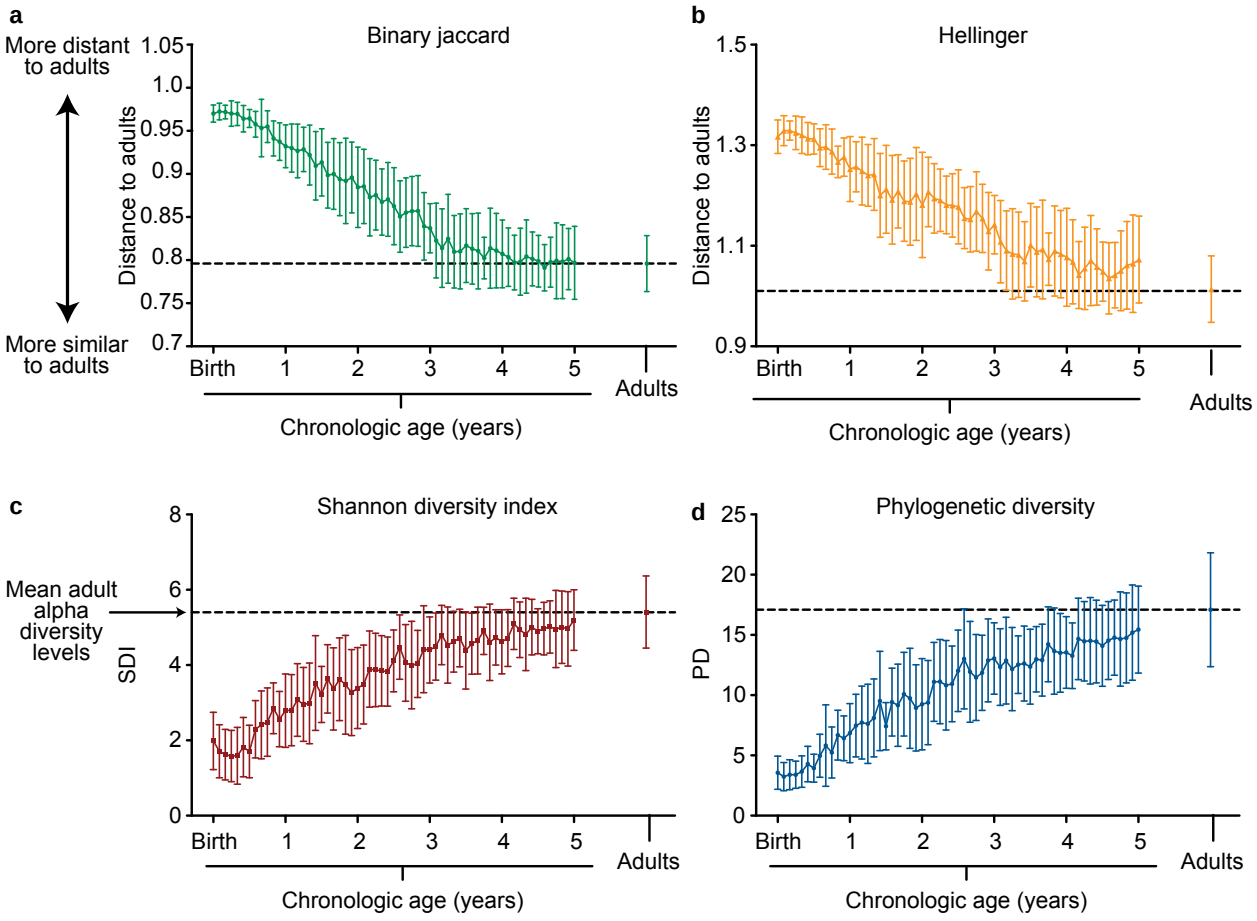

Extended Data Figure 5

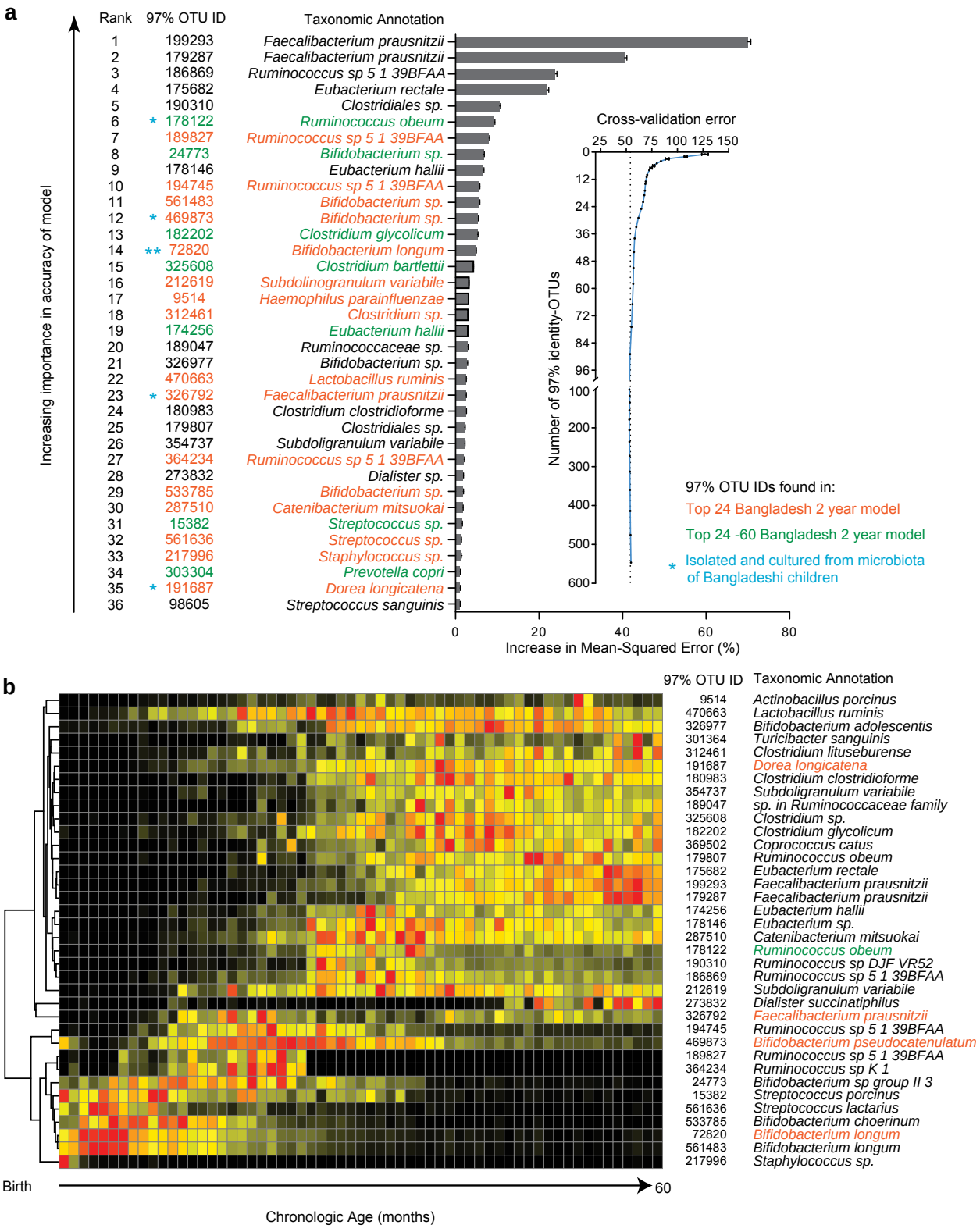

Extended Data Figure 6

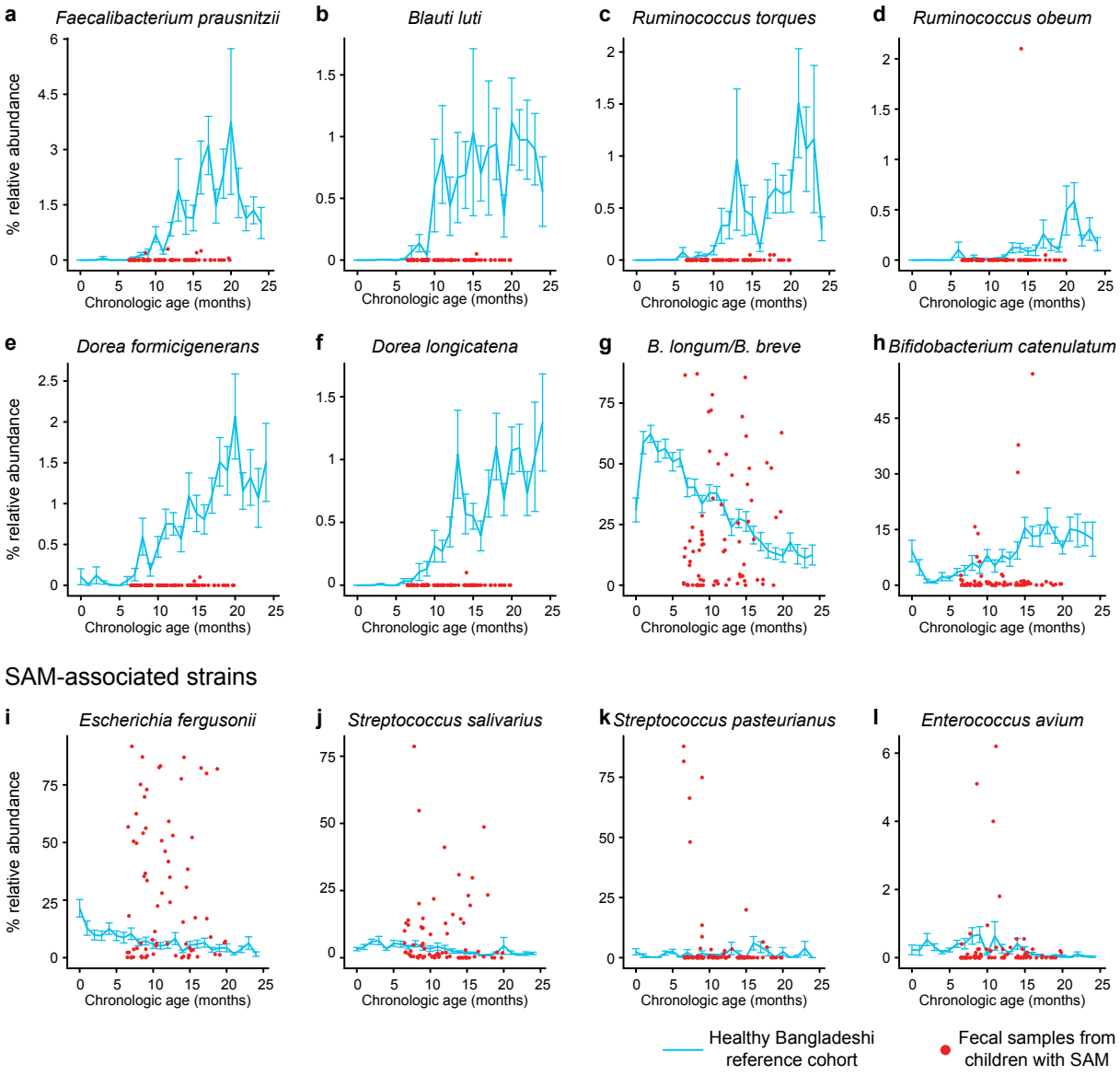

Extended Data Figure 7

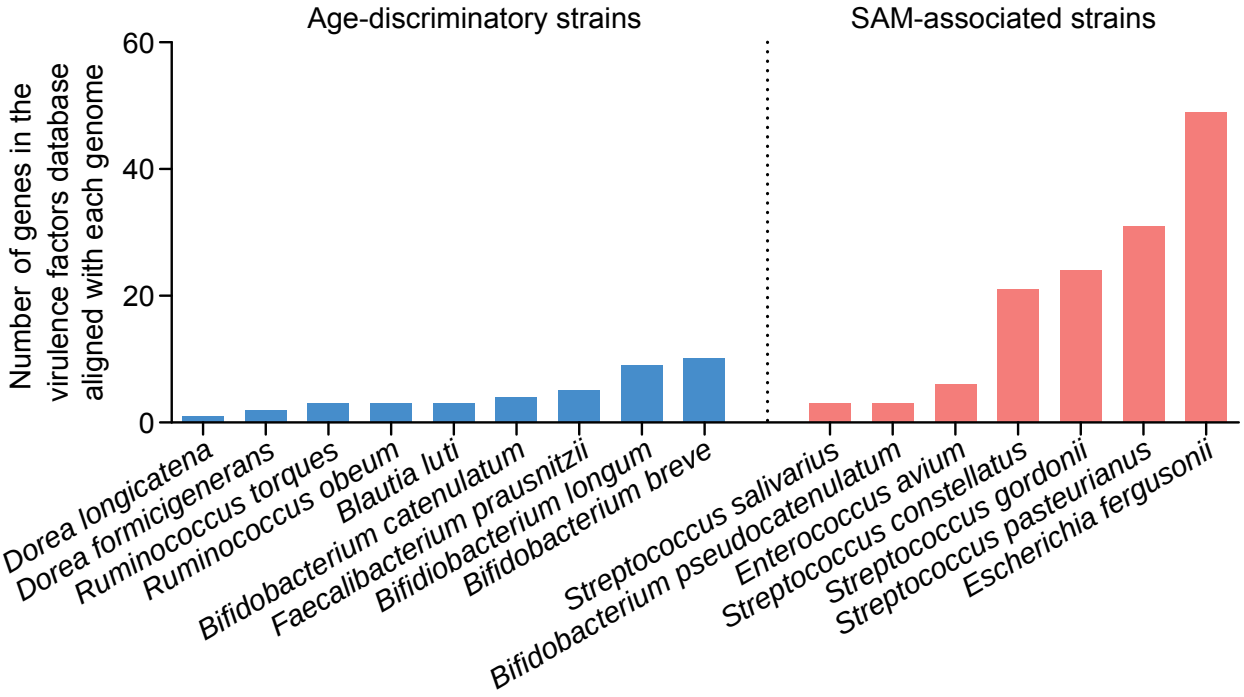

Extended Data Figure 8

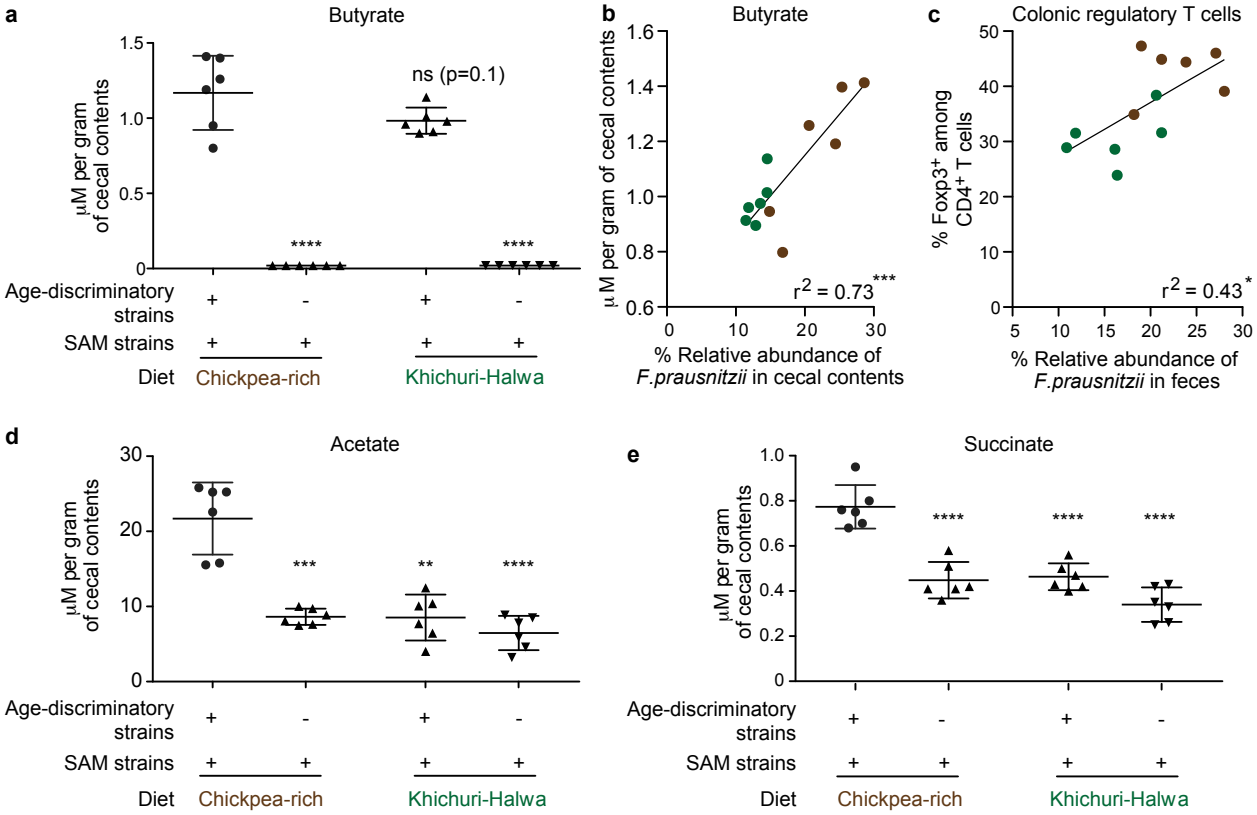

Extended Data Table Legends

Extended Data Table 1 - Metadata for healthy children sampled monthly during the first two years of life from four different MAL-ED sites

Extended Data Table 2 – Information associated with individual fecal samples collected from consistently healthy children followed from birth from four different MAL-ED sites

Extended Data Table 3 - Information associated with fecal samples collected from Bangladeshi children sampled monthly from birth through 60 months of age.

Extended Data Table 4 – Cultured age-discriminatory and SAM-associated bacterial strains.

Extended Data Table 5 – Analysis of virulence factor gene content and the representation of metabolic pathways involved in short chain fatty acid production in cultured age-discriminatory bacterial strains.

Extended Data Table 6 - Composition and nutritional analysis of diets used in the diet-oscillation experiments.

Extended Data Table 7 - Pairwise testing for collinearity between food ingredients.

Extended Data Table 8 - Sequence of diets administered during diet-oscillation experiment shown in Figure 3.

Extended Data Table 9 - Diets administered to mice in the experiment shown in Figure 4.

Extended Data Table 10 - Information associated with fecal samples obtained from the diet oscillation experiment shown in Figure 3.

Extended Data Table 11 - Associations between relative abundances of bacterial strains in the fecal microbiota of gnotobiotic mice treated with the chickpea-enriched MDCF or Khichuri-Halwa, with or without addition of the nine age-discriminatory taxa.

Supplementary Information

Supplementary Methods

Metabolic reconstructions of cultured age-discriminatory bacterial strains

Analysis of virulence factors present in cultured SAM-enriched taxa

Microbial RNA-Seq analysis of community and individual strain responses to the chickpea-enriched MDCF.

Chapter 4

Future Directions

Introduction

This chapter focuses on ways for testing the generalizability by which a complementary food could promote maturation of the gut microbiota, and how these lines of inquiry may extend to future field-based research.

Generalizability of chickpea-associated effects on age-discriminatory taxa isolated from different donors and 'background' recipient donors

The discovery that a chickpea-based diet supplement can increase the relative abundances of several age-discriminatory taxa, increase butyrate production by the artificial, defined, human gut microbiota installed in gnotobiotic mice and increase the regulatory T cell population in the colon serves as a starting point for a systematic evaluation of two factors: 'effector-strain' variation in relation to phenotypes and secondly, the effect of background-community variation to an established effector strain-mediated phenotype. As an example, assuming that the phenotypes observed are shown to be dependent on a single member of the 9-member consortium of age-discriminatory strains, (e.g., *Faecalibacterium prausnitzii*), the following systematic matrix of experimental manipulations could be highly informative.

Firstly, multiple OTUs with a taxonomic annotation of *Faecalibacterium prausnitzii* were identified in each of the Random Forests models constructed from Bangladesh, Peru, India, as well as the extended five year Bangladeshi model. Several of these are exact matches in terms of their V4 16S rRNA gene sequence, while others are distinct sequences. Isolation and comparative genomic analyses of these strains would enable an understanding of the extent to which their gene content is conserved. It is notable that the OTU variants (strains) of *Faecalibacterium prausnitzii* that were cultured have distinct sequences from the strain with the highest feature importance score in the five year Bangladeshi Random Forests model of microbiota maturation. One hypothesis is that different strains of *F. prausnitzii* have somewhat different niches at different stages of gut microbial community development: e.g., at earlier ages, breast milk is a prominent component of the diet whereas a child is completely weaned by their fifth postnatal year.

Isolating multiple strains of *F. prausnitzii* would allow a series of precise substitution experiments to be performed. The Bangladeshi strain of *F.prausnitzii* within the 16-member community described in Chapter 3, could be systematically substituted with other Bangladeshi *F.prausnitzii* strains that have been cultured from donors having similar chronologic ages, with several different age bins represented in the culture collection. Similarly, the Bangladeshi strain could be removed from the artificial, defined, human gut microbiota that was used to colonized gnotobiotic mice and strains from other donors representing other geographic sites (e.g. Malawi, Peru) but comparable ages at the Bangladeshi donors introduced instead. Once these manipulated communities are transplanted into gnotobiotic mice, animals could be divided into chickpea-supplemented and control diets to determine the extent to which strain-level variation can influence butyrate production, colonic regulatory T cell homeostasis and other phenotypes that might be identified in the future.

Another equally interesting approach to exploring the robustness of chickpea-based effects observed in Chapter 3 would be to repeat the food intervention on a number of different microbiota, ideally obtained from children who following SAM and therapeutic food-interventions continue to harbor a persistently immature gut microbiota relative to healthy reference controls. Here, the chickpea-based intervention could be applied to gnotobiotic animals with transplanted intact uncultured donor microbiota to see if the food intervention can promote age-discriminatory strains that are already resident in the input fecal sample. One advantage to this approach is that an uncultured intact microbiota sample encompasses more diversity than a derived culture collection and multiple samples from multiple donors (each transplanted into a separate group of germ-free mice) captures interpersonal variations in community structure that are present in a human population. However, this is also a major caveat compared to the defined community approach used in Chapter 3: the defined community approach enables a consistent community to be installed across many different mice so that the effects of a given or different complementary foods on members of that cultured consortia can be analyzed within members of a given treatment group and across experiments. In contrast, depending upon the speed in which a donor's fecal sample is frozen at -80^{o}C, microbial viability is affected resulting in varying colonization efficiencies and variations

in the representation of age-discriminatory taxa in recipient animals. An alternative is to introduce a consortium of age-discriminatory effector strains together with an intact uncultured fecal sample so that these strains can be reliably represented in recipient mice: the effects of a chickpea supplemented diet can then be tested in different community contexts.

Impact of complementary foods on host metabolism, immunity and other phenotypes

The effects of a microbiota-directed complementary food (MDCF) on host metabolism can be evaluated in gnotobiotic mice using an approach similar to that described in Chapter 3 where chickpea MDCF versus the Khichuri-Halwa therapeutic food administered to animal with the 9-member consortium of age-discriminatory strains plus the 7 SAM-associated strains and targeted and non-targeted mass spectroscopy performed on serum, liver, skeletal muscle and brain samples. A recent study of children with severe undernutrition in Uganda prior to, during and after dietary rehabilitation, showed that as children gained weight, there were dramatic changes in serum levels of fatty acids, amino acids and hormones including leptin and insulin (Bartz et al., 2014). Leptin was found to be a predictor of mortality in this study. However it is still unclear as to how these metabolic profiles compare to healthy reference age-matched controls. To clarify this question, further assays of metabolites and hormones using serum samples from the same children at the MAL-ED sites that were used for our analyses of gut microbiota maturation could be compared to children with SAM in an ongoing clinical trial in Bangladesh. Moreover, such a study would provide a point of comparison for our gnotobiotic mouse models and help us in our efforts to identify robust and potentially translatable metabolic biomarkers of responses to lead MDCFs. Food ingredient/bacterial strain combinations can be tested in our preclinical gnotobiotic models for their ability to modulate metabolic phenotypes identified as being transmitted by immature microbiota obtained from children with SAM, or those who having been treated for SAM still manifest severe stunting and are underweight [i.e. those with post-SAM moderate acute malnutrition (MAM)].

In addition to perturbations in metabolism, another important feature of undernutrition is immune dysfunction, whether manifested by frequent pulmonary infections, recurrent diarrhea or

impaired vaccine responses. Children with SAM and MAM are particularly vulnerable to enteric pathogens in part due to poor sanitation. The role of microbiota immaturity in susceptibility to enteropathogen invasion and on the maturation of the gut mucosal immune system, and reciprocally the effects of a large enteropathogen burden on microbiota maturation and gut barrier function are not known. In Chapter 1, I speculate that these factors are interrelated and contribute to the still ill-defined entity known as environmental enteric dysfunction (EED; also see Kosek et al., 2014). Intriguingly, the benefits of promoting Treg representation in the gut have been explored primarily in preclinical models of colitis and food-allergen sensitization (Stefka et al., 2014; Atarashi et al., 2013; Faith, Ahern et al., 2014). Characterizing the effects of an MCDF intervention in mice with an immature donor microbiota on (i) Treg induction, (ii) maturation of the mucosal immune system (e.g., by monitoring IgA responses to members of the microbiota), gut barrier integrity (characterized by histochemical and immunocytochemical assays of the epithelium and/or by functional genomics-based studies of laser capture microdissected epithelium), (iii) resistance to invasion by enteropathogens, and (iv) growth (as judged by gain of lean body mass as assayed by quantitative magnetic resonance or by micro-CT assays of bone phenotypes) could help inform the design of clinical studies in children with undernutrition (Kau et al., 2015).

Development of new approaches with improved efficacy for treating impaired linear growth (stunting) rather than just improved ponderal growth represents a major aspirational goal of the field. Stunting is associated with a variety of co-morbidities including impaired cognitive development. Studies in the Lancet series using pooled data from five different countries showed an association between height at 2 years of age and number of years of schooling completed, after adjusting for household wealth and maternal education (Bhutta, 2013, Adair et al., 2013). The observations that gut bacterial strains can increase butyrate levels in the context of a specific diet in our studies are intriguing in the context of another study, which reported that propionate and butyrate promote intestinal gluconeogenesis via a gut-brain circuit (De Vadder et al., 2014). The investigators were able to test their hypothesis by administration of short-chain fatty acids directly to control mice and mice deficient in the intestine glucose-6 phosphatase catalytic unit. Moreover

gene expression analyses of different regions of the brain and radioactive tracers implicated specific brain signaling pathways, which should be explored in analogous mouse models of undernutrition.

Point of care diagnostics and the capacity building for microbiota research in low-income countries

An exciting aspect related to the development of metrics for defining microbiota maturation that generalize to populations of children representing different geographic locations and cultural traditions, is that these assays could be conducted at the sites where the burden of undernutrition is great. The goal would be to apply these measurements to patient populations so that their microbiota could be phenotyped, the children better stratified and efficacy better defined in clinical trials of MDCF or other interventions. This would be the first step in a journey ultimately designed to develop new ways for prevention. Another effect would be to develop a new cadre of researchers from these countries who themselves could lead clinical and basic science studies in the area of human microbial ecology.

Much, if not all, of the work presented in my thesis was made possible by large-scale research collaborations involving basic and clinical scientists from several countries. Several ethical issues have been discussed regarding large-scale research collaborations and the importance of openness in the process and challenges with informed consent (Chokshi et. al, 2006). Another related challenge for the future is the ability to prosecute 'personalized medicine' in a cost-effective manner to reach members of society that have low income and limited access to healthcare (Alyass et al., 2015).

In a parallel universe, students at the Center for Genome Sciences and Systems Biology at Washington University in St. Louis have had unrestricted floor-level access to state of the art, next-generation sequencing instruments for many years. A striking observation during my studies, has been the ability for students to make unprecedented connections in all aspects of their projects by virtue of their direct access to biospecimens (including their role in the design and execution of

plans for proper collection, storage and archiving these specimens and related de-identified meta-data), submitting DNA from those samples directly to sequencing instruments, and working on the high-performance cluster computing required for downstream analyses (including the design of new algorithms for data-mining). The interconnections between people representing different disciplinary perspectives and skill sets ('inter-connected neurons') and these materials and technology, allow dramatic moments of discovery ('synaptogenesis'), and new understanding of host biology. One could imagine that the specific technologies involved in this pipeline could in future extend to the developing world with potentially far-reaching consequences. The decreasing cost of sequencing, including the release of newer long-read, portable technology (e.g. MinION nanopore), plus the advances in cloud computing that facilitate easy installation of microbiota analysis software and publically available microbiota datasets on Amazon Web Services, hint at new and exciting possibilities (Jain et al., 2015). Looking back in time, the experimental medicine research conducted by Dr. Norbert Hirschorn and colleagues at the International Centre for Diarrhoeal Disease Research, Bangladesh (icddr,b) in 1968 that resulted in the development of oral rehydration solution has saved millions of lives and remains truly inspirational (Hirschhorn et al., 1968). The solutions to undernutrition and other vexing global health problems may very well originate in the blend of these two worlds, in societies afflicted by the condition with access to the technology to engage in further research. I am confident that the factors/forces and personal commitments needed to enable these discoveries are going to become even more permissive in the years to come.

References

Adair, L.S., Fall, C.H., Osmond, C., Stein, A.D., Martorell, R., Ramirez-Zea, M., Sachdev, H.S., Dahly, D.L., Bas, I., Norris, S.A., et al. (2013). Associations of linear growth and relative weight gain during early life with adult health and human capital in countries of low and middle income: findings from five birth cohort studies. The Lancet *382*, 525–534.

Alyass, A., Turcotte, M., and Meyre, D. (2015). From big data analysis to personalized medicine for all: challenges and opportunities. BMC Medical Genomics *8*, 33.

Atarashi, K., Tanoue, T., Oshima, K., Suda, W., Nagano, Y., Nishikawa, H., Fukuda, S., Saito, T., Narushima, S., Hase, K., et al. (2013). Treg induction by a rationally selected mixture of Clostridia strains from the human microbiota. Nature *500*, 232–236.

Bartz, S., Mody, A., Hornik, C., Bain, J., Muehlbauer, M., Kiyimba, T., Kiboneka, E., Stevens, R., Bartlett, J., St Peter, J.V., et al. (2014). Severe acute malnutrition in childhood: hormonal and metabolic status at presentation, response to treatment, and predictors of mortality. J. Clin. Endocrinol. Metab. *99*, 2128–2137.

Bhutta, Z.A. (2013). Early nutrition and adult outcomes: pieces of the puzzle. The Lancet *382*, 486–487.

Chokshi, D.A., Parker, M., and Kwiatkowski, D.P. (2006). Data sharing and intellectual property in a genomic epidemiology network: policies for large-scale research collaboration. Bull. World Health Organ. *84*, 382–387.

Hirschhorn, N., Kinzie, J.L., Sachar, D.B., Northrup, R.S., Taylor, J.O., Ahmad, S.Z., and Phillips, R.A. (1968). Decrease in Net Stool Output in Cholera during Intestinal Perfusion with Glucose-Containing Solutions. New England Journal of Medicine *279*, 176–181.

Jain, M., Fiddes, I.T., Miga, K.H., Olsen, H.E., Paten, B., and Akeson, M. (2015). Improved data analysis for the MinION nanopore sequencer. Nat Meth *12*, 351–356.

Kau, A.L., Planer, J.D., Liu, J., Rao, S., Yatsunenko, T., Trehan, I., Manary, M.J., Liu, T.-C., Stappenbeck, T.S., Maleta, K.M., et al. (2015). Functional characterization of IgA-targeted bacterial taxa from undernourished Malawian children that produce diet-dependent enteropathy. Science Translational Medicine *7*, 276ra24–ra276ra24.

Kosek, M., Guerrant, R.L., Kang, G., Bhutta, Z., Yori, P.P., Gratz, J., Gottlieb, M., Lang, D., Lee, G., Haque, R., et al. (2014). Assessment of environmental enteropathy in the MAL-ED cohort study: theoretical and analytic framework. Clin. Infect. Dis. *59 Suppl 4*, S239–S247.

Stefka, A.T., Feehley, T., Tripathi, P., Qiu, J., McCoy, K., Mazmanian, S.K., Tjota, M.Y., Seo, G.-Y., Cao, S., Theriault, B.R., et al. (2014). Commensal bacteria protect against food allergen sensitization. PNAS *111*, 13145–13150.

De Vadder, F., Kovatcheva-Datchary, P., Goncalves, D., Vinera, J., Zitoun, C., Duchampt, A., Bäckhed, F., and Mithieux, G. (2014). Microbiota-Generated Metabolites Promote Metabolic Benefits via Gut-Brain Neural Circuits. Cell *156*, 84–96.

Appendices

Appendix A

Bokulich, N.A., Subramanian, S., Faith, J.J., Gevers, D., Gordon, J.I., Knight, R., Mills, D.A., and Caporaso, J.G. (2013). **Quality-filtering vastly improves diversity estimates from Illumina amplicon sequencing.** Nat Meth *10*, 57–59.

Quality-filtering vastly improves diversity estimates from Illumina amplicon sequencing

Nicholas A Bokulich[1–3], Sathish Subramanian[4], Jeremiah J Faith[4], Dirk Gevers[5], Jeffrey I Gordon[4], Rob Knight[6,7], David A Mills[1–3] & J Gregory Caporaso[8,9]

High-throughput sequencing has revolutionized microbial ecology, but read quality remains a considerable barrier to accurate taxonomy assignment and α-diversity assessment for microbial communities. We demonstrate that high-quality read length and abundance are the primary factors differentiating correct from erroneous reads produced by Illumina GAIIx, HiSeq and MiSeq instruments. We present guidelines for user-defined quality-filtering strategies, enabling efficient extraction of high-quality data and facilitating interpretation of Illumina sequencing results.

Recent advances in high-throughput, short-amplicon sequencing are revolutionizing efforts to describe microbial diversity within and across complex biomes, including the human body[1] and Earth's biosphere[2]. The greater sequence coverage and lower per-base cost of the Illumina GAIIx, HiSeq and MiSeq instruments relative to the more expensive, lower-coverage platforms aids this progress. Given unknown sequencing error rates for amplicon data generated by these rapidly evolving instruments and changing chemistries, and the potential for PCR error introduced during short-amplicon sample preparation, quality filtering is integral to the analysis of high-throughput sequencing data because it removes erroneous reads that otherwise overestimate microbial diversity. 'Denoising'[3,4], an approach developed for quality-filtering amplicons sequenced on the Roche 454 Life Sciences pyrosequencer, does not scale to Illumina instruments, which generate tens (MiSeq) to hundreds (GAIIx) to thousands (HiSeq2000) of times more data per run.

Illumina systems provide Phred quality scores for every nucleotide, which represent the probability that a given base call is erroneous. How best to incorporate these scores in marker-gene–based microbial ecology studies has not been thoroughly investigated, and stringent filtration that discards many reads has been recommended to avoid exaggerated diversity estimates[5]. Our strategy works on a per-nucleotide basis, truncating reads at the position where their quality begins to drop. It therefore differs from Illumina's quality-filtering software CASAVA, which filters on a per-read basis. Previous investigation into quality filtering of Illumina data[6] focused on whole-genome sequencing applications, where error profiles are expected to differ from those in amplicon-sequencing runs.

We tested the effects of different quality-filtering parameters on taxonomic classification, α-diversity (within-sample diversity) and β-diversity (between-sample diversity comparison) estimates, using the 'quantitative insights into microbial ecology' (QIIME)[7] pipeline (**Fig. 1** and **Supplementary Table 1**). We tested four different 'mock' communities sequenced on the GAIIx (1 sequencing run), HiSeq (2 sequencing runs) and MiSeq (3 sequencing runs) (**Supplementary Table 2**). These comprised deliberately combined collections of 12–67 bacterial or fungal species whose genomes had been previously sequenced (**Supplementary Tables 3–6**). We also compared free-living and host-associated communities[5,8], which were samples with high β diversity, and wine[9] and spontaneous beer fermentation–associated communities[10], which were samples with lower β diversity, to evaluate the effects of filtering settings on β-diversity comparisons of different community types. Raw read counts and sample counts for all data sets are presented in **Supplementary Table 7**.

We evaluated how primary quality-filtering parameters (p, minimal high-quality read length, q Phred score, r maximum of consecutive low-quality calls and n maximum of ambiguous calls allowed) and secondary (c, operational taxonomic unit (OTU) threshold) quality-filtering parameters affect analyses using the following five separate evaluations. Evaluation 1 was an analysis of α diversity and qualitative taxonomic composition, using mock communities, to test which settings best measure true community composition, minimizing spurious additional OTUs (**Fig. 2** and **Supplementary Figs. 1–7**). Evaluation 2 was an analysis of quantitative taxonomic composition, using defined mock communities, to test whether different settings introduce biases in specific taxa (**Supplementary Figs. 8–10**). Evaluation 3 was an analysis of β diversity, using mock communities, to determine whether different settings cause significant ($P < 0.05$) differences in phylogenetic composition between identical communities (**Supplementary Table 8**). Evaluation 4 was an analysis of β diversity, using real communities, to test whether different

[1]Department of Viticulture and Enology, University of California, Davis, Davis, California, USA. [2]Department of Food Science and Technology, University of California, Davis, Davis, California, USA. [3]Foods for Health Institute, University of California, Davis, Davis, California, USA. [4]Center for Genome Sciences and Systems Biology, Washington University School of Medicine, St. Louis, Missouri, USA. [5]Microbial Systems & Communities, Genome Sequencing and Analysis Program, Broad Institute of MIT and Harvard, Cambridge, Massachusetts, USA. [6]Department of Chemistry and Biochemistry, University of Colorado, Boulder, Colorado, USA. [7]Howard Hughes Medical Institute, Boulder, Colorado, USA. [8]Institute for Genomics and Systems Biology, Argonne National Laboratory, Argonne, Illinois, USA. [9]Department of Computer Science, Northern Arizona University, Flagstaff, Arizona, USA. Correspondence should be addressed to J.G.C. (gregcaporaso@gmail.com).

RECEIVED 15 AUGUST; ACCEPTED 20 OCTOBER; PUBLISHED ONLINE 2 DECEMBER 2012; DOI:10.1038/NMETH.2276

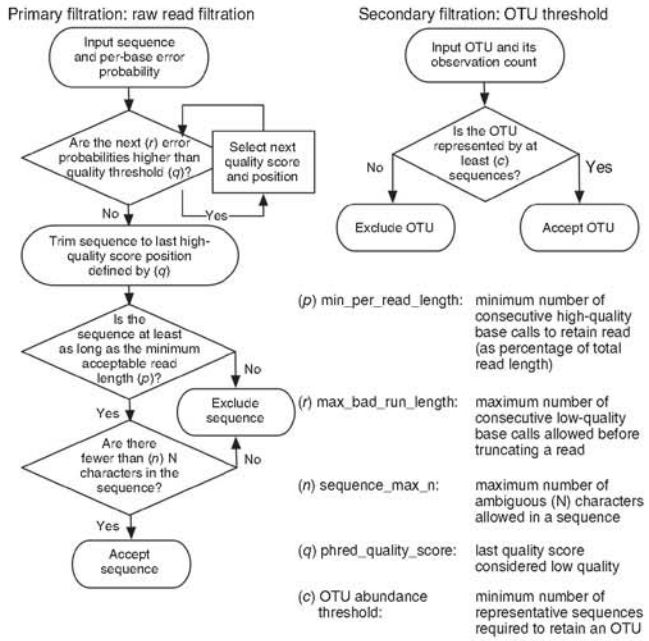

Figure 1 | Quality-filtration process flow in QIIME v1.5.0.

settings affect our ability to differentiate sample types in principal coordinates analysis (PCoA) plots (**Fig. 2**, **Supplementary Table 9** and **Supplementary Figs. 11–16**). Evaluation 5 was an analysis of β diversity, using real communities, to test whether differences detected between communities on different sequencing platforms are consistent.

Our results revealed general patterns. First, parameters *p*, *q* and *c* had a marked effect on α diversity and estimates of taxonomic composition, whereas *n* and *r* did not (**Fig. 2a**,**b** and **Supplementary Figs. 1–7**). The effects of *p* and *q* were variable across runs in an apparently platform-independent fashion (**Supplementary Figs. 4–5**). All settings except high *q* values required secondary filtration with *c* to reach expected taxon counts, but the required level varied between 0.01% to 0.0001% of total sequences, depending on *q* and *p* settings. Increasing *p* also decreased abundance of unassigned sequences and sequences given shallow taxonomic assignment. In all mock data sets studied, extreme settings of *q* and *p*, but not *r* and *n*, had a marked impact on taxonomic distribution (**Supplementary Figs. 8–10** and **Supplementary Note**). Second, weighted UniFrac[11] distances between mock communities (**Supplementary Note**) were more robust to changes in parameter settings than unweighted UniFrac distances at low *c*; however, these differences disappeared at high *c*. Thus, as expected, differences in low-abundance OTUs have a larger impact on the unweighted metric. We note that any filtering strategies that remove low-abundance reads make it impossible to apply richness estimation metrics such as abundance-based coverage estimator (ACE) and Chao1, which incorporate low-abundance read counts in their calculations. These metrics are unlikely to be accurate, however, if many of these reads actually represent sequencing errors.

Because observations in microbial ecology are often based on PCoA of samples, we applied Procrustes analysis to compare PCoA plots from different parameter settings on both biological and mock communities. We found that conclusions derived from PCoA plots were also robust to differences in parameter settings: the only notable differences occurred at stringent *q*, *p* and *c*, which resulted in extreme levels of read filtration that blurred the known major distinction between host-associated and free-living communities (**Fig. 2c–e** and **Supplementary Figs. 11**, **12**), and closely related wine and beer fermentation–associated communities (**Supplementary Figs. 13–16** and **Supplementary Note**).

Finally, these observations generalized from the GAIIx to the HiSeq2000 and MiSeq platforms. We observed the same β-diversity trends (such as separation in host-associated and free-living communities) on all three platforms, and heavily decreased *p* ($p = 0.25$) and increased *q* ($q \geq 20$) were the only factors that caused these sample types to erroneously cluster together in the HiSeq data (**Supplementary Note**).

To calibrate optimal filtering settings, we highly recommend including a standardized mock community in each individual sequencing run. We believe this will be necessary for confident comparison of samples from multiple sequencing runs to normalize run-to-run PCR and sequencing error, but additional work is

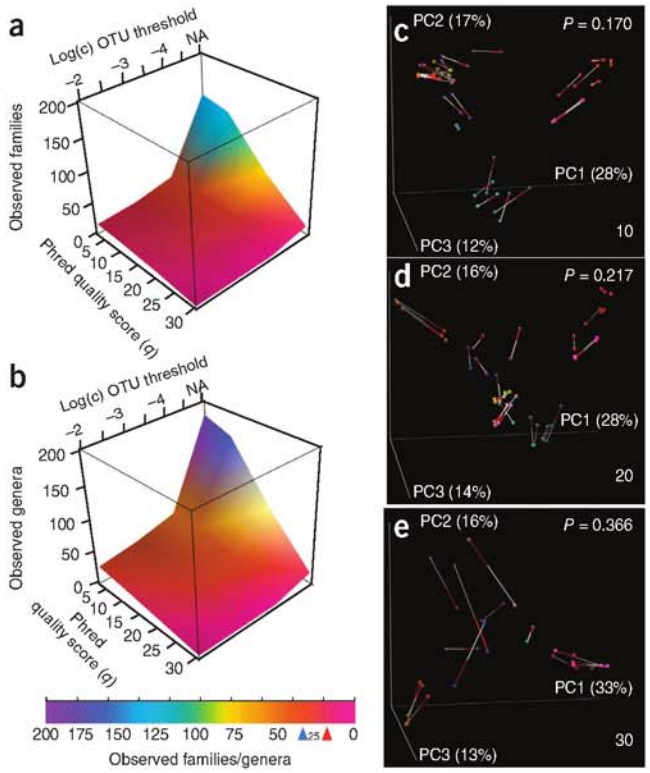

Figure 2 | The α and β diversity comparisons of mock community reads filtered using select phred_quality_score (*q*) settings (data set 1). (**a**,**b**) Family-level (**a**) and genus-level (**b**) taxon counts for mock communities filtered with variable (*q*) values at multiple OTU minimum abundance thresholds (*c*) (as percentages). Arrowheads below color key indicate expected genus-level (blue) and family-level (red) taxon counts. NA, no *c* filtering applied. (**c**–**e**) Procrustes PCoA biplot of GAIIx weighted UniFrac distance comparing variation in *q*. Comparison of *q* setting listed in bottom right corner to $q = 3$. Top right corner indicates Bonferroni-corrected *P* value for Procrustes goodness of fit. Red, human feces; magenta, mock community; cyan, human skin; dark cyan, human tongue; blue, freshwater; orange, freshwater creek; purple, ocean; yellow, estuary sediment; pink, soil. All other settings represent defaults in both α- and β-diversity comparisons.

needed to evaluate which factors (such as community composition and complexity) define optimal mock communities for filter calibration under different experimental conditions. For data sets where a mock community is not included for calibration, we recommend a conservative OTU threshold of $c = 0.005\%$. Additional work is also required to address the impact of filtering strategies on the analysis of paired-end reads.

Users can process sequencing data under specific filtering conditions to support different downstream analyses. For example, users with a majority of high-quality, full-length sequences may wish to increase Phred score (q) and minimum of high-quality calls (p) in lieu of limiting OTU abundance (c), thereby retrieving only full-length sequences with low error rates, potentially increasing the discovery rate of rare OTUs (as sequence selection will be based on length and quality, not count). Users with shorter reads or reads truncated by early low-quality base calls may wish to increase the maximum number of consecutive low-quality calls (r), lower minimum of high-quality calls (p) and use a higher OTU threshold. In this way, lower-quality but taxonomically useful reads will be retained, and reliable sequences will be selected based on abundance rather than error probability. Other users may be more interested in maximizing read count for implementation of machine-learning tools, identifying OTUs with different abundances across metadata categories or treatment regimes, or jackknifing or permutational tests for β diversity, all of which benefit from increased sample sizes. In this scenario, reads should be filtered using primary filters of Phred score and minimum high-quality calls instead of OTU abundance, which greatly reduces read count.

With these guidelines, users can confidently extract more, higher-quality sequences and decrease OTU filtration thresholds, increasing acuity for rare OTU discrimination and β-diversity comparisons. The Earth Microbiome Project (EMP)[2] is adopting these guidelines for routine analysis of all small-subunit rRNA gene sequencing on the Illumina HiSeq and MiSeq systems, facilitating deeper, more efficient insight into how microbial diversity varies over spatial and temporal scales across our planet. The conclusions drawn from this study are conserved for data from HiSeq2000, MiSeq and GAIIx systems, supporting confident cross-platform data handling. In addition, we recommend new default settings for Illumina processing in QIIME ($r = 3$; $p = 0.75$ total read length; $q = 3$; $n = 0$; $c = 0.005\%$; **Supplementary Note**), incorporated in the recent release of QIIME 1.5.0. Finally, although quality parameters tested here were evaluated using QIIME, these conclusions are relevant to Illumina amplicon quality filtering across all bioinformatics pipelines for improved diversity estimates in all taxa and environments.

METHODS

Methods and any associated references are available in the online version of the paper.

Note: Supplementary information is available in the online version of the paper.

ACKNOWLEDGMENTS

We thank G. Giannoukos (Broad Institute of MIT and Harvard), I. Rasolonjatovo (Illumina), M. Gebert (University of Colorado, Boulder) and L. Wegener Parfrey (University of Colorado, Boulder) for contributing mock community sequencing data used in this study, and S. Huse and A. Gonzalez for useful feedback and discussions of this manuscript. This work was supported in part by grants from the US National Institutes of Health (NIH DK78669 to J.I.G., NIH R01HD059127 to D.A.M. and NIH U54HG004969 to D.G.), the Juvenile Diabetes Research Fund (D.G.), the Crohn's and Colitis Foundation of America (J.I.G. and D.G.), and the Howard Hughes Medical Institute. N.A.B. was supported by the 2012–2013 Dannon Probiotics Fellow Program (The Dannon Company) and a *Wine Spectator* scholarship.

AUTHOR CONTRIBUTIONS

N.A.B., J.G.C., D.A.M. and R.K. conceived and designed the experiments; N.A.B. performed the experiments and data analysis. All authors contributed sequencing data sets and wrote the manuscript.

COMPETING FINANCIAL INTERESTS

The authors declare no competing financial interests.

Published online at http://www.nature.com/doifinder/10.1038/nmeth.2276.

1. Yatsunenko, T. *et al. Nature* **486**, 222–227 (2012).
2. Gilbert, J.A. & Meyer, F. *ASM Microbe* **7**, 64–69 (2012).
3. Reeder, J. & Knight, R. *Nat. Methods* **7**, 668–669 (2010).
4. Quince, C. *et al. Nat. Methods* **6**, 639–641 (2009).
5. Caporaso, J.G. *et al. Proc. Natl. Acad. Sci. USA* **108**, 4516–4522 (2011).
6. Minoche, A.E. *et al. Genome Biol.* **12**, R112 (2011).
7. Caporaso, J.G. *et al. Nat. Methods* **7**, 335–336 (2010).
8. Caporaso, J.G. *et al. ISME J.* **6**, 1621–1624 (2012).
9. Bokulich, N.A. *et al. PLoS ONE* **7**, e36357 (2012).
10. Bokulich, N.A., Bamforth, C.W. & Mills, D.A. *PLoS ONE* **7**, e35507 (2012).
11. Lozupone, C. & Knight, R. *Appl. Environ. Microbiol.* **71**, 8228–8235 (2005).

ONLINE METHODS

Data availability. Raw data can be found in the QIIME database (http://microbio.me/qiime/) under the following study identifiers, where data set number can be found in **Supplementary Table 7**: data set 1, 719; data set 2, 1685; data set 3, 1686; data set 4, 1626; data set 5, 1687; data set 6, 1688; data set 7, 1683; data set 8, 1684; data set 9, 1689; and data set 10, 1690.

Sample data. Data analyzed in this study were generated in ten separate sequencing runs on the Illumina GAIIx (3 sequencing runs), HiSeq2000 (3 sequencing runs) and MiSeq (4 sequencing runs) (**Supplementary Table 7**). In the first phase of this study, this consisted of six different sequencing runs analyzing four different bacterial and fungal mock communities (**Supplementary Table 2**); of these, only data set 1 comprised previously published data and contained biological samples in addition to mock community samples[5]. In the second phase of this study, β-diversity comparisons were made between biological samples analyzed in four different, previously published studies using Illumina GAIIx system[5,9,10] (data sets 1, 9, 10; **Supplementary Table 7**), and HiSeq2000 system[8] (data set 7) and MiSeq system[8] (data set 8). DNA extraction, PCR and sequencing for all sequencing runs were performed described previously[5,8–10]. Mock community data sets 2 and 3 (**Supplementary Table 2**) were acquired using a protocol described previously[8] except that singleton PCRs were performed, the PCRs contained only 25 cycles and the extension step was extended by 5 min. Additionally, data set 2 was prepared using the Illumina TruSeq v2 paired-end library preparation kit, and data set 3 was prepared with the TruSeq v1 paired-end library kit. Mock communities analyzed in this study were derived from six total sequencing runs on the GAIIx, HiSeq and MiSeq with reads between 90 nt and 250 nt (**Supplementary Table 2**). The taxonomic compositions of the four mock communities analyzed by these runs are presented in **Supplementary Tables 3–6**. These sequencing runs were performed on different instruments at different sites with the goal of assessing the impact of filtering parameters across a broad set of sequencing conditions: Illumina Cambridge (data sets 1, 3, 7 and 8), Broad Institute (data sets 2 and 4), Washington University School of Medicine (data sets 5 and 6) and University of California DNA Technologies Core (data sets 9 and 10). Although all sequencing runs in this study were paired-end runs, only the forward reads were analyzed for the purposes of this study, as QIIME's filtering pipeline currently handles each read independently and does not use a scheme for aligning or concatenating paired-end reads.

Sequence analysis. Raw Illumina fastq files were de-multiplexed, quality filtered and analyzed using QIIME (v. 1.4.0-dev)[7]. Reads were filtered using variable manual settings, as modulated by the parameters p, q, r and n (**Supplementary Table 1**). OTUs were assigned using the QIIME UCLUST[12] wrapper, with a threshold of 97% pair-wise nucleotide sequence identity, and the cluster centroid for each OTU was chosen as the OTU representative sequence. OTU representative sequences were then classified taxonomically using the QIIME-based wrapper of the Ribosomal Database Project (RDP) naive Bayesian classifier[13] retrained on the Greengenes 16S rRNA gene database[14] prefiltered at 97% identity, using a 0.80 confidence threshold for taxonomic assignment. After taxonomic assignment, variable OTU minimum abundance thresholds (c) were applied to remove any OTU representing fewer sequences than the defined threshold. Representative sequences were aligned using PyNAST[15] against a template alignment of the Greengenes database, filtered at 97% identity, and phylogenetic trees were constructed using FastTree. β-diversity estimates were calculated within QIIME using UniFrac[11] distances between samples, with even subsampling at 2,000 sequences per sample with 1,000 Monte Carlo iterations. Procrustes analysis was performed on UniFrac distance matrices with 1,000 Monte Carlo randomizations to compute goodness of fit (M^2) and visualized using PCoA.

12. Edgar, R.C. *Bioinformatics* **26**, 2460–2461 (2010).
13. Wang, Q., Garrity, G.M., Tiedje, J.M. & Cole, J.R. *Appl. Environ. Microbiol.* **73**, 5261–5267 (2007).
14. DeSantis, T.Z. *et al. Appl. Environ. Microbiol.* **72**, 5069–5072 (2006).
15. Caporaso, J.G. *et al. Bioinformatics* **26**, 266–267 (2010).

doi:10.1038/nmeth.2276

Appendix B

Hsiao, A., Ahmed, A.M.S., Subramanian, S., Griffin, N.W., Drewry, L.L., Petri, W.A., Haque, R., Ahmed, T., and Gordon, J.I. (2014). **Members of the human gut microbiota involved in recovery from Vibrio cholerae infection.** Nature *515*, 423–426.

LETTER

doi:10.1038/nature13738

Members of the human gut microbiota involved in recovery from *Vibrio cholerae* infection

Ansel Hsiao[1], A. M. Shamsir Ahmed[2,3], Sathish Subramanian[1], Nicholas W. Griffin[1], Lisa L. Drewry[1], William A. Petri Jr[4,5,6], Rashidul Haque[3], Tahmeed Ahmed[3] & Jeffrey I. Gordon[1]

Given the global burden of diarrhoeal diseases[1], it is important to understand how members of the gut microbiota affect the risk for, course of, and recovery from disease in children and adults. The acute, voluminous diarrhoea caused by *Vibrio cholerae* represents a dramatic example of enteropathogen invasion and gut microbial community disruption. Here we conduct a detailed time-series metagenomic study of faecal microbiota collected during the acute diarrhoeal and recovery phases of cholera in a cohort of Bangladeshi adults living in an area with a high burden of disease[2]. We find that recovery is characterized by a pattern of accumulation of bacterial taxa that shows similarities to the pattern of assembly/maturation of the gut microbiota in healthy Bangladeshi children[3]. To define the underlying mechanisms, we introduce into gnotobiotic mice an artificial community composed of human gut bacterial species that directly correlate with recovery from cholera in adults and are indicative of normal microbiota maturation in healthy Bangladeshi children[3]. One of the species, *Ruminococcus obeum*, exhibits consistent increases in its relative abundance upon *V. cholerae* infection of the mice. Follow-up analyses, including mono- and co-colonization studies, establish that *R. obeum* restricts *V. cholerae* colonization, that *R. obeum luxS* (autoinducer-2 (AI-2) synthase) expression and AI-2 production increase significantly with *V. cholerae* invasion, and that *R. obeum* AI-2 causes quorum-sensing-mediated repression of several *V. cholerae* colonization factors. Co-colonization with *V. cholerae* mutants discloses that *R. obeum* AI-2 reduces *Vibrio* colonization/pathogenicity through a novel pathway that does not depend on the *V. cholerae* AI-2 sensor, LuxP. The approach described can be used to mine the gut microbiota of Bangladeshi or other populations for members that use autoinducers and/or other mechanisms to limit colonization with *V. cholerae*, or conceivably other enteropathogens.

We used an approved protocol for recruiting Bangladeshi adults living in Dhaka Municipal Corporation area for this study. Of the 1,153 patients with acute diarrhoea who were screened, seven passed all entry criteria (Methods) and were enrolled (Supplementary Tables 1 and 2). Faecal samples collected at monthly intervals during the first 2 postnatal years from 50 healthy children living in the Mirpur area of Dhaka city, plus samples obtained at approximately 3-month intervals over a 1-year period from 12 healthy adult males also living Mirpur, allowed us to compare recovery of the microbiota from cholera with the normal process of assembly of the gut community in infants and children, and with unperturbed communities from healthy adult controls.

Using the standard treatment protocol of the International Centre for Diarrhoeal Disease Research, Bangladesh, study participants with acute cholera received a single oral dose of azithromycin and were given oral rehydration therapy for the duration of their hospital stay. Patients were discharged after their first solid stool. We divided the diarrhoeal period (from the first diarrhoeal stool after admission to the first solid stool) into four proportionately equal time bins: diarrhoeal phase 1 (D-Ph1) to D-Ph4. Every diarrhoeal stool was collected from every participant. Faecal samples were also collected every day for the first week after discharge (recovery phase 1, R-Ph1), weekly during the next 3 weeks (R-Ph2), and monthly for the next 2 months (R-Ph3). For each individual, we selected a subset of samples from D-Ph1 to D-Ph3 (Methods), plus all samples from D-Ph4 to R-Ph3, for analysis of bacterial composition by sequencing PCR amplicons generated from variable region 4 (V4) of the 16S ribosomal RNA (rRNA) gene (Supplementary Information, Extended Data Fig. 1a and Supplementary Table 3). Reads sharing 97% nucleotide sequence identity were grouped into operational taxonomic units (97%-identity OTUs; Methods).

We identified a total of 1,733 97%-identity OTUs assigned to 343 different species after filtering and rarefaction (Methods). *V. cholerae* dominated the microbiota of the seven patients with cholera during D-Ph1 (mean maximum relative abundance 55.6%), declining markedly within hours after initiation of oral rehydration therapy. The microbiota then became dominated by either an unidentified *Streptococcus* species (maximum relative abundance 56.2–98.6%) or by *Fusobacterium* species (19.4–65.1% in patients B–E). In patient G, dominance of the community passed from a *Campylobacter* species (58.6% maximum) to a *Streptococcus* species (98.6% maximum) (Supplementary Table 4). Of the 343 species, 47.9 $\pm$ 6.6% (mean $\pm$ s.d.) were observed throughout both the diarrhoeal and recovery phases, suggesting that microbiota composition during the recovery phase may reflect an outgrowth from reservoirs of bacteria retained during disruption by diarrhoea (Extended Data Fig. 2a–d and Supplementary Information).

Indicator species analysis[4] (Methods) was used to identify 260 bacterial species consistently associated with the diarrhoeal or recovery phases across members of the study group, and in a separate analysis for each subject (Supplementary Table 5). The relative abundance of each of the discriminatory species in each faecal sample was compared with the mean weighted phylogenetic (UniFrac[5]) distance between that microbiota sample and all microbiota samples collected from the reference cohort of healthy Bangladeshi adults. The results revealed 219 species with significant indicator value assignments to diarrhoeal or recovery phases, and relative abundances with statistically significant Spearman's rank correlation values to community UniFrac distance to healthy control microbiota (Supplementary Table 6 and Extended Data Fig. 2d). Not surprisingly, the abundance of *V. cholerae* directly correlated with increased distance to a healthy microbiota. *Streptococcus* and *Fusobacterium* species, which bloomed during the early phases of diarrhoea, were also significantly and positively correlated with distance from a healthy adult microbiota. Increases in the relative abundances of species in the genera *Bacteroides*, *Prevotella*, *Ruminococcus/Blautia*, and *Faecalibacterium* (for example, *Bacteroides vulgatus*, *Prevotella copri*, *R obeum*, and *Faecalibacterium prausnitzii*) were strongly correlated with a shift in community structure towards a healthy adult configuration (Extended Data Fig. 2d and Supplementary Table 6).

[1]Center for Genome Sciences and Systems Biology, Washington University School of Medicine, St Louis, Missouri 63108, USA. [2]School of Population Health, The University of Queensland, Brisbane, Queensland 4006, Australia. [3]Centre for Nutrition and Food Security, International Centre for Diarrhoeal Disease Research, Dhaka 1212, Bangladesh. [4]Department of Medicine, University of Virginia School of Medicine, Charlottesville, Virginia 22908, USA. [5]Department of Microbiology, University of Virginia School of Medicine, Charlottesville, Virginia 22908, USA. [6]Department of Pathology, University of Virginia School of Medicine, Charlottesville, Virginia 22908, USA.

Previously we used Random Forests, a machine-learning algorithm, to identify a collection of age-discriminatory bacterial taxa that together define different stages in the postnatal assembly/maturation of the gut microbiota in healthy Bangladeshi children living in the same area as the adult patients with cholera[3]. Of those 60 most age-discriminatory 97%-identity OTUs representing 40 different species, 31 species were present in adult patients with cholera. Intriguingly, they followed a similar progression of changing representation during diarrhoea to recovery as they do during normal maturation of the healthy infant gut microbiota (Extended Data Fig. 2d). Twenty-seven of the 31 species were significantly associated with recovery from diarrhoea by indicator species analysis (see Supplementary Information and Extended Data Figs 3–5 for OTU-level and community-wide analyses). These 27 species, which serve as indicators and are potential mediators of restoration of the gut microbiota after cholera, guided construction of a gnotobiotic mouse model that examined the molecular mechanisms by which some of these taxa might affect *V. cholerae* infection and promote restoration.

We assembled an artificial community of 14 sequenced human gut bacterial species (Supplementary Table 7) that included (1) five species that directly correlated with gut microbiota recovery from cholera and with normal maturation of the infant gut microbiota (*R. obeum*, *Ruminococcus torques*, *F. prausnitzii*, *Dorea longicatena*, *Collinsella aerofaciens*), (2) six species significantly associated with recovery from cholera by indicator species analysis (*Bacteroides ovatus*, *Bacteroides vulgatus*, *Bacteroides caccae*, *Bacteroides uniformis*, *Parabacteroides distasonis*, *Eubacterium rectale*), and (3) three prominent members of the adult human gut microbiota that have known capacity to process dietary and host glycans (*Bacteroides cellulosilyticus*, *Bacteroides thetaiotaomicron*, *Clostridium scindens*[6–8]; as noted in Extended Data Fig. 6 and Supplementary Table 8, shotgun sequencing of diarrhoeal- and recovery-phase human faecal DNA samples revealed that genes encoding enzymes involved in carbohydrate metabolism were the largest category of identified genes specifying known enzymes that changed in relative abundance within the faecal microbiome during the course of cholera). One group of mice was directly inoculated with approximately 10^9 colony-forming units (c.f.u.) of *V. cholerae* at the same time they received the 14-member community to simulate the rapidly expanding *V. cholerae* population during diarrhoea ('D1invasion' group). A separate group was gavaged with the community alone and then invaded 14 days later with *V. cholerae* ('D14invasion' group) (Extended Data Fig. 1c).

V. cholerae levels remained at a high level in the D1invasion group over the first week (maximum 46.3% relative abundance), and then declined rapidly to low levels (<1%). Introduction of *V. cholerae* into the established 14-member community produced much lower levels of *V. cholerae* infection (range of mean abundances measured daily over the 3 days after gavage of the enteropathogen, 1.2–2.7%; Supplementary Table 9). Control experiments demonstrated that *V. cholerae* was able to colonize at high levels for at least 7 days when it was introduced alone into germ-free recipients (10^9–10^{10} c.f.u. per milligram wet weight of faeces; Fig. 1a). Together, these data suggest that a member or members of the artificial human gut microbiota had the ability to restrict *V. cholerae* colonization.

Changes in relative abundances of the 14 community members in faecal samples in response to *V. cholerae* were consistent for most species across the D1invasion and D14invasion mice (Supplementary Table 9). We focused on one member, *R. obeum*, because its relative abundance increased significantly after introduction of *V. cholerae* in both the D1invasion and D14invasion groups (Extended Data Fig. 7a and Supplementary Table 9) and because it is a prominent age-discriminatory taxon in the Random Forests model of gut microbiota maturation in healthy Bangladeshi children[3] (Extended Data Fig. 4b). Mice were mono-colonized with either *R. obeum* or *V. cholerae* for 7 days and then the other species was introduced (Extended Data Fig. 1d). When *R. obeum* was present, *V. cholerae* levels declined by 1–3 logs (Fig. 1a). Germ-free mice were also colonized with the defined 14-member community or the same community without *R. obeum* for 2 weeks, and *V. cholerae* was

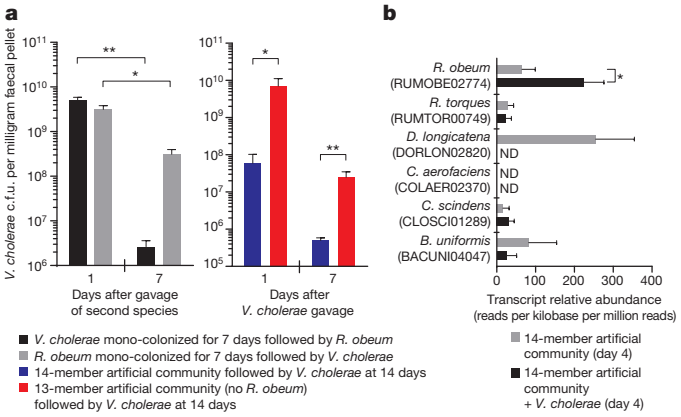

Figure 1 | *R. obeum* restricts *V. cholerae* colonization in adult gnotobiotic mice. **a**, *V. cholerae* levels in the faeces of mice colonized with the indicated human gut bacterial species ($n = 4$–6 mice per group). **b**, Expression of *R. obeum luxS* AI-2 synthase in the 14-member community 4 days after introduction of 10^9 c.f.u. of *V. cholerae* or no pathogen ($n = 5$ mice per group). Note that *D. longicatena* levels fall precipitously after *V. cholerae* invasion (Supplementary Table 9). Mean values ± s.e.m. are shown. ND, not detected. $^*P < 0.05$, $^{**}P < 0.01$ (unpaired Mann–Whitney *U*-test).

then introduced by gavage (Extended Data Fig. 1e). *V. cholerae* levels 1 day after gavage were 100-fold higher in the community that lacked *R. obeum*; these differences were sustained over time (50-fold higher after 7 days; $P < 0.01$, unpaired Mann–Whitney *U*-test; Fig. 1a).

Having established that *R. obeum* restricts *V. cholerae* colonization, we used microbial RNA sequencing (RNA-seq) of faecal RNAs to determine the effect of *R. obeum* on expression of known *V. cholerae* virulence factors in mono- and co-colonized mice. Co-colonization led to reduced expression of *tcpA* (a primary colonization factor in humans[9,10]), *rtxA* and *hlyA* (encode accessory toxins[11,12]), and *VC1447–VC1448* (RtxA transporters) (threefold to fivefold changes; $P < 0.05$ compared with *V. cholerae* mono-colonized controls, Mann–Whitney *U*-test; see Supplementary Information and Supplementary Table 10 for other regulated genes that could impact colonization, plus Extended Data Fig. 8 for an ultra-performance liquid chromatography mass spectrometry (UPLC–MS) analysis of bile acids reported to effect *V. cholerae* gene regulation[13]).

Two quorum-sensing pathways are known to regulate *V. cholerae* colonization/virulence[14–17]: an intra-species mechanism involving cholera autoinducer-1, and an inter-species mechanism involving autoinducer-2 (refs 18, 19). Quorum sensing disrupts expression of *V. cholerae* virulence determinants through a signalling pathway that culminates in production of the LuxR-family regulator HapR[15,16]. Repression of quorum sensing in *V. cholerae* is important for virulence factor expression and infection[20–22]. The *luxS* gene encodes the S-ribosylhomocysteine lyase responsible for AI-2 synthesis. Homologues of *luxS* are widely distributed among bacteria[18,19], including 8 of the 14 species in the artificial human gut community (Supplementary Table 11 and Extended Data Fig. 9). RNA-seq of the faecal meta-transcriptomes of D1invasion mice colonized with the 14-member artificial community plus *V. cholerae*, and mice harbouring the 14-member consortium without *V. cholerae*, revealed that of predicted *luxS* homologues in the community, only expression of *R. obeum luxS* (*RUMOBE02774*) increased significantly in response to *V. cholerae* ($P < 0.05$, Mann–Whitney *U*-test; Fig. 1b). Moreover, *R. obeum luxS* transcript levels directly correlated with *V. cholerae* levels (Extended Data Fig. 7c).

In addition to *luxS*, the *R. obeum* strain represented in the artificial community contains homologues of *lsrABCK* that are responsible for import and phosphorylation of AI-2 in Gram-negative bacteria[23], as well as homologues of two genes, *luxR* and *luxQ*, that play a role in AI-2 sensing and downstream signalling in other organisms[24]. Expression of all these *R. obeum* genes was detected *in vivo*, consistent with *R. obeum*

having a functional AI-2 signalling system (Extended Data Fig. 7b). (See Supplementary Information for results showing that *R. obeum* AI-2 production is stimulated by *V. cholerae in vitro* and in co-colonized animals (Extended Fig. 7d–f), plus (1) a genome-wide analysis of the effects of *V. cholerae* on *R. obeum* transcription in co-colonized mice (Supplementary Table 10c) and (2) a community-wide view of the transcriptional responses of the 14-member consortium to *V. cholerae* (Supplementary Table 12).)

Quorum sensing downregulates the *V. cholerae tcp* operon that encodes components of the toxin co-regulated pilus (TCP) biosynthesis pathway required for infection of humans[9,10]. To confirm that *R. obeum* LuxS could signal through AI-2 pathways, we cloned *R. obeum* and *V. cholerae luxS* downstream of the arabinose-inducible P_{BAD} promoter in plasmids that were maintained in an *Escherichia coli* strain unable to produce its own AI-2 (DH5α)[25]. High *tcp* expression can be induced in *V. cholerae* after slow growth in AKI medium without agitation followed by rapid growth under aerobic conditions[26]. Addition of culture supernatants harvested from the *E. coli* strains expressing *R. obeum* or *V. cholerae luxS* caused a two- to threefold reduction in *tcp* induction in *V. cholerae* ($P < 0.05$, unpaired Student's *t*-test; replicated in four independent experiments). Supernatants from a control *E. coli* strain with the plasmid vector lacking *luxS* had no effect (Fig. 2a). These findings are consistent with our *in vivo* RNA-seq results and provide direct evidence that *R. obeum* AI-2 regulates expression of *V. cholerae* virulence factor.

Germ-free mice were then colonized with *V. cholerae* and *E. coli* bearing either the P_{BAD}-*R. obeum luxS* plasmid or the vector control. Mice that received *E. coli* expressing *R. obeum luxS* showed a significantly lower level of *V. cholerae* colonization 8 h after gavage than mice that received *E. coli* with vector alone (Fig. 2b; there was no statistically significant difference in levels of *E. coli* between the two groups (data not shown)). Together, these results establish a direct causal relationship between *R. obeum*-mediated restriction of *V. cholerae* colonization and *R. obeum* AI-2 synthesis.

Several *V. cholerae* mutants were used to determine whether known *V. cholerae* AI-2 signalling pathways are required for the observed effects of *R. obeum* on *V. cholerae* colonization. LuxP is critical for sensing AI-2 in *V. cholerae*. Co-colonization experiments in gnotobiotic mice revealed that levels of isogenic Δ*luxP* or wild-type $luxP^+$ *V. cholerae* strains were not significantly different as a function of the presence of *R. obeum* (Extended Data Fig. 10a), suggesting that *R. obeum* modulates *V. cholerae* levels through other quorum-sensing regulatory genes. The *luxO* and *hapR* genes encode central regulators linking known *V. cholerae* quorum-signalling and virulence regulatory pathways. Deletion of *luxO* typically results in increased *hapR* expression[15]. However, our RNA-seq analysis had shown that both *luxO* and *hapR* are repressed in the presence of *R. obeum* (six- to sevenfold, $P < 0.0001$; Mann–Whitney *U*-test), as are two important downstream activators of virulence repressed by HapR[16], encoded by *aphA* and *aphB*. These findings provide additional evidence that *R. obeum* operates to regulate virulence through a novel regulatory pathway.

The quorum-sensing transcriptional regulator VqmA was upregulated more than 25-fold when *V. cholerae* was introduced into mice monocolonized with *R. obeum* (Fig. 2c and Supplementary Table 10). When germ-free mice were gavaged with *R. obeum* and a mixture of Δ*vqmA* (Δ*lacZ*)[27] and wild-type *V. cholerae* ($lacZ^+$) strains, the Δ*vqmA* mutant exhibited an early competitive advantage (Fig. 2d), suggesting that *R. obeum* may be able to affect early colonization of *V. cholerae* through VqmA. VqmA is able to bind to and activate the *hapR* promoter directly[27]. Since RNA-seq showed that *hapR* activation did not occur in gnotobiotic mice despite high levels of *vqmA* expression (Extended Data Fig. 10b and Supplementary Table 10), we postulate that the role played by VqmA in *R. obeum* modulation of *Vibrio* virulence genes involves an uncharacterized mechanism rather than the known pathway passing through HapR.

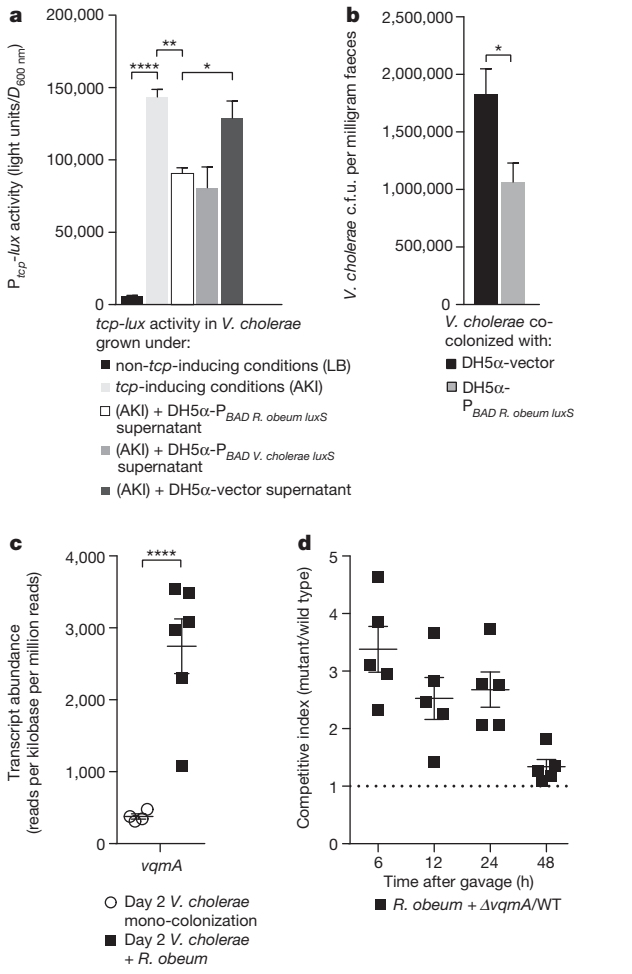

Figure 2 | *R. obeum* AI-2 reduces *V. cholerae* colonization and virulence gene expression. **a**, *R. obeum* AI-2 produced in *E. coli* represses the *tcp* promoter in *V. cholerae* (triplicate assays; results representative of four independent experiments). **b**, Faecal *V. cholerae* levels in gnotobiotic mice 8 h after gavage with *V. cholerae* and an *E. coli* strain containing either the P_{BAD}-*R. obeum luxS* plasmid or vector control. **c**, Faecal *vqmA* transcript abundance in mono- or co-colonized mice. **d**, Competitive index of Δ*vqmA* versus wild-type *V. cholerae* during co-colonization with *R. obeum* ($n = 5$ animals per group). Mean values ± s.e.m. are shown. $*P < 0.05$, $**P < 0.01$, $****P < 0.0001$ (unpaired two-tailed Student's *t*-test).

We have identified a set of bacterial species that strongly correlate with a process in which the perturbed gut bacterial community in adult patients with cholera is restored to a configuration found in healthy Bangladeshi adults. Several of these species are also associated with the normal assembly/maturation of the gut microbiota in Bangladeshi infants and children, raising the possibility that some of these taxa may be useful for 'repair' of the gut microbiota in individuals whose gut communities have been 'wounded' through a variety of insults, including enteropathogen infections. Translating these observations to a gnotobiotic mouse model containing an artificial human gut microbiota composed of recovery- and age-indicative taxa established that one of these species, *R. obeum*, reduces *V. cholerae* colonization. As an entrenched member of the gut microbiota in Bangladeshi individuals, *R. obeum* could function to increase median infectious dose (ID_{50}) for *V. cholerae* in humans and thus help to determine whether exposure to a given dose of this enteropathogen results in diarrhoeal illness. The modest effects of *R. obeum* AI-2 on *V. cholerae* virulence gene expression in our adult gnotobiotic mouse model may reflect the possibility that we have only identified a small fraction of the microbiota's full repertoire of virulence-suppressing mechanisms. Culture collections generated from the faecal microbiota

of Bangladeshi subjects are a logical starting point for 'second-generation' artificial communities containing *R. obeum* isolates that have evolved in this population, and for testing whether the observed effects of *R. obeum* generalize across many different strains from different populations. Moreover, the strategy described in this report could be used to mine the gut microbiota of Bangladeshi or other populations where diarrhoeal disease is endemic for additional species that use quorum-related and/or other mechanisms to limit colonization by *V. cholerae* and potentially other enteropathogens.

Online Content Methods, along with any additional Extended Data display items and Source Data, are available in the online version of the paper; references unique to these sections appear only in the online paper.

Received 10 October 2013; accepted 6 August 2014.
Published online 17 September 2014.

1. World Health Organization Cholera, 2013. *Wkly Epidemiol. Rec.* **89,** 345–356 (2014).
2. Chowdhury, F. *et al.* Impact of rapid urbanization on the rates of infection by *Vibrio cholerae* O1 and enterotoxigenic *Escherichia coli* in Dhaka, Bangladesh. *PLoS Negl. Trop. Dis.* **5,** e999 (2011).
3. Subramanian, S. *et al.* Persistent gut microbiota immaturity in malnourished Bangladeshi children. *Nature* **510,** 417–421 (2014).
4. Dufrene, M. & Legendre, P. Species assemblages and indicator species: the need for a flexible asymmetrical approach. *Ecol. Monogr.* **67,** 345–366 (1997).
5. Lozupone, C. & Knight, R. UniFrac: a new phylogenetic method for comparing microbial communities. *Appl. Environ. Microbiol.* **71,** 8228–8235 (2005).
6. Martens, E. C. *et al.* Recognition and degradation of plant cell wall polysaccharides by two human gut symbionts. *PLoS Biol.* **9,** e1001221 (2011).
7. McNulty, N. P. *et al.* Effects of diet on resource utilization by a model human gut microbiota containing *Bacteroides cellulosilyticus* WH2, a symbiont with an extensive glycobiome. *PLoS Biol.* **11,** e1001637 (2013).
8. McNulty, N. P. *et al.* The impact of a consortium of fermented milk strains on the gut microbiome of gnotobiotic mice and monozygotic twins. *Sci. Translat. Med.* **3,** 106ra106 (2011).
9. Taylor, R. K., Miller, V. L., Furlong, D. B. & Mekalanos, J. J. Use of phoA gene fusions to identify a pilus colonization factor coordinately regulated with cholera toxin. *Proc. Natl Acad. Sci. USA* **84,** 2833–2837 (1987).
10. Herrington, D. A. *et al.* Toxin, toxin-coregulated pili, and the toxR regulon are essential for *Vibrio cholerae* pathogenesis in humans. *J. Exp. Med.* **168,** 1487–1492 (1988).
11. Olivier, V., Salzman, N. H. & Satchell, K. J. Prolonged colonization of mice by *Vibrio cholerae* El Tor O1 depends on accessory toxins. *Infect. Immun.* **75,** 5043–5051 (2007).
12. Olivier, V., Haines, G. K., III, Tan, Y. & Satchell, K. J. Hemolysin and the multifunctional autoprocessing RTX toxin are virulence factors during intestinal infection of mice with *Vibrio cholerae* El Tor O1 strains. *Infect. Immun.* **75,** 5035–5042 (2007).
13. Yang, M. *et al.* Bile salt-induced intermolecular disulfide bond formation activates *Vibrio cholerae* virulence. *Proc. Natl Acad. Sci. USA* **110,** 2348–2353 (2013).
14. Miller, M. B., Skorupski, K., Lenz, D. H., Taylor, R. K. & Bassler, B. L. Parallel quorum sensing systems converge to regulate virulence in *Vibrio cholerae*. *Cell* **110,** 303–314 (2002).
15. Zhu, J. *et al.* Quorum-sensing regulators control virulence gene expression in *Vibrio cholerae*. *Proc. Natl Acad. Sci. USA* **99,** 3129–3134 (2002).
16. Kovacikova, G. & Skorupski, K. Regulation of virulence gene expression in *Vibrio cholerae* by quorum sensing: HapR functions at the aphA promoter. *Mol. Microbiol.* **46,** 1135–1147 (2002).
17. Higgins, D. A. *et al.* The major *Vibrio cholerae* autoinducer and its role in virulence factor production. *Nature* **450,** 883–886 (2007).
18. Pereira, C. S., Thompson, J. A. & Xavier, K. B. AI-2-mediated signalling in bacteria. *FEMS Microbiol. Rev.* **37,** 156–181 (2013).
19. Sun, J., Daniel, R., Wagner-Dobler, I. & Zeng, A. P. Is autoinducer-2 a universal signal for interspecies communication: a comparative genomic and phylogenetic analysis of the synthesis and signal transduction pathways. *BMC Evol. Biol.* **4,** 36 (2004).
20. Duan, F. & March, J. C. Engineered bacterial communication prevents *Vibrio cholerae* virulence in an infant mouse model. *Proc. Natl Acad. Sci. USA* **107,** 11260–11264 (2010).
21. Liu, Z. *et al.* Mucosal penetration primes *Vibrio cholerae* for host colonization by repressing quorum sensing. *Proc. Natl Acad. Sci. USA* **105,** 9769–9774 (2008).
22. Liu, Z., Stirling, F. R. & Zhu, J. Temporal quorum-sensing induction regulates *Vibrio cholerae* biofilm architecture. *Infect. Immun.* **75,** 122–126 (2007).
23. Taga, M. E., Semmelhack, J. L. & Bassler, B. L. The LuxS-dependent autoinducer AI-2 controls the expression of an ABC transporter that functions in AI-2 uptake in *Salmonella typhimurium*. *Mol. Microbiol.* **42,** 777–793 (2001).
24. Bassler, B. L., Wright, M. & Silverman, M. R. Multiple signalling systems controlling expression of luminescence in *Vibrio harveyi*: sequence and function of genes encoding a second sensory pathway. *Mol. Microbiol.* **13,** 273–286 (1994).
25. Surette, M. G., Miller, M. B. & Bassler, B. L. Quorum sensing in *Escherichia coli*, *Salmonella typhimurium*, and *Vibrio harveyi*: a new family of genes responsible for autoinducer production. *Proc. Natl Acad. Sci. USA* **96,** 1639–1644 (1999).
26. Iwanaga, M. *et al.* Culture conditions for stimulating cholera toxin production by *Vibrio cholerae* O1 El Tor. *Microbiol. Immunol.* **30,** 1075–1083 (1986).
27. Liu, Z., Hsiao, A., Joelsson, A. & Zhu, J. The transcriptional regulator VqmA increases expression of the quorum-sensing activator HapR in *Vibrio cholerae*. *J. Bacteriol.* **188,** 2446–2453 (2006).

Supplementary Information is available in the online version of the paper.

Acknowledgements We thank S. Wagoner, J. Hoisington-López, M. Meier, J. Cheng, D. O'Donnell, and M. Karlsson for technical support, J. Zhu for providing strains of *V. cholerae* and *Vibrio harveyi*, and W.-L. Ng for providing Δ*luxP V. cholerae*. This work was supported in part by a grant from the Bill & Melinda Gates Foundation. The singleton birth cohort of Bangladeshi children was supported by a grant from the National Institutes of Health (AI 43596). The post-doctoral fellowship stipend of A.H. was funded in part by NIH training grants (T32DK077653, T32AI007172) and by the Crohn's and Colitis Foundation of America. The International Centre for Diarrhoeal Disease Research, Bangladesh, acknowledges the following donors, which provided unrestricted support: the Australian Agency for International Development, the Government of Bangladesh, the Canadian International Development Agency, the Swedish International Development Cooperation Agency, and the Department for International Development, UK.

Author Contributions A.H. and J.I.G. designed the metagenomic and gnotobiotic mouse study; A.M.S.A., R.H., and T.A. designed and implemented the clinical study, participated in patient recruitment, sample collection, sample preservation and clinical evaluations; R.H. and W.A.P. participated in recruitment of and sample collection from healthy Bangladeshi controls; A.H. generated the 16S rRNA, AI-2, RNA-seq, shotgun microbial community DNA sequencing, and *V. cholerae* colonization data. S.S. generated 16S rRNA data from extended sampling of the Bangladeshi singleton birth cohort. L.L.D. performed 16S rRNA sequencing of the additional samples from patients C and E and helped generate the colonization data in *in vivo* competition experiments involving isogenic wild-type, Δ*vqmA* and Δ*luxP* strains of *V. cholerae* C6706; A.H., S.S., N.W.G., and J.I.G. analysed the data; A.H. and J.I.G. wrote the paper.

Author Information All 16S rRNA, shotgun sequencing, and RNA-seq data sets generated from faecal samples have been deposited in the European Nucleotide Archive in raw format before post-processing and data analysis under accession number PRJEB6358. Reprints and permissions information is available at www.nature.com/reprints. The authors declare competing financial interests: details are available in the online version of the paper. Readers are welcome to comment on the online version of the paper. Correspondence and requests for materials should be addressed to J.I.G. (jgordon@wustl.edu).

METHODS

Human studies. Subject recruitment. Protocols for recruitment, enrollment, and consent, procedures for sampling the faecal microbiota of healthy Bangladeshi adults and children, and the faecal microbiota of adults during and after cholera infection, plus the subsequent de-identification of these samples, were approved by the Human Studies Committees of the International Centre for Diarrhoeal Disease Research, Bangladesh, and Washington University School of Medicine in St. Louis.

Enrollment into the adult cholera study was based on the following criteria: residency in the Dhaka Municipal Corporation area, a positive stool test for *V. cholerae* as judged by dark-field microscopy, diarrhoea for no more than 24 h before enrollment, and a permanent address that allowed follow-up faecal sampling after discharge from Dhaka Hospital (International Centre for Diarrhoeal Disease Research, Bangladesh). Non-prescription antibiotic usage is prevalent in Bangladesh[28,29]. Since a history of previous antibiotic consumption could be a confounder when interpreting the effects of cholera on the gut microbiota, we excluded individuals if they had received antibiotics in the 7 days preceding admission to the hospital. Since this was an observational study with no experimental treatment arm, blinding for study inclusion was not necessary. See Supplementary Table 1 for the number of individuals screened for inclusion in the study, the number of potential subjects excluded from the study and the reasons for their exclusion, and the number of subjects enrolled who satisfied all criteria for inclusion.

The healthy adults were fathers in a cohort of healthy twins, triplets, and their parents living in Mirpur that is described in ref. 3. Fathers were sampled every 3 months during the first 2 years of their offspring's postnatal life. Histories of diarrhoea and antibiotic use were not available for these fathers. However, histories of diarrhoea and antibiotic use in their healthy children were known: 46 of the 49 paternal faecal samples used were obtained during periods when none of their children had diarrhoea; 36 of these 49 samples were collected at a time when there had been no antibiotic use by their children in the preceding 7 days.

DNA extraction from human faecal samples, sequencing, and analysis. All diarrhoeal stools were collected from each participant (one sterilized bowl per sample), frozen immediately at −80 °C, then subjected to the same bead beating and phenol chloroform extraction procedure for DNA purification that was applied to the formed frozen faecal samples collected from these individuals during the recovery phases (and previously to a wide range of samples collected from individuals representing different ages, cultural traditions, geographical locations, and physiological and disease states[3,30]).

DNA was isolated from all frozen faecal samples from D-Ph1 to D-Ph4, from the period of frequent sampling during the first week following discharge (recovery phase 1; R-Ph1), the period of less frequent sampling during weeks 2–3 (R-Ph2), and from weeks 4 to 12 of recovery (R-Ph3) ($n = 1{,}053$ samples in total). For analyses involving healthy adult and child control groups, samples were excluded from our analysis where antibiotic use or diarrhoea was known to have occurred in the 7 days before sample collection.

For each participant in the cholera study, we selected one sample with high DNA yield (≥2 μg) from each 2-hour period during D-Ph1 to D-Ph3. An additional 7 ± 2 samples (mean ± s.d.) that had been collected during the approximately 5-h period before the rate of diarrhoea began to decrease at the beginning of D-Ph3 were included. All faecal samples collected after this time point (that is, from the remainder of D-Ph3 to R-Ph3), were also included in our analysis ($n = 19.7 \pm 7.4$ total samples (mean ± s.d.) per individual in the diarrhoeal phase, and 14 ± 3.3 total samples per individual in the recovery phase). Two patients (C and E) were chosen for additional sequencing of all their diarrhoeal samples ($n = 100$ and 50, respectively; see Supplementary Table 3b).

The V4 region of bacterial 16S rRNA genes represented in each selected faecal microbiota sample was amplified by PCR using primers containing sample-specific barcode identifiers. Amplicons were purified, pooled, and paired-end sequenced with an Illumina MiSeq instrument (250 nucleotide paired-end reads; 86,315 ± 2,043 (mean ± s.e.m.) assembled reads per sample; see Supplementary Table 3). Healthy control samples were analysed using the same sequencing platform and chemistry ($n = 293$ total samples).

Sequences were assembled, then de-multiplexed and analysed using the QIIME software package[31] and custom Perl scripts. For analysis of diarrhoeal and recovery phase samples, rarefaction was performed to 49,000 reads per sample. For analyses including samples from healthy adults and children, samples were rarefied to 7,900 reads per sample. Reads sharing 97% nucleotide sequence identity were grouped into operational taxonomic units (97%-identity OTUs). To ensure that we retained less abundant bacterial taxa in our analysis of the faecal samples of patients with cholera, a 97%-identity OTU was called 'distinct and reliable' if it appeared at 0.1% relative abundance in at least one faecal sample. Taxonomic assignments of OTUs to species level were made using the Ribosomal Database Project version 2.4 classifier[32] and a manually curated Greengenes database[33].

Indicator species analysis[4] was used to classify bacterial species as highly associated with either diarrhoeal phases or recovery. This approach is used in studies of macroecosystems to identify species that associate with different environmental groupings; it assigns for each species an indicator value that is a product of two components: (1) the species' specificity, which is the probability that a sample in which the species is found came from a given group; and (2) the species' fidelity, which is the proportion of samples from a given group that contains the species. We performed indicator species analysis in the set of 236 faecal specimens, selected from the seven patients according to the subsampling scheme described above, to identify bacterial species consistently associated with the diarrhoeal or recovery phases across members of the study group; statistical significance was defined using permutation tests in which permutations were constrained within subjects. We also conducted a separate indicator species analysis for each subject, using each individual's replicate diarrhoeal and recovery phase samples as the groupings.

For analyses of variation across communities, we used UniFrac[5], a metric that measures the overall degree of phylogenetic similarity of any two communities based on the degree to which they share branch length on a bacterial tree of life; low pairwise UniFrac distance values indicate that communities are more similar to one another. Unifrac distances were calculated using the QIIME software package[31].

The gut microbiomes of study participants were characterized by paired-end 2 × 250 nucleotide shotgun sequencing of faecal DNA using an Illumina MiSeq instrument (mean 216,698 reads per sample; Supplementary Table 3). Paired sequences were assembled into single reads using the SHERA software package[34], and annotated by mapping to version 58 of the Kyoto Encyclopedia of Genes and Genomes (KEGG) database[35] using UBLAST[36].

Gnotobiotic mouse experiments. All experiments involving animals used protocols approved by the Washington University Animal Studies Committee. Germ-free male C57BL/6J mice were maintained in flexible plastic film gnotobiotic isolators and fed an autoclaved, low-fat, plant polysaccharide-rich mouse chow (B&K, catalogue number 7378000, Zeigler Bros) *ad libitum*. Mice were 5–8 weeks old at time of gavage. The number of mice used in each experiment is reported in the text, relevant figure legends, and summarized in Extended Data Fig. 1.

Bacterial strains and plasmids. Supplementary Table 7 lists the sequenced human gut-derived bacterial strains used to generate the artificial communities and their sources. Since all Bangladeshi faecal samples were devoted to DNA extraction, we were unable to utilize strains that originated from culture collections generated from study participants' faecal biospecimens. Thus, the strains incorporated into the artificial community were from public repositories, represented multiple individuals, and were typically not accompanied by information about donor health status or living conditions.

A P_{tcp}-*lux* reporter strain was constructed by introducing P_{tcp}-*lux* (pJZ376) into *V. cholerae* C6706 via conjugation from SM10λpir. P_{BAD}-*luxS* expression vectors were produced by first amplifying the *luxS* sequences of *V. cholerae* C6706 and *R. obeum* ATCC2917 using PCR and the primers described in Supplementary Table 13. Amplicons were then cloned into pBAD202 (TOPO TA Expression Kit; Life Technologies), and introduced into *E. coli* DH5α by electroporation.

All cultures of *V. cholerae* C6706, the isogenic Δ*luxS* mutant (MM883), and *E. coli* strains containing *luxS* expression vectors were grown aerobically in Luria Broth (LB) medium with appropriate antibiotics (Supplementary Table 13). All members of the 14-member artificial human gut microbiota, including *R. obeum* ATCC29174, were propagated anaerobically in MegaMedium[37].

Colonization of gnotobiotic mice. All animal experiments involved administration of known consortia of bacterial species; as such, no blinding to group allocation was performed. The order of administration of microbial species to given groups of recipient mice was intentionally varied, as described in Extended Data Fig. 1c–e.

Mono-colonized animals received either 200 μl of overnight cultures of *R. obeum* strain ATCC29174 or *V. cholerae* strain C6706. All *V. cholerae* colonization studies in mice used the current pandemic El Tor biotype (strain C6706). Mice receiving the defined 13- or 14-member communities of sequenced human bacterial symbionts were gavaged with 200 μl of an equivalent mixture of bacteria assembled from overnight monocultures of each strain ($D_{600\,nm} \approx 0.4$ per strain; grown in MegaMedium). In the case of mice that received mixtures of *V. cholerae* and *E. coli* strains with *R. obeum luxS*-expressing plasmids (or vector controls), the *E. coli* strains were first grown overnight in LB medium containing 50 μg ml^{-1} kanamycin. Two millilitres of the culture were removed and cell pellets were obtained by centrifugation, washed three times with 2 ml LB medium to remove antibiotics, and re-suspended in 6 ml LB medium containing 0.1% arabinose. The suspension of *E. coli* cells was then incubated at 37 °C for 90 min, and mixed with *V. cholerae* C6706 such that each mouse was gavaged with ~50 μl and ~2.5 μl of overnight cultures of each organism, respectively. All gavages involving *V. cholerae* were preceded by a gavage of 100 μl sterile 1 M sodium bicarbonate to neutralize gastric pH. Colonization levels of *V. cholerae* were determined by serial dilution plating of faecal homogenates on selective medium.

Competitive index assays were performed with mice gavaged with 50 µl aliquots of cultures of mutant and wild-type *V. cholerae* C6706 strains that had been grown to $D_{600\,nm} = 0.3$. For experiments involving competitive index calculations as a function of the presence of *R. obeum*, 100 µl of an overnight *R. obeum* culture was co-inoculated with the mixture of *V. cholerae* strains. Faecal samples from recipient gnotobiotic mice were subjected to dilution plating and aerobic growth on LB agar with the LacZ substrate Xgal; blue–white screening was used to determine colonization levels of the individual *V. cholerae* strains.

Community profiling by shotgun sequencing (COPRO-seq). Shotgun sequencing of faecal community DNA was used to define the relative abundance of species in the artificial communities; experimental and computational tools for COPRO-seq have been described previously[8].

Microbial RNA-seq analysis of faecal samples collected from mice colonized with the 14-member artificial community with and without *V. cholerae*. Faecal samples were collected from colonized gnotobiotic mice and immediately snap-frozen in liquid nitrogen. RNA was extracted using bead-beating in phenol/chloroform/isoamyl alcohol followed by further purification using MEGAClear (Life Technologies). Purified RNA was depleted of 16S rRNA, 5S rRNA, and transfer RNA as previously described[8] or by using a RiboZero kit (Epicentre). Complementary DNA (cDNA) libraries were generated and sequenced (50 nucleotide unidirectional reads; Illumina GA-IIx, HiSeq 2000 or MiSeq instruments; see Supplementary Table 3). Reads were mapped to the genomes of members of the artificial community using Bowtie[38].

To profile transcriptional responses to *V. cholerae*, all cDNA reads that mapped to the genomes of the 14 consortium members were binned based on enzyme classification level annotations from KEGG. ShotgunFunctionalizeR[39] was then used compare the faecal meta-transcriptomes of 'D14invasion' animals sampled 4 days after gavage of the 14-member community to the faecal meta-transcriptomes of D1invasion mice sampled 4 days after gavage of the 14-member community plus *V. cholerae*. A mean twofold or greater difference in expression between the conditions, with an adjusted *P* value less than 0.0001 (ShotgunFunctionalizeR) was considered significant. This approach of binning to enzyme classifications mitigates issues with low-abundance transcripts being insufficiently profiled owing to limitations in sequencing depth[8].

Owing to the higher sequencing depth achieved for *R. obeum* and *V. cholerae* in mono- and co-colonization experiments, reads were mapped to reference genomes using Bowtie, and changes at the single transcript level were analysed using DESeq[40] (Supplementary Table 11). Transcripts that satisfied the criteria of (1) having greater than twofold differential expression after DESeq normalization, (2) an adjusted *P* value less than 0.05, and (3) a minimum mean count value more than 10 were retained.

AI-2 assays. Previously frozen faecal pellets from gnotobiotic mice were resuspended in AB medium[24] by agitation with a rotary bead-beater (25 mg faecal pellet per millilitre of medium). AI-2 assays were performed using the *V. harveyi* BB170 bioassay strain[24], with reported results representative of at least two independent experiments, each with five technical repeats. *V. harveyi* BB170 cultures were grown aerobically overnight in AB medium, and diluted 1:500 in this medium for use in the AI-2 bioassay[24]. Luminescence was measured using a BioTek Synergy 2 instrument after 4 h of growth at 30 °C with agitation (300 r.p.m. using a rotatory incubator).

For *in vitro* measurements of *R. obeum* AI-2 production, a 100 µl aliquot from an overnight monoculture of the bacterium grown in MegaMedium without glucose was diluted 1:20 in fresh MegaMedium without glucose. In addition, cells pelleted from 100 µl of an overnight culture of *V. cholerae* Δ*luxS* (MM883 (ref. 14)) grown in LB medium were added to *R. obeum* that had also been diluted 1:20 in MegaMedium without glucose. The resulting mono- and co-cultures were incubated anaerobically at 37 °C for 16 h. Cells were pelleted by centrifugation, and supernatants were harvested and then added to *V. harveyi* BB170 cultures for AI-2 bioassay.

UPLC–MS. Procedures for UPLC–MS of bile acids have been described in ref. 37.

28. Faiz, M. A. & Basher, A. Antimicrobial resistance: Bangladesh experience. *Reg. Health Forum* **15,** 1–18 (2011).
29. Morgan, D. J., Okeke, I. N., Laxminarayan, R., Perencevich, E. N. & Weisenberg, S. Non-prescription antimicrobial use worldwide: a systematic review. *Lancet Infect. Dis.* **11,** 692–701 (2011).
30. Yatsunenko, T. *et al.* Human gut microbiome viewed across age and geography. *Nature* **486,** 222–227 (2012).
31. Caporaso, J. G. *et al.* QIIME allows analysis of high-throughput community sequencing data. *Nature Methods* **7,** 335–336 (2010).
32. Cole, J. R. *et al.* The ribosomal database project (RDP-II): introducing myRDP space and quality controlled public data. *Nucleic Acids Res.* **35,** D169–D172 (2007).
33. DeSantis, T. Z. *et al.* Greengenes, a chimera-checked 16S rRNA gene database and workbench compatible with ARB. *Appl. Environ. Microbiol.* **72,** 5069–5072 (2006).
34. Rodrigue, S. *et al.* Unlocking short read sequencing for metagenomics. *PLoS ONE* **5,** e11840 (2010).
35. Kanehisa, M. & Goto, S. KEGG: Kyoto Encyclopedia of Genes and Genomes. *Nucleic Acids Res.* **28,** 27–30 (2000).
36. Edgar, R. C. Search and clustering orders of magnitude faster than BLAST. *Bioinformatics* **26,** 2460–2461 (2010).
37. Ridaura, V. K. *et al.* Gut microbiota from twins discordant for obesity modulate metabolism in mice. *Science* **341,** 1241214 (2013).
38. Langmead, B., Trapnell, C., Pop, M. & Salzberg, S. L. Ultrafast and memory-efficient alignment of short DNA sequences to the human genome. *Genome Biol.* **10,** R25 (2009).
39. Kristiansson, E., Hugenholtz, P. & Dalevi, D. ShotgunFunctionalizeR: an R-package for functional comparison of metagenomes. *Bioinformatics* **25,** 2737–2738 (2009).
40. Anders, S. & Huber, W. Differential expression analysis for sequence count data. *Genome Biol.* **11,** R106 (2010).

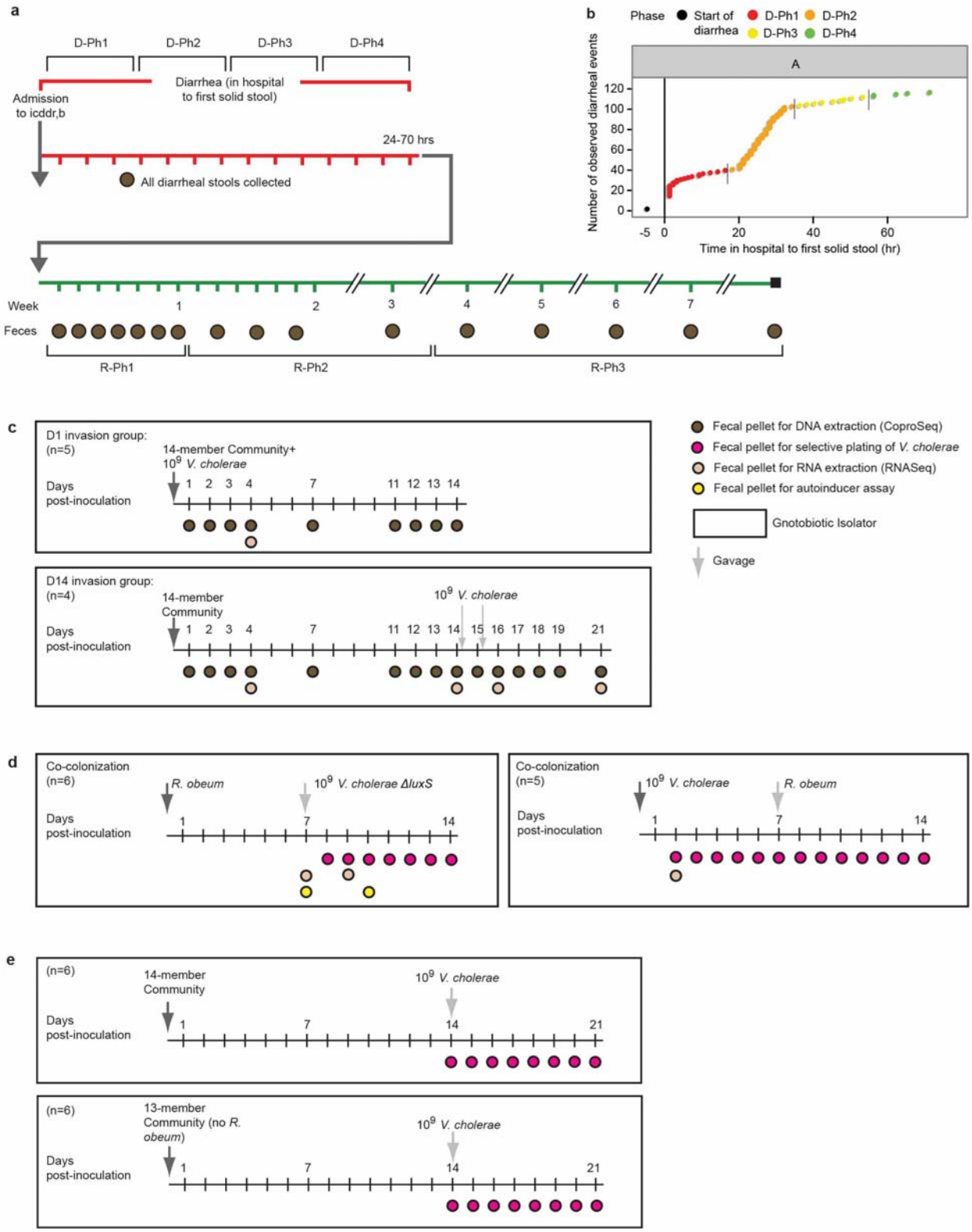

Extended Data Figure 1 | Experimental designs for clinical study and gnotobiotic mouse experiments. **a**, Sampling schedule for human cholera study. **b**, Frequency of diarrhoeal episodes over time for a representative participant (patient A). Initial time (black circle) represents beginning of diarrhoea. The long vertical line marks enrollment into the study. Colours and short vertical lines denote boundaries of study phases defined in **a**. **c**–**e**, Gnotobiotic mouse experimental design. The number (*n*) of animals in each treatment group is shown.

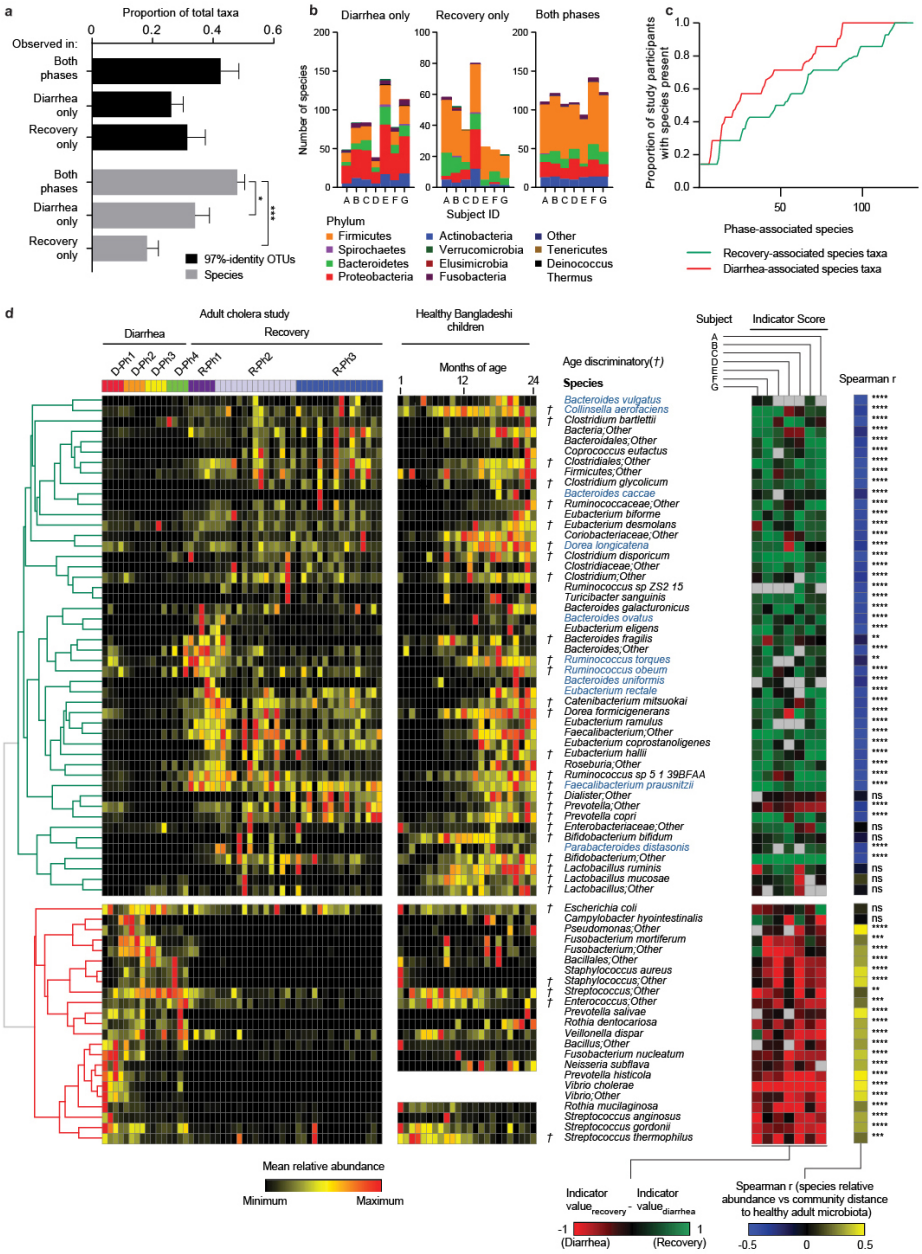

Extended Data Figure 2 | Bacterial taxa associated with diarrhoeal and recovery phase. a, Proportion of bacterial species-level taxa that were observed in both diarrhoeal and recovery phases, in D-Ph1 to D-Ph4 only, and in R-Ph1 to R-Ph3 only. Mean values ± s.e.m. are plotted. $*P < 0.05$, $***P < 0.001$ (unpaired Mann–Whitney *U*-test). **b**, Phylum-level analysis. Mean values are plotted. **c**, Proportion of study participants having bacterial taxa associated by indicator species analysis with the diarrhoeal or recovery phase. The *x* axis shows species associated with each phase, ranked by proportion of subjects harbouring that species. For each species, 'representation in study participants' is the average presence/absence of all 97%-identity OTUs with that species taxonomic assignment. The OTU table was rarefied to 49,000 reads per sample. **d**, Bacterial species identified by indicator analysis as indicative of diarrhoea or recovery phases in adult patients with cholera, and species identified by Random Forests analysis as discriminatory for different stages in the maturation of the gut microbiota of healthy Bangladeshi infants/children aged 1–24 months (denoted by the symbol †). The heat map in the left-hand portion of the panel shows mean relative abundances of species across all individuals during D-Ph1 to D-Ph4, with each phase subdivided into four equal time bins. For recovery time points, columns represent the mean relative abundances for each sampling time point during R-Ph1 to R-Ph3. Mean relative abundance values are also presented for these same species in the faecal microbiota of 50 healthy Bangladeshi children sampled from 1 to 2 years of age at monthly intervals. Unsupervised hierarchical clustering used relative abundances of species in the faecal microbiota of the patients with cholera. The green portion of the tree encompasses species that are more abundant during recovery whereas the red portion encompasses species that are more abundant during diarrhoea. Indicator scores are presented in the right-hand portion of the panel, with 'score' for a given taxon defined as its indicator value for recovery minus its indicator value for diarrhoea (−1, highly diarrhoea-associated; +1, highly recovery-associated). Spearman's rank correlation coefficients of mean relative abundances of species by sample in the cholera study versus the mean sample-weighted UniFrac distance to healthy adult faecal microbiota are shown at the extreme right together with the statistical significance of correlations after Benjamini–Hochberg false discovery rate correction for multiple hypothesis testing (NS, not significant; $*P < 0.05$; $**P < 0.01$; $***P < 0.001$). Higher coefficients indicate increasing divergence from a healthy configuration with higher relative abundance of a given species. Species shown satisfied two or more of the following criteria: (1) presence among the list of the top 40 age-discriminatory species in the Random-Forests-based model of gut microbiota maturation in healthy infants and children; (2) indicator value score greater than 0.7; (3) significant correlation (Spearman's *r*) between relative abundance in the faecal microbiota of patients with cholera and UniFrac distance to healthy adult faecal microbiota; and (4) inclusion in the artificial 14-member human gut community (species name highlighted in blue).

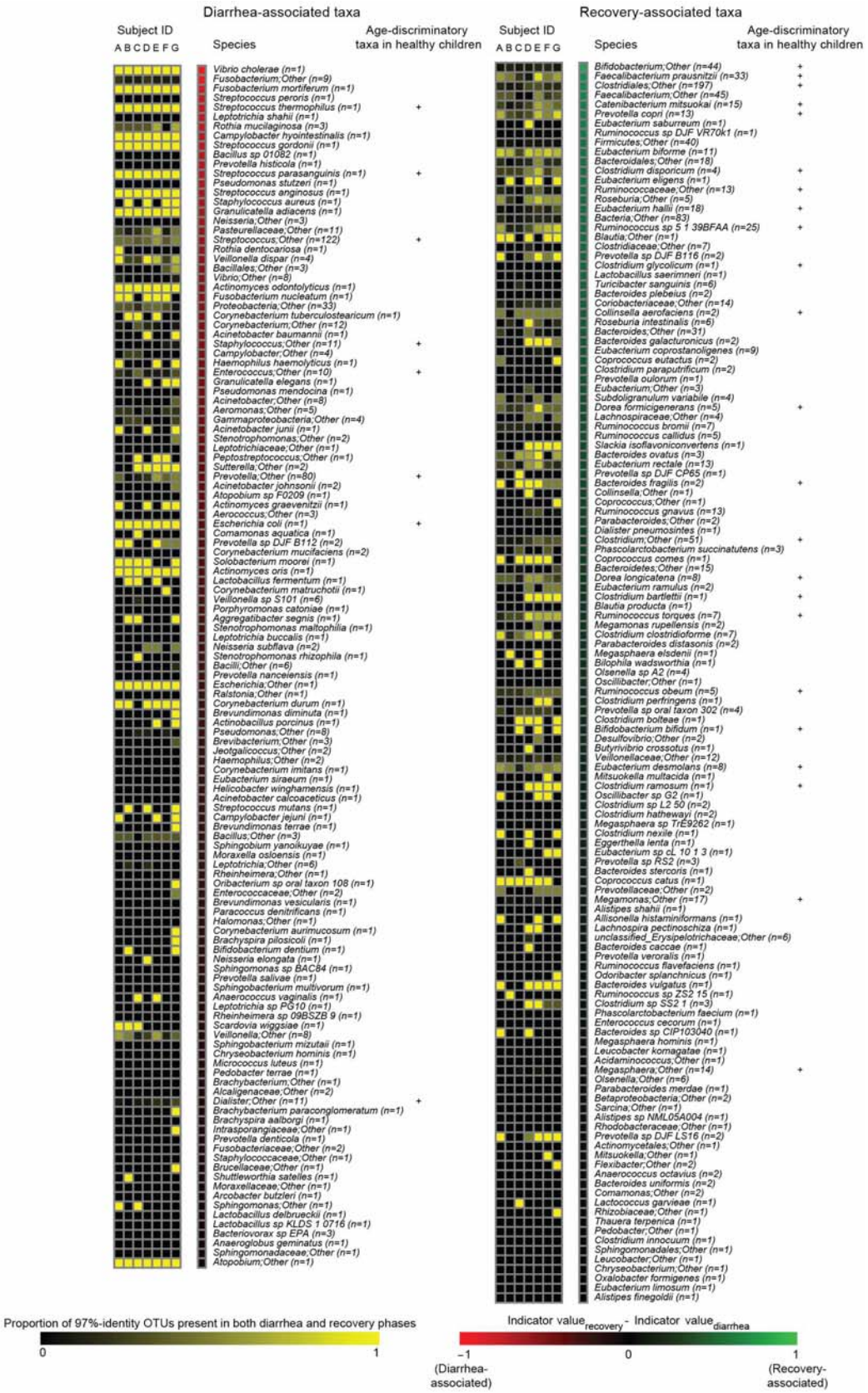

Extended Data Figure 3 | The 97%-identity OTUs observed in both diarrhoeal and recovery phases. The proportion of 97%-identity OTUs with a given species-level taxonomic assignment that were present in both diarrhoeal and recovery phases is shown for each individual in the study. The number of 97%-identity OTUs with a given species assignment is shown in parentheses. Species are ordered based on their 'indicator scores' (defined as indicator $\text{value}_{\text{recovery}}$ minus indicator $\text{value}_{\text{diarrhoea}}$). Age-discriminatory bacterial species incorporated into a Random-Forests-based model for defining relative microbiota maturity and microbiota-for-age *z*-scores[3] in healthy Bangladeshi infants and children are marked with a '+' symbol. The 97%-identity OTUs were derived from data sets generated from all samples from adult patents with cholera; the OTU table was rarefied to 49,000 reads per sample.

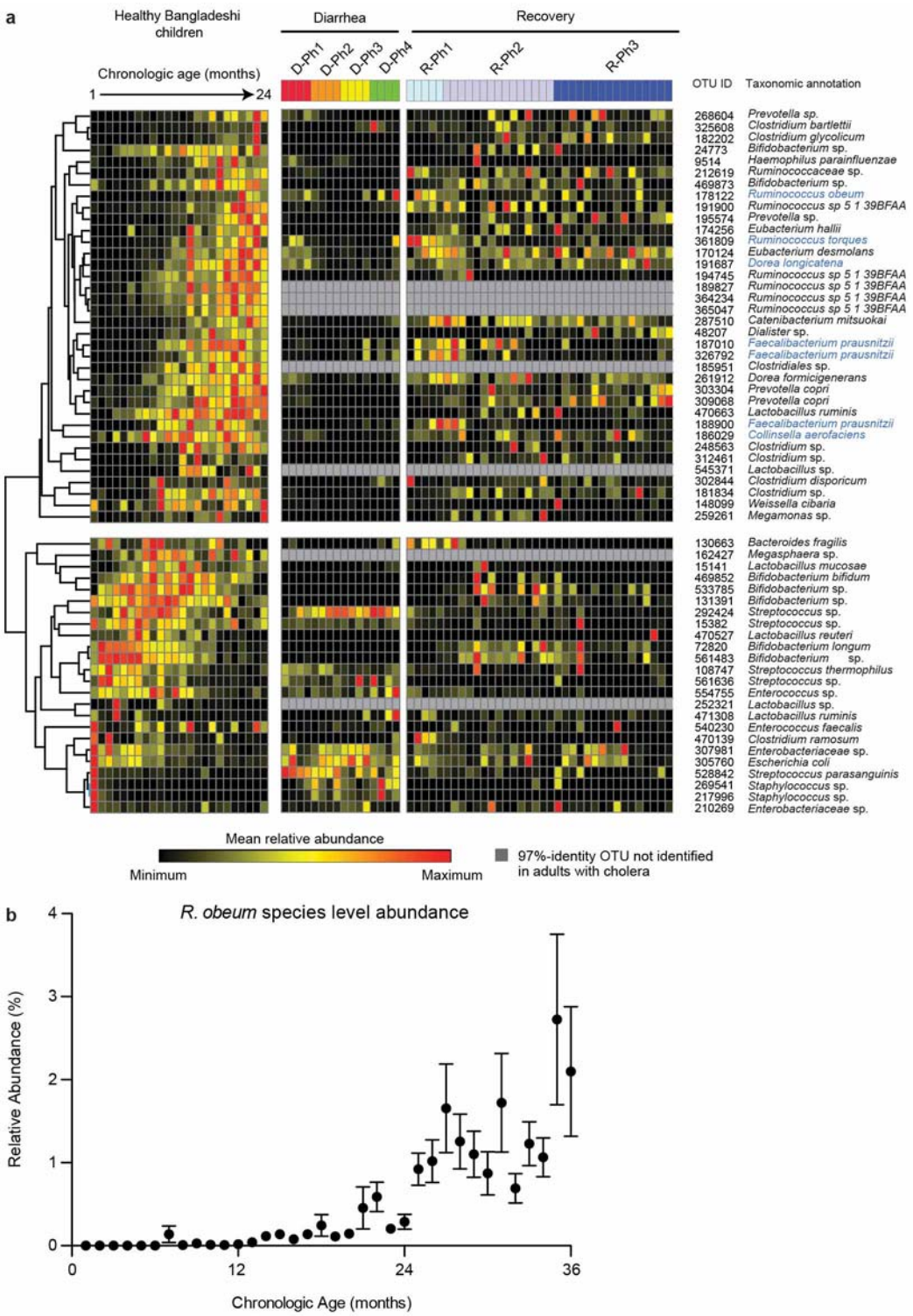

Extended Data Figure 4 | Pattern of appearance of age-discriminatory 97%-identity OTUs in the faecal microbiota of patients with cholera mirrors the normal age-dependent pattern in the faecal microbiota of healthy Bangladeshi infants and children. **a**, Left portion of the panel shows hierarchical clustering of relative abundance values for each of the top 60 most age-discriminatory 97%-identity OTUs in a Random-Forests-based model of normal maturation of the microbiota in healthy Bangladeshi infants/children (importance scores for the age-discriminatory taxa defined by Random Forests analysis are reported in ref. 3; these 60 97%-identity OTUs can be grouped into 40 species-level taxa). Right portion of the panel presents the mean relative abundances of these OTUs in samples obtained from patients with cholera during D-Ph1 to D-Ph4, and R-Ph1 to R-Ph3. The 97%-identity OTUs corresponding to species included in the artificial community that was introduced into gnotobiotic mice are highlighted in blue. **b**, Relative abundance of *R. obeum* strains in the faecal microbiota of healthy Bangladeshi children sampled monthly through the first 3 years of life. Mean values ± s.e.m. are plotted.

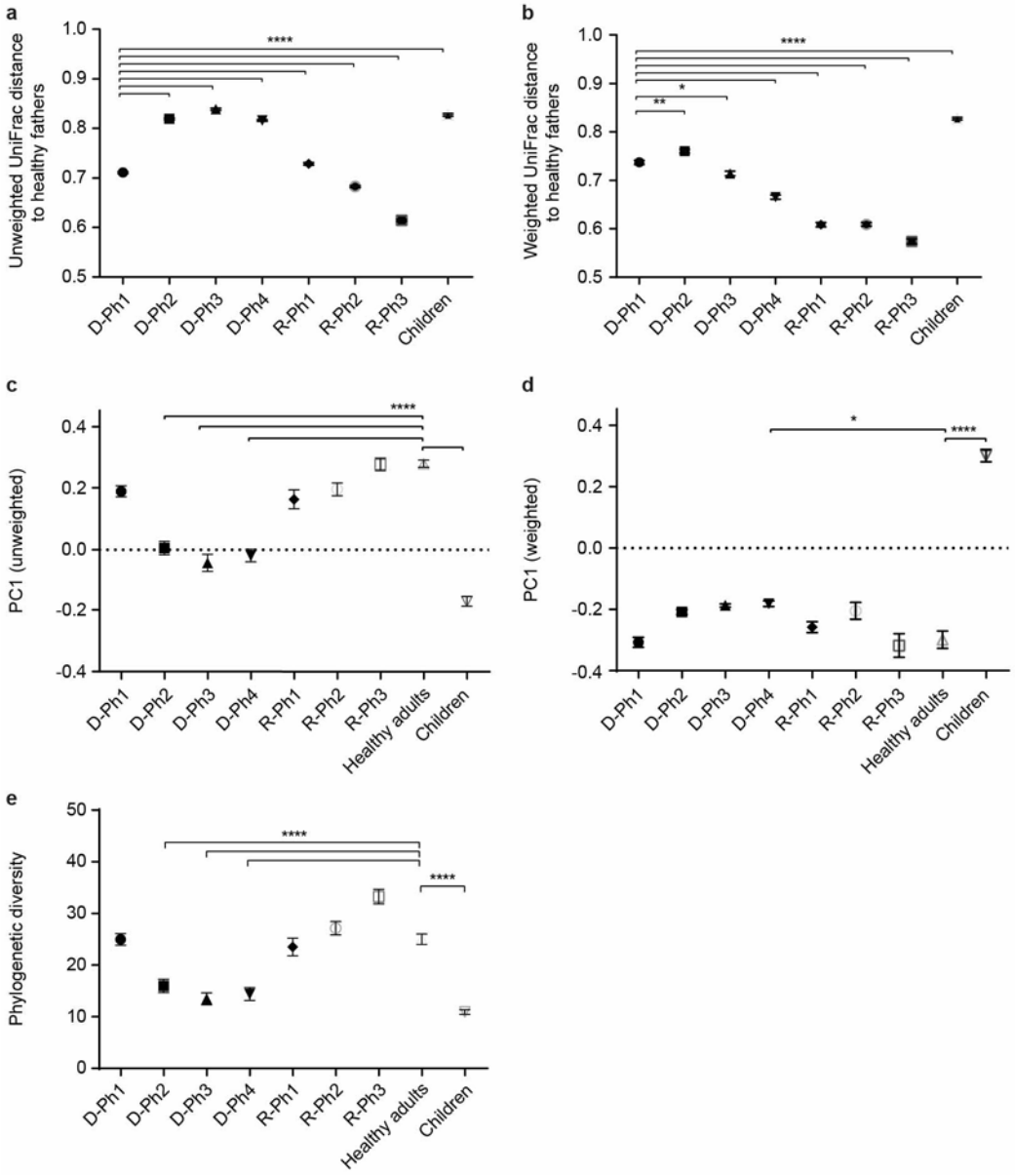

Extended Data Figure 5 | Pattern of recovery of the gut microbiota in patients with cholera. **a**, **b**, Mean unweighted (**a**) and weighted (**b**) UniFrac distances to healthy adult controls at each of the defined phases of diarrhoea and recovery. **c**, **d**, Principal coordinates analysis of UniFrac distances between gut microbiota samples. Location along the principal axis of variation (PC1) shows how acute diarrhoeal communities first resemble those of healthy Bangladeshi children sampled during the first 2 years of life, then evolve their phylogenetic configurations during the recovery phase towards those of healthy Bangladeshi adults. PC1 accounts for 34.3% variation for weighted and 17.7% variation for unweighted UniFrac values. **e**, Alpha diversity (whole-tree phylogenetic diversity) measurements of faecal microbial communities through all study phases. Mean values ± s.e.m. are plotted. $*P < 0.05$, $**P < 0.01$, $****P < 0.0001$ (Kruskal–Wallis analysis of variance followed by multiple comparisons test).

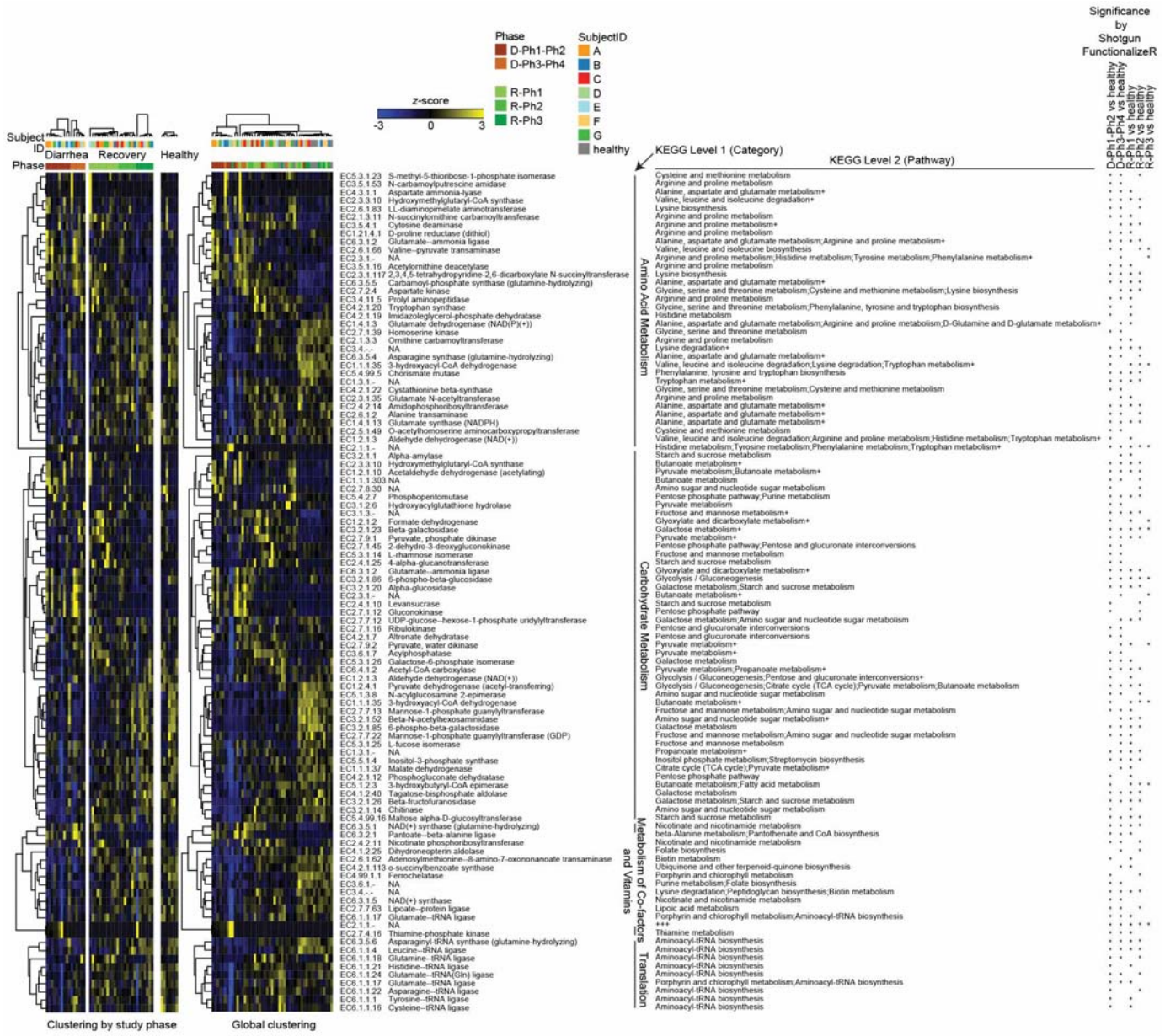

Extended Data Figure 6 | Proportional representation of genes encoding enzymes (classified according to Enzyme Commission number identifiers) in faecal microbiomes sampled during the diarrhoeal and recovery phases of cholera. Shotgun sequencing of faecal community DNA was performed (MiSeq 2000 instrument; 2 × 250bp paired-end reads; 341,701 ± 145,681 reads (mean ± s.d. per sample)). Read pairs were assembled (SHERA software package[34]). Read counts were collapsed based on their assignment to Enzyme Commission (EC) number identifiers. The significance of differences in EC abundances compared with faecal microbiomes in healthy adult Bangladeshi controls was defined using ShotgunFunctionalizeR[39]. Unsupervised hierarchical clustering identifies groups of ECs that characterize the faecal microbiomes of patients with cholera at varying diarrhoeal and recovery phases. The heat map on the left shows the results of EC-based clustering by phase (diarrhoea/recovery). An asterisk on the extreme right of the figure indicates that differences in EC abundance observed across the specified study phases were statistically significant (adjusted $P < 0.00001$, ShotgunFunctionalizeR). The heat map on the right presents the results of a global clustering of all time-points and study phases. Genes encoding 102 ECs were identified with (1) at least 0.1% average relative abundance across the study and (2) significant differences in their representation relative to healthy microbiomes in at least one comparison (adjusted $P < 0.00001$ based on ShotgunFunctionalizeR). In each of the heat maps, *z*-scores for each EC across all samples are plotted. ECs are grouped by KEGG level 1 assignment and further annotated based on their KEGG Pathway assignments. A '+' symbol indicates that the EC has additional KEGG level 2 annotations (see Supplementary Table 8 for a list of all assignable functional annotations). Note that the majority of the 46 ECs that were more prominently represented in faecal microbiomes during diarrhoeal phases in study participants are related to carbohydrate metabolism. The faecal microbiomes of patients during recovery are enriched for genes involved in vitamin and cofactor metabolism (Supplementary Table 8).

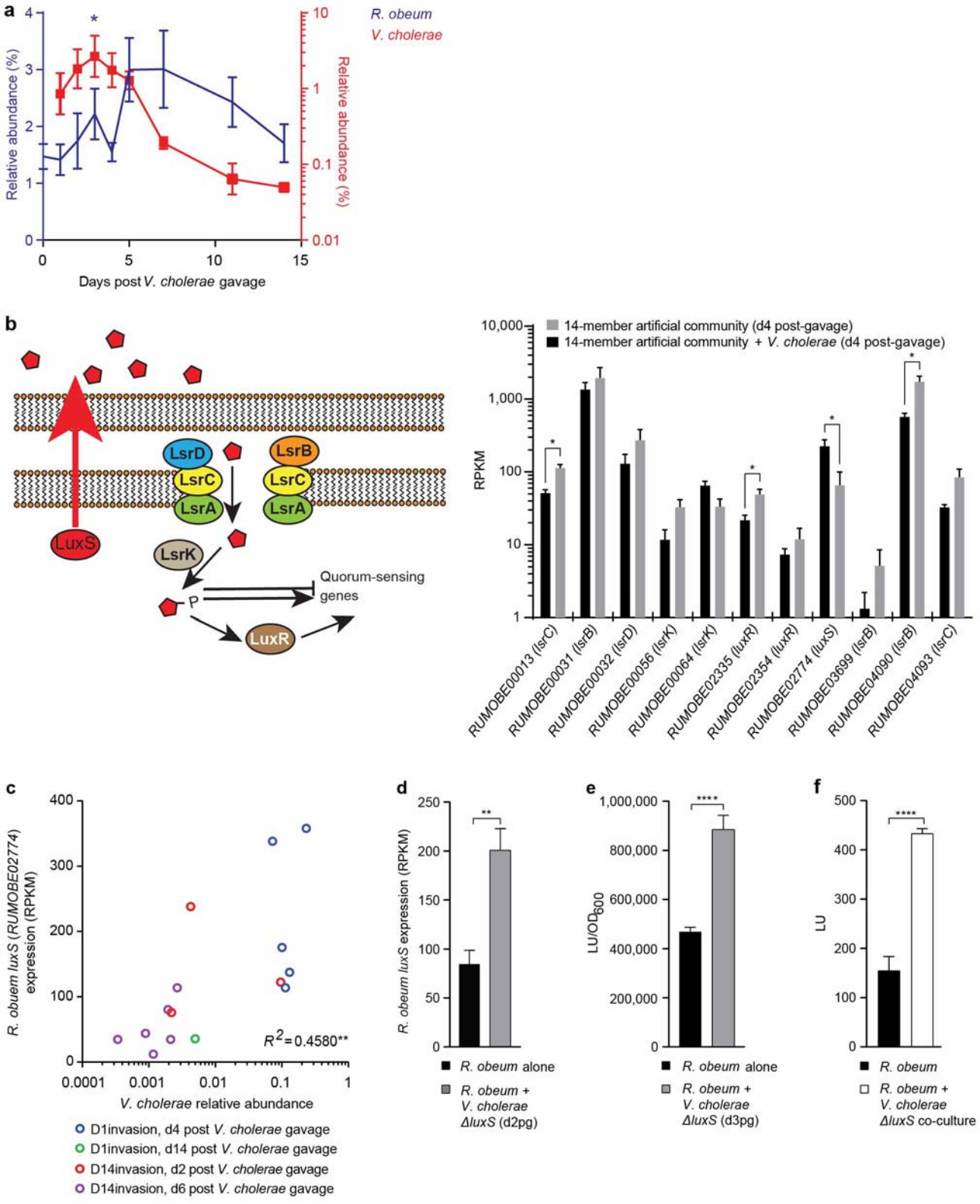

Extended Data Figure 7 | *R. obeum* encodes a functional AI-2 system, and *R. obeum* AI-2 production is stimulated by the presence of *V. cholerae*. **a**, Relative abundances of *R. obeum* and *V. cholerae* in the faecal microbiota after introduction of *V. cholerae* into mice harbouring the artificial 14-member human gut community (D14invasion group, see Extended Data Figure 1c). 'Days post *V. cholerae* gavage' refers to the second of two daily gavages of 10^9 c.f.u. *V. cholerae* into animals that had been colonized 14 days earlier with the 14-member community. Mean values ± s.e.m. are shown ($n = 4$ or 5 mice, $^*P < 0.05$, unpaired Student's *t*-test). **b**, Left panel shows AI-2 signalling pathway components represented in the *R. obeum* genome. Right panel plots changes in expression of these components as defined by microbial RNA-seq of faecal samples obtained (1) 4 days after colonization of mice with the 14-member community and (2) 4 days after gavage of mice with the 14-member community together with 10^9 c.f.u. of *V. cholerae* ($n = 4$–6 animals per group; one faecal sample analysed per animal). Mean values ± s.e.m. are shown. $^*P < 0.05$ (Mann–Whitney *U*-test). **c**, RNA-seq of faecal samples collected at the time points and treatment groups indicated reveals that *R. obeum luxS* transcription is directly correlated to *V. cholerae* abundance in the context of the 14-member community. $^{**}P < 0.01$ (*F* test). **d**, *R. obeum luxS* expression. Mice were colonized first with *R. obeum* for 7 day. Faecal samples were collected for microbial RNA-seq analysis 1 day before gavage of 10^9 c.f.u. of a *V. cholerae* Δ*luxS* mutant, and then 2 days post-gavage (d2pg). Mean values for relative *R. obeum luxS* transcript levels (± s.e.m.) are shown ($n = 5$ or 6 animals per group per experiment, $n = 3$ independent experiments; $^{**}P < 0.01$ unpaired Mann–Whitney *U*-test). **e**, AI-2 levels in faecal samples, taken 1 day before and 3 days after gavage of the *V. cholerae* Δ*luxS* strain, from the same mice as those analysed in **a**. AI-2 levels were measured based on induction of bioluminescence in *V. harveyi* BB170 using the same mass of input faecal sample for all assays. Mean values ± s.e.m. are shown; $^{****}P < 0.0001$ (unpaired Mann–Whitney *U*-test). **f**, *R. obeum* produces AI-2 when co-cultured with *V. cholerae in vitro*. Aliquots of the supernatant from cultures containing *R. obeum* alone, or *R. obeum* plus the *V. cholerae* Δ*luxS* mutant, were assayed for their ability to induce *V. harveyi* bioluminescence. Mean values ± s.e.m. are presented ($n = 4$ independent experiments). LU, light units; RPKM, reads per kilobase per million reads. $^{****}P < 0.0001$ (unpaired Mann–Whitney *U*-test). Note that (1) the number of *R. obeum* c.f.u. present in the samples obtained from mono-cultures of the organism was similar to the number in co-culture, as measured by selective plating, and (2) the *V. cholerae* Δ*luxS* mutant cultured alone produced levels of AI-2 signal that were not significantly different from that of *R. obeum* in mono-culture (data not shown).

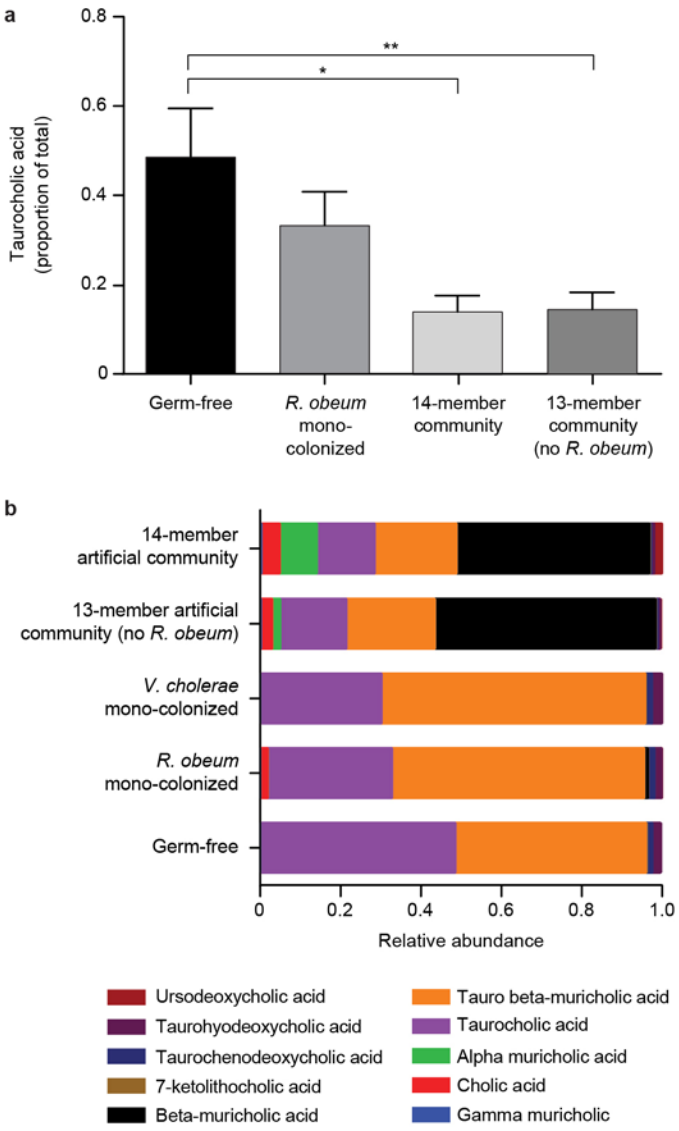

Extended Data Figure 8 | UPLC–MS analysis of faecal bile acid profiles in gnotobiotic mice. Targeted UPLC–MS used methanol extracts of faecal pellets obtained from age- and gender-matched germ-free C57BL/6J mice and gnotobiotic mice colonized for 3 days with *R. obeum* alone, for 7 days with the 14-member community ('D1invasion group'), and for 3 days with the 13-member community that lacked *R. obeum* ($n = 4$–6 mice per treatment group; one faecal sample analysed per animal). **a**, Faecal levels of taurocholic acid. Mean values ± s.e.m. are plotted. $^{*}P < 0.05$, $^{**}P < 0.01$, Mann–Whitney *U*-test. **b**, Mean relative abundance of ten bile acid species in faecal samples obtained from the mice shown in **a**.

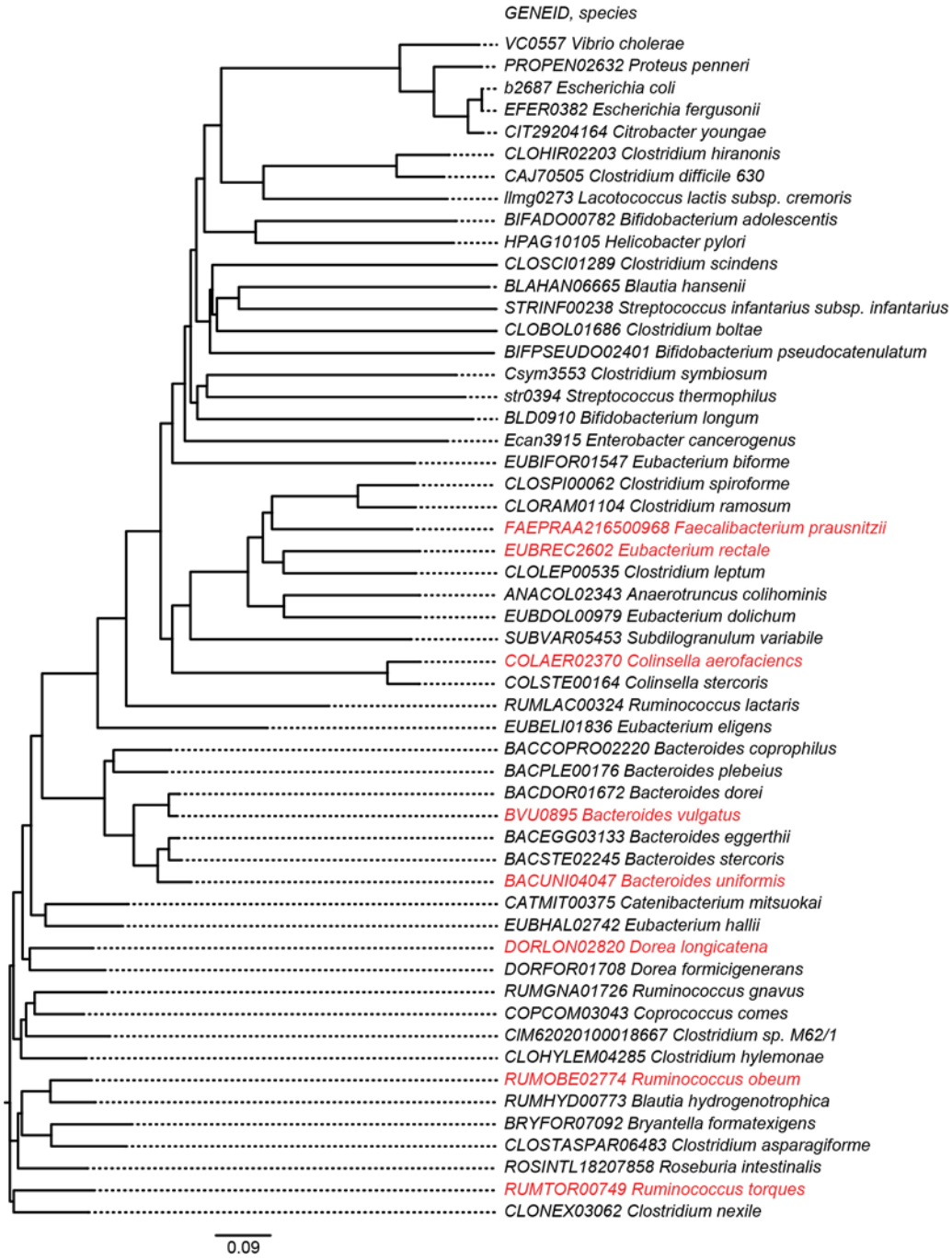

Extended Data Figure 9 | Phylogenetic tree of *luxS* genes present in human gut bacterial symbionts and enteropathogens. The tree was constructed from amino-acid sequence alignments using Clustal X. Red type indicates that the homologue is represented in the genomes of members of the 14-member artificial human gut bacterial community.

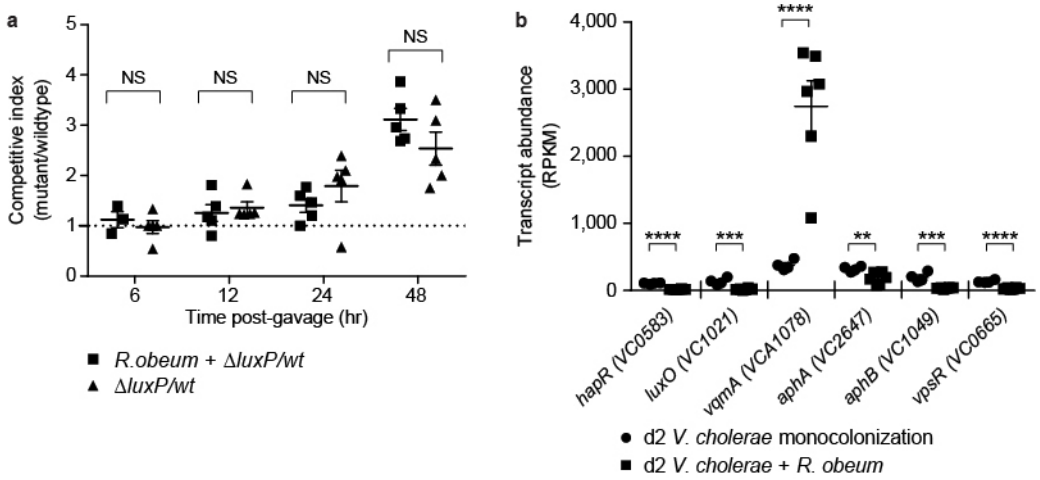

Extended Data Figure 10 | *In vivo* tests of the effects of known quorum-sensing components on *R. obeum*-mediated reductions in *V. cholerae* colonization. **a**, Competitive index of Δ*luxP* versus wild-type C6706 *V. cholerae* when colonized with or without *R. obeum* ($n = 4$–6 animals per group). Horizontal bars, mean values. Data from individual animals are shown using the indicated symbols. **b**, Transcript abundance (reads per kilobase per million reads) for selected quorum-sensing and virulence gene regulators in *V. cholerae*. Microbial RNA-seq was performed on faecal samples collected 2 days after mono-colonization of germ-free mice with *V. cholerae* (circles), or 2 days after *V. cholerae* was introduced into mice that had been mono-colonized for 7 days with *R. obeum* (squares) ($n = 5$ animals per group; NS, not significant ($P \geq 0.05$); $^{**}P < 0.01$, $^{***}P < 0.001$, $^{****}P < 0.0001$ (unpaired two-tailed Student's *t*-test)).